Texas A&M Transportation Institute

Developing a Surface Drainage Rating for Inclusion in TxDOT's Asset Management System: Technical Report

Technical Report 0-6896-R1

Cooperative Research Program

TEXAS A&M TRANSPORTATION INSTITUTE

COLLEGE STATION, TEXAS

1. Report No. FHWA/TX-18/0-6896-R1	2. Government Accession No.	3. Recipient's Catalog No.
4. Title and Subtitle DEVELOPING A SURFACE DRAINAGE RATING FOR INCLUSION IN TXDOT'S ASSET MANAGEMENT SYSTEM: TECHNICAL REPORT		5. Report Date Published: January 2019
		6. Performing Organization Code
7. Author(s) Charles Gurganus, Tom Scullion, Nasir Gharaibeh, Deepika Ravipati, and Saurav Neupane		8. Performing Organization Report No. Report 0-6896-R1
9. Performing Organization Name and Address Texas A&M Transportation Institute The Texas A&M University System College Station, Texas 77843-3135		10. Work Unit No. (TRAIS)
		11. Contract or Grant No. Project 0-6896
12. Sponsoring Agency Name and Address Texas Department of Transportation Research and Technology Implementation Office 125 E. 11th Street Austin, Texas 78701-2483		13. Type of Report and Period Covered Technical Report: September 2015–November 2017
		14. Sponsoring Agency Code

15. Supplementary Notes

Project performed in cooperation with the Texas Department of Transportation and the Federal Highway Administration.
Project Title: Developing a Surface Drainage Rating for Inclusion in TxDOT's Asset Management System
URL: http://tti.tamu.edu/documents/0-6896-R1.pdf

16. Abstract

This project develops a surface drainage rating for inclusion in the Texas Department of Transportation's asset management system. The surface drainage rating includes paved surface attributes and roadside attributes. During development of the rating, special care was taken to account for safety aspects inherent to drainage features. A key element of the surface drainage rating was the automated data collection process using a mobile light detecting and ranging (LiDAR) device. The mobile LiDAR device allowed for the collection of surface measurements at near highway speeds, improving raters' safety. Mobile LiDAR's effectiveness in producing vast amounts of data presents challenges with converting data into useful information such as a drainage rating. Within this project, proof of concept computer code was developed to display how mobile LiDAR data can be collected and processed with minimal intervention to create an efficient rating scheme. The paved surface features within the rating are traveled way width, cross-slope, and hydroplaning potential. The roadside surface features within the rating are front slope steepness, ditch depth, and ditch flowline grade. In addition to the network level rating, the project provides a thorough review of the accuracy of the single laser mobile LiDAR device used to collect data and a method to evaluate the accuracy. Four project level evaluations were also performed that illustrate the use of mobile LiDAR device to measure and analyze surface features to assist in plan development or identification of maintenance locations.

17. Key Words LiDAR, Surface Drainage, Network-Level Rating		18. Distribution Statement No restrictions. This document is available to the public through NTIS: National Technical Information Service Alexandria, Virginia http://www.ntis.gov	
19. Security Classif. (of this report) Unclassified	20. Security Classif. (of this page) Unclassified	21. No. of Pages 226	22. Price

Form DOT F 1700.7 (8-72) Reproduction of completed page authorized

DEVELOPING A SURFACE DRAINAGE RATING FOR INCLUSION IN TXDOT'S ASSET MANAGEMENT SYSTEM: TECHNICAL REPORT

by

Charles F. Gurganus
Associate Research Engineer
Texas A&M Transportation Institute

and

Tom Scullion
TTI Senior Research Engineer
Texas A&M Transportation Institute

Nasir Gharaibeh
Associate Professor
Texas A&M University Civil Engineering Department

Deepika Ravipati
Graduate Research Assistant
Texas A&M Transportation Institute

and

Saurav Neupane
Graduate Research Assistant
Texas A&M University Civil Engineering Department

DISCLAIMER

This research was performed in cooperation with the Texas Department of Transportation (TxDOT) and the Federal Highway Administration (FHWA). The contents of this report reflect the views of the authors, who are responsible for the facts and the accuracy of the data presented herein. The contents do not necessarily reflect the official view or policies of the FHWA or TxDOT. This report does not constitute a standard, specification, or regulation.

This report is not intended for construction, bidding, or permit purposes. The engineer in charge of the project was Charles F. Gurganus, P.E. #101096.

The United States Government and the State of Texas do not endorse products or manufacturers. Trade or manufacturers' names appear herein solely because they are considered essential to the object of this report.

ACKNOWLEDGMENTS

TABLE OF CONTENTS

LIST OF FIGURES

LIST OF TABLES

INTRODUCTION

The rapid evolution of technology allows roadway agencies to collect vast amounts of data through automated means. Paramount to using these data is their conversion into information and metrics aggregated along data collection sections. As the Texas Department of Transportation (TxDOT) begins to implement automated data collection for pavement distress, it also seeks to capitalize on other emerging technologies to gather additional data. Mobile light detecting and ranging (LiDAR) presents an attractive option for collecting data on the surface geometry of both the roadway and roadside.

Geometric information provides insight into surface drainage and design compliance of geometric elements. Including this information into TxDOT's asset management plan represents an expansion of TxDOT's current asset management system. Ultimately, this information can be used in project decision making, network management, and performance evaluation.

This report contains the following sections:

- Introduction.
- Drainage rating background, needs, and literature review.
- Mobile LiDAR equipment used for this study.
- Development of the surface drainage rating.
- Application of the surface drainage rating.
- Project level case studies.
- Summary, conclusions, and recommendations.

DRAINAGE RATING BACKGROUND, NEEDS, AND LITERATURE REVIEW

This section of the report summarizes the current state-of-practice of drainage rating systems, discusses what data collection techniques are used within those systems, and provides a literature review of relevant topics. Drainage assets are diverse and range from the simplicity of the roadway cross-slope to major structures such as bridges. This study does not focus on drainage structures but rather on surface elements that contribute to drainage and can be measured through automated means. The use of mobile LiDAR for transportation-related applications continues to grow and provides significant data on surface features. A cost effective, single-laser mobile LiDAR provides measurements for the surface assets included in the surface drainage rating system.

NATIONWIDE DEPARTMENT OF TRANSPORTATION SURVEY

Prior to the study, researchers reached out to engineers from other departments of transportation (DOTs) to determine how drainage features are currently being evaluated or rated. Additionally, an inquiry on the use of LiDAR within the agency was made. To provide background on why this information was being sought, the following introduction was provided:

> My name is Charles Gurganus and I am an Associate Research Engineer with the Texas A&M Transportation Institute. We have just embarked on a project with TxDOT to develop a surface drainage rating program. If you would be so kind as to take a look at the three quick questions at the bottom of the email to assist with understanding state-of-practice in DOTs. Here is a little background regarding the project; essentially, we are using a LiIDAR device to capture continuous transverse cross-sections in hopes of capturing information on the following elements:
> - Ditch depth.
> - Ditch profile.
> - Roadway cross-slope.
> - Roadway profile.
> - Paved-to-unpaved edge conditions.
> - Rutting.
> - Front and back slope steepness.
>
> Eventually, the data will be combined to create a performance measure. The hope is that we can capture roadway sections that have surface drainage issues, such as poor superelevations, steep front slopes, prone to overtopping or any combination of factors. This is not a culvert inspection project. If you could provide any insight into what your agency is doing, it would be extremely helpful.

Rather than simply leave the response open-ended, three questions were provided to assist in the response. These questions were:

1. Does your agency do anything similar to what is described above?
2. How, if at all, does your agency use LiDAR or other automated data collection means?
3. Do you have a formal culvert inspection program?

Responses were received from 21 state DOTs, a response rate of 42 percent. Some DOTs provided detailed responses, while others succinctly answered the questions provided. Table 1 summarizes the responses.

Table 1. Summary of State DOT Responses.

State	Does your agency continuously capture surface characteristics for drainage or other uses?	Does your agency use LiDAR for data collection?	Does your agency have a formal culvert inspection program?	Contact Person
Alabama				
Alaska	No.	No.	No.	Carolyn H. Morehouse (carolyn.morehouse@ alaska.gov)—considering a similar project and interested in these results
Arizona	No.	No.	No.	Lonnie Hendrix (LHendrix@azdot.gov)
Arkansas				
California	Caltrans does **not** use LiDAR devices for the specific purpose to capture ditch depth, ditch profile, roadway cross-slope, roadway profile, bank-slope steepness, etc. as identified in researcher's email below, but this type of data could be extracted and filtered from a Caltrans LiDAR survey if needed. In other words, this type of data could be a byproduct from a typical roadway project survey.	Caltrans collects LiDAR data by stationary scanning, mobile scanning, and airborne scanning. The following are merely examples of applications for each of the LiDAR collection methods: stationary scanning has been used for mapping structures and assessing pavement, mobile scanning has been used for developing 3D alignments and linear referencing, and airborne scanning has been used for obtaining topography in rural areas with dense vegetation cover and obtaining bathymetry for hydraulic/hydrologic studies.	Caltrans has a formal culvert inspection program. Under the Culvert Inventory Program, Caltrans' culverts and other drainage structures and assets are inspected, assessed, and inventoried by state forces. The field data are logged into a statewide database and used when considering rehabilitating or replacing various drainage assets.	Bruce Swanger (bruce.swanger@ dot.ca.gov) or Michael Whiteside (mike.whiteside@ dot.ca.gov)
Colorado	The transverse cross-section data are not collected as described. Pavement condition and rutting are collected.	All pavement data collection is outsourced. Vendors use various automated data collection tools. These include lasers, inertial profilers, and global positioning system (GPS).	CDOT inspects both major and minor culverts using National Bridge Inspection Standards. The Minor Structures Program includes all structures with a clear opening of 4–20 feet.	William Johnson (will.johnson@ state.co.us)

State	Does your agency continuously capture surface characteristics for drainage or other uses?	Does your agency use LiDAR for data collection?	Does your agency have a formal culvert inspection program?	Contact Person
Connecticut	Connecticut does have a procedure to use a drainability index using data collected by our pavement and photolog data collection vehicles (automated collection). It is simpler than the one described above, but I have attached a summary of how it is done at the CTDOT.	The CTDOT owns and operates two right-of-way (ROW) photolog and pavement-data-collection vehicles that complete an annual survey of all approx. There are 3,800 centerline miles of our highway network that are state-maintained (driving [right] lane, both directions). In addition to high-definition photolog records, the vans are used to collect pavement data, including: Roughness (Roline sensors), rutting cracking, macrotexture, cross-slope, grade (Pavemetrics 3-D laser system combined with gyroscope and GPS).	Culverts with a span over 6 feet in length are inspected regularly as part of the CTDOT bridge inspection program.	Ed Block (Edgardo.Block@ct.gov)
Delaware				
Florida				
Georgia	Georgia has used a contract to look at drainage in problem areas. This evaluation led to the development of projects. This was focused around the metro Atlanta area.	GDOT Maintenance has begun a project using LiDAR to detect roadway elements.	Minor structures are monitored by local personnel. State Bridge Maintenance inspects major structures.	Melany Reynolds (mreynolds@dot.ga.gov)
Hawaii				
Idaho	Idaho does not currently have a program like the one described.	Idaho currently uses ground based LiDAR for survey and are exploring the uses of LiDAR for roadway inventory. The digital storage space requirements are a limiting factor. Idaho currently uses a Pathways Profiler van to perform automatic data collection for roadway conditions throughout the system, including international roughness index (IRI), video, rutting, and cross-slope measurements.	No.	J. Caleb Lakey (caleb.lakey@itd.idaho.gov)
Illinois				

6

State	Does your agency continuously capture surface characteristics for drainage or other uses?	Does your agency use LiDAR for data collection?	Does your agency have a formal culvert inspection program?	Contact Person
Indiana				
Iowa				
Kansas				
Kentucky	Similar information is collected for individual projects, but not at the network level.	To date LiDAR has been beneficial in determining cross, bridge height determination, and subgrade height QA/QC. It is also used for ADA ramp compliance, asset inventory, and landslide analysis. Separately, we use a Laser Crack Measurement System to collect pavement information for rutting and cracking.	Not for culverts less than 20' in span length.	Jon Wilcoxson (jon.wilcoxson@ ky.gov)
Louisiana	Do not have a drainage rating program and have not captured specific data to support one. However, many components listed in the question are captured for Pavement Management Analysis by the Fugro-supplied ARAN data capture vehicle.	Do not use LiDAR. Continually monitoring its feasibility, but have not found a good fit based on data accuracy needs. Current data are captured with the Fugro ARAN vehicle. There is a consideration to move to 3D technology. Collected data will trigger pavement recommendations in the Deighton software DTIMS.	A culvert inspection program is currently being developed with one district piloting a culvert rating form. Districts will collect the data. Data will be stored in the AgileAssets Maintenance Management system.	Mark Suarez (mark.suarez@ LA.GOV)
Maine	No. LiDAR is not used for cross-sections.	When LiDAR is used it is for engineering specific locations, hydrologic studies, airport safety reviews, and other site specific work.	There is a formal inspection program for culverts greater than 5' in diameter.	Andrew Bickmore (andrew.bickmore@ main.gov)
Maryland				
Massachusetts				
Michigan				

State	Does your agency continuously capture surface characteristics for drainage or other uses?	Does your agency use LiDAR for data collection?	Does your agency have a formal culvert inspection program?	Contact Person
Minnesota	The metro district in the Minneapolis/St. Paul area has used LiDAR to collect asset data. Other districts are exploring its use, but not to the level of the metro district.	MnDOT inspects its entire system annually. Through automated means, it collects IRI, faulting, rutting, and cracking. The info is input into an Oracle database and MnDOT uses its Highway Pavement Management Application to identify treatments.	MnDOT uses HydInfra to store location, material type and condition of culverts with less than 10' span. http://www.dot.state.mn.us/bridge/hydraulics/hydinfra.html is a link to MnDOT's culvert inspection program. A contact is provided on this website.	Kirby Becker (kirby.becker@state.mn.us)
Mississippi	There is no drainage rating program or something similar to the work in this project.	Many assets are now being collected with LiDAR. This is being done incrementally, with the desire to eventually cover the entire system.	Culverts are inspected as part of the maintenance quality assessment (MQA) condition assessment. This is performed on 2400 0.1-mile segments annually.	Heath Patterson (hpatterson@mdot.ms.gov)—expressed interest in the results of the project
Missouri				
Montana				
Nebraska	No.	LiDAR has been used for preliminary survey information. Profiler vans collect similar roadway information.	No.	Mark Osborn (mark.osborn@nebraska.gov)
Nevada	No.	NDOT uses both static and mobile LiDAR. We use the static LiDAR on smaller project. Some examples would be bridge and culvert scour, rock stabilization, stockpiles, and various other point projects. Currently doing first mobile LiDAR project. On the project it became necessary to get a very accurate surface for the drainage study.	Yes.	Anita Bush (abush@dot.state.nv.us)
New Hampshire				
New Jersey				
New Mexico				

State	Does your agency continuously capture surface characteristics for drainage or other uses?	Does your agency use LiDAR for data collection?	Does your agency have a formal culvert inspection program?	Contact Person
New York				
North Carolina				
North Dakota	Cross-sectional data as described are not collected. Pavement data are collected, including roughness, rutting, longitudinal and transverse profile (w/ a gyro), distress, and images. This info is collected annually on the entire system.	LiDAR is not used, but is being considered for incorporation when the pavement data collection van is replaced, likely in two years.	Not on a statewide level, but one is being developed for pollutant-discharge monitoring and compliance. This development is early in the process.	Scott D. Zainhofsky (szainhofsky@nd.gov) —interested in our results
Ohio	Inventory data are not collected via LiDAR.	Not for inventory data collection.	Yes.	Drew Williams (Andrew.Williams@dot.ohio.gov)
Oklahoma				
Oregon				
Pennsylvania				
Rhode Island				
South Carolina				
South Dakota				
Tennessee	No program to evaluate cross-section elements.	LiDAR is used. Both static and mobile LiDAR are used to map slopes and elevation data for specific drainage issues at isolated locations. TDOT is in the process of contracting the collection of pavement condition, asset inventory, and overhead clearance through LiDAR, photolog, laser profiles, downward-facing images, and 3D crack detection.	There is no formal culvert inspection; however a pilot program is planned for culvert inspection.	Chris Harris (chris.harris@tn.gov)
Texas				

State	Does your agency continuously capture surface characteristics for drainage or other uses?	Does your agency use LiDAR for data collection?	Does your agency have a formal culvert inspection program?	Contact Person
Utah	Utah does not have a surface drainage rating program. Utah collects vast amounts of asset data via automated means.	Utah has a geospatial inventory of most of its assets. The major omission is subsurface utilities, including storm drain.	There is no formal culvert program. However, over the past four summers, students have been used to locate and inspect storm drain facilities. A 1 to 10 scale was used for the rating. There is an estimate of 31,000 culverts with span less than 20'. Utah is focusing this effort on major roadway.	Stan Burns (sburns@utah.gov)
Vermont	Vermont does not directly measure these elements for a drainage rating. There is an annual collection of roadway conditions that includes rutting. Rutting is seen as a primary drainage related distress. The other drainage related distress is ditch adequacy. This is a major issue in winter months when lack of storage can case icing issues. Ditch adequacy is identified and addressed by regional employees. There is a move toward creating routine maintenance work programs to ensure proper evaluation and maintenance of these types of drainage structures.	LiDAR has been used in our Agency sparingly at this point. In response to Hurricane Irene, the Agency contracted out close to 100 miles of aerial LiDAR that was used in place of land surveying to measure the amount of material lost from damaged roadways and support the development of contract plans for repair without having to rely on survey staff to complete their work before starting design.	The Agency has been working on a culvert inventory and inspection program over the last 7 years. Currently we have reviewed 94% of our state mileage and house an inventory of over 50,000 culverts ranging in diameter from 12" to 72". Next field season will represent our first season of re-inspection with a goal of our four regions re-inspecting 20% of their culverts each year.	Kevin Viani (kevin.viani@vermont. gov)
Virginia				

State	Does your agency continuously capture surface characteristics for drainage or other uses?	Does your agency use LiDAR for data collection?	Does your agency have a formal culvert inspection program?	Contact Person
Washington	WSDOT uses terrestrial LiDAR as a data collection tool that collects the data described. They are using Ptech, Leica or Faro terrestrial scanners. Another responder from Washington indicated there was a limited method to deal with drainage trouble spots.	Consultants are on contract to collect mobile LiDAR data, but the services have not been used to date. Another response detailed the use of LiDAR for bridge clearance.	WSDOT has a program to collect culvert location and condition information. The data are gathered by Region Maintenance while performing routine cleaning of culverts. The data are stored in an iPad application built by WSDOT and transmitted wirelessly to the Highway Activity Tracking System in Olympia. The information is shared with WSDOT's hydraulic community to identify culverts in need of rehabilitation. http://hatsprod.wsdot.loc/Maintenance/management/activities/Inventory	Steve Palmen (PalmenS@ wsdot.wa.gov)
West Virginia				
Wisconsin				
Wyoming	No.	No.	No.	Martin Kidner (martin.kidner@ wyo.gov)—expressed interest in the project and have a 2017 project of their own

The responses above indicate that a network-level surface drainage rating program is nonexistent in other DOTs. Most DOTs that collect surface drainage characteristics are doing so to evaluate localized problem areas. Many DOTs rely heavily on regional employees to identify drainage problems and mitigate as necessary, which is similar to the expectation of maintenance supervisors and area engineers (AEs) within TxDOT. Concerning the use of LiDAR for data collection, many of the responses included a discussion on automated data collection, not necessarily LiDAR. Very few, if any DOTs, are using LiDAR to collect data at the network level. Some DOTs have experience using LiDAR that is mainly focused on localized areas or specific data elements. When using LiDAR, both static and mobile LiDAR are mentioned. Static LiDAR offers a high degree of precision targeted toward a specific area, similar to traditional surveying. The use of mobile LiDAR has significant upside, but precision in the readings is an issue raised by multiple managers.

TXDOT SURVEY OF NEEDS

A web-based survey was sent to the five participating districts to gain an understanding of drainage performance. Two different surveys were circulated. One survey targeted maintenance supervisors and sought insight into current drainage problems. The other survey was disseminated to district engineers, district staff, and AEs in hopes that an understanding of anticipated or desired drainage performance could be deduced.

The surveys were simplistic in nature, specifically designed to maximize participation while minimizing the time required for each participant. Both the surveys sent to maintenance supervisors and to staff/AEs consisted of three main questions. The questions attempted to capture information on three separate drainage zones/areas within the ROW. These areas are roadway drainage, immediate roadside drainage, and extended roadside drainage. The drainage areas are fairly intuitive, with roadway drainage consisting of elements on the pavement where vehicles are expected to travel. Immediate roadside drainage are those elements near the edge of pavement (EOP) or traveled way that are not expected to consistently carry traffic but that can be impacted by turning movements and traffic wander. These elements can greatly influence how water leaves the travel lanes or paved surface. Extended roadside drainage assets are those elements farther away that help convey the water to a crossing or exit point on ROW.

While the survey consisted of three primary questions, participants were given the opportunity to comment on the three drainage areas described above and the ability to include other information that might be useful about the performance or expectation of drainage assets. For the maintenance supervisor, these questions are listed below:

1. Rank the roadway elements about how much trouble each one gives you with maintenance. The element that gives you the most trouble should receive a one (1) and the element that gives you the least trouble should receive a four (4).
   a. Cross-slope.

     b. Rut depth.

     c. Longitudinal profile.

     d. Superelevations.

2. Rank the roadside elements on how much trouble each one gives you for maintenance. The element that gives you the most trouble should receive a one (1) and the element that gives you the least trouble should receive a six (6).

     a. Edge drop-offs.

     b. High edges.

     c. Barrier and rail openings.

     d. Curb and gutter.

     e. Inlets.

     f. Intersection radii.

3. Rank the extended roadside elements on how much trouble each one gives you for maintenance. The element that gives you the most trouble should receive a one (1) and the element that gives you the least trouble should receive a five (5).

     a. Front slopes.

     b. Ditch lines.

     c. Back slopes.

     d. Parallel structures.

     e. Cross structures.

Table 2 provides a summary of the survey sent to maintenance supervisors.

Table 2. Maintenance Supervisor Survey Summary.

District	Surveys Sent	Surveys Completed	% Completed
Atlanta	7	3	43%
Bryan	10	5	50%
Corpus Christi	11	4	36%
Houston	9	3	33%
Tyler	8	3	38%
Total	**45**	**18**	**40%**

Figure 1 through Figure 3 and Table 3 through Table 5 provide survey results. For maintenance supervisors, the number of participants who provided information was 22, a response rate of 55 percent, with 18 surveys completed.

Table 3. Maintenance Supervisor Survey Question 1 Summary.

Statistic	Cross-slope	Rut depth	Longitudinal profile	Super-elevations
Min Value	1	1	1	1
Max Value	4	4	4	4
Mean	2.09	2	2.45	3.45
Standard Deviation	0.87	1.15	0.86	1.01

Figure 1 provides a graphical representation of these results. This graph is constructed by Qualtrics software. The bars within each category represent the number assigned to the feature for the problems it creates related to maintenance. For example, for cross-slope, six maintenance supervisors believe it causes the most trouble, while nine supervisors believe it causes the second most trouble, six the third most, and one supervisor feels it causes the least amount of trouble.
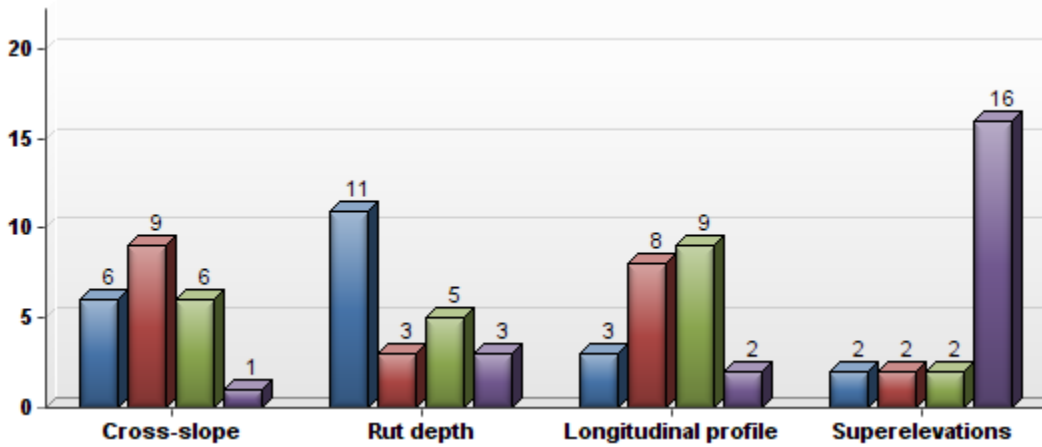
Figure 1. Maintenance Supervisor Survey Question 1 Summary.

Table 4. Maintenance Supervisor Survey Question 2 Summary.

Statistic	Edge Drop-offs	High Edges	Barrier and Rail Openings	Curb and Gutter	Inlets	Intersection Radii
Min Value	1	1	1	1	1	1
Max Value	6	6	6	6	6	6
Mean	2.41	2.68	4.41	4.05	3.64	3.82
Standard Deviation	1.82	1.46	1.56	1.7	1.36	1.56
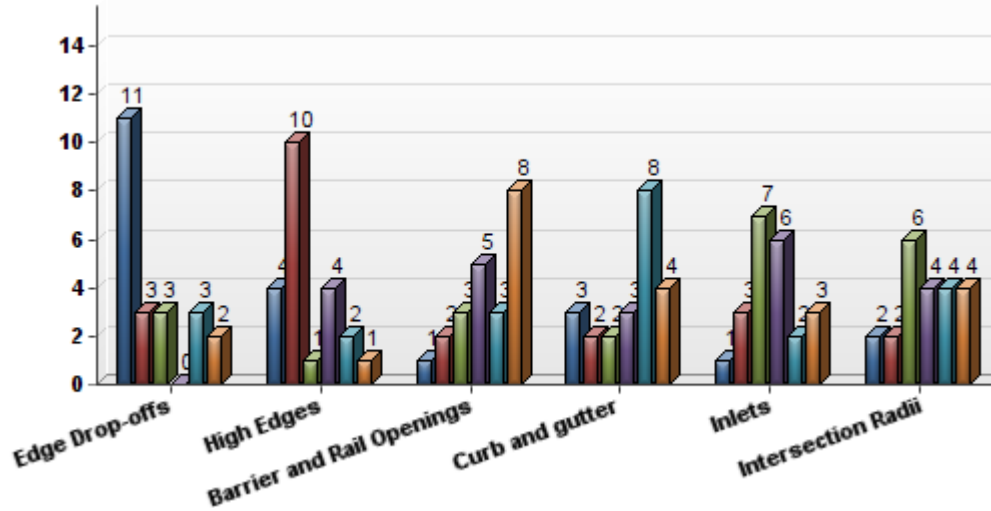
Figure 2. Maintenance Supervisor Survey Question 2 Summary.

Table 5. Maintenance Supervisor Survey Question 3 Summary.

Statistic	Front slopes	Ditch lines	Back slopes	Parallel structures	Cross structures
Min Value	1	1	1	1	1
Max Value	5	5	5	5	5
Mean	3.05	1.95	3.91	3.18	2.91
Standard Deviation	1.29	1.17	1.27	1.33	1.41
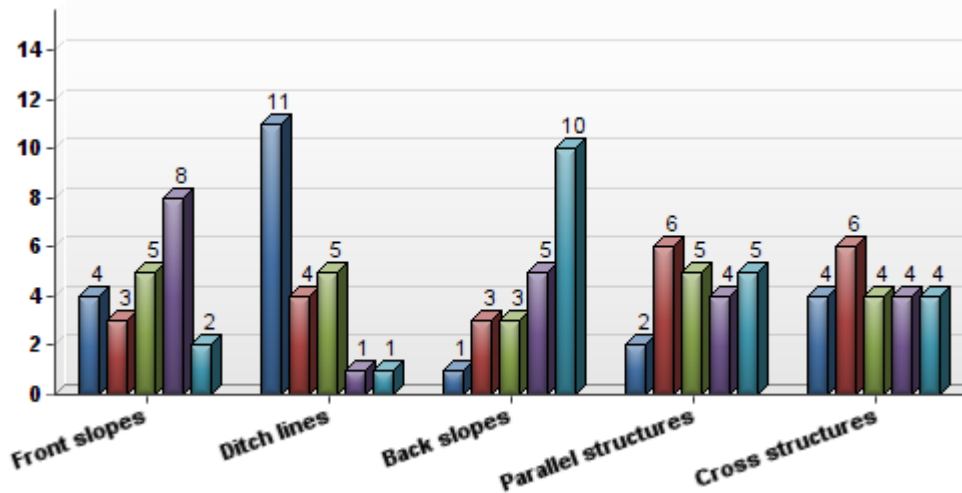
Figure 3. Maintenance Supervisor Survey Question 3 Summary.

Of the 22 maintenance supervisors who provided responses, 21 felt the three drainage areas were appropriate. The responder who indicated that the drainage areas did not make sense did not provide additional information on how the areas should be changed. Six maintenance supervisors provided additional comments. These comments are listed verbatim below:

15

- Hot mix asphalt (HMA) covering curb reveal is becoming a big problem.
- Outfall drainage.
- Drainage issues in this area are mostly a direct result of poor Storm Water Prevention Planning by development contractors. There is not enough oversight to the massive land clearing and building happening now. Silt accumulation from this projects collect in our drainage system causing all kinds of erosion around cross structures, cause high edge problems, and some areas promotes water to run down the edge of the road causing edge drop offs. Until a law enforcement agency starts requiring silt fence or other prevention methods at this construction sites, this will continue to be a problem for TxDOT.
- Not having a curb and gutter and bridge sweeping contract is starting to give us problems at times of rainy weather. Ditch cleaning contract would help us so that we can focus on energy sector areas on the roadway.
- Outfall ditches, more defined and mapped out.
- In our area, we have a high volume of truck traffic, which brings a large amount of dirt and debris on to our ROW, which causes high shoulder. This prevents proper water drainage, water pooling up and encroaching in to the travel lanes.

The survey issued to staff/AEs was structured differently than the survey sent to maintenance supervisors. While the primary goal with maintenance supervisors was to capture current drainage problems, with staff/AEs the goal was to determine current perspectives on the importance of drainage assets. While maintenance supervisors rank drainage assets with no overlap, staff/AEs provide importance levels to drainage assets and have the ability to assign the same importance level to multiple assets. The same drainage areas within the ROW were used, and the ability to comment on those areas or add additional information was offered within the survey. The three primary questions presented to staff/AEs are listed below:

1. Think about the roadway elements below and move the slider to the importance rating it should receive for its effect on surface drainage. One (1) represents no importance at all, while nine (9) indicates the element is very important. Do not worry about rating overlap, it is perfectly acceptable to assign the same importance weight to multiple elements:
    a. Cross-slope.
    b. Rut depth.
    c. Longitudinal profile.
    d. Superelevations.
2. Repeat the rating for the roadside elements below:
    a. Edge drop-offs.
    b. High edges.
    c. Barrier and rail openings.
    d. Curb and gutter.
    e. Inlets.
    f. Intersection radii.

3. Repeat the rating for the extended roadside elements below:
    a. Front slopes.
    b. Ditch lines.
    c. Back slopes.
    d. Parallel structures.
    e. Cross structures.

Table 6 provides a summary of the survey sent to staff and AEs.

Table 6. District Staff/AE Survey Summary.

District	Surveys Sent	Surveys Completed	% Completed
Atlanta	7	4	57%
Bryan	8	5	63%
Corpus Christi	7	3	43%
Houston	9	5	56%
Tyler	9	4	44%
Total	**40**	**21**	**53%**

Table 7 and Figure 4 summarize the survey results for each question.

Table 7. Staff/AE Survey Question 1 Summary.

	Min Value	Max Value	Average Value	Standard Deviation
Cross-slope	5	9	8.19	0.98
Rut depth	5	9	7.62	1.28
Longitudinal profile	2	9	6.62	1.86
Superelevations	3	9	7.1	1.92
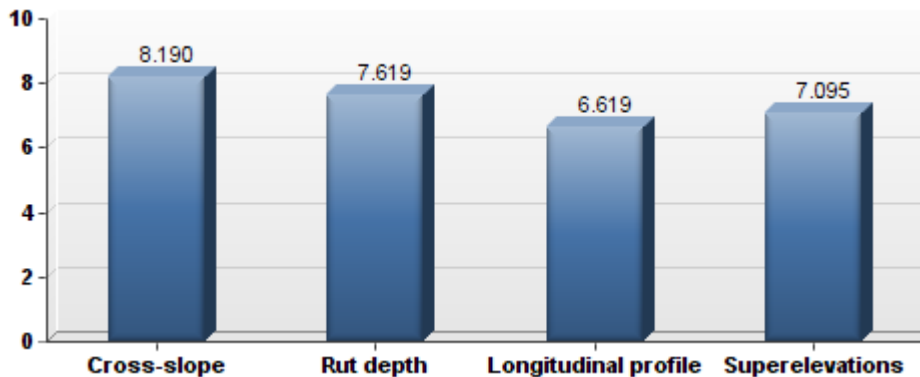
Figure 4. Staff/AE Survey Question 1 Summary.

A review of the results of Question 1 indicates that while cross-slope and rut depth are considered the most important, the degree of importance for roadway elements does not vary significantly across elements. Table 8 seems to indicate that some may view longitudinal slope and superelevations less importantly, while cross-slope and rutting never receive an importance rating of less than five. Figure 5 graphically presents the information in Table 8.

Table 8. Staff/AE Survey Question 2 Summary.

	Min. Value	Max. Value	Average Value	Standard Deviation
Edge Drop-offs	1	9	5.19	2.6
High Edges	4	9	7.24	1.45
Barrier and Rail Openings	3	9	6.52	1.91
Curb and gutter	3	9	6.76	1.89
Inlets	5	9	7.76	1.26
Intersection Radii	1	9	4.85	2.8
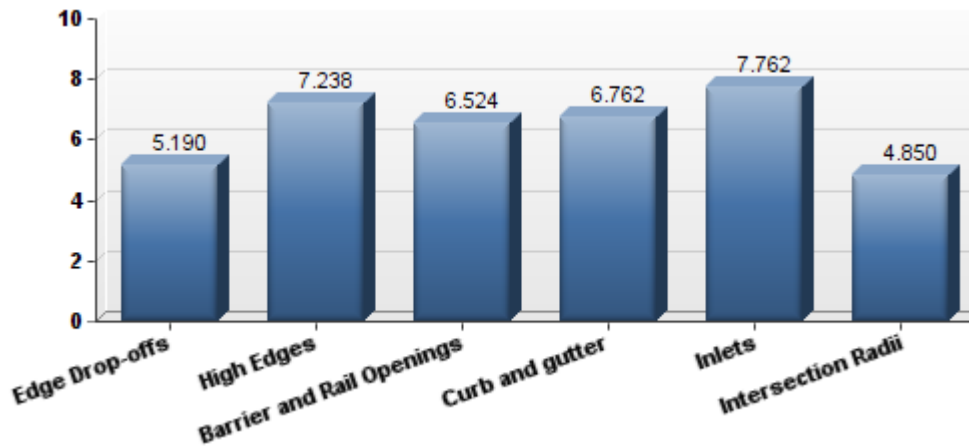
Figure 5. Staff/AE Survey Question 2 Summary.

An interesting observation from Figure 5 is that edge drop-offs rank near the bottom in terms of importance weighting, while inlets are the highest. Maintenance supervisors rank edge drop-offs as one of the highest trouble areas and inlets as one of the least.

Table 9. Staff/AE Survey Question 3 Summary.

	Min Value	Max Value	Average Value	Standard Deviation
Front slopes	1	9	5.38	2.33
Ditch lines	3	9	7.24	1.67
Back slopes	1	9	4.81	2.14
Parallel structures	3	9	6.57	1.72
Cross structures	3	9	7.52	1.63
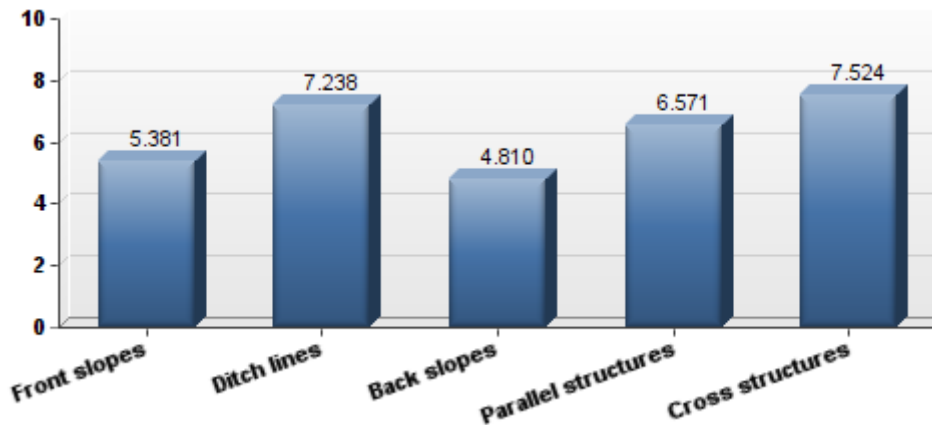
Figure 6. Staff/AE Survey Question 3 Summary.

For the staff/AE survey, 21 were completed. In the section of the survey where participants are asked if the three drainage areas are reasonable, 20 of the respondents indicated that they are reasonable. The respondent who indicated the area did not make sense provided additional feedback. It appears that in order for this participant to clearly state whether or not the areas make sense, a more formal definition of each area needs to be provided. Eleven additional comments were provided in the open comment box. These comments are listed verbatim below:

- Actually falls under superelevation, but partial overlay with TOM (approx. ¾ in.) has been known to cause minor accumulation of water on superelevated inside shoulders (Interstate section) and concentrated flow across travel lanes. Specific example, but something that has occurred. Also possible effects of the various methods of overlay in curb and gutter sections.
- Moving trunkline outfalls. These should be considered but I do not know how to capture them.
- Type of pavement, speed of facility, and traffic volume.
- Intersections that are built to a tabletop to facilitate traffic flow in both directions (i.e., flattened for the main road and the crossroad), resulting in poor drainage if inlets are not placed in the approach gutters, or if the intersection plane is too flat.

- Curb openings on curbed roads with ditches or in raised medians where they allow drainage to cross the roadway on the surface in areas of superelevation.
- Combination of features (i.e., longitudinal grade at zero in location where the superelevation transition goes to zero).
- Slope drains extending down the header bank at bridge ends (some are blocked deliberately because of erosion alongside the drain, while others are blocked by curbing installed for a retrofitted thrie-beam connection).
- Width of pavement if built-in single cross-slope.
- Birdbath built into surface grade due to combination of superelevation and curb/bridge rail.
- Flooding allegations by private property owners. Storm water pollution prevention plan (SWP3) device effects on roadway drainage retention/detention for capacity improvement projects.
- Use of slotted drains in wide pavement sections in superelevation.

ADDITIONAL BACKGROUND INFORMATION AND LITERATURE REVIEW

Asset Management Overview

Asset management has been a rapidly evolving field within transportation since 1998 when the American Association of State Highway and Transportation Officials (AASHTO) created an asset management task force. Over this 15-plus-year evolution, the state of implementation of an asset management programs across state DOTs has varied widely, but the Moving Ahead for Progress in the 21st Century Act (MAP-21) appears to be the catalyst for nationwide implementation of an asset management approach. Under MAP-21 legislation, states must build a risk-based asset management plan for roads and bridges. Plans for other assets are encouraged, but not required. State plans must include:

- A summary listing of the pavement and bridge assets on the National Highway System, including the condition of those assets.
- Asset management objectives and measures.
- Performance gap identification.
- Lifecycle cost and risk management analysis.
- A financial plan.
- Investment strategies (*1, 2*).

Obviously, asset management takes on many forms throughout the industry. In the literature, the point has been made that while asset management has been studied for decades, there is no common understanding of what it is and how it looks within an agency. Ultimately, it should help achieve more value with fewer resources, but for public agencies, this remains difficult because of the following issues:

- The function of infrastructure assets is complex as is the expected performance of those assets.
- How asset failure and asset benefit is defined is not always known, and there is no standard within the industry.
- Once failure and benefit are defined, they must be quantified and measured, a difficult task itself (*3*).

As agencies try to piece together their asset management program, the National Cooperative Highway Research Program (NCHRP) published a synthesis in 2013 that offers a fairly comprehensive review of what is taking place around the country. This synthesis was published in response to MAP-21. Asset management principles are pushing agencies to make decisions based on data, with the understanding that data-driven decisions are more defensible and will ultimately be performance based. This synthesis reinforces the readily available data for pavements and bridges but indicates that while some agencies are beginning to collect data on other assets, their use in decision making is almost nonexistent (*4*).

Current Asset Management Systems with TxDOT

TxDOT has a plethora of historical pavement and bridge data. TxDOT collects distress data on all on-system (state-owned) facilities on an annual basis. These data include ride quality and distress ratings. This information is stored in the Pavement Management Information System (PMIS). Much of these data are aggregated to provide three primary scores: a condition score (CS), a distress score, and a ride score. Condition and distress scores range from 1 to 100, with 1 representing the worst condition and 100 representing the best condition. Ride score can range from 0.1 to 5.0, with higher numbers representing smoother pavements. PMIS has long been used to describe the condition of Texas pavements and provide a benchmark associated with the 90 percent good or better goal (*5, 6*).

A bridge is defined as a "structure erected over a depression or an obstruction, such as water, a highway, or a railway that carries traffic and has an opening of more than 20 feet between faces of abutments" (*7*). TxDOT inspects all bridges at least every two years. For Texas, this requires the inspection of 52,536 structures, about 76 percent more than any other state (*7, 8*).

While PMIS and the bridge inventory are well developed, such a comprehensive database does not exist for other assets. For other assets on the ROW, TxDOT uses the Texas Maintenance Assessment Program (TxMAP). The Texas Traffic Assessment Program (TxTAP) is also used to evaluate signs, works zones, and other traffic-related elements. Unlike PMIS, these systems only sample a portion of the network. The annual program collects data on 4,000 1-mi roadway sections and adjacent ROW. This equates to 5 percent of non-interstate highway centerline miles and 10 percent of interstate centerline miles. TxMAP collects data on pavement condition and roadside performance using a windshield survey on a statistically determined sample size.

The roadside elements include:

- Vegetation.
- Litter.
- Sweeping.
- Trees/Brush.
- Drainage.
- Encroachments.
- Guard rails.
- Guard rail end treatments.
- Mail boxes.

Data are collected on these elements through visual inspection while driving. During a peer review of the program, this process was questioned by several other state DOTs. Kansas DOT asked, "If you are driving, how is pipe condition determined?" North Carolina Department of Transportation (NCDOT) pointed out that they measure blocked pipes within its program. This peer review is part of a process to evaluate the creation of a Texas Condition Assessment Program (TxCAP), which will combine TxTAP, TxMAP, and PMIS. The initial formulation for TxCAP uses a 25 percent multiplier for TxMAP and TxTAP and a 50 percent multiplier for PMIS. Double counting can occur within these multipliers because of the PMIS and TxMAP pavement condition data.

The peer review revealed what other DOTs are using in measuring asset performance. Caltrans indicated they have a five-year maintenance program that leads their largest condition rating effort, but they do not have all components inventoried. Caltrans categorizes assets in terms of safety, preservation, and service. NCDOT indicated that they would love an inventory, but it is too much effort, so inventory is estimated on 34 different areas. Each area has a performance target used for planning and seeking additional money from the legislature (*9, 10*).

Lack of good data beyond pavements and bridges is a common area of concern voiced by transportation decision makers. The small sample size and the use of a windshield survey within TxMAP leaves decision makers wanting better and more reliable data for which decisions can be made. Geometric elements and how those elements relate to pavement and other asset performance are not commonly collected, particularly at the network level.

Literature Review of Mobile LiDAR Applications

The use of mobile LiDAR to measure and inventory roadway attributes is on the rise (*11-14*). However, applying the results of mobile LiDAR measurements and incorporating the results into asset management systems and processes often requires tailor-made techniques. NCHRP Report 748 suggested that applying mobile LiDAR to transportation-related applications has the

potential to revolutionize the industry, particularly if data are shared across agency silos from project planning to facility maintenance (*15*).

The use of LiDAR for specific infrastructure applications is well documented in the literature. A LiDAR study conducted on over 90 miles of roadway in North Carolina evaluated LiDAR data against manually collected data and found that mobile data compare reasonably well to manual collection (*14*). Potential LiDAR application at the network level includes the measurement of roadway cross-slope with a device that generates over 10,000 laser points per second (*13*). An algorithm referred to as the horizontal alignment finder was created to inventory highway curves (*16*). Studies related to storm water surface drainage infrastructure have also been performed. The use of LiDAR data within an Italian storm water study sought to overcome the challenge of not knowing the in-field condition because as-built data are often out of date or inaccurate (*17*). Lantieri used mobile LiDAR data to determine water runoff conditions on the pavement surface and to understand how improper surface drainage can lead to pavement striping and delamination (*18*). The Florida Department of Transportation has evaluated methods to analyze cross-slope from mobile data collection. The analysis of highway geometric conditions assists agencies in evaluating accidents related to surface geometry or surface drainage (*19*).

A major application of LiDAR intensity that has been widely studied is to classify natural and urban surface covers such as asphalt roads, grass, trees, and house roof. Intensity has also been used to discriminate snow-covered areas from bare ice in a glacier, aging lava flows, rock properties, coastal land cover, flood modeling, and wetland hydrology (*20*). Further, LiDAR intensity has been used with other measurements to improve the accuracy of results.

LiDAR-based elevation data were qualitatively analyzed for highway drainage analysis by comparing against standard USGS-based elevation data for watershed and drainage pattern delineation along a section of highway on Iowa 1. The study used flow-modeling tools from the Hydrologic Engineering Center and GIS with terrain obtained from LiDAR data and USGS Digital Elevation Models (DEMs). The study did not find significant benefit due to additional detail from aerial LiDAR data in terms of highway hydrology in the area studied (*21*).

With in-depth technical details, rapidly emerging technology, and various applications, a 2013 synthesis was performed on LiDAR applications. Along with this synthesis, an NCHRP report offers much of the same information and guidelines for the use of mobile LiDAR for transportation applications. These two references almost serve as a one-stop shop for the state-of-practice of LiDAR within transportation. These documents were created because this technology is being rapidly deployed, and while the benefits seem obvious, limited experience and vast amounts of created data can prove challenging for transportation agencies. One of the primary benefits with the use of mobile laser scanning is the safety to the raters and the traveling public; a second is an almost elimination of roadway delays (*11, 15*).

Puente et al. provided a thorough review of laser scanning technology available on the market (*22*). This review evaluated multiple pieces of technology and their capabilities for positioning, scanning, and imaging. When determining what type of mobile scanning system needs to be used, an agency needs to understand if it is primarily concerned with mapping of features or surveying features. Making this determination dictates which equipment should be selected and the associated price for that equipment. The article evaluated seven separate scanning devices. These devices and a brief conclusion on their capabilities are:

- Roadscanner (Siteco): Good performance and one of most effective, especially for road inspections.
- IP-S2 (Topcon): Provides panoramic views but requires more detailed point data to be used in surveys and roadway inspections. Better in situations where low accuracy is acceptable.
- MX8 (Trimble): Good performance for roadway inspections but not as high as the Optech equipment.
- Streetmapper Portable (3d Laser Mapping, Ltd.): Good performance for roadway inspections but not as high as the Optech equipment.
- VMX-250 (Riegl): Good performance for roadway inspections but not as high as the Optech equipment.
- Dynascan (MDL Laser Systems): Lower precision, but great range. The range component can help in mining or environmental monitoring where large scale mapping is needed.
- Lynx Mobile Mapper (Optech): Best laser specifications on the market, providing high performance for roadway inspections (*22*).

Hydraulic and Hydrologic Literature Review

To simulate surface drainage on the roadway and roadside, LiDAR readings must be linked together to form a grid that can be used in grid-based algorithms. O'Callaghan and Mark created the deterministic eight-direction (D8) single-flow algorithm to extract data from DEMs in 1984 (*23*). Choi et al. continued the use of grid-based algorithms in a study used to capture manmade storm water infrastructure (*24*). TopoToolbox is a set of Matlab commands built upon the D8 algorithm to assist with hydraulic analysis of topographic data (*25, 26*).

Hydroplaning can be defined as the actual separation of the tire from the pavement surface, caused by a layer of fluid (*27, 28*). Hydroplaning potential is a function of geometric conditions such as cross-slope, longitudinal grade, and pavement width. Surface textures also effect hydroplaning by directly impacting the fluid thickness between the tire and roadway. On pavements, this thickness is called the water film thickness (WFT) or water film depth (WFD) (*27-33*). Parameters beyond the control of the agency also influence hydroplaning, such as tire wear, tire pressure, driver's speed, and rainfall intensity (*33*).

Both empirical and analytical models have been developed to predict WFT. Ultimately, researchers have sought to move beyond the geometric and textural analysis that calculates a WFT into an analysis of the speed at which hydroplaning will occur. In 1963, NASA developed a hydroplaning speed (HPS) formula that was modified in 1986 to account for the width to length ratio of the tire footprint. Gallaway's work at the Texas Transportation Institute in the 1970s culminated in the development of a WFT formula and HPS formula (*27*). PAVDRN software was created as part of an NCHRP in the late 1990s that also developed WFT and HPS formulas (*31, 34*). Recent work at the University of Southern Florida created HPS formulas based on numerical predications (*35*). Work in the field continues in an effort to move past empirical equations that can be limited to specific values. Analytical methods using finite element analysis to predict skid resistance and HPS have been built to apply to broader conditions and include factors such as tire pressure and wheel load (*28*).

LiDAR measurements can be analyzed to delineate drainage areas within the roadway and roadside infrastructure. Knowledge of drainage areas allows researchers to capitalize on hydraulic analysis equations with long histories of use. For example, the developer of the PAVDRN model settled upon a one-dimensional kinematic model for WFT calculations (*31*). A popular hydraulic model, the kinematic wave model, has a long history in overland and channel flow calculations (*36-39*). The Rational Method can be applied to surface runoff calculations when the intensity and duration of rainfall are known or assumed. The Rational Method is typically limited to smaller areas (less than 200 acres). Manning's equation can be used to calculate water velocity while accounting for the roughness of the surface (*40*). Manning's equation uses the hydraulic radius for velocity calculation, but when the bottom width of a channel or flow path is extremely wide, particularly as it relates to water depth, the hydraulic radius is equal to the flow depth (*39, 41*). The continuity equation is a conservation equation in fluid mechanics that includes discharge, velocity, and cross-sectional drainage area (*42*). The continuity equation, Manning's equation, and the discharge equation can often be combined to calculate important flow parameters.

MOBILE LIDAR EQUIPMENT USED TO DEVELOP TXDOT'S SURFACE DRAINAGE RATINGS

MOBILE LIDAR SYSTEM

In this study, a single-laser mobile LiDAR system (MLS) was used to collect roadway and roadside surface geometry. Knowledge of roadway and roadside geometry permits the analysis of surface drainage and also permits the comparison of roadway and roadside elements to design standards. Design standards are developed to balance safety and drainage requirements while placing paramount importance on the safety of the users. Therefore, because of the nature of the MLS equipment used in this study and the nature of highway surface drainage, both safety and drainage elements are included.

The common components of MLSs include the hardware technology mounted to the vehicle, the in-vehicle software interface for data collection, and the software package for post-processing. The MLSs used in this study included the Road Doctor CamLink camera, a single SICK laser scanner, a NovAtel GPS, a NovAtel inertial measurement unit (IMU), a 3D accelerometer, Road Doctor CamLink 7.0 in-vehicle software, and Road Doctor 3 post-processing software. The laser scanner package was constructed by Roadscanners Oy of Finland (*43*). Two primary pieces of data are generated by the laser: the reflectivity of the target object and the straight-line distance to the object in relation to the angle of the laser. Figure 7 illustrates the geometry associated with LiDAR measurements.
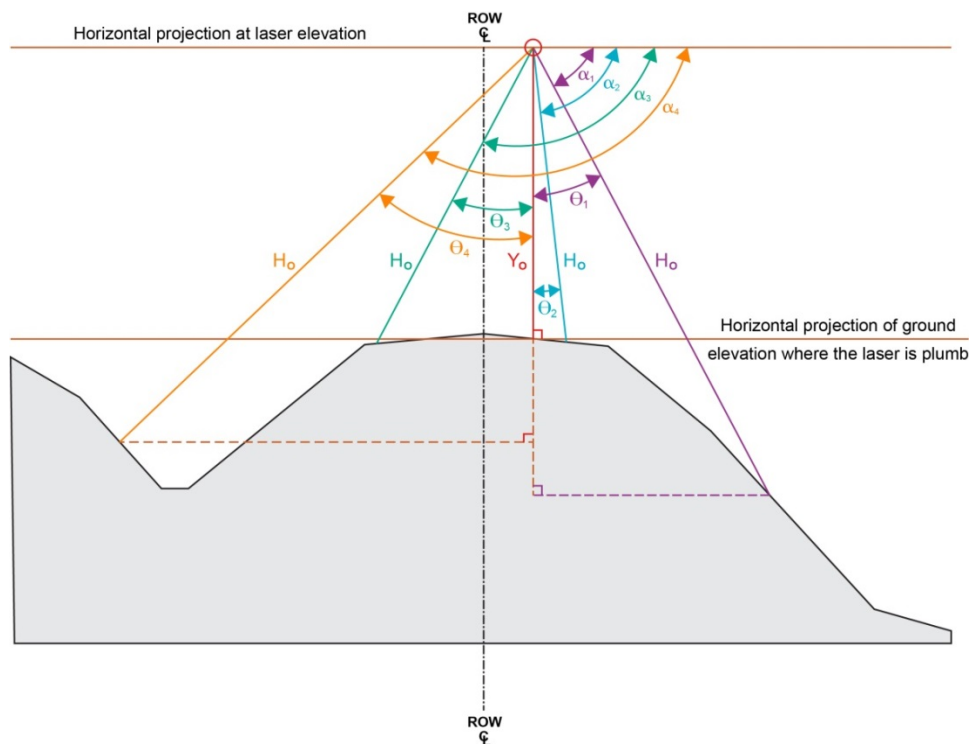
Figure 7. Laser Scanner Geometry.

Figure 7 depicts four relevant measurements as the scanner collects data within the ROW. Descriptions of the variables in Figure 7 are:

- Y_0 represents the height of the laser source when the laser is vertically plumb to the target object (i.e., the road surface). This height is approximately 10 ft (3.05 m).
- H_0 is the distance from the laser source to the target object.
- α is the angle between a horizontal projection at the height of the laser and the laser shot.
- θ is the angle between Y_0 and the laser shot.

The α value represents the angular resolution. Angular resolution is defined as the angular movement in the laser between measurements (*44*). In this study, the angular resolution is 0.6667°. The angular resolution increment spacing does not change, so more data points are collected in close proximity to the laser source. This can be seen in Figure 8, which includes laser lines on approximately 5° increments.
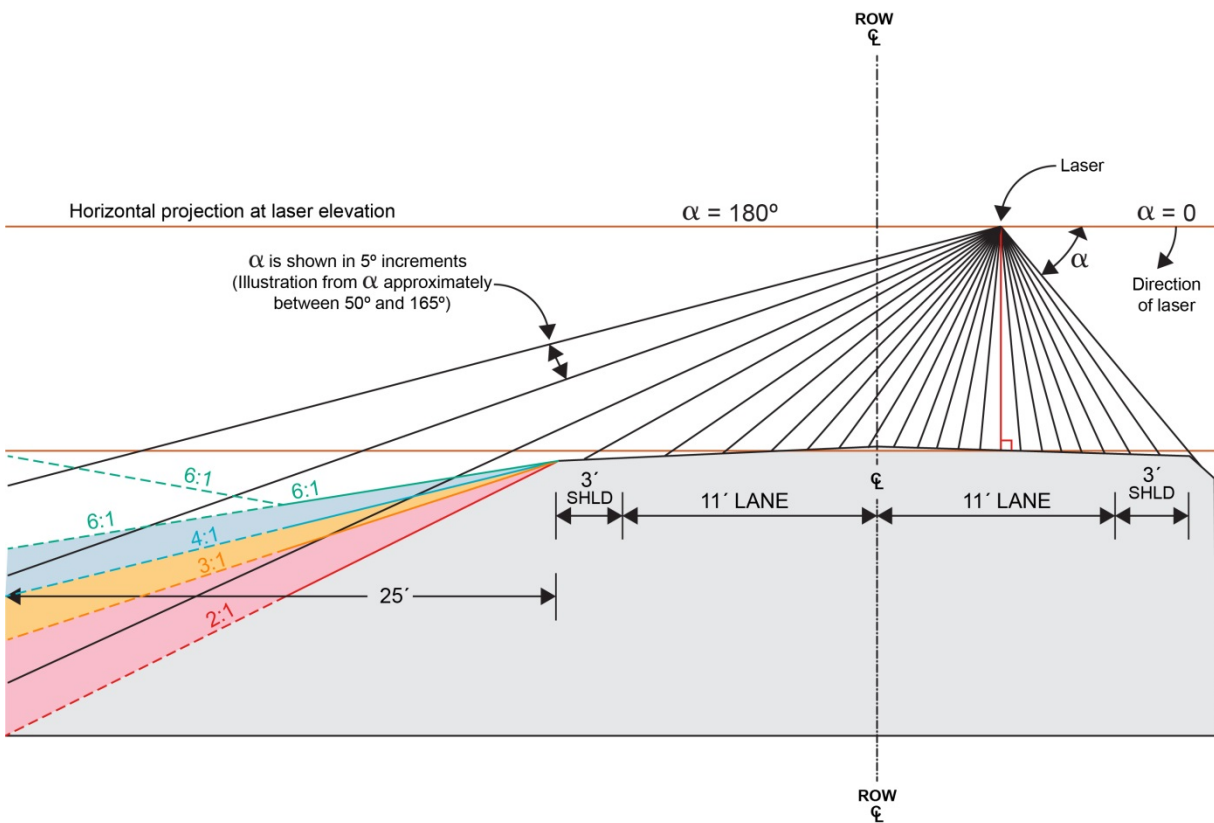
Figure 8. Transverse Laser Geometry.

Point density is the number of LiDAR measurements (i.e., points) per unit area. Point density changes in relation to laser proximity and the speed of the MLS vehicle. Within a 0.1-mi (161 m) data collection section, between 100,000 and 200,000 points are generated over a 100-ft (30.5 m) wide field of view while driving at 45 mph (72.5 kph) average speed. In the data collection lane, approximately 19,000 points are generated within a 0.1-mi (161 m) section. The mobile LiDAR

unit in this study has a point density of approximately 190,000 points per lane mile in the data collection lane at 45 mph. At 70 mph, the point density reduces to approximately 127,000 points per lane mile. Figure 8 illustrates the point density reduction as the target object distance becomes farther from the laser source or the target surface becomes steeper.

Data processing begins in the collection vehicle. Within the vehicle is a software interface to initiate and stop data collection. Road Doctor Camlink 7.0 was used in this study. Data management is an integral element within the network-level process. An approximately 0.93-mi (1500 m) long project level section on US 75 in Sherman, Texas, generates between 275,000 KB and 300,000 KB of data per run. A multi-mile roadway segment for inclusion into a network rating will generate several million kilobytes of information. Much of the used disk space is video files. For US 75, video constitutes over 250,000 KB of data. On approximately 7.5 mi of FM 320 in the Tyler District, over 2.8 million KB of data are produced, but 2.6 million KB of the data are video. The other 7 percent to 10 percent of data are scanner data used to generate point clouds and compute elevations.

The Surface Analytics module of Roadscanners' Road Doctor 3 software package was used in this study. Many software options are available from Roadscanners. The various modules of Road Doctor 3 can be found at http://www.roadscanners.com/product/road-doctor-3/. The Surface Analytics module includes the following features:

- Road Doctor Survey Laser Scanner Data Processing.
- Point Cloud Creation.
- 3D Surface Data Extraction from Laser Scanner Data.
- Rutting Calculation from Laser Scanner Data.
- IRI Calculation from Accelerometer Data.
- Semiautomatic Road Shape Calculation from Laser Scanner Data.
- Longitudinal Data Filtering Tool.

CONVERSION OF MLS DATA INTO A GRIDDED FORMAT

For this study, LiDAR points were organized in a surface grid for reduction and hydraulic analysis purposes. This was done for both the paved surface and the roadside after the different surfaces were extracted as described above. Post-processing software was used to extract an elevation from each grid. Locations close to the laser have multiple points within a single grid, while points far from the laser may have no points within the grid and must rely upon interpolation.

Figure 9 displays a 1-ft × 1-ft grid on the paved surface. The longitudinal spacing between cross-sections remains somewhat constant, but the spacing between points within a cross-section increases moving away from the laser. This is displayed in Figure 10, which depicts 3-ft × 3-ft grids used on the roadside. At far distances from the laser, it is possible no discrete

29

measurements are taken within a 3-ft × 3-ft grid. Cross-sections are generated on a slight skew, as illustrated in Figure 9 and Figure 10.
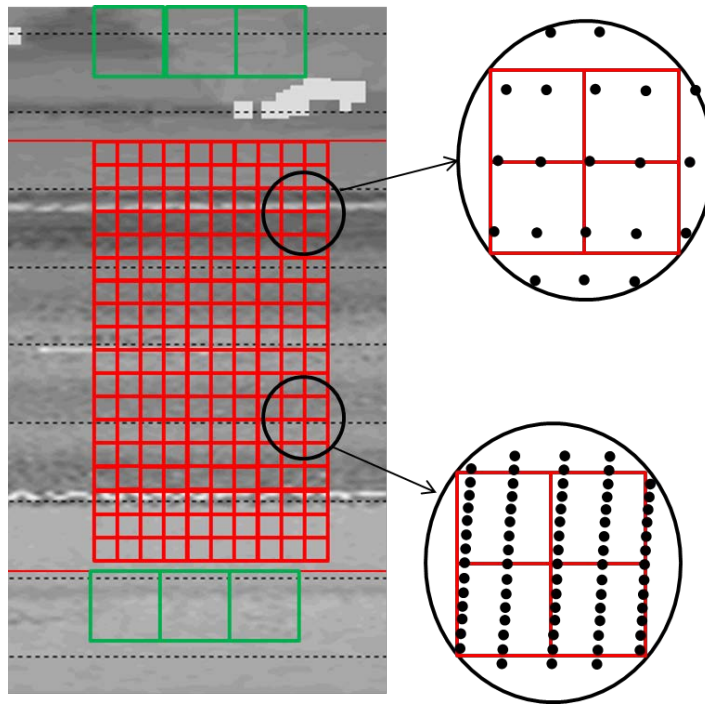
Figure 9. Paved Surface Grid Example.
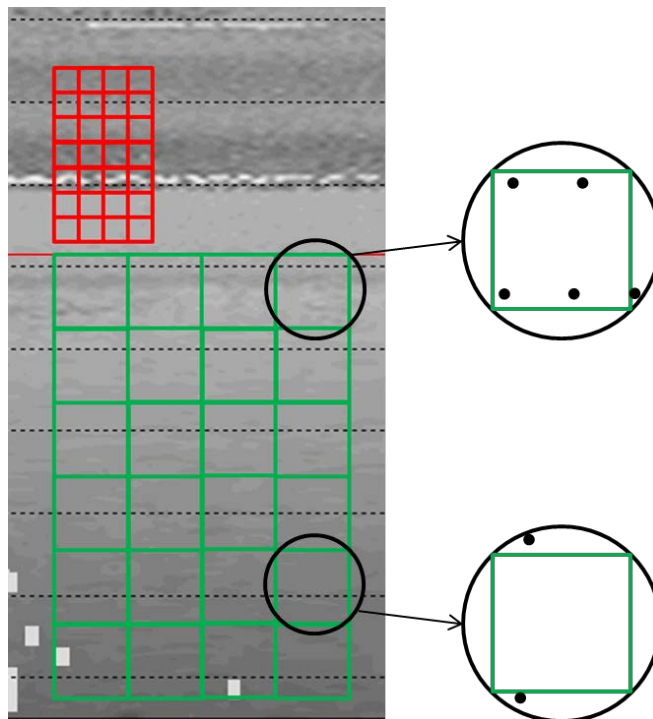
Figure 10. Roadside Grid Example.

The three factors that can affect the data orientation and data density of the roadway surface grid for mobile LiDAR data were briefly illustrated and discussed above. These factors are:

- Skew created in collecting data from a mobile apparatus.
- Longitudinal spacing between cross-sections.
- Transverse spacing within cross-sections.

Longitudinal Skew

Longitudinal skew—the difference between creating a perfectly perpendicular cross-section to the centerline and one that crosses the centerline at an angle—is created by collecting data from a mobile device. Because the laser scans through the horizon and the data collection vehicle is moving, each point within a cross-section is in a different longitudinal location from the centerline. Table 10 shows the longitudinal skew at various data collection speeds (i.e., speed of the MLS vehicle).

Table 10. Longitudinal Skew Associated with Mobile LiDAR Data.

Vehicle Speed (mph)	Max Longitudinal Skew (in.)	Longitudinal Skew across Collection Lane (in.)	Longitudinal Skew from EOP to EOP (in.)
5	0.47	0.20	0.29
10	0.93	0.39	0.59
15	1.39	0.59	0.88
20	1.86	0.78	1.17
25	2.32	0.98	1.47
30	2.79	1.17	1.76
35	3.25	1.37	2.05
40	3.72	1.56	2.35
45	4.18	1.76	2.34
50	4.64	1.96	2.93
55	5.11	2.15	3.23
60	5.57	2.35	3.52
65	6.04	2.54	3.81
70	6.50	2.74	4.11
75	6.97	2.93	4.40
80	7.43	3.13	4.69

The maximum longitudinal difference represents the laser reading 190° apart, or 5° above the horizon created by the laser. This distance is often of no interest because the laser is likely reading leaves on trees or a target object far in the distance. For practical purposes, the skew created by collecting the data from a mobile apparatus will often be less than 3 in. and will almost always be less than 6 in. Within the context of a roadway cross-section, this can be considered negligible and will be ignored from this point forward.

Longitudinal Spacing

Longitudinal spacing represents the spacing between cross-section measurements and must be accounted for during data reduction. Using mobile LiDAR, transverse cross-sections are taken on small intervals, typically less than 1 ft. Figure 11 displays transverse cross-section spacing for a 6.5-mi section of rural highway. On this roadway, 54,621 cross-sections were created. The average spacing between these cross-sections is 0.63 ft (less than 8 in.) apart. Data were collected on this roadway section at an average vehicle speed of 42.9 mph.

Statistic	Dist. (ft)
Count	54621
Mean	0.630
Median	0.640
Std. Dev.	0.072
95th Percentile	0.755
Max	0.889
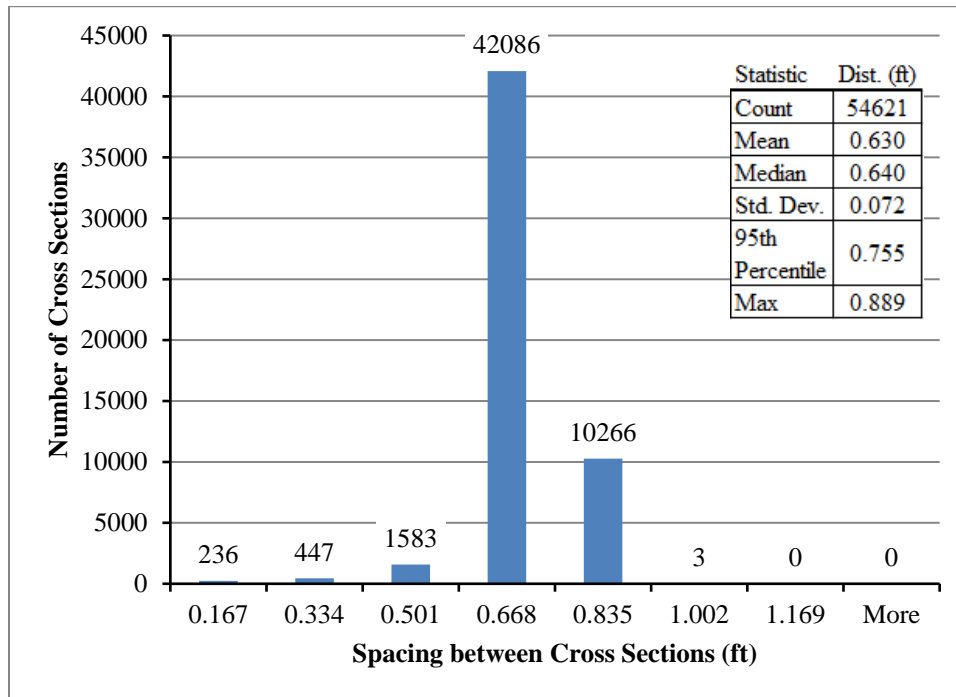
Figure 11. Transverse Cross-Section Spacing over Multiple Miles Traveling at Approximately 43 mph.

Transverse Spacing within a Cross-Section

Skew and cross-section spacing deal with measurements moving in the direction of the data collection vehicle, but transverse spacing deals with the distance between measurements within a cross-section. Transverse spacing (i.e., spacing within a cross-section) is a function of the following four variables:

- Laser frequency.
- Angular resolution.
- Distance from laser source.
- Slope of target surface.

The laser dictates the first two variables, while the roadway geometry controls the latter two. Because the angular resolution does not change, if a target surface moves steeply away from the

laser, measurements become farther apart. Figure 12 displays the spacing across a typical two-lane roadway with varying front slopes.
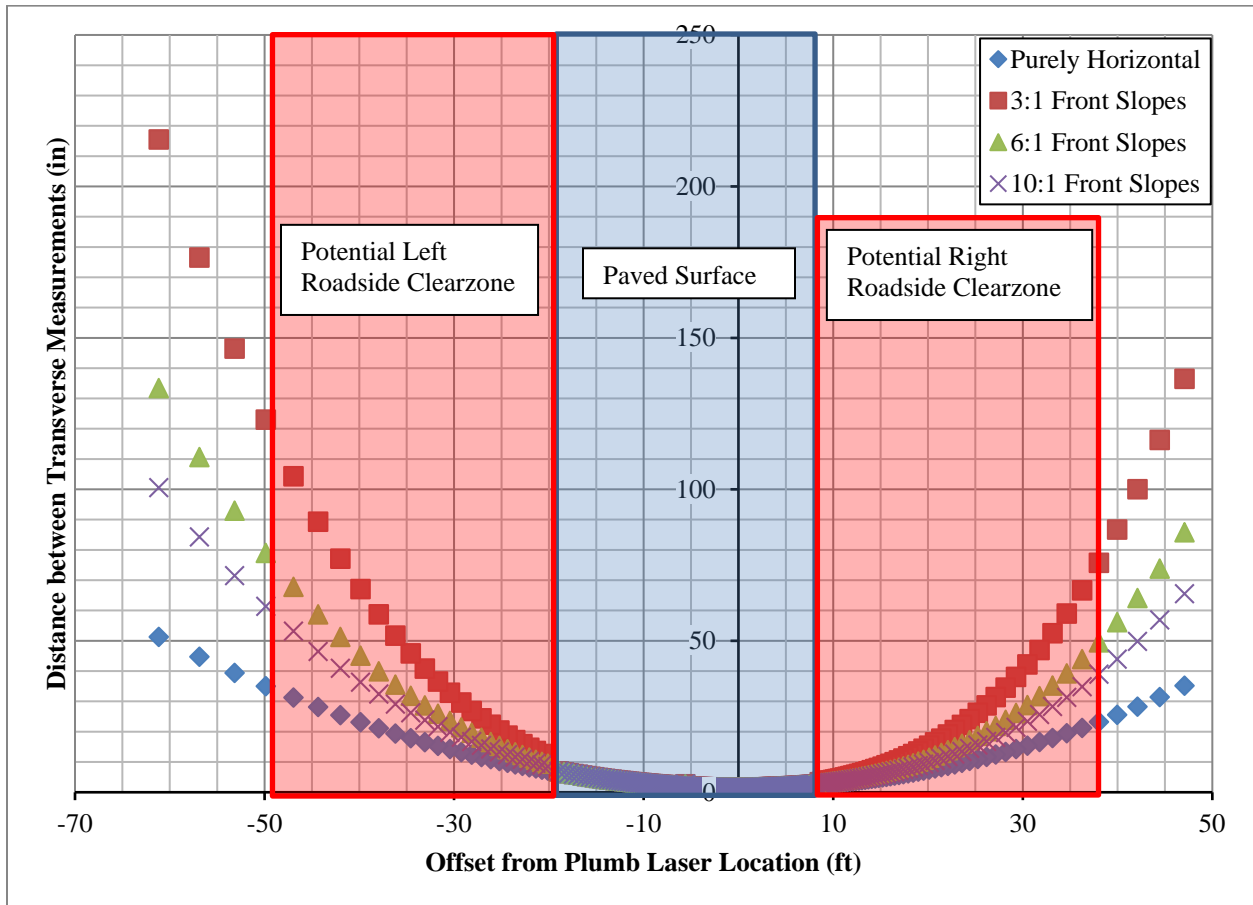
Figure 12. Transverse Spacing for a Two-Lane Roadway.

The grid size for pavements must be small enough so that no interpolation is required. For example, if the transverse spacing is 12 in., then the grid size should not be smaller than 12 in.[2] to avoid interpolation. The largest spacing between skew, longitudinal spacing, and transverse spacing dictates the grid size for pavements. For a paved-surface-only analysis, a 1-ft × 1-ft grid can be used on most sections with no interpolation between points. For wider geometric sections, it might be necessary to collect data for pavement analysis and for roadside analysis in different MLS runs. Grid size is a function of the following variables:

- Number of lanes.
- Data collection lane.
- Width of paved surface.
- Slope of the target surface.

Roadside geometry varies greatly depending on the topography of the site. Thus, the distance from the laser to the target surface requires a change in grid size. The clear zone concept often

dictates the horizontal offset area of concern. Because roadside geometry is not typical, knowledge of the potential clear zone widths can help define the appropriate roadside grid size. The clear zone is based off of the edge of the traveled way, not the EOP, and can be much smaller than 30 ft depending on posted speed and traffic volume. Because motorists do not directly interact with the roadside, interpolation between points can be allowed, so a 3-ft × 3-ft grid size is used for roadsides. At this grid size, along the right roadside of a rural roadway with a shoulder, no interpolation is required between the EOP and 15 ft away. If no shoulder exists, this distance increases to 24 ft. For a left roadside with a shoulder, interpolation begins approximately 8 ft from the EOP. If no shoulder exists, it begins 17 ft from the EOP. In summary, for typical rural two-lane facilities, one data collection run in either travel lane can be used for network-level analysis. A 1-ft × 1-ft grid size should be used for pavement analysis, and a 3-ft × 3-ft grid size should be used for roadside analysis. Table 11 provides the results of the analysis with transverse spacing shown at each EOP and near the middle of each lane. The data collection lane is indicated in red font.

Table 11. Various Pavement Type Configuration.

No. Thru Lanes	Potential Roadway Type	Paved Width (ft)	Lane Configuration	Data Collection Lane	Distance between Transverse Measurments at Specific Locations (inches)		
					LT Edge of Pavement	Middle of Lanes	RT Edge of Pavement
2	One roadbed of a divided hwy	38	4'/12'/12'/10' (Shld./2 Lanes/Shld.)	Outside Lane	7.75	3.70/1.50	4.60
4	Opposing traffic with no median or single direction multi-lane facility	56	4'/48'/4' (Shld./4 Lanes/Shld.)	Outside Lane	25.37	18.08/9.50/3.70/1.50	2.77
4	Opposing traffic with no median; 4 lane single direction multi-lane facility	56	4'/48'/4' (Shld./4 Lanes/Shld.)	Inside Lane	14.8	8.57/3.46/1.50/3.47	7.21
3	Super-2 or passing lane in a single direction; 3 lane single direction facility	50	10'/36'/4' (Shld./3 Lanes/Shld.)	Outside Lane	21.26	9.00/3.70/1.50	2.77
3	Super-2 or passing lane in a single direction; 3 lane single direction facility	50	10'/36'/4' (Shld./3 Lanes/Shld.)	Inside Lane	10.7	3.46/1.50/3.47	7.21
3	Super-2 or passing lane in a single direction; 3 lane single direction facility	50	10'/36'/4' (Shld./3 Lanes/Shld.)	Single lane direction	14.8	8.57/3.46/1.50	4.6
5	5 lane single direction facility; two-way traffic with a flush median or turn lane.	74	4'/60'/10' (Shld./5 Lanes/Shld.)	Middle Lane	18.59	10.62/3.70/1.50/3.47/9.32	28.51
5	5 lane single direction facility; two-way traffic with a flush median or turn lane.	74	4'/60'/10' (Shld./5 Lanes/Shld.)	Outside Lane	54.36	36.86/22.07/10.62/3.70/1.50	4.77
5	Crowned two-way traffic with flush median or turn lane	82	10'/24'/14'/24'/10' (Shld./2 Lanes/Turn Lane/2 Lanes/Shld)	Inside Lane	33.49	19.16/10.39/4.05/1.50/3.47	11.1

MOBILE LIDAR EQUIPMENT ACCURACY VALIDATION

Within this study, validation of the accuracy of mobile LiDAR readings occurred through a multistep approach. The raw accuracy of the laser and other MLS components were established by manufacturers and assumed to be valid. For this study, the accuracy of initially post-processed data to measure roadway and roadside surface geometric features was of primary concern. Sections of known geometry were used to validate the accuracy of MLS measurements from processed data. These sections and the accuracy use of each section include:

- Validation of the accuracy of length measurements. To accomplish this, a pavement run of known length located on Runway 35C at the Texas A&M University RELLIS campus was used. Length measurements on this facility are provided on 10-ft (3.05 m) increments.
- For cross-slope validation between the data collection vehicle wheel paths, 11 locations spaced 50 ft (15.24 m) apart along the known length section had cross-slopes measured using a 6-ft (1.83 m) straight edge and digital protractor.
- Cross-slope validation across an entire travel lane occurred on a 0.1-mile (161 m) section of New Main, located on Texas A&M University Campus, with cross-sections professionally surveyed on 10-ft increments.
- Validation of the paved surface continued by evaluating the cross-slope of the adjacent lane along New Main.
- Similar to New Main, a 0.1-mile (161 m) section of SH 30 was surveyed to establish cross-sections on 10-ft (3.05 m) increments. Figure 13 shows the various points professionally surveyed along SH 30. SH 30 cross-section data were used to analyze cross-slopes measured while collecting in opposite directions. For example, the cross-slope in the eastbound direction should be the same regardless if it was collected in the eastbound lane or the westbound lane.
- SH 30 data were also used to validate the accuracy of the roadside slopes while collecting in only one direction. The front slope can be measured using Points 2 and 3 and Points 9 and 10. Back slopes can be measured using Points 1 and 2 and 10 and 11.
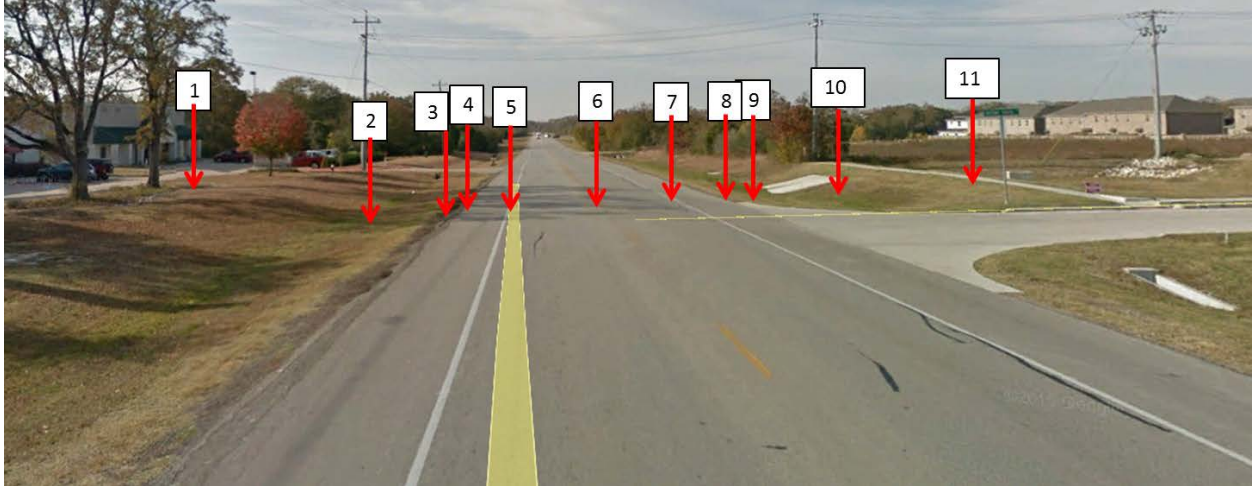
Figure 13. SH 30 Ground Truth Cross-Section.

- In addition to the professionally surveyed ground truth cross-sections, an inverted rut track located at the Texas A&M University RELLIS campus was used to evaluate the accuracy of mobile LiDAR for depth measurements.
- This same inverted rut track was used to analyze area calculations for drainage basins along the roadway. Figure 14 displays the inverted rut track containing steel plates 40-ft (12.2 m) long with 42 in. (1.07 m) between plates.

Figure 14. Rut Track Located at Texas A&M RELLIS Campus with Inverted Rut Plates of Known Dimensions.

Mobile LiDAR Length Analysis

A precisely measured test track of known length, stratified on 10-ft (3.05 m) increments exists at the Texas A&M University RELLIS campus. This track has a long history of use with inertial profiler certifications as specified in TxDOT's Standard Specifications. A piece of reflective tape was placed at 0 ft and another at 1640 ft (499.872 m). Mobile LiDAR data repeatedly measured this length to within 0.15 percent. Table 12 displays the results of the length analysis.

Table 12. Mobile LiDAR Measured Length Analysis.

Run Number	Field Measured Distance (ft)	Field Measured Distance (m)	LiDAR Measured Distance (ft)	LiDAR Measured Distance (m)	Difference (ft)	Difference (m)	% Difference
1			1639.15	499.61	0.85	0.259	0.05%
2			1638.15	499.31	1.85	0.564	0.11%
3	1640	499.872	1637.57	499.13	2.43	0.741	0.15%
4			1638.62	499.45	1.38	0.421	0.08%
5			1638.62	499.45	1.38	0.421	0.08%

Cross-Slope between Data Collection Vehicle Wheel Paths

A 6-ft (1.83 m) straight edge and digital protractor were used to precisely measure the cross-slope on 50-ft (15.24 m) increments along the same track used for the known length measurements. MLS data were processed into cross-sections of 6-in. (0.1524 m) spacing with transverse measurements within the cross-sections spaced 3 in. (0.0762 m) apart. MLS data were collected dynamically and processed into predefined grids, so accuracy analyses consider a window around the discretely measured point. A 2-ft (0.6096 m) window around the discretely measured locations was used to compare the accuracy of the MLS cross-slope. Table 13 shows these results. The top portion of Table 13 compares the field measurement with the average of the four cross-slopes generated by the MLS in the 2-ft (0.6096 m) window. The bottom portion of Table 13 compares the accuracy of the cross-section most similar to the field-measured location. In summary, a single cross-section within a small window around a discretely measured location will likely be within 0.05 percent and will at times identically match. If the average value is used, the accuracy between the MLS and the finite location is near 0.15 percent.

Table 13. Mobile LiDAR Cross-Slope Analysis.

| Location | Field Measured Cross-Slope (%) (1) | Mobile LiDAR Run 1 | | Mobile LiDAR Run 2 | | Mobile LiDAR Run 3 | |
		2-ft Average (%) (2)	Difference (1) – (2)	2-ft Average (%) (2)	Difference (1) – (2)	2-ft Average (%) (2)	Difference (1) – (2)
1 (0-ft)	1.75%	1.71%	0.04%	1.92%	-0.17%	2.18%	-0.43%
2 (50-ft)	2.09%	1.94%	0.15%	1.95%	0.14%	1.83%	0.26%
3 (100-ft)	2.27%	2.06%	0.21%	2.34%	-0.07%	2.00%	0.27%
4 (150-ft)	2.44%	2.62%	-0.18%	1.95%	0.49%	2.34%	0.10%
5 (200-ft)	2.44%	2.42%	0.02%	2.12%	0.32%	2.33%	0.11%
6 (250-ft)	2.27%	1.90%	0.37%	1.73%	0.54%	2.15%	0.12%
7 (300-ft)	2.09%	2.07%	0.02%	2.20%	-0.11%	2.14%	-0.05%
8 (350-ft)	2.27%	2.05%	0.22%	1.95%	0.32%	2.01%	0.26%
9 (400-ft)	1.92%	1.75%	0.17%	1.80%	0.12%	1.65%	0.27%
10 (450-ft)	2.44%	2.18%	0.26%	2.04%	0.40%	2.27%	0.17%
11 (500-ft)	2.27%	2.03%	0.24%	1.97%	0.30%	2.18%	0.09%
Location	Field Measured Cross-Slope (%) (1)	Mobile LiDAR Run 1		Mobile LiDAR Run 2		Mobile LiDAR Run 3	
		2-ft Average (%) (2)	Difference (1) – (2)	2-ft Average (%) (2)	Difference (1) – (2)	2-ft Average (%) (2)	Difference (1) – (2)
1 (0-ft)	1.75%	1.74%	0.01%	1.85%	-0.10%	1.82%	-0.07%
2 (50-ft)	2.09%	2.09%	0.00%	2.09%	0.00%	2.08%	0.01%
3 (100-ft)	2.27%	2.23%	0.04%	2.30%	-0.03%	2.10%	0.17%
4 (150-ft)	2.44%	2.52%	-0.08%	2.13%	0.31%	2.44%	0.00%
5 (200-ft)	2.44%	2.47%	-0.03%	2.43%	0.01%	2.46%	-0.02%
6 (250-ft)	2.27%	2.18%	0.09%	2.29%	-0.02%	2.25%	0.02%
7 (300-ft)	2.09%	1.99%	0.10%	2.18%	-0.09%	1.98%	0.11%
8 (350-ft)	2.27%	2.21%	0.06%	2.16%	0.11%	2.28%	-0.01%
9 (400-ft)	1.92%	1.89%	0.03%	1.90%	0.02%	1.99%	-0.07%
10 (450-ft)	2.44%	2.56%	-0.12%	2.22%	0.22%	2.43%	0.01%
11 (500-ft)	2.27%	2.34%	-0.07%	2.11%	0.16%	2.36%	-0.09%

Cross-Slope across Data Collection Lane

To expand the accuracy analysis of the MLS, the cross-slope measured and processed across the entire data collection lane was compared with professionally surveyed locations. The lane used for analysis was the outside inbound lane of New Main Dr., entering the Texas A&M University campus. This lane consists of both a travel lane and bicycle lane with concrete curb on the outside. Over approximately a 0.1-mi (161 m) section, professionally surveyed cross-sections were acquired on 10-ft (3.05 m) spacing. The cross-slope evaluated for accuracy began in the middle of the white lane striping to the left of the data collection vehicle and proceeded to the base of the curb at the outside edge. MLS data were processed into cross-sections spaced on 1-ft (0.3048 m) increments with 3-in. (0.0762 m) transverse spacing between points within a cross-section. Once again, because of the dynamic nature of MLS data collection and because the

precise location of the survey point is only as accurate as the survey equipment used, both a 1-ft (0.3048 m) longitudinal and transverse window are used for accuracy comparison. Three repeat runs and 39 cross-sections were used for comparison. The histogram in Figure 15 consolidates the 39 cross-sections from each of the three repeat runs. The population count in Figure 15 is 117 with 103 cross-sections, or 88 percent of cross-sections, within an accuracy of ±0.1 percent. Approximately 92 percent of all cross-slopes are within ±0.15 percent, and more than 95 percent of cross-sections are within ±0.2 percent.
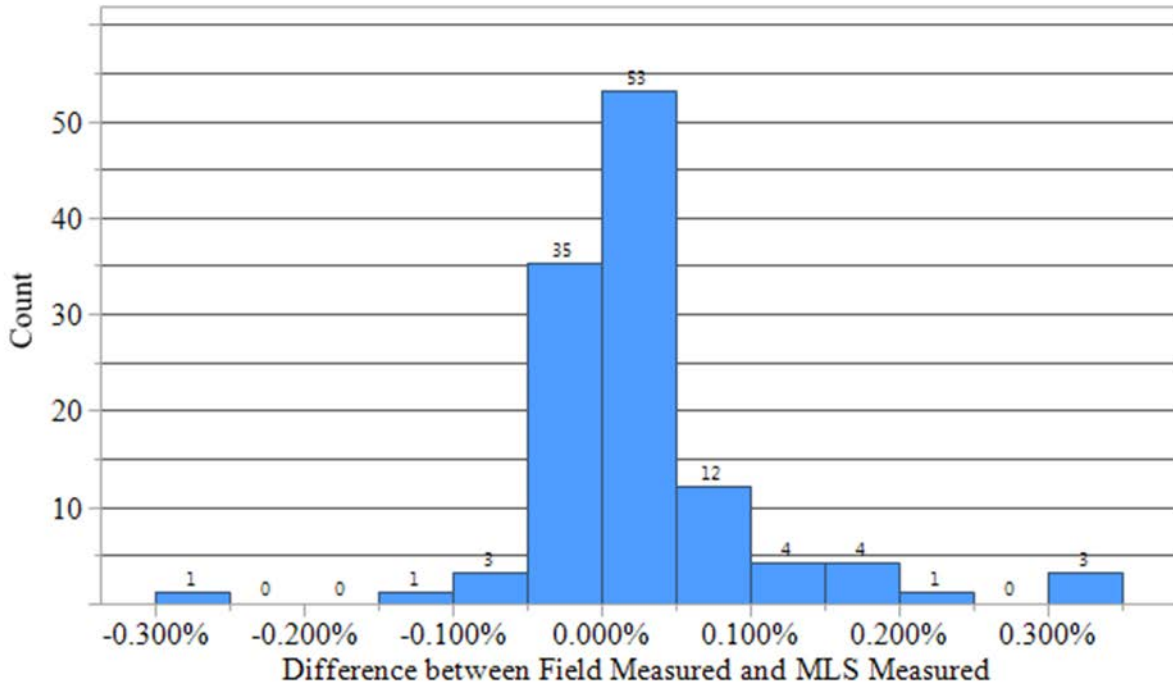
Figure 15. Histogram of Data Collection Lane Cross-Slope Accuracy.

The multiple runs associated with this accuracy analysis allows for a comparison of the repeatability of the cross-slope measurement. Figure 16 shows that 83 percent of cross-sections have cross-slope repeatability within 0.10 percent and 91 percent within 0.15 percent.
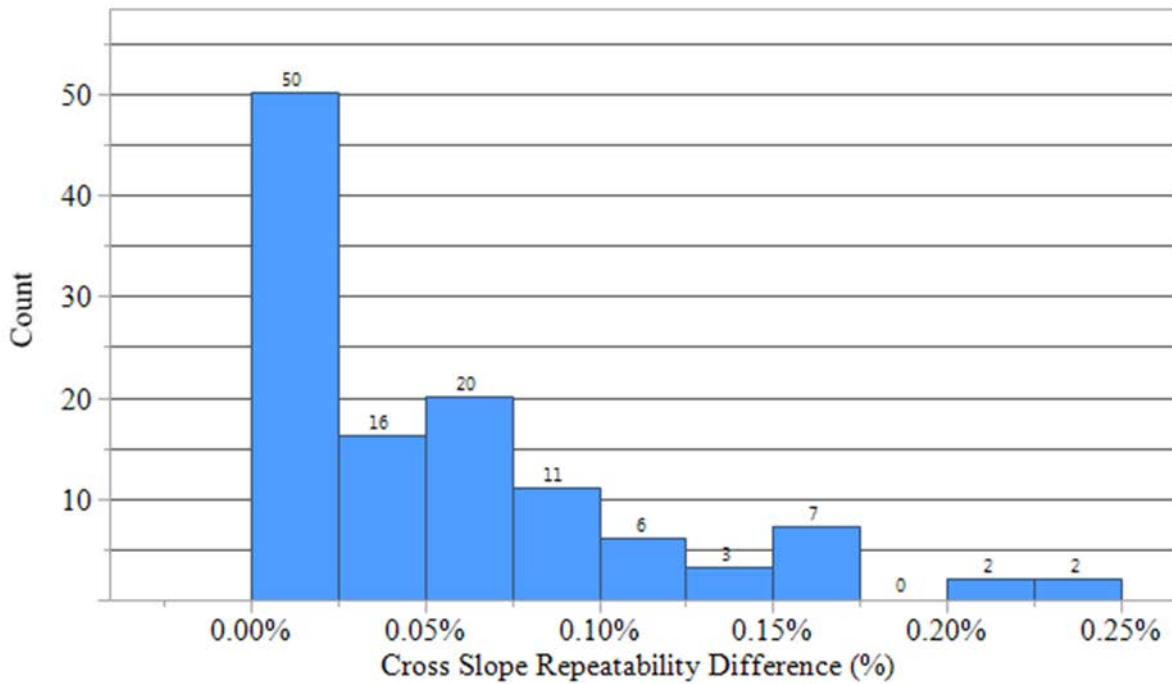
Figure 16. Histogram of Cross-Slope Repeatability between MLS Runs.

Adjacent Lane Cross-Slope

The expansion of the accuracy analysis includes the lane adjacent to the data collection lane. This analysis was also performed on New Main. Two processing methods were used to evaluate the accuracy of the processed data. The first method created 6-in. (0.1524 m) × 6-in. (0.1524 m) grids for processing, and the other method increased the size of the grid to 1-ft (0.3048 m) × 1-ft (0.3048 m) grids. For each method, a 2-ft (0.6096 m) window around the discretely surveyed location was used, and the LiDAR processed the cross-section most similar to the surveyed cross-section for accuracy comparison. Figure 17 displays the results of comparing 47 ground truth cross-sections with MLS-generated cross-sections using processed data on 6-in. (0.1524 m) × 6-in. (0.1524 m) grids. With this grid size, the cross-section within a 2-ft (0.3096 m) window of the surveyed cross-section that is most similar is very nearly identical to the surveyed cross-section. Increasing the grid size to 1 ft (0.3048 m) × 1 ft (0.3048 m) slightly increased the difference, as shown in Figure 18. Using 1-ft (0.3048 m) × 1-ft (0.3048 m) spacing, 70 percent of cross-sections were within 0.10 percent of the surveyed measurements, while 96 percent were within 0.20 percent of the surveyed measurements.
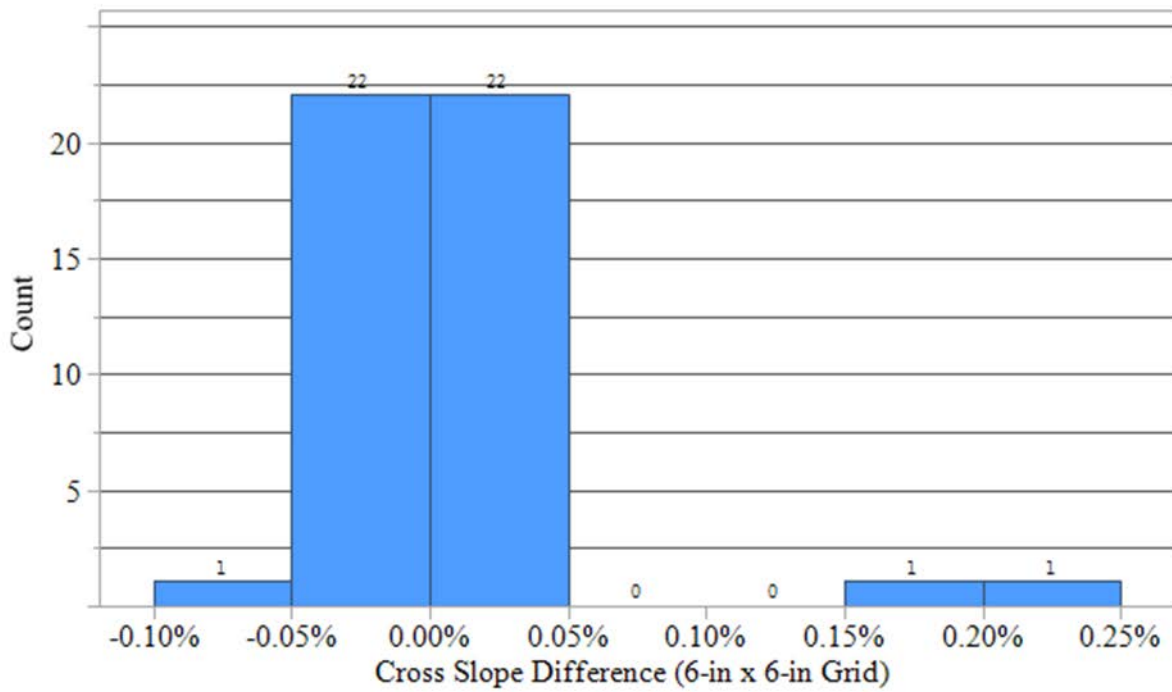
**Figure 17. Histogram of Adjacent Lane Cross-Slope Accuracy Comparison Using a 6-in. ×
6-in. Grid.**
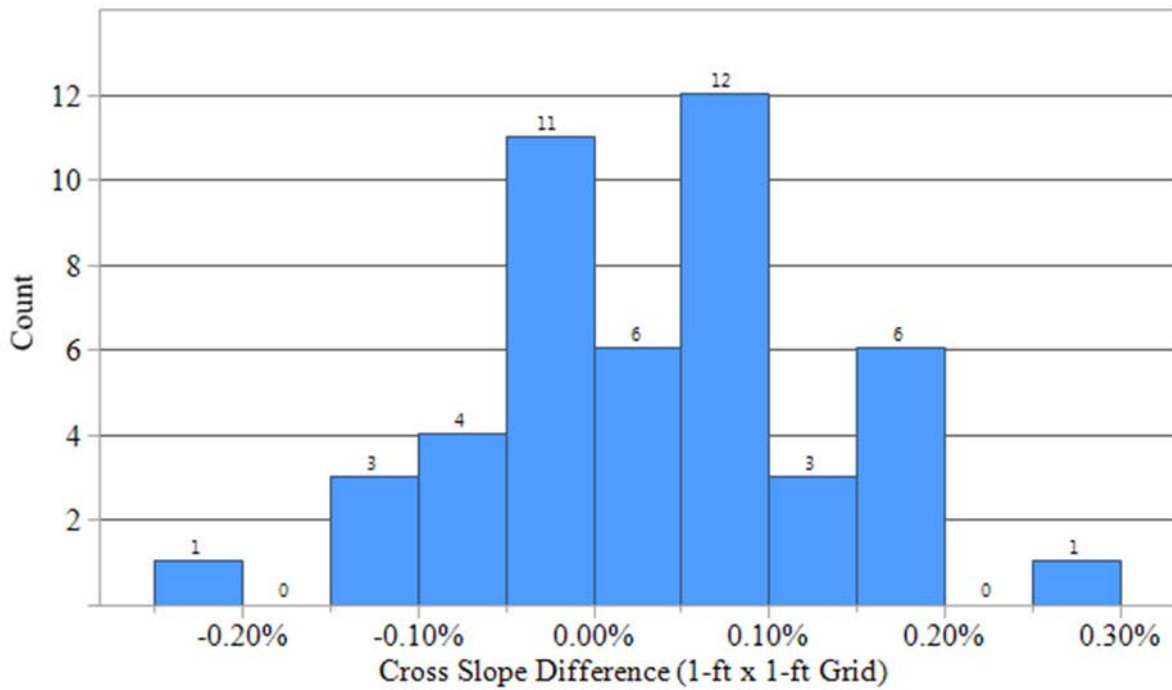
**Figure 18. Histogram of Adjacent Lane Cross-Slope Accuracy Comparison Using 1-ft × 1-ft
Grids.**

Repeatability of Measurements Collecting in Opposite Direction

LiDAR measurements in the lane adjacent to the data collection are often within 0.10 percent of the actual cross-slope using 1-ft (0.3048 m) × 1-ft (0.3048 m) grids. For this reason, the accuracy of a particular location measured traveling in one direction is compared with its accuracy while traveling in the other direction. In more practical terms, if a measurement occurs at STA 1+00, the cross-slope of the eastbound lane at this point should be the same regardless of whether or not the eastbound lane was the data collection lane or if the data were collected in the adjacent lane. This comparison was performed on 33 cross-sections generated on SH 30. MLS measurements occurred in both the eastbound and westbound directions. When the data collection lane was the eastbound lane, cross-sections processed in the data collection lane were compared with cross-sections at the same location processed from the adjacent lane when data collection occurred in the westbound lane. The same methodology was used for cross-sections generated for the westbound lane. Figure 19 shows that approximately 50 percent of the time the difference between a specific cross-slope when measured in the data collection lane as opposed to the adjacent lane is within 0.10 percent, and 73 percent of the time it is within 0.20 percent.
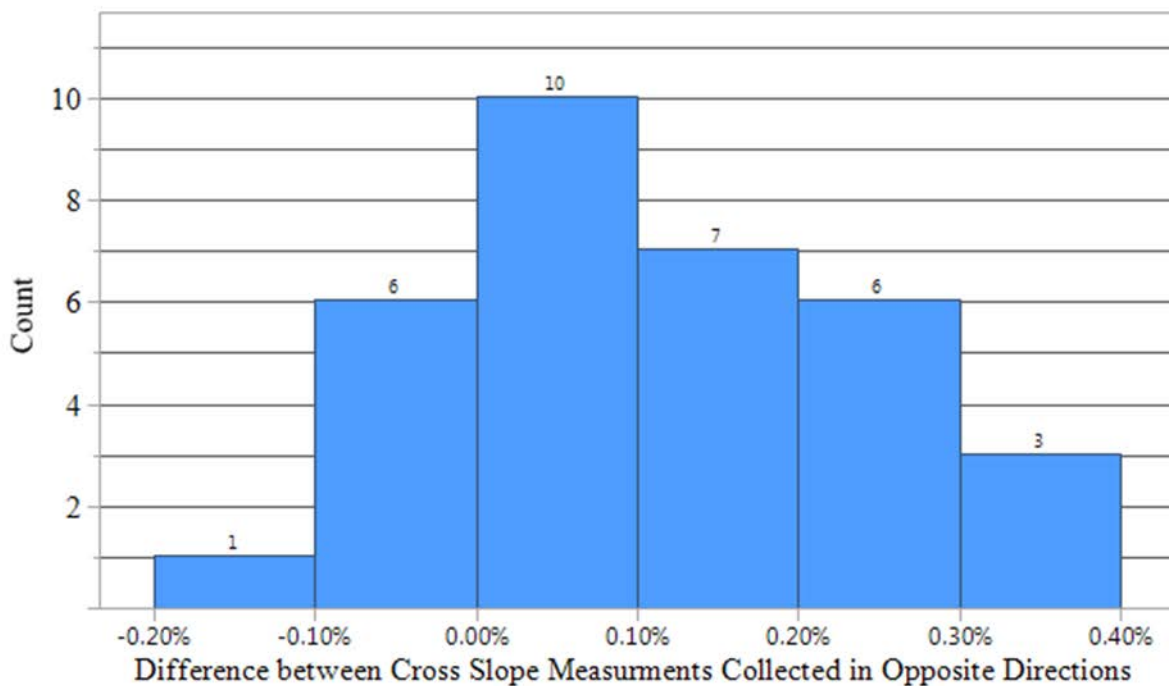
Figure 19. Cross-Slope Comparison with Data Collected in Opposite Direction.

Ditch Analysis

Data were collected on SH 30 in a single direction to compare actual roadside conditions with LiDAR processed measurements. Using a single data collection run in one direction, both the left and right roadsides were analyzed. Due to the increase in spacing as the target moves away from

the laser, a 3-ft (0.9144 m) × 3-ft (0.9144 m) grid is used to process the data on the roadsides. Along a 150-ft (45.72 m) longitudinal section of SH 30, 16 cross-sections are available on 10-ft (3.05 m) increments for right and left ditch analysis. Table 14 shows the comparison of the MLS generated ditch offset within the 3-ft (0.9144 m) × 3-ft (0.9144 m) grid to the surveyed offset. Along the right side of the roadway, adjacent to the data collection lane, all ditch offsets are within 3-ft (0.9144 m). Even though the laser has to travel farther to the target surface on the left side of the roadway, the accuracy remains within 3-ft. Data are not available for cross-sections 4 through 11 on the left side because a driveway exists in this location. Table 15 compares the ditch depth from the processed data with the survey data. In Table 15, it is clear that the surveyed ditch depth is deeper than that measured by the MLS. This is most likely because of the vegetation along the ROW. The laser returns to the source after striking a surface, so when it encounters grass, it returns a measurement without completely reaching the ground. The area along SH 30 was finish mowed during MLS collection. Figure 20 is a screenshot from the MLS software on the day of data collection, showing how tightly the ROW is mowed along with the driveway on the left side of the screen reference with the omitted data.

Table 14. Ditch Flowline Offset Accuracy Comparison.

Cross-Section No.	Right Side Ditch Flowline			Left Side Ditch Flowline		
	Surveyed Offset (ft)	MLS Processed Offset (ft)	Difference (ft)	Surveyed Offset (ft)	MLS Processed Offset (ft)	Difference (ft)
1	30.21	28.784	1.426	42.63	43.2126	-0.5826
2	30.05	28.784	1.266	41.57	40.2126	1.3574
3	30.1	28.784	1.316	40.43	40.2126	0.2174
4	29.98	28.784	1.196	49.9		
5	30.21	28.784	1.426	40.22		
6	29.99	28.784	1.206	50.22		
7	30.44	28.784	1.656	39.87		
8	30.38	28.784	1.596	49.65		
9	30.18	28.784	1.396	49.67		
10	30.75	28.784	1.966	50.43		
11	31.24	28.784	2.456	40.37	40.2126	0.1574
12	30.16	28.784	1.376	40.37	40.2126	0.1574
13	29.92	28.784	1.136	39.24	40.2126	-0.9726
14	30.07	28.784	1.286	38.56	40.2126	-1.6526
15	30.34	28.784	1.556	38.08	40.2126	-2.1326
16	30.71	28.784	1.926	38.29	40.2126	-1.9226

Table 15. Ditch Flowline Depth Comparison.

Cross-Section No.	Right Side Ditch Flowline			Left Side Ditch Flowline		
	Surveyed Depth (ft)	MLS Processed Depth (ft)	Difference (ft)	Surveyed Depth (ft)	MLS Processed Depth (ft)	Difference (ft)
1	2.19	2.09	0.10	2.77	2.45	0.32
2	2.20	1.99	0.21	2.78	2.57	0.21
3	2.19	1.97	0.22	2.83	2.54	0.29
4	2.14	1.89	0.25			
5	2.04	1.94	0.10			
6	2.09	1.94	0.15	0.66		
7	2.04	1.92	0.12	0.65		
8	2.08	1.93	0.15	0.62		
9	2.08	1.95	0.13	0.55		
10	2.13	1.95	0.18	0.61		
11	1.87	1.85	0.02	2.28	1.89	0.39
12	2.04	2.00	0.04	2.07	1.88	0.19
13	2.15	2.07	0.08	1.86	1.62	0.24
14	2.12	2.04	0.08	1.84	1.60	0.24
15	2.12	1.96	0.16	1.96	1.65	0.31
16	2.02	1.92	0.10	2.09	1.72	0.37

Figure 20. SH 30 on the Day of MLS Data Collection.

Along the right roadside, a finish mowed surface creates a ditch or roadside surface between 1 and 3 in. higher than the actual ground surface. Vegetation also affects the measured slopes of the roadside. For rural areas, vegetation is expected to be higher. Ideally, data collection should occur immediately following the TxDOT mowing cycle. Under Item 730 in TxDOT's Standard Specifications, roadside mowers should be set to between 5-in. and 7-in. *(45)*.

Roadside Slope(s) Analysis

Using 3-ft (0.9144 m) × 3-ft (0.9144 m) grids, the LiDAR processed roadside slopes were compared against ground truth surveyed slopes. Along SH 30, 26 cross-sections were used for the analysis. Data were collected in a single direction, but both the left and right roadsides were processed for comparison. Entering this analysis, it was expected that the accuracy of the left side would be lower than the right side because the laser travels farther to reach left roadside slopes. Figure 21 shows the absolute value of the difference between the MLS-processed right front and back slopes compared with survey-measured values. Figure 22 shows the same information using the same scaling for the left roadside. For both the right front and back slope, 26 cross-sections were used for analysis, but on the left side only 18 cross-sections were used for the front slope and 16 for the back slope. The availability of more sections on the right side (i.e., the side adjacent to the data collection vehicle) indicates cleaner data. In this case, cleanliness of data speaks to the ability of the laser to reach the target surface. This ability becomes more difficult on the left side because the laser must cross opposing traffic, or the laser encounters an obstruction rather than reaching the target surface. Encountering an obstruction can take place on the right side as well, but it can be easier to deal with in post-processing because multiple points can be available near the obstruction since the laser is closer to its source. On the left side, spacing between laser readings can be far enough apart that the reading on the obstruction is the only value to use in post-processing.
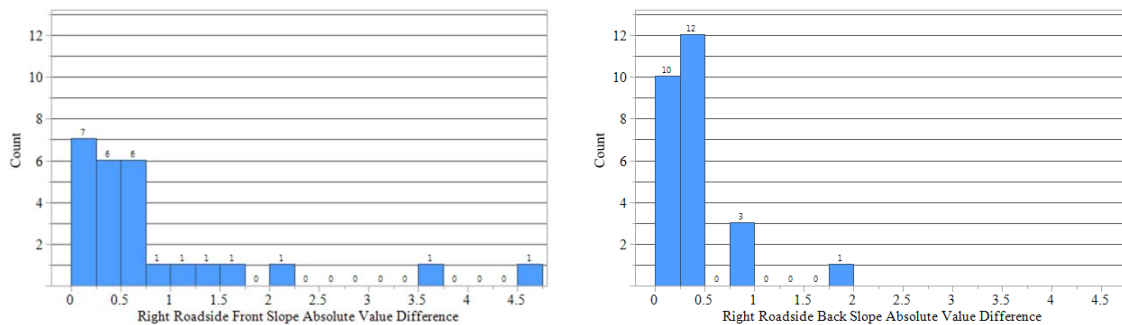
Figure 21. Right Roadside Slope Comparison.
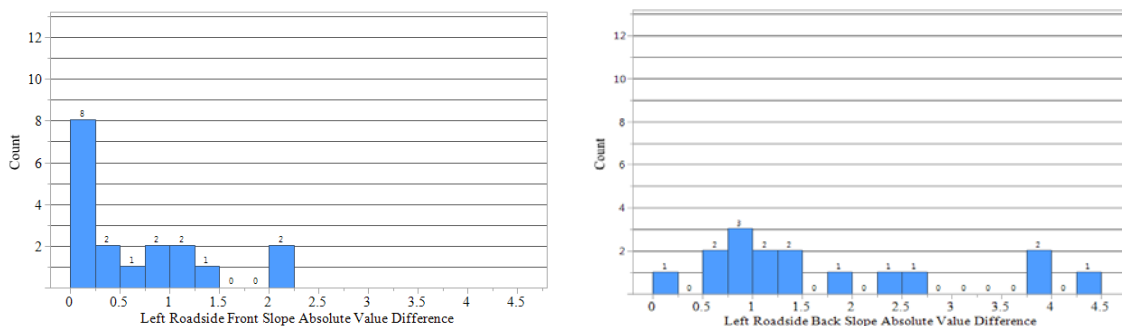
Figure 22. Left Roadside Slope Comparison.

Figure 21 shows that the difference between the survey-measured front slope and MLS-processed front slope is typically less than 0.75. For the back slope, values are typically within 0.5, more accurate than the front slope. Initially, this appears counterintuitive because the back slope is farther from the laser source than the front slope. However, front slope surfaces, by definition, are moving away from the laser source. Essentially, the laser chases the front slope downward to reach the surface. The back slope, however, moves upward and more easily back into the laser trajectory. For this reason, when the back slope is not significantly far from the laser source, it has the potential to be more accurate than the front slope. Moving to the left side of the roadway, the front slope is accurate on almost half of its readings to within 0.25. The accuracy of the left roadside back slope is much more variable as the laser begins to exceed 75 ft (22.86 m) from source to target surface. Table 16 shows the average, median, and standard deviation for the histograms referenced in Figure 21 and Figure 22. Analysis of the median value helps minimize the effect of outliers and shows that the right roadside accuracy, regardless of front or back slope, is within 0.5. More often than not, the MLS-processed front slope is flatter than the surveyed front slope. This result is expected since vegetation in the ditch flowline raises the elevation of the target surface. When using the pavement as the tie-point, the flatter slope is generated with a raised flowline. Table 17 shows the direct comparison for 16 cross-sections on the right roadside along SH 30. A larger number associated with the horizontal measurement indicates a flatter slope. In every instance in Table 17, the MLS-processed slope is flatter than the surveyed slope.

Table 16. Roadside Difference Statistics.

Roadside Attribute	Number of Cross-Sections	Mean	Median	Standard Deviation
Right Front Slope	26	0.835	0.481	1.101
Right Back Slope	26	0.394	0.331	0.379
Left Front Slope	18	0.698	0.439	0.707
Left Back Slope	16	1.729	1.297	1.277

Table 17. Direct Right Roadside Slope Comparison.

Cross-Section Number	Surveyed Front Slope	MLS-Processed Front Slope	Surveyed Back Slope	MLS-Processed Back Slope
1	7.53(H):1(V)	7.59(H):1(V)	8.80(H):1(V)	8.51(H):1(V)
2	7.46(H):1(V)	8.04(H):1(V)	8.38(H):1(V)	8.27(H):1(V)
3	8.18(H):1(V)	7.97(H):1(V)	7.90(H):1(V)	7.68(H):1(V)
4	7.59(H):1(V)	8.47(H):1(V)	7.76(H):1(V)	7.68(H):1(V)
5	8.18(H):1(V)	8.49(H):1(V)	7.67(H):1(V)	7.36(H):1(V)
6	8.04(H):1(V)	8.60(H):1(V)	7.29(H):1(V)	6.88(H):1(V)
7	8.77(H):1(V)	9.11(H):1(V)	7.01(H):1(V)	6.94(H):1(V)
8	8.48(H):1(V)	8.91(H):1(V)	6.75(H):1(V)	6.59(H):1(V)
9	8.44(H):1(V)	8.86(H):1(V)	6.74(H):1(V)	6.80(H):1(V)
10	8.40(H):1(V)	8.94(H):1(V)	6.44(H):1(V)	6.73(H):1(V)
11	10.23(H):1(V)	10.22(H):1(V)	6.86(H):1(V)	7.73(H):1(V)
12	8.72(H):1(V)	9.02(H):1(V)	6.73(H):1(V)	7.15(H):1(V)
13	7.77(H):1(V)	8.27(H):1(V)	6.55(H):1(V)	6.93(H):1(V)
14	8.41(H):1(V)	8.58(H):1(V)	6.43(H):1(V)	6.86(H):1(V)
15	8.05(H):1(V)	8.61(H):1(V)	6.26(H):1(V)	6.65(H):1(V)
16	8.41(H):1(V)	8.46(H):1(V)	6.24(H):1(V)	6.68(H):1(V)

Rut Depth Measurements

By using the inverted rut track located at the Texas A&M University RELLIS campus, the ability of the MLS device to measure rut depth was analyzed. Using 3-in. (7.62 cm), 1-in. (2.54 cm), 0.5-in. (1.27 cm), and 0.25-in. (0.635 cm) inverted rut plates of approximately 40 ft (12.19 m), three MLS measurements along each plate were compared with the known height. Figure 23 displays the reflection data and cross-section for the 1-in. (2.54 cm) rut plates. The rut plates are easily visible in the cross-section view. Table 18 shows the MLS measurements of the rut plates. To develop the measurements in Table 18, 3-in. (7.62 cm) transverse spacing was used in processing. Each measurement dot in Figure 23 is spaced 3-in. (7.62 cm) apart.
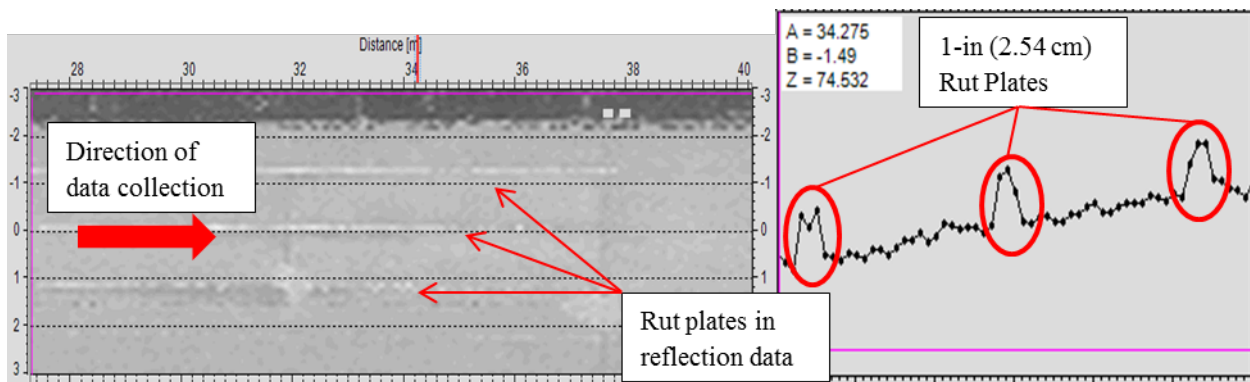
Figure 23. 1-in. (2.54 cm) Rut Plate Display.

Table 18. MLS Rut Height Measurement Comparison.

3-in. (7.62 cm) Rut Plate Measurements					
	MLS Measurements (in.)			Difference (in.) (Actual – MLS)		
Location No.	Left Plate	Middle Plate	Right Plate	Left Plate	Middle Plate	Right Plate
1	3.11	2.91	3.15	−0.11	0.09	−0.15
2	2.95	2.83	3.07	0.05	0.17	−0.07
3	2.95	3.07	2.87	0.05	−0.07	0.13
1-in. (2.54 cm) Rut Plate Measurements					
	MLS Measurements (in.)			Difference (in.) (Actual – MLS)		
Location No.	Left Plate	Middle Plate	Right Plate	Left Plate	Middle Plate	Right Plate
1	0.98	0.98	1.02	0.02	0.02	−0.02
2	0.94	1.02	1.18	0.06	−0.02	−0.18
3	0.87	0.98	1.06	0.13	0.02	−0.06
0.5-in. (1.27 cm) Rut Plate Measurements					
	MLS Measurements (in.)			Difference (in.) (Actual – MLS)		
Location No.	Left Plate	Middle Plate	Right Plate	Left Plate	Middle Plate	Right Plate
1	0.55	0.51	0.79	−0.05	−0.01	−0.29
2	0.67	0.47	0.63	−0.17	0.03	−0.13
3	0.59	0.51	0.47	−0.09	−0.01	0.03
0.25-in. (0.635 cm) Rut Plate Measurements					
	MLS Measurements (in.)			Difference (in.) (Actual – MLS)		
Location No.	Left Plate	Middle Plate	Right Plate	Left Plate	Middle Plate	Right Plate
1	0.20	0.24	0.20	0.05	0.01	0.05
2	0.12	0.20	0.28	0.13	0.05	−0.03
3	0.16	0.20	0.31	0.09	0.05	−0.06

MLS-Processed Area Delineation

The inverted rut track was also used to validate the MLS's ability to capture areas along a pavement surface. The need to delineate an area on a pavement surface ties into the need to identify drainage areas for various hydraulic analyses. The inverted rut track provides easily discernable areas, with the rut plates serving as dividing lines. Area accuracy was analyzed by directly driving over the rut track and by driving adjacent to the rut track. This methodology is similar to the methodology used to evaluate cross-slope in both the data collection lane and adjacent lane. The goal is to determine the accuracy for both lanes and develop an understanding of the confidence in the data as the target surface moves away from the laser source. TopoToolbox in Matlab was used outside of the MLS post-processing software to assist in the identification of areas *(25)*. Figure 24 displays the TopoToolbox output for the 1-in. (2.54 cm) rut track section. The x-axis in Figure 24 represents the horizontal distance from the laser source. The middle inverted track coincides with the zero horizontal offset. All dimensions in Figure 24 are in SI units. The y-axis represents the longitudinal distance or direction of travel for the data

collection vehicle. The z-axis represents the elevation, ranging approximately 14 in. (0.35 m) for the plot. The three rut plates are easily identifiable in Figure 24. Grass growth creates the elevation spike on the right side at the end of the rut track. The screenshot in Figure 25 displays this elevation.
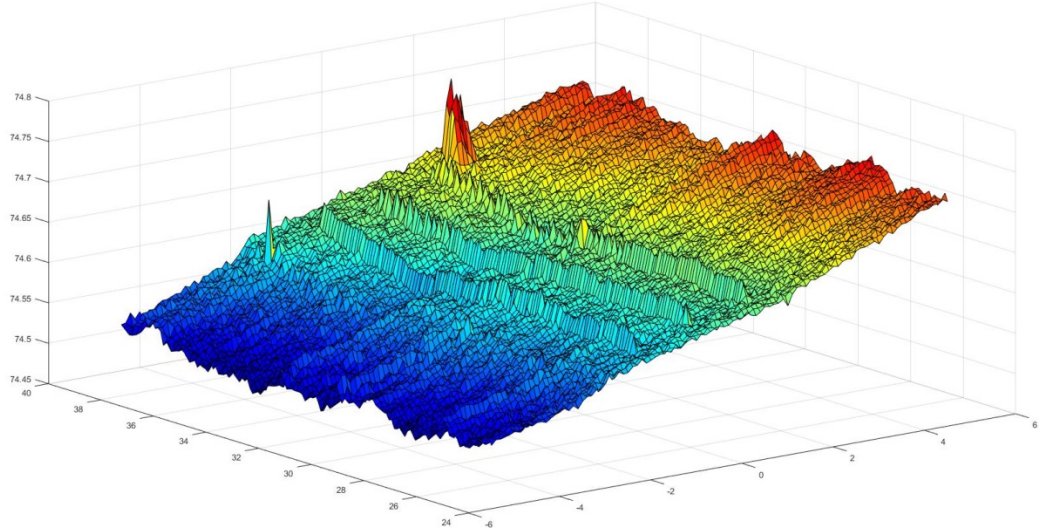
Figure 24. 1-in. (2.54 cm) Rut Track Area Delineation Display.

Figure 25. Screenshot of 1-in. (2.54 cm) Rut Track Area.

Further processing of the data using 1-ft (3.05 m) × 1-ft (3.05 m) grids also delineated the areas on the pavement when processing the data collected directly over the rut tracks and to the side of

the rut tracks. Figure 26 displays the 1-in. (2.54 cm) rut plates generated from the gridded data collected directly over the plates, while Figure 27 displays the same area but in the opposite direction as if collecting from the adjacent travel lane.
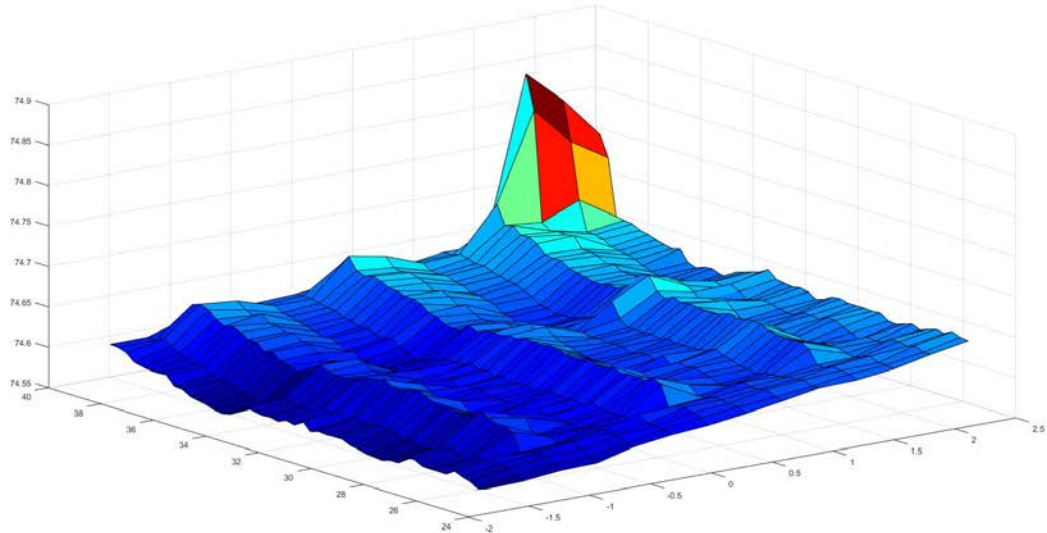
Figure 26. Pavement Area Delineation Using 1-ft × 1-ft Grids and Direct Data Collection.
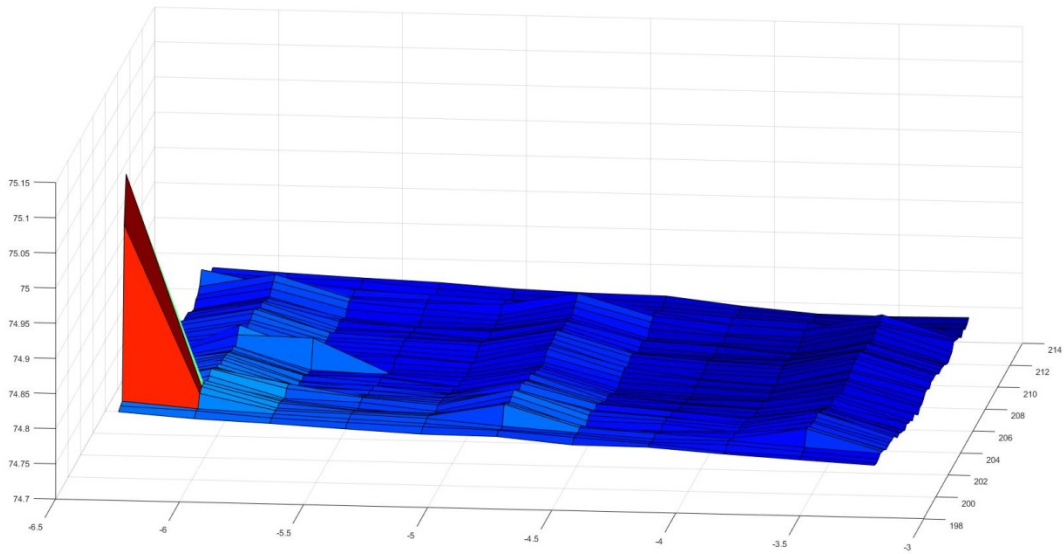
Figure 27. Pavement Area Delineation Using 1-ft × 1-ft Grids and Adjacent Data Collection.

MLS Accuracy Summary

The MLS used in this study accurately measures length and provides post-processed length data to within 0.15 percent of the actual length and often provides length measurements to within 0.10 percent of the actual length. The dynamic nature of MLS data collection implies that in length measurements, as with any other piece of MLS data, there will be a processing decision made that will deviate from actual conditions. Regardless of this, the MLS in this study provided a high degree of accuracy as it relates to length measurements.

The MLS accuracy of the cross-slope in the data collection lane is typically between 0.05 percent and 0.10 percent. Cross-slope accuracy in lanes adjacent to the data collection lane remains near the accuracy seen in the data collection lane. As data processing moves into a gridded analysis, some accuracy can be lost. This accuracy loss is marginal; 1-ft (0.305 m) × 1-ft (0.305 m) gridded data yielded an adjacent lane cross-slope accuracy of within 0.20 percent and often remained within 0.10 percent. Cross-slope repeatability also performed well in accuracy, and the ability of the MLS to measure the same cross-slope when collecting from different was accurate to within 0.20 percent.

Ditch offsets can be identified almost 100 percent of the time. When using 3-ft (0.9144 m) × 3-ft (0.9144 m) gridded data, the comparison between MLS-processed ditch offsets and actual measured offsets resulted in MLS offsets always falling within a 3-ft (0.9144 m) window on both the right and left roadside. Ditch depths are also accurately measured, but roadside vegetation will indicate a shallower ditch than actually exists. Roadside vegetation also results in roadside slopes that are flatter in MLS data than in reality. Although the roadside slopes are slightly flatter, they are often within 0.5H:1V accuracy along the right roadside. The left roadside is more variable, and if a detailed evaluation of both roadsides is required, it is recommended that data are collected in both directions.

The MLS used in this study measured rut depth to within 0.10-in. (0.254 cm) and often measured rut depth to within 0.05-in. (0.127 cm). The MLS, aided by post-processing tools, can identify and delineate various areas along the pavement surface.

DEVELOPMENT OF SURFACE DRAINAGE RATING

Based on the results from the accuracy analysis, LiDAR data within the data collection lane and lanes adjacent to the data collection are processed into 1-ft × 1-ft grids. This grid spacing avoids any interpolation between data points and provides multiple points within the grid from which to choose. Because water always flows downhill, researchers use the minimum elevation from each grid for analysis. For the roadside analysis, 3-ft × 3-ft grids are used. When the data collection lane is adjacent to the right roadside, little to no interpolation is required between data points. For the left roadside, the distance from the laser will cause gaps in the data where interpolation is required to generate output. As will be shown later in the report, researchers decided to apply the rating only to the roadside adjacent to the data collection lane.

The nature of mobile LiDAR leads to the creation of large data sets complete with measurements from the laser source to the target surface and the reflectivity of the target surface. Off-the-shelf post-processing software readily converts straight-line distances into x, y, and z data sets. The x, y, and z data sets consist of longitudinal location in the direction of travel, horizontal offset from the laser source, and elevation of the target surface. While the mobile LiDAR unit is equipped with a high-end GPS, the accuracy remains approximately ±1 m (±3 ft). For this reason, measurements and analysis are conducted in relative terms. The location established at the beginning of data collection serves as an initiation point and all measurements remain relative to the coordinates used upon initiation. Therefore, asset measurements used to develop ratings and provide information are accurate, but the ability to transfer these measurements to a precise point in space has equipment-based limitations. For example, a measured ditch depth of 2 ft is an accurate measurement, but the actual real-world elevation of the flowline at 585 ft above sea level is only accurate to within ±3 ft. Because relative measurements can be used to analyze roadway features, GPS limitations have no impact on the network-level application within this project.

Surface geometry within the ROW line consists of a number of elements (or assets) that have a safety and drainage nature. This paradox requires a balancing act during design, where drainage efficacy must often be sacrificed to create a geometrically safe cross-section. For example, along a tangent portion of roadway, a 6 percent cross-slope would efficiently move the water off of the travel lane quickly, but a cross-slope with this steepness presents a number of safety-related issues. The same is true along the roadside. Steep front slopes are hydraulically desirable, but front slopes steeper than 3H:1V are unacceptable unless protected. With the ability to measure surfaces, mobile LiDAR provides a tool to analyze a section's design compliance and evaluate drainage performance. Because design compliance must be considered for geometric features, an effective section from a drainage perspective might receive a rating deduction because of design incompliance. For example, a front slope of 2H:1V might provide reasonable drainage, but because it violates design standards, the section will receive a lower rating.

While mobile LiDAR can provide measurements in both directions of travel, ratings were developed only for the direction of travel. This ensures accuracy for roadside ratings with little to no interpolation required between LiDAR measurements and provides the most precise measurement of surface drainage basins along the traveled way. Additionally, rating in a single direction provides a consistent approach to rate the same direction year after year to begin to generate temporal data associated with surface drainage ratings. Researchers used data collected with mobile LiDAR to rate:

- Traveled way width.
- Travel lane cross-slope.
- Hydroplaning potential.
- Front slope steepness.
- Ditch depth.
- Ditch flowline steepness.

Additionally, the rating provides a horizontal alignment descriptor for the roadway and determines if the roadway surface section is in shape. The roadside in the direction of travel is also provided a descriptor based on the majority of the geometry along the roadside. When the section contains more than 50 percent ditch, the roadside is described as primarily ditch, but if the section consists primarily of a front slope, the descriptor captures this instead. Each of these elements is discussed in more detail below.

TRAVELED WAY WIDTH

The traveled way along a roadway consists of a lane and shoulder. The traveled way width is the only element measured not using gridded data. Within this study, mobile LiDAR reflectivity data were used to determine the location of pavement striping and the interface between pavement and roadside vegetation. Researchers use this interface to perform specific analysis of either the roadway or roadside. The reflectivity data generated by the mobile LiDAR unit are stored in a table that includes the straight-line distance to the target surface. This table is unprocessed in the sense that the data have not been placed in a grid. Each string of data generated by the mobile LiDAR unit is available within this table. Each reflectivity and measurement relate to an angle, referred to as α throughout the report. The α angle represents the angle in relation to the horizon projected to the right of the data collection vehicle. Predetermined α-based search windows are included in the algorithm to find changes in the reflectivity data that would indicate a material surface change. The pseudocode, located in the Appendix, provides the rules used in the algorithms. The pseudocode for locating the right edge stripe is listed below:

- Evaluate each transverse string of data within the data collection section.
- For $25° \leq \alpha \leq 75°$:

- o If $225 \le R \le 254$ output α, distance, and "Stripe Found" for the transverse string being analyzed:
  - Elseif R is never between 225 and 254, output "No Stripe."
- o If "Stripe Found" frequency < 35 percent of all transverse strings, output "No Stripe in this Section."
- o If "Stripe Found" frequency ≥ 35 percent:
  - Find five most common α values ($α_{XS}$, $α_S$, $α_M$, $α_L$, $α_{XL}$):
    - If $α_{XL} - α_{XS} \le 9.5°$ (increased to five most common and 9.5° to account for up to 2 ft wander in the striping):
      - o And Σ $α_{XS}$, $α_S$, $α_M$, $α_L$, $α_{XL}$ ≥ 35 percent of "Stripe Found" count, calculate the associated average α and distance. Use the average values to calculate an offset to the right edge stripe, X_{RS}.
      - o X_{RS} is calculated using the following geometry:
        - If $α < 90°$, $X_{RS} = Distance*sin(90°-α)$.
        - For the right side, α will always be less than 90°.
      - o Output, "Right Edge Stripe at X_{RS} distance."
  - Elseif, "Stripe Found" frequency ≥ 35 percent, but the other conditions are not met, output "Error."

Researchers developed the lane width rating using TxDOT's Roadway Design manual. Design lane widths are based on daily traffic, roadway functional classification, and the extent of the planned project. 4R design requirements are the most robust and include new location and reconstruction projects. The lane widths within 4R requirements are further delineated based on functional class, daily traffic, and posted speed. 3R projects include rehabilitation and require less extensive design elements.

While 4R design standards represent the ideal, 3R standards provide guidance on what is acceptable for the existing system. For rating purposes, the ideal represents a perfect score, and the acceptable represents a passing score. For traveled lane width, a section receives a perfect rating if it complies with 4R collector requirements at 60 mph. The section receives a 30 percent deduction if it complies with 3R requirements. Further graduated deductions are made to transition the rating curves to zero for different traffic levels. Table 19 shows the derived deductions from the design guidelines, followed by the graphical presentation of the rating curves for a rural roadway in Figure 28.

Table 19. Rural Roadway Lane Width Rating.

Rating	< 400 ADT			400 –1500 ADT			> 1500 ADT		
	Lane Width (ft)	Shld. Width (ft)	Tot. Width (ft)	Lane Width (ft)	Shld. Width (ft)	Tot. Width (ft)	Lane Width (ft)	Shld. Width (ft)	Tot. Width (ft)
1.0	11	2	13	11	4	15	12	8	20
0.7	10	0	10	11	1	12	11	3	14
0.5	9.5	0	9.5	10	0	10	11	1	12
0.0	9	0	9	9.5	0	9.5	10	0	10
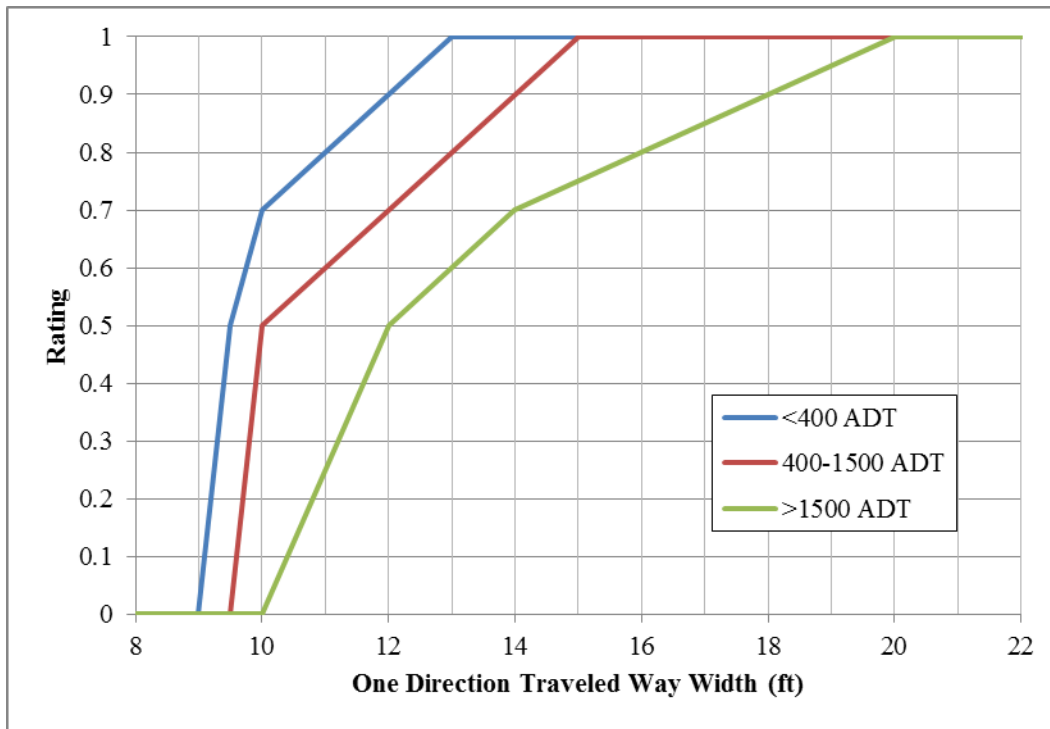
Figure 28. Rural Roadway Deduction Curves for Traveled Way Width.

TRAVEL LANE CROSS-SLOPE

The cross-slope along the roadway changes as tangent sections transition into horizontal curves. The inclusion of an inertial measurement unit (IMU) in the mobile LiDAR package provides a piece of equipment that maintains an accurate measurement of the vehicle heading. Chunking the data into 0.1-mile increments allows researchers to evaluate the vehicle azimuth at the beginning and ending of the section to determine the presence of horizontal curves. Researchers used Table 2-4 within TxDOT's Roadway Design manual to determine the potential change in azimuth bearing when superelevation becomes required. Table 2-4 provides the minimum curve radius to maintain a 2 percent crown. Figure 29 displays horizontal curve geometry and a horizontal curve equation. Using a known length of 528 ft for L and minimum radius to maintain a crown at a

given speed, the allowable azimuth difference, I, is calculated. Speeds and minimum radii are shown in Table 20, along with calculated azimuth difference within the data collection section.

$$L = 2\pi R \left(\frac{I}{360°}\right)$$

WHERE:
L = LENGTH OF CURVE ALONG ARC
R = CURVE RADIUS
I = DIFFERENCE BETWEEN AZ_{PC} AND AZ_{PT}
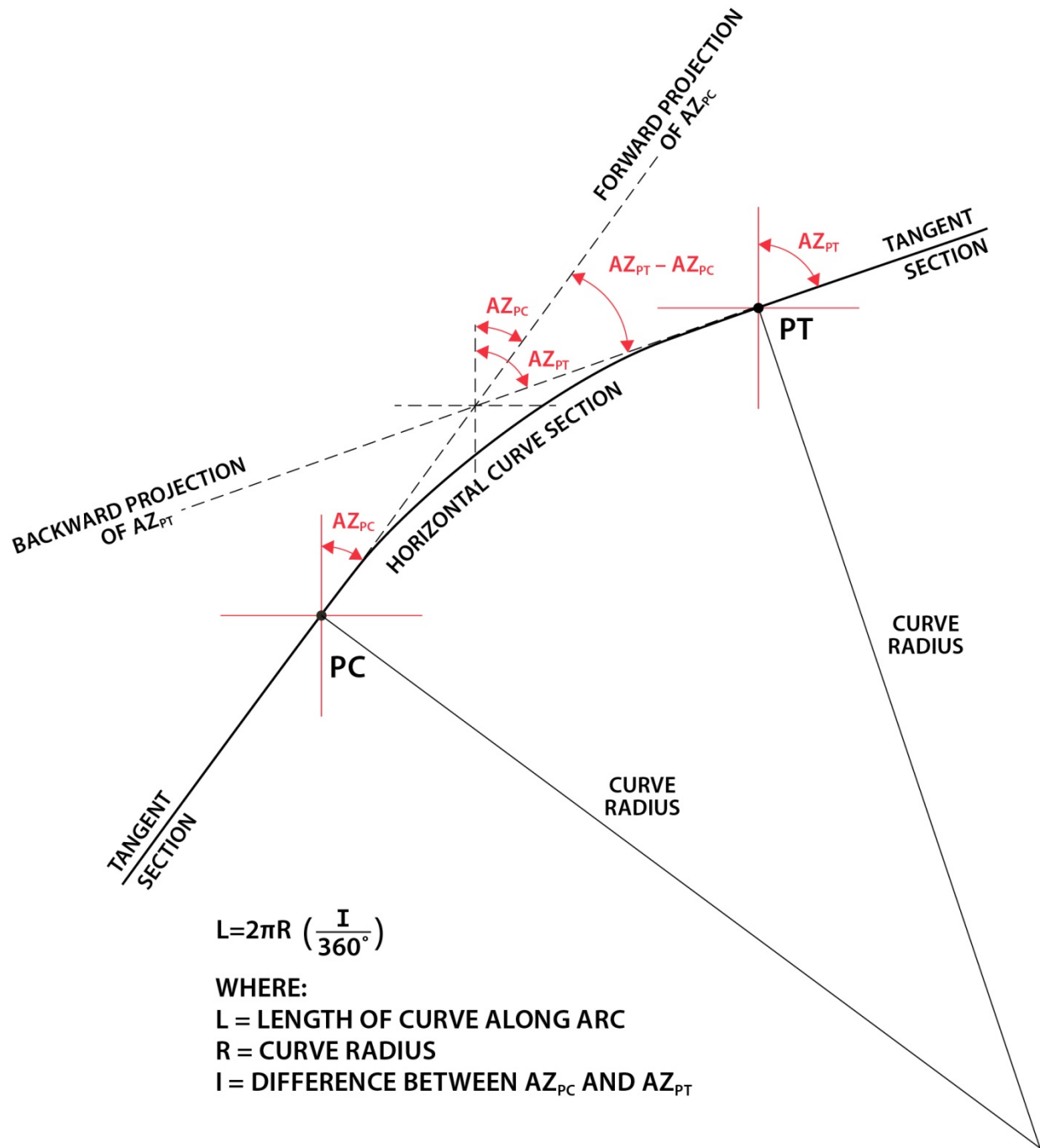
Figure 29. Horizontal Curve Geometry.

Table 20. Azimuth Difference within 0.1-mi Data Collection Section.

Design Speed	6% Superelevation		8% Superelevation	
	Min. Radius (ft)	Azimuth Δ in 528 ft	Min. Radius (ft)	Azimuth Δ in 528 ft
45	6,480	4.67	6,710	4.51
50	7,870	3.84	8,150	3.71
55	9,410	3.21	9,720	3.11
60	11,100	2.73	11,500	2.63
65	12,600	2.40	12,900	2.35
70	14,100	2.15	14,500	2.09
75	15,700	1.93	16,100	1.88
80	17,400	1.74	17,800	1.70

Using the IMU azimuth information, researchers classify a data collection section as either tangent, right curve, or left curve. However, just because the bearing of the roadway indicates a particular geometrical behavior, the cross-sections within the data collection section do not always adhere to the expected behavior. For tangent sections, it is typically expected that the highpoint on the paved surface falls near the centerline, while curved sections have highpoints offset toward the EOP. When this does not occur, the section is determined to be out of shape and cannot be rated.

Tangent Section Cross-Slope Rating

The equipment accuracy of ±0.15 percent for cross-slopes must be taken into account in the rating scheme. Design standards recommend different maximum cross-slopes for tangent sections depending on regional rainfall. For wet weather regions, the recommended tangent cross-slope is 2 percent with up to 2.5 percent considered acceptable. In dry regions, the recommended tangent cross-slope is 1.5 percent with 2 percent considered acceptable.

Researchers use 1-ft × 1-ft grids for cross-slope analysis. For a 0.1-mile data collection section, up to 528 cross-sections are available. However, rarely will 100 percent of cross-sections be analyzed. Some cross-sections are lost due to physical obstructions, while others are removed from analysis because of noisy data. Within the study, a 50 percent threshold was set. To analyze the pavement within a data collection section, 264 cross-sections must be available for analysis, otherwise the section is classified as out of shape. Using recommended design cross-slopes and accounting for measurement error in the equipment, the rating curves in Figure 30 were used to rate each cross-section that meets the highpoint criteria. Researchers developed stepwise curves for both wet and dry regions. Stepwise curves are required because of the error window that must be accounted for when making deductions. For example, because equipment accuracy is ±0.15 percent, within a wet region a cross-slope can be measured between 1.85 percent and 2.65 percent and receive no deduction because it lies between 2 percent and 2.5 percent

±0.15 percent. The stepwise curves allow drier climates to maintain flatter cross-slopes. Despite the fact that this is not as beneficial for drainage, the curves are built to comply with design requirements that were established with safety and drainage in mind.
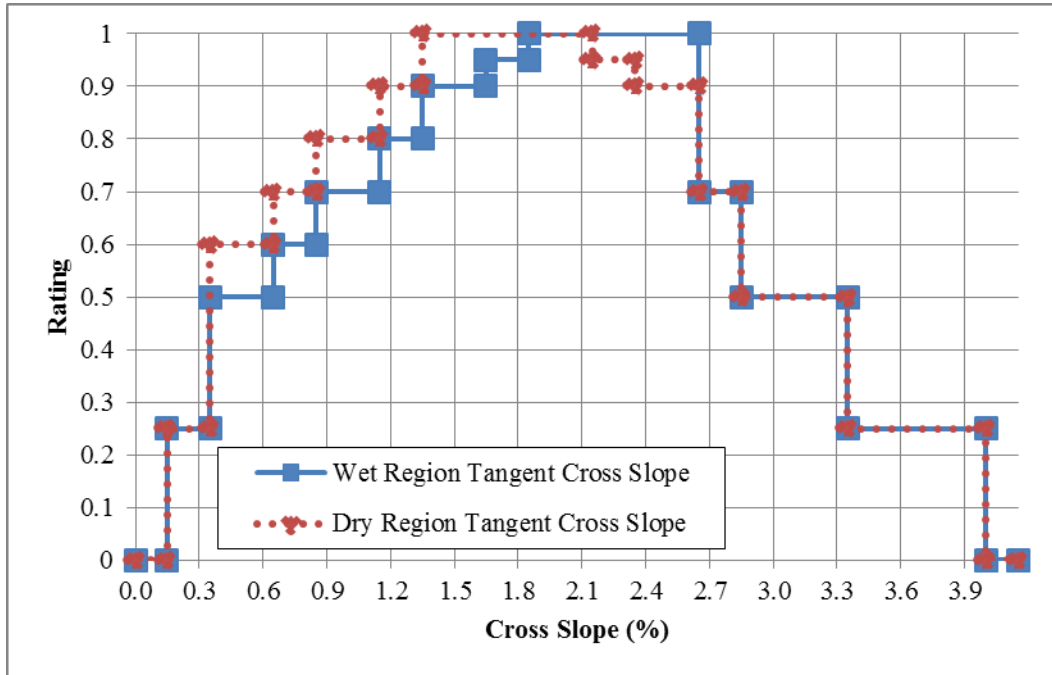
Figure 30. Tangent Rating Curves.

The rating is applied to each cross-section that is available for analysis rather than calculating an average cross-slope for the 0.1-mile data collection section and then applying the rating. This helps ensure that averaging the cross-slopes does not cover a poor cross-section that should impact the section's rating. For example, the average cross-slope within a section can be 2.2 percent, indicating no deduction if the rating was only applied to the average cross-slope. However, if within the section there was a very flat cross-section of 0.8, that particular cross-section would receive a rating of 0.6 (i.e., a 40 percent deduction) that would then prevent the section from receiving a perfect rating. In summary, each cross-section receives a numerical value between zero and one. These values are summed and divided by the available number of cross-sections to attach a paved cross-slope score to each lane. The follow equation displays this calculation:

$$\frac{\sum R_k}{j} = Section\ Rating \tag{1}$$

Where,
R_k = the rating between 0 and 1 of cross-section k.
j = the available number of cross-sections to analyze (min. 264).
$Section\ Rating$ = the percentage rating between 0 and 100 that defines the cross-slope compliance for a data collection section.

During the application of the method to roadways with poor ride quality and a history of pavement distress, researchers found that the highpoint did not match the expected location based on the IMU bearing. Sections such as these are by definition, out of shape. From an alignment perspective, the section can be defined, but the cross-slope cannot be calculated because the highpoint does not comply with either a tangent or curve definition. These sections are given a rating of 0.0, with the descriptor out of shape. From a drainage perspective, out of shape does not necessarily mean poor drainage, but the conclusion is made based on design criteria.

Horizontal Curve Section Rating

While the amount of superelevation within a curve is a design element, the radius of the curve serves as the controlling design variable. Initially, researchers use the IMU alignment data to determine if a curve is present on the roadway. If curves are detected, the shape of the section is reviewed to determine if the highpoint fits the requirement of a horizontal curve. For sections meeting the shape requirement, the rating continues, and a cross-slope rating of 0.0 is applied for those sections out of shape.

For sections in shape, researchers calculate the average superelevations for sections completely within a curve. Using this superelevation, researchers calculate the as-built or existing required curve radius. This calculation follows the traditional superelevation equation shown below:

$$e + f = \frac{V^2}{15R} \tag{2}$$

Where,

e = superelevation rate, in decimal format.
f = side friction factor.
V = vehicle speed, mph.
R = curve radius, feet.

Researchers calculate the superelevation rate using the 1-ft × 1-ft gridded data. The side friction factor is taken from the AASHTO Green Book and is recreated in Table 21. Using information based on posted speed rather than design speed, the required radius is calculated and can be compared with the actual field radius for rating purpose. Researchers calculate the field radius using sections completely contained within a curve based on the IMU alignment. Using the known arc length of the curve and the change in IMU bearing, the curve radius can be determined using the following horizontal curve equation:

$$L = 2\pi R \left(\frac{I}{360°}\right) \tag{3}$$

Where,

L = arc length of curve.
R = curve radius.
I = Difference in curve bearing from start point to end point.

Table 21. AASHTO Side Friction Factors for Horizontal Curves.

Design Speed (mph)	Max Side Friction factor, f
45	0.15
50	0.14
55	0.13
60	0.12
65	0.11
70	0.10
75	0.09
80	0.08

To rate horizontal curves, researchers use the posted speed limit and guidance from the Texas Manual on Uniform Traffic Control Devices (TMUTCD) on sign requirements when the curves must be navigated at a speed lower than the posted speed limit. A horizontal curve receives a perfect rating when the existing radius exceeds the radius required with the existing superelevation and a side friction factor of 0.08, or the minimum side friction factor allowable in the AASHTO Green Book. A rating of 0.9 or higher is applied when the existing radius is as long as or exceeds the radius required at the existing superelevation and the side friction factor associated with the posted speed limit. From this point, deductions are made based on the difference in navigable speed with posted speed using the side friction factor for the posted speed limit. Researchers use the deduction curve in Figure 31 to make these calculations. Deductions are based on the posted speed limit, and while the rating will penalize curves based on radius length and superelevation, TxDOT has various measures to address horizontal issues arising from alignment constraints. One of the ways to address these issues is through sign and chevron placement based on guidance in the TMUTCD. The zones shown in Figure 31 have related TMUTCD guidance as described below:

- Zone 1: No signs required, curve is very gentle and can easily be navigated at the posted speed limit.
- Zone 2: No signs required, curve can be navigated at the posted speed limit.
- Zone 3: Both a curve sign and advisory speed plaque for 5 mph lower than the posted speed limit are recommended.
- Zone 4: A curve sign, an advisory speed plaque for 15 mph lower than the posted speed limit, and chevrons are required.

- Zone 5: A curve sign, an advisory speed plaque for 25 mph lower than the posted speed limit, and chevrons are required.
- Zone 6: These curves should be avoided and represent locations where TxDOT might consider alignment changes.
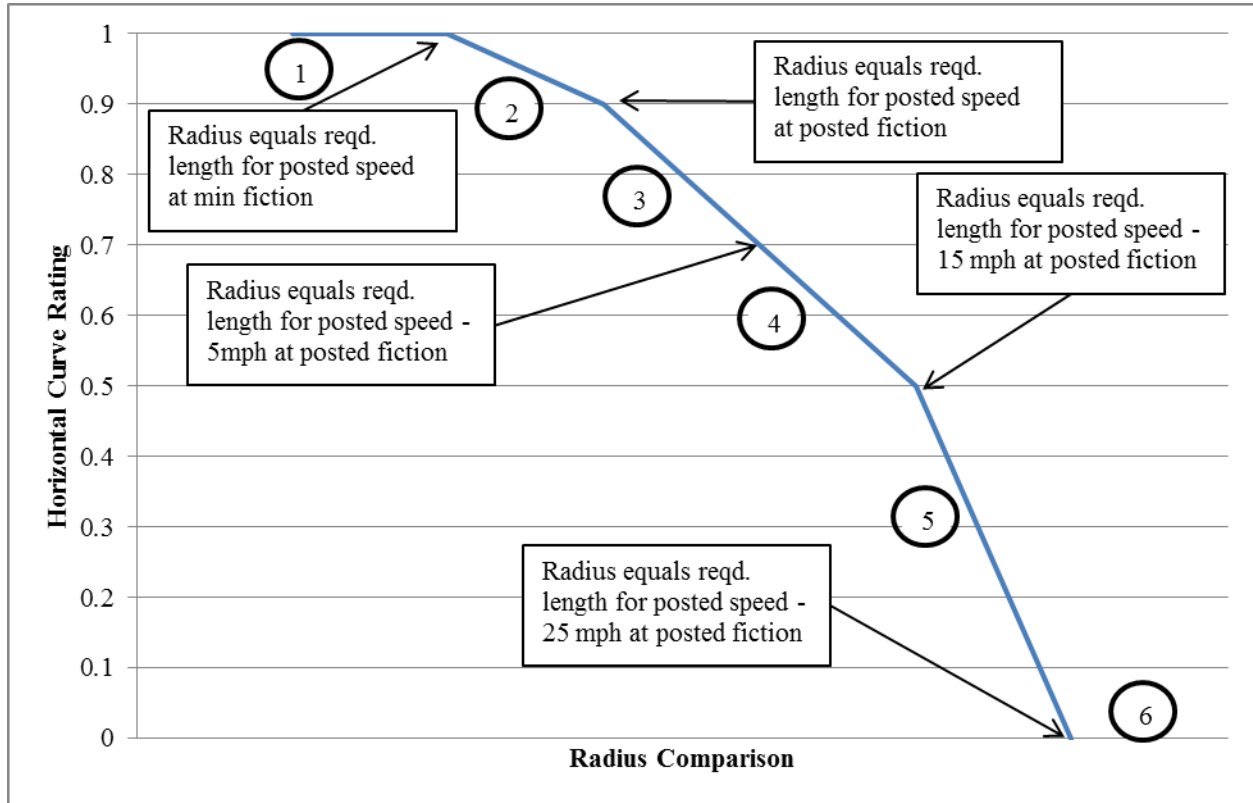
Figure 31. Horizontal Curve Rating Curve.

Based on the zones described above, a curve can reside in Zone 3 and have a rating between 0.7 and 0.9. This rating indicates to the maintenance supervisor or area engineer that this curve cannot be safely navigated at the posted speed limit. However, signage can be placed to mitigate this risk that complies with the TMUTCD. Therefore, while the rating might be below 1.0, measures can be in place that are appropriate for the roadway. Therefore, the curve rating should be considered informative and not necessarily punitive.

Additionally, the location of the highpoint is used to determine when adjacent sections are within curve transitions rather than being classified as out of shape. When a section longitudinally resides between a curve and a tangent (or vice versa), it can be classified as a curve transition and receives a rating that is equally weighted between the tangent rating and the curve rating. Rating horizontal curves follows the steps listed in the flowchart in Figure 32.

Partition the IMU data into 0.1-mi (528 ft) sections

Calculate the azimuth difference between the beginning of the section and the end of the section.

Based on azimuth difference and speed limit determine if the section is a tangent or curve

If the section is a tangent, proceed with tangent rating

Using IMU data determine how many adjacent sections are included in the curve

Determine if the curve sections are within geometric compliance using the highpoint analysis

Transition sections receive a rating weighted 50/50 based on the curve rating and the tangent rating entering the curve

If the curve sections are in-shape, evaluate adjacent sections to determine extent of curve transitions

Rate in-shape curves based on LiDAR measured super-elevation and calculated radius

Calculate average super-elevation for sections completely within the curve based on IMU alignment.

Calculate the curve radius using super-elevation and length of curve based on sections completely within the curve

Rate the curve based on radius using the following control points and linear connections between control points:

- Rating = 1.0 if radius length equals or exceeds the length required for minimum side friction (0.08) and existing super-elevation
- Rating = 0.9 if radius length equals the length required for the posted speed limit side friction and existing super-elevation
- Rating = 0.7 if radius length equals the length required for the posted speed limit minus 5 mph at the existing super-elevation and posted speed side friction factor
- Rating = 0.5 if radius length equals the length required for the posted speed limit minus 15 mph at the existing super-elevation and posted speed side friction factor
- Rating = 0.0 if radius length equals or is less than the length required for the posted speed limit minus 25 mph at the existing super-elevation and posted speed side friction factor

Figure 32. Horizontal Curve Rating Flowchart.

HYDROPLANING POTENTIAL

Hydroplaning potential is a function of surface geometry (i.e., cross-slope, longitudinal grade, and pavement width), surface texture, rainfall intensity, vehicle characteristics, and vehicle speed. Surface geometry and surface texture are the only variables within the control of TxDOT. Surface geometry is particularly applicable to this study because mobile LiDAR allows researchers to measure hydraulically important areas on the pavement surface. Nonetheless, previous research helps to calculate HPS while accounting for elements within and not within the control of TxDOT. Producing an HPS helps engineers understand how hydroplaning potential relates to the posted speed limit. Each of the hydroplaning elements listed above are discussed within, moving from the later to the former.

Vehicle Speed

Vehicle speed at the time of hydroplaning is of great interest to engineers. Ideally, the HPS will occur close to or higher than the posted speed limit. Two models are considered for computing HPS. One was developed in the 1970s by Gallaway, and a more recent one was developed by Ong and Fwa using finite element methods *(27, 28)*. These two models are presented with the calculation of WFT determined using LiDAR data.

Gallaway's formula is:

$$HPS = SD^{0.04} P_t^{0.3} (TD + 1)^{0.06} A \tag{4}$$

Where,
HPS = hydroplaning speed (mph).
SD = spindown (fixed at 0.10).
P_t = tire pressure (psi).
TD = tire tread depth (in 32nd inch).
A is the greater of:

$$\frac{10.409}{WFT^{0.06}} + 3.507 \tag{5}$$

$$\left[\frac{28.952}{WFT^{0.06}} - 7.817\right] MTD^{0.14} \tag{6}$$

Where,
WFT = water film thickness (in.).
MTD = mean texture depth of pavement surface (in.).

Ong and Fwa's formula is:

$$HPS = WL^{0.2}P_t^{0.5}\left(\frac{0.82}{WFT^{0.06}} + 0.49\right) \qquad (7)$$

Where,
HPS = hydroplaning speed (kph).
WL = wheel load (N).
P_t = tire pressure (kPa).
WFT = water film thickness (mm).

Ultimately, a Monte Carlo simulation is performed using the daily traffic as the number of iterations to predict an HPS for each data collection section. A Monte Carlo simulation is used because varying vehicle characteristics are included within the HPS calculations. The Monte Carlo simulation assumes vehicle characteristics are normally distributed around a mean value.

Vehicle Characteristics

As shown in the previous section, the calculation of HPS requires assumptions on vehicle characteristics. Within the Gallaway equation, tire pressure and tread depth are required. Within the finite element method (FEM) equation, tire pressure and wheel load are required. To perform a Monte Carlo simulation, researchers selected mean values and standard deviations for each vehicle characteristic.

For tire tread depth, 7/32 in. was selected as the mean value, with 2.4/32 in. selected as the standard deviation. Typical new tires have approximately 11/32-in. tread depth and 2/32-in. tread depth is typically considered the legal limit of tire wear (*46*). The average of these two values is 6.5/32, but was rounded up to 7/32 in. for this project. With a standard deviation of 2.4/32 in., the 95 percent range used in the Monte Carlo simulation is between 3/32 in. and 11/32 in., where 11/32 in. is established as the maximum.

Researchers selected a mean tire pressure of 35 psi with a standard deviation of 7 psi. Typical passenger vehicle tire pressures range from 30 psi to 35 psi (*47*). Within the Monte Carlo simulation, a normal tire pressure distribution using these values simulates 95 percent of vehicles with a tire pressure between 21 psi and 49 psi.

Texas has an eclectic group of vehicles that use its roadways. A compact car such as a Toyota Corolla weighs approximately 2850 lb, and a larger sedan such as a Toyota Camry weighs approximately 3400 lb. In Texas, many users drive trucks and SUVs. A Chevrolet Tahoe weighs approximately 5500 lb, and a Ford F-150 pick-up weighs approximately 4600 lb. The average of these numbers is 4100 lb. To account for the larger-size vehicle use in Texas, researchers selected a mean vehicle weight of 4400 lb with a standard deviation of 950 lb. Within the simulation, 95 percent of vehicles will weigh between 2500 lb and 6300 lb.

Using the roadway daily traffic as the iteration number, normally distributed random values are generated for the aforementioned vehicle characteristics. This helps in creating a realistic estimate of HPS.

Rainfall Intensity

TxDOT's Hydraulic Design manual includes a table in Chapter 4 that details the appropriate storm to use for design calculations. For freeways and principle arterials, the 50-year storm serves as the design standard (*42*). Moving forward, intensities associated with the 50-year event are used for analysis. Hydroplaning potential is at its highest when the WFT is deepest. This situation will occur during a short-duration, heavy rain event when the entire drainage area contributes to the critical point. Within this study, the critical point for hydroplaning is the wheel path with the largest drainage area and therefore the largest accumulation of water.

The shortest storm period provided in the work done by USGS for Texas is 15 minutes. Within the HPS calculations, the 15-minute, 50-year storm intensity is used. This value is taken from the depth-duration maps within the USGS work (*48*). The use of a 15-minute storm implies the time of concentration within the drainage area will not exceed 15 minutes. This implication exists because the hydraulic calculations for hydroplaning assume that the entire drainage area contributes water to the critical location at the same time. A check exists within the proof of concept code to ensure the time of concentration does not exceed 15 minutes. For the districts within this study, the following 50-year, 15-minute rainfall intensities were used:

- Atlanta District = 7.6 in./hr.
- Bryan District = 8.4 in./hr.
- Corpus Christi = 8.0 in./hr.
- Houston District = 8.0 in./hr.
- Tyler District = 8.0 in./hr.

Surface Texture

For hydroplaning potential calculations generated for this study, the pavement surface type was noted during data collection, and mean surface texture depths (MTDs) for various surface types were taken from literature. The ability to detect surface texture with mobile LiDAR remains in development and requires advancements in technology. Average MTD values were developed based on a thorough 41-pavement study performed by Gallaway and Rose in 1970 (*49*). That study provided multiple data points for seal-coated surfaces, dense-graded hot-mix surfaces, concrete surfaces, and flushed seal-coated surfaces. Researchers interpolated between a seal-coated surface and a flushed seal-coated surface to establish an MTD for partially flushed surfaces. When a surface is known to be an asphaltic surface, but it is not clear exactly what type of surface (e.g., a limestone rock asphalt overlay patch), the MTD is set to slightly shallower than a dense-graded surface. These values, along with Manning's *n* values from TxDOT's

Hydraulic Design Guide and abbreviations used in the pseudocode are shown in Table 22 (*42, 49*).

Table 22. Surface Type Hydroplaning Variables.

Surface Type	Surface Abbreviation	MTD (in.)	TxDOT's Manning's n
Concrete	CONC	0.023	0.015
Dense Graded Mix	HMA	0.024	0.013
Open Graded Mix	OGC	0.15	0.02
Seal Coat	ST	0.055	0.016
Partially Flushed Seal Coat	PFST	0.03	0.012
Flushed Seal Coat	FST	0.004	0.01
Unknown Asphaltic Surface	ASPH	0.02	0.013

Surface Geometry

TxDOT has the ability to control the surface texture and surface geometry of a roadway section. Historically, hydroplaning models use design profile grades and design cross-slopes to determine hydroplaning susceptibility. The use of as-built conditions in a hydroplaning analysis has not previously been plausible because of the lack of data. With mobile LiDAR, dense data sets are created that contain elevations associated to specific longitudinal and horizontal coordinates. Converting these data into a gridded format assists in further hydraulic analysis. Using 1-ft × 1-ft gridded data of the paved surface and Matlab's TopoToolbox (*25, 26*), drainage basins along the paved surface within a data collection section can be delineated. Researchers calculate WFT using the surface area characteristics of the LiDAR-generated drainage basins combined with the Rational Method and Manning's equation.

Hydroplaning Speed Calculation

Researchers chose the Rational Method as the foundational formula to calculate HPS because of its historical use for small drainage areas (*40*). Inputting the area generated from LiDAR data into the Rational Method allows researchers to calculate peak discharge. Using the peak discharge as an input into Manning's equation and using the assumption that for overland sheet flow the hydraulic radius equals the flow depth, calculations can continue to solve for water depth. The kinematic wave equation can be derived by combining the Rational Method and Manning's equation with the hydraulic radius equal to water depth. The kinematic wave equation has commonly been used for overland flow calculations, including water depth on pavements (*31, 34, 40*).

Manning's n represents the hydraulic roughness of a specific surface and must be determined through lab or field experiments. Vast amounts of work have been done on Manning's n determination. Researchers use TxDOT's published values, shown in Table 22, and the

calculation developed during PAVDRN model work. The PAVDRN model work relies on the Reynold's number calculation (*31*). Figure 33 is a flow chart of the HPS analysis. Figure 33 is followed by the equations used to calculate water depth on the surface.
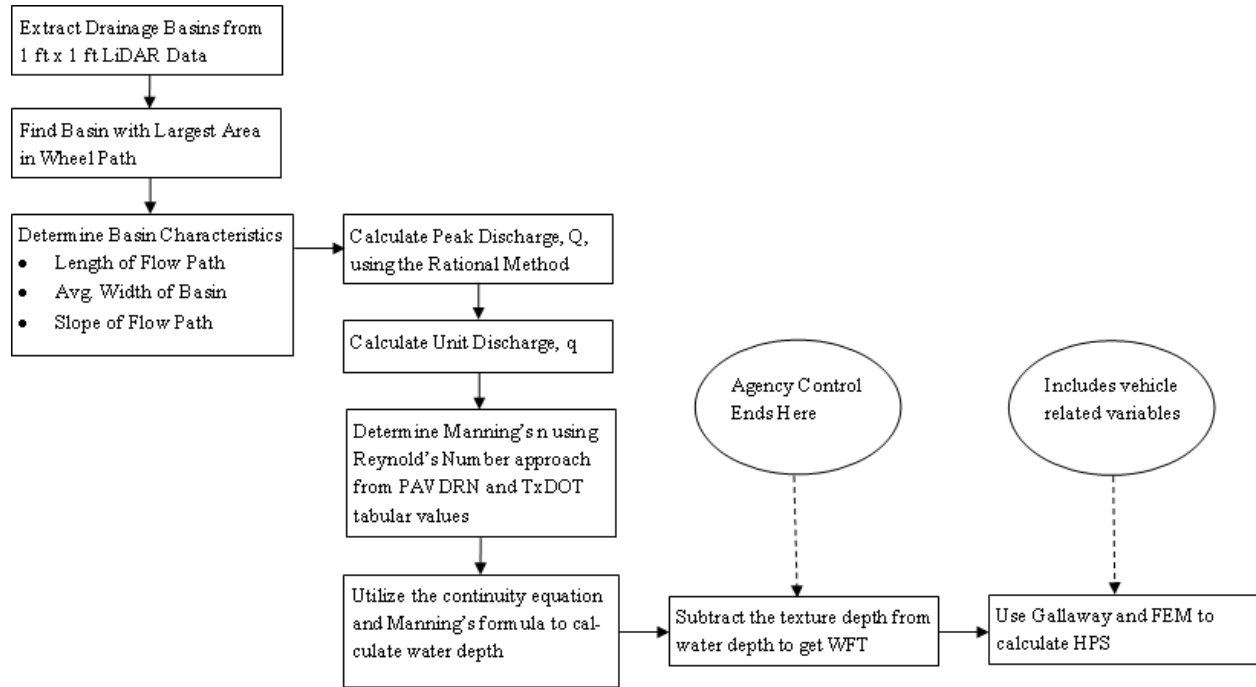
Figure 33. Hydroplaning Calculation Flow Chart.

Calculating the peak discharge using the Rational Method:

$$Q = CIA \tag{8}$$

Where,
Q = peak discharge (ft³/s).
C = runoff coefficient, assumed to be 1.0 for all non-permeable pavements.
A = drainage basin area (acres).
I = rainfall intensity (in./hr)

Converting peak discharge to an average unit discharge requires dividing the previously calculated Q by the average width of the drainage basin as defined using LiDAR data. To capture the hydraulic resistance of surfaces, the PAVDRN approach was used by first calculating Reynold's number with the following equation:

$$N_R = \frac{q}{\nu} \tag{9}$$

Where,
N_R = Reynold's number.

68

q = unit discharge (ft^3/s/ft).
v = kinematic viscosity of water (ft^2/s).

Calculations continue using the continuity equation and Manning's formula to ultimately calculate water depth. Surface texture is subtracted from water depth to determine WFT, the primary input into HPS formulas. The calculation of water depth proceeds in the following fashion:

$$\text{Continuity Equation: } \boldsymbol{Q = AV = wdV} \tag{10}$$

Where,
Q = peak discharge (ft^3/s).
A = cross-sectional area of flow (ft^2).
V = water velocity (ft/s).
w = width of flow (ft).
d = water depth (ft).

$$\text{Manning's Equation: } \boldsymbol{V = \frac{1.49}{n} R^{2/3} S^{1/2} = \frac{1.49}{n} d^{2/3} S^{1/2}} \tag{11}$$

Where,
V = water velocity (ft/s).
n = Manning's roughness number, taken from the PAVDRN approach.
R = hydraulic radius, which equals the depth of flow, d, when the depth is small compared with the width.
S = slope of drainage basin, calculated from LiDAR data.
The calculation of water depth is completed using the following equations.

$$\boldsymbol{\frac{Q}{w} = q = dV = \frac{1.49}{n} d^{5/3} S^{1/2}} \tag{12}$$

$$\boldsymbol{d = \left(\frac{qn}{1.49 S^{1/2}}\right)^{3/5}} \tag{13}$$

The above calculations result in a water depth, not WFT. The WFT consists of water above the pavement texture depth, thus the computation of WFT requires subtracting the MTD from the water depth found using the above equations. The WFT and MTD feed the HPS calculations described in the Vehicle Speed portion of this section.

Hydroplaning Speed Calculation Conclusion

Using mobile LiDAR data, researchers were able to extract drainage basins along the paved surface. With knowledge of the dimensions associated with the drainage basins, researchers were able to apply commonly used hydraulic equations to calculate water depth. These equations

require assumptions about pavement texture. Two models were used for HPS calculations. Each of these models traditionally used design parameters to calculate HPS, but in this study researchers extracted as-built geometry from LiDAR scans. A Monte Carlo simulation, using daily traffic as the number of iterations and typical values for tire pressure, tread depth, and vehicle weight, produced an HPS for each data collection section.

Researchers developed a deductions scheme for hydroplaning potential by comparing the calculated HPSs to the posted speed limit. Previous work has found that during rain events, motorists will slow below the speed limit by 3 mph to 6 mph, but the primary cause of slowing is visibility, not hydroplaning risk (*32*). In other words, motorists expect the roadway to function in a way that hydroplaning is not likely. The 50-year, 15-minute storm event used in the calculations would generate enough rain that visibility would be impacted, so prudent motorists will likely reduce their speed by approximately 5 mph. This threshold is used to develop a tiered deduction curve, as shown in Figure 34.
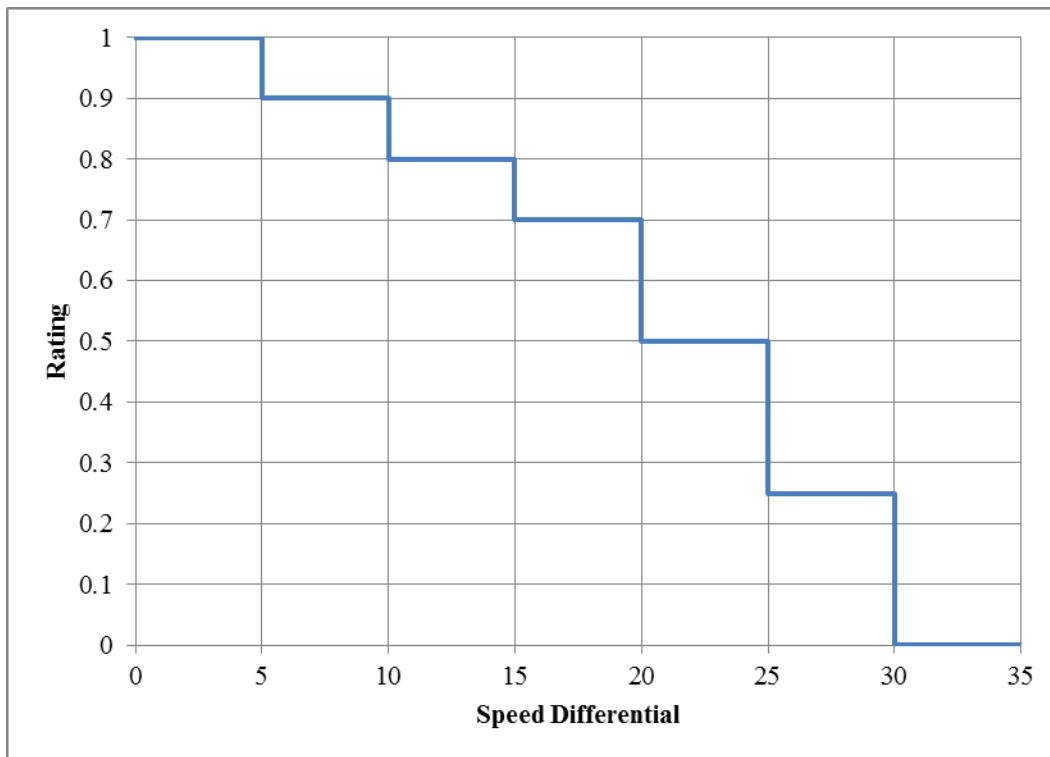
Figure 34. HPS Deduction Curve.

Figure 34 shows that if the calculated HPS is within 5 mph of the posted speed limit, no deduction is made to the section. For up to a 20-mph speed differential from the HPS and posted speed limit, the deduction occurs in 10 percent increments for each 5-mph difference. Therefore, if the posted speed limit is 70 mph and the HPS is calculated as 52 mph, the section will receive a hydroplaning potential rating of 0.7. Beyond this point, the deductions occur on 25 percent

increments for each 5-mph change. Ultimately, if the speed differential exceeds 30 mph, the section receives a 0.0 rating for hydroplaning potential.

This methodology was selected over a smooth curve because of the expected distribution associated with HPS. The HPS calculations rely on vehicle characteristic assumptions and a Monte Carlo simulation. In reality, hydroplaning occurs because of a series of unfortunate events. The drainage area is the only measured value within the calculation and, for the purposes of surface drainage, is the primary element within control of the managing agency. Water depth is the primary output from calculations using LiDAR-processed drainage area data. Water depth is not used as the primary rating element because it is difficult for engineers to visualize if a particular water depth is problematic. On the other hand, comparing a speed at which hydroplaning might occur to the posted speed limit helps in understanding the susceptibility in the field.

FRONT SLOPE STEEPNESS

The front slope represents the first element encountered along the roadside. Vegetation along the roadside creates a surface for the laser to encounter. To mitigate the impact of vegetation, data were collected within a couple of weeks of TxDOT's summer mowing cycle. TxDOT's specifications require the roadside to be mowed to a height of 5 in. to 7 in. Minimizing the time between data collection and the mowing cycle produces data on a uniformly mowed roadside where a reasonable assumption can be made about grass height.

A front slope is categorized in one of three ways: recoverable, non-recoverable, or critical. A recoverable front slope has a slope of 1V:4H or flatter. A non-recoverable front slope is traversable, but not recoverable. Slopes between 1V:3H and 1V:4H are often considered non-recoverable. Front slopes steeper than 1V:3H are considered critical because of the probability that a vehicle could overturn (*50*). The TxDOT Roadway Design Manual notes that about 1/3 of all highway fatalities are associated with single-vehicle, run-off-the-road accidents. TxDOT's desirable front slope is 1V:6H (*51*). The AASHTO Roadside Design guide indicates a 1V:4H front slope is desired, but 1V:3H is acceptable. When a 1V:3H is required, a vehicle will likely reach the bottom of the front slope before it is able to stop, and the vehicle will not likely be able to return to the pavement (*50*).

As discussed earlier in Transverse Spacing within a Cross-Section, the roadside should be analyzed using a 3-ft × 3-ft grid. Within a 0.1-mi data collection section, 176 cross-sections are produced. The roadside often consists of multiple elements, such as vegetated slopes, driveways, and turn-outs, but each of these elements should comply with front slope design requirements. Therefore, researchers calculate front slope steepness for each of the 176 cross-sections. Similar to the paved cross-slope, a rating is also calculated for each cross-section, and then the ratings are averaged to generate the section rating. This calculation can have a greater impact on the overall rating for front slope steepness than for the paved cross-slope. While outliers exist on the

paved cross-slope, for the most part a typical section exists having cross-slopes within a small window of values. The roadside can have slopes that vary significantly within a data collection section. For example, a 0.1-mi section might have slopes near 3H:1V, with two driveways built up within the section. The driveways will likely be much flatter than 3H:1V and could influence the overall average cross-slope to make the section appear to have a flatter roadside than in reality. By capturing the many cross-sections that have a steeper front slope and accounting for that element within the rating, the overall rating of the section reflects the steepness that exists.

Researchers rate each cross-section within a data collection section using the curve shown in Figure 35. For sections flatter than 6H:1V, no deduction is made. Many districts specify a 6H:1V front slope steepness as desired. A 10 percent linear deduction takes place from 6H:1V to 4H:1V. A 4H:1V or flatter slope is considered recoverable, so only a small deduction is applied at 4H:1V. Another 20 percent deduction occurs from 4H:1V to 3H:1V as the slope transitions from recoverable to non-recoverable. A front slope steepness of 3H:1V represents the steepest front slope that meets design criteria and receives a rating of 0.7. A linear deduction from a rating of 0.7 to 0.0 occurs between steepness values of 3H:1V and 2H:1V. Anything steeper than 2H:1V receives a rating of 0.0. Not only do slopes steeper than 2H:1V create safety issues, they often cannot be constructed without a stabilization technique such as riprap (*40*).

Figure 35. Front Slope Rating Curve.

Very flat front slopes can create drainage-related issues. However, researchers chose not to select a too flat value to begin deductions. This decision was made not only to acknowledge the safety element associated with flatter roadside but also to avoid double counting. Ditch depth is the next element rated, and shallow ditches receive a poorer rating, essentially capturing very flat roadside front slopes.

DITCH DEPTH

As a design element, ditch depth often competes with front slope steepness. In narrow ROW situations, deeper ditches often require steeper front slopes. For this reason, researchers attempt to balance geometric elements from a design compliance and drainage perspective, a challenge similar to the challenges faced by designers and network managers.

Each data collection section receives a descriptive label during analysis of either primarily front slope or primarily ditch. Researchers establish these labels using the majority of cross-sections within the data collection section. Regardless of whether or not a section is categorized as primarily a front slope or primarily a ditch section, ditch depth is captured on any roadside section that is identified as having a ditch. Therefore, sections that are classified as primarily front slope still have a ditch depth rating to ensure problematic locations are identified.

Researchers discovered that the desirable ditch depth is under-researched. A recent study from Nordic countries in Europe indicated that general practice was to have the bottom of the ditch at least 8 in. below the bottom of the pavement structure (*52*). Occasionally, in plans, designers include a typical ditch depth from the pavement surface. A common depth shown in plans is 2 ft, similar to Figure 36, taken from 0151-01-051. TxDOT's design manual recommends a ditch depth at least 6 in. below the crown of the subgrade (*51*). Iowa DOT uses a desirable ditch depth from the pavement surface of 3 ft and an absolute minimum of 2 ft (*53*). New York recommends a typical depth of 30 in. below the surface of the EOP (*54*). Illinois' Bureau of Local Roads and Streets recommends a 2 ft ditch depth with an absolute minimum of 1.5 ft (*55*).

The depth to the bottom of the pavement structure is critical, and mobile LiDAR provides surface measurements. Depth of pavement structure varies from roadway to roadway. For example, in Figure 36 the pavement structure includes a seal coat, 2 in. of TY D HMA, 4 in. of TY B HMA, and 8 in. of flex base for a total depth of 14 in. plus a seal-coated surface.
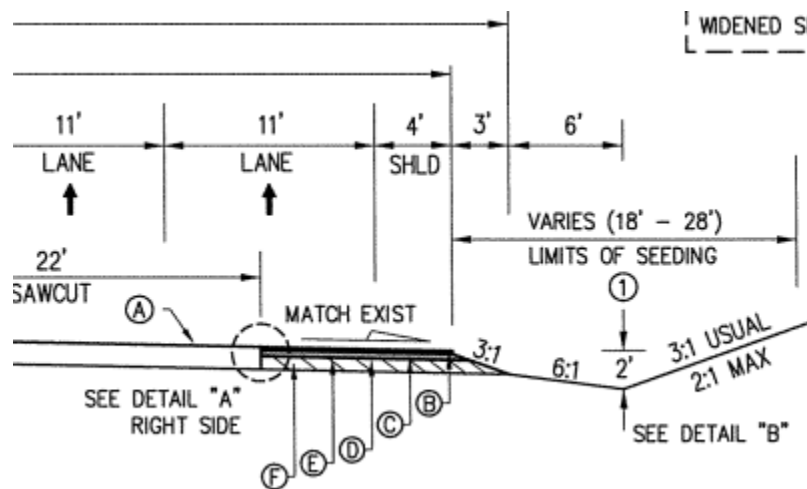
Figure 36. Ditch Depth Shown in Proposed Typical Section.

73

Researchers originally developed a stepwise curve to rate the average ditch depth within a data collection section. Through application of the system, researchers discovered that the stepwise curve was too punitive. Adjustments were made to create a curve-based deduction system based on desired ditch depth while accounting for potential noise in the data. One of the primary causes of noise along the ROW is vegetation. Grass growth impedes the laser from reaching the actual bottom of the ditch. Collecting data shortly after conclusion of a mowing cycle allows for the assumption that the ditch bottom is between 5 in. and 7 in. lower than the LiDAR measurements. This assumption is valid because of the specification associated with roadside mowing. Researchers use 6 in. within the study. However, it is possible that in areas of thin vegetation or if data are collected following the fall mowing cycle once the grass is dormant, the laser will reach the ground. Therefore, the rating should account for the fact that a margin of error exists by accounting for vegetation.

Based on field feedback and information similar to that shown in Figure 36, researchers discovered that the minimum desired ditch depth ranged from between 1 ft and 2 ft below the bottom of the pavement structure, or approximately 2 ft to 3 ft from the pavement surface. To provide some latitude for grass growth on the roadside, researchers selected 3.5 ft as the depth to receive a perfect rating. Ideally, enough ROW exists that deep ditches exist far from the EOP, producing water surface flows significantly below the pavement structure while maintaining safe front slopes. This feature creates the balancing mechanism between ditch depth and front slope steepness. Researchers do not consider ditch offset in the rating because doing so would double count its effect with the combination of ditch depth and front slope steepness. A maximum ditch depth is not required within the rating because a too-deep ditch depth creates too steep of a front slope and will be reflected in the rating. The rating uses the curve in Figure 37.
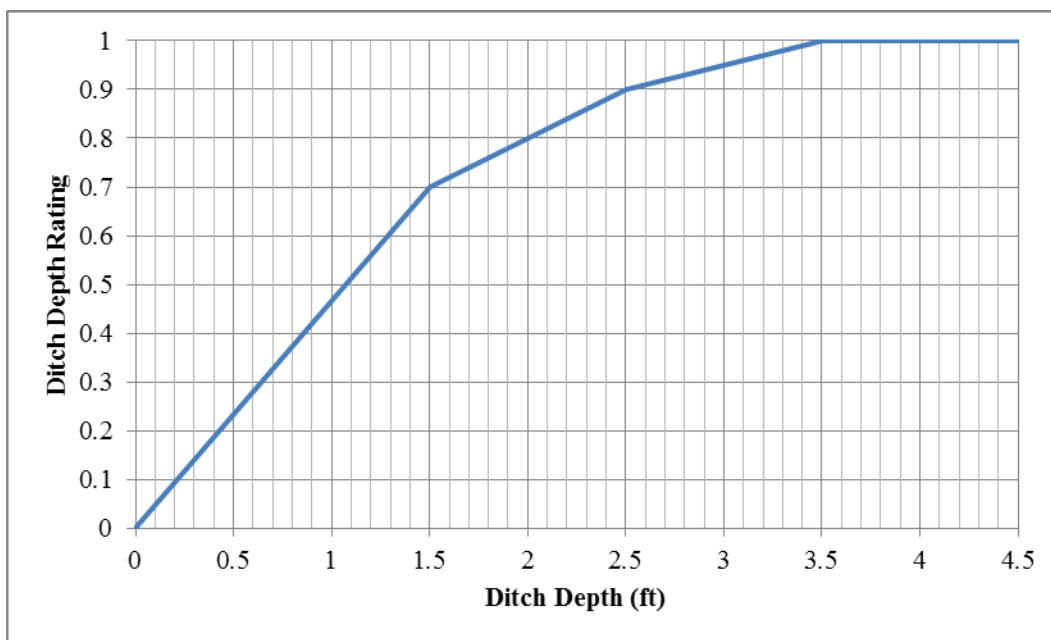
Figure 37. Ditch Depth Rating Curve.

DITCH FLOWLINE GRADE

Measuring the ditch flowline grade functions similarly to the HPS analysis except that rather than calculating water depth, the flowline steepness within a drainage basin is of interest. Water velocity within the channel impacts erosion or sedimentation potential. Water velocity is a function of many variables, including channel geometry, channel slope, and water depth. Water depth in a roadside ditch is a function of the size of the drainage basin using the ditch as a conduit to a lower elevation. Often, the drainage basin includes large portions of property off of ROW. These areas cannot be measured with mobile LiDAR. With the ability for mobile LiDAR to delineate roadside drainage basins and calculate a flowline grade for the drainage basin, researchers relate flowline slope to potential water velocity.

Figure 38 shows the relationship between depth of water and water velocity. Figure 38 illustrates that the deeper the water, the faster it flows. Figure 39 shows the relationship between front slope geometry and water velocity. Reviewing the front slope geometry captures the impact of the wetted perimeter. While some impact is revealed in Figure 39, the impact of front slope geometry is much less than that of water depth. Figure 40 shows the relationship between Manning's *n* and water velocity. As Manning's *n* goes down, water velocity increases, but the magnitude of the velocity impact is much less than the contribution of water depth.
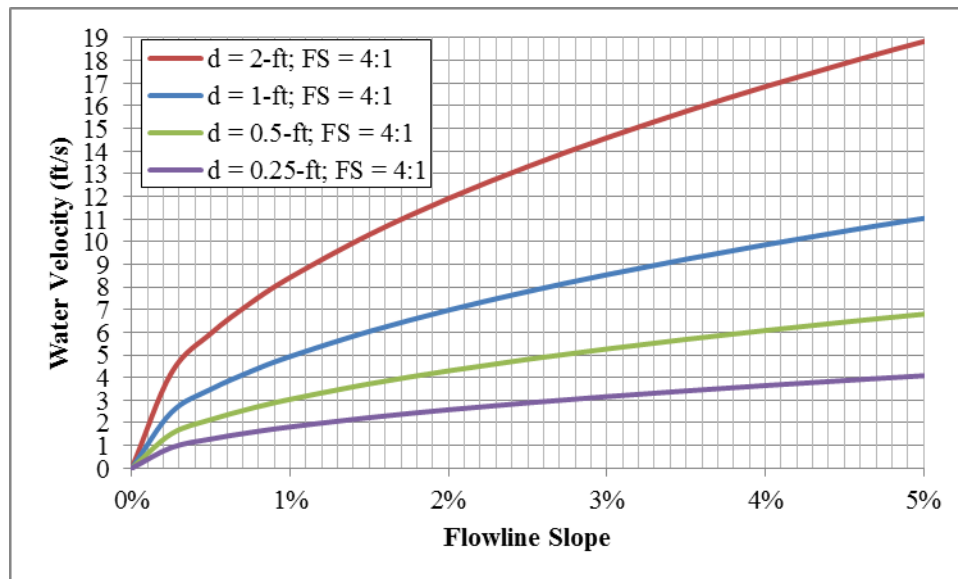
Figure 38. Depth of Water Effect on Water Velocity.
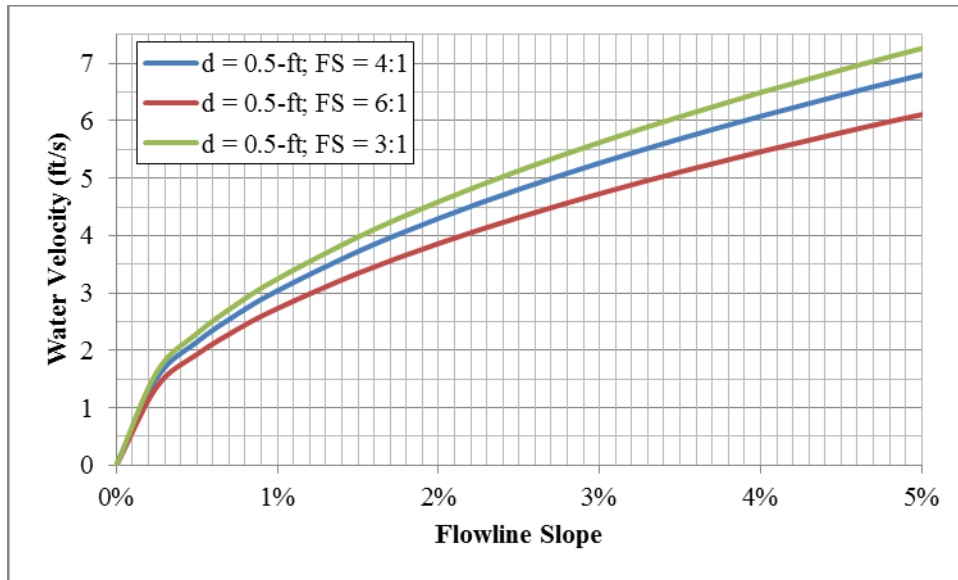
Figure 39. Front Slope Geometry Effect on Water Velocity.
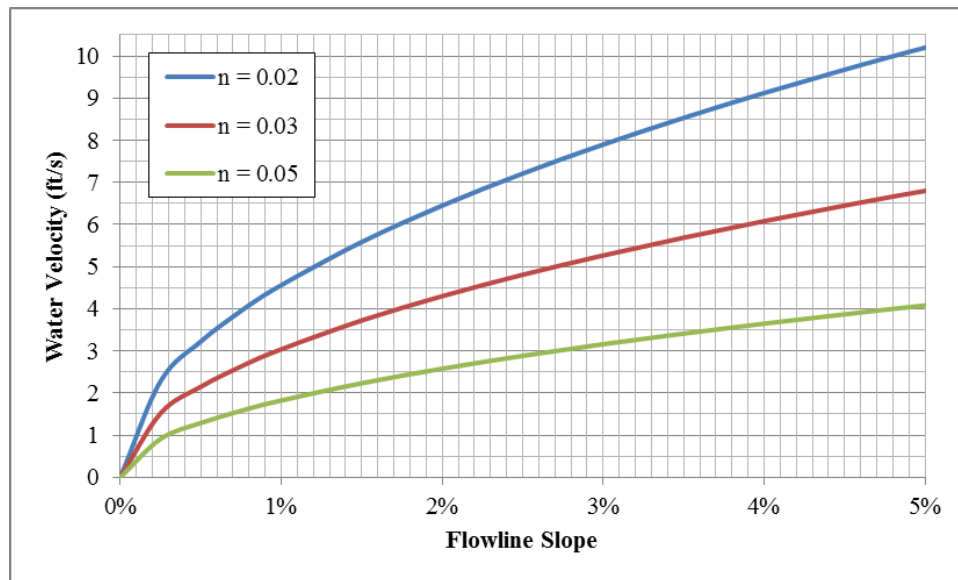
Figure 40. Manning's *n* Effect on Water Velocity.

Regardless of the variable in question, each curve begins to rapidly descend toward zero velocity near a flowline slope of 0.3 percent. Based on this, researchers selected 0.3 percent as the absolute minimum flowline slope.

Maximum slope is typically controlled by the profile grade of the roadway and safety considerations associated with front slope steepness. While slopes too flat can lead to sedimentation, slopes too steep can lead to erosion. Other DOTs have general guidelines to address ditch steepness. Iowa uses desirable ditch grades of between 1 percent and 3 percent with a minimum acceptable grade between 0.2 percent and 1 percent (*53*). Washington DOT establishes a 6 percent maximum ditch line grade or 5 ft/s water velocity before requiring special

lining techniques (*56*). Michigan DOT and New York DOT provide desired minimums of 0.3 percent and 0.5 percent, but provide no maximums (*54, 57*).

For pavement preservation, sedimentation causes more concern because silting in the flowline raises the water elevation and creates potential for water within pavement structural layers. Initially, researchers implemented a stepwise function that included punitive measures for slopes that were too flat and too steep. This method was overly punitive for slope approaching cross-culverts or flowlines at the toe of slope in front slope only sections. Additionally, the challenge of distinguishing between surface types along the ROW can lead to steep slopes being penalized when in reality erosion measures such as riprap are in place. While different material types can be distinguished at the project level, doing so at the network level becomes difficult. Therefore, the final rating for flowline slope focuses on providing information on ditches that are steep enough, rather than trying to identify slopes that might be too steep. Researchers selected a 1 percent fall as the threshold to receive a perfect rating. Anything steeper than that also receives a perfect rating, while flatter flowlines follow the deduction curve in Figure 41.
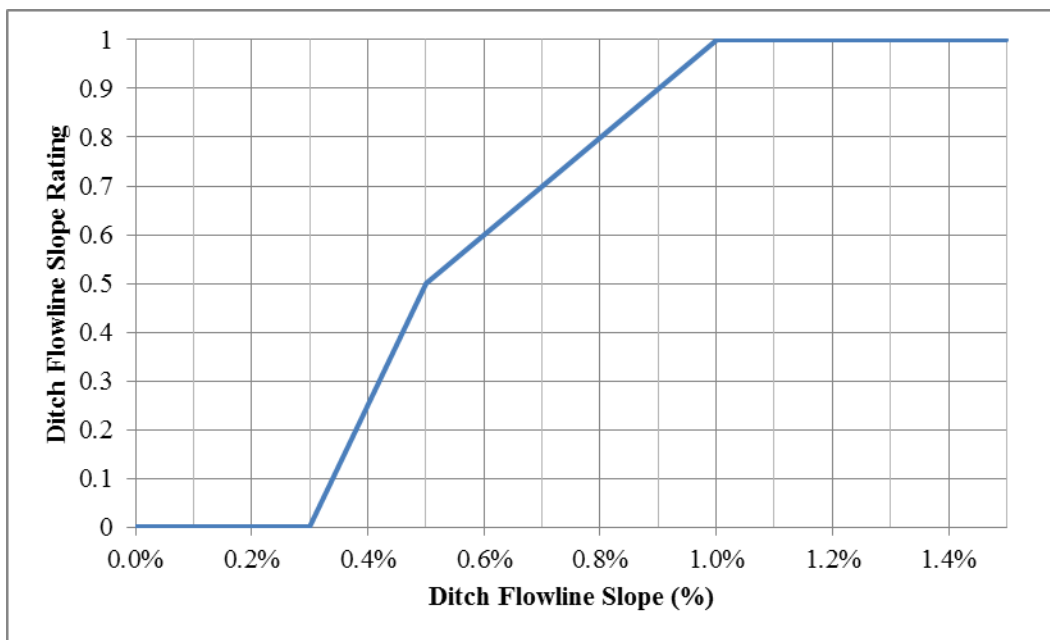
Figure 41. Ditch Flowline Slope Stepwise Rating Curve.

A NOTE ON RUTTING

Researchers chose not to include rutting into the surface drainage rating scheme. Rutting measurements currently take place during the annual pavement condition inspection. The annual condition score for a pavement section includes rutting measurements. However, rutting can play a significant role in pavement drainage, particularly if ruts create a trough to channelize water flow. The use of drainage area calculations for HPS analysis captures water channelization, and WFT calculations near the outside wheel path provide a critical analysis point. Therefore, while

rutting does not explicitly contribute to the drainage rating, it implicitly effects drainage area calculations, contributing to the overall drainage rating.

SURFACE DRAINAGE RATING SUMMARY

The surface drainage rating consists of paved surface elements and roadside elements measured through automated means. Researchers collect mobile LiDAR data at near highway speeds. Through this project, methods have been developed to extract mobile LiDAR data, process it, and generate ratings with minimal manual interaction. The goal of the network-level rating was to implement a proof of concept that could efficiently rate miles of roadway without spending large amounts of time evaluating video.

Using off-the-shelf processing software that accompanies the data collection equipment, mobile LiDAR data were extracted on both 1-ft × 1-ft grids and 3-ft × 3-ft grids. The raw LiDAR scanner data were used to differentiate between the paved surface and the vegetated roadside. Once this delineation has been made, 1-ft × 1-ft gridded data are used to analyze the paved surface, and 3-ft × 3-ft gridded data are used to analyze the roadside.

The rating balances design requirements and drainage needs. Paved surface elements include lane width, lane cross-slope, and hydroplaning potential. Lane cross-slope is rated only if the data collection section is determined to be in shape as it relates to the expected location of the highpoint on the paved surface. Hydroplaning analysis includes evaluating the drainage areas along the paved surface and calculating the WFT created in the outside wheel path. The actual calculation of HPS requires several assumptions on vehicle characteristics, so a Monte Carlo simulation was used to generate an average HPS for the section.

Roadside elements compete against each other within the rating. The roadside front slope must meet design requirements in terms of steepness, but a deep ditch is desired for drainage. This competition between rated elements is shown in more detail in the Application of Surface Drainage Rating section. Calculation of the ditch flowline requires generating a drainage area along the roadside and determining the flowline slope within the drainage area. In addition to rating the drainage elements along the roadside, roadsides are provided a descriptor to classify if the section has a ditch, is primarily a front slope, or has varying drainage geometry.

This drainage rating applies primarily to rural roadways with consistent geometry. While other sections can be rated, automatic extraction of data and automatic processing requires as much consistency as possible. Changes in geometry or loss of roadside features due to curb and gutter or barrier require manual intervention. In the following section, the drainage rating is applied to roadways with paved surface and roadside features. This rating meets the needs identified by TxDOT to address pavement cross-slope, horizontal curve shape and radius, front slope, and roadside ditch geometry. Unfortunately, due to the nature of data collection, inlets and barrier rail openings cannot be identified. This limits the current application at the network level to rural

sections. Sections with curb and gutter and barrier can be analyzed, but the effort requires significant manual interaction and does not lend itself to network-level analysis. These sections should be treated similar to project level applications with specific features targeted.

APPLICATION OF SURFACE DRAINAGE RATING

The surface drainage rating described in the previous section was applied to 73.5 mi of rural roadway. Road Doctor software was initially used to process the mobile LiDAR data and extract it for additional use. Following the extraction of mobile LiDAR data into a gridded format, Matlab software was used to develop a proof of concept code to generate network-level ratings. Ratings were generated on 0.1-mi data collection sections and reported in an Excel environment. Because the rating is derived from multiple pieces of information, additional tabular data can be provided to drill down into individual pieces of the rating. Currently, the proof of concept code requires approximately 10 minutes per mile to generate ratings. This process occurs after the data have been processed, and an additional aesthetic step is required to generate the final tabular summary of the rating. In total, processing a mile of data to create gridded data in LiDAR specific software requires approximately one hour, followed by additional time to push the data through the proof of concept Matlab code and additional aesthetic steps for the final output. Economies of scale are realized in the initial processing. While it takes approximately one hour to process 1 mi of raw LiDAR data, it only takes marginally longer to process 10 mi.

Roadway sections were taken from the Atlanta, Bryan, Corpus Christi, and Tyler Districts. Roadway types were chosen that included both paved surface features and roadside drainage features. As the drainage rating was applied to the various networks, it became obvious that comparing drainage features within an urban or metro environment was significantly different than comparing drainage features in a rural environment. Within a rural environment, both paved surface geometry and roadside geometry contribute to the surface drainage. In addition to the contribution, these elements can be measured using mobile LiDAR, and additional post-processing methods can be developed to develop ratings at the network level.

Within an urban environment with curb and gutter, calculations can be made for lane width, cross-slope, and drainage areas. However, it is difficult to delineate the location of an inlet or outfall point at the network level. This information can easily be captured at the project level when video and mobile LiDAR data are coupled together. At the network level, researchers focused on developing methods that could process vast amounts of data with minimal manual interaction. Therefore, in curb and gutter sections, the outside ponding width developed at the network level often far exceeds allowable results because the flow of water into an inlet is not automatically captured without manual processing.

Urban sections with curb and gutter are void of roadside geometry that impacts drainage in the same way as rural sections. The lack of influence of roadside geometry is also true for large metro sections with multiple lanes in each direction. Sections such as those encountered on IH 45 and IH 610 in the Houston District have many geometric features, but the width of the section impacts the ability to measure network-level information in a single data collection run. Collecting from the center lane provides the most information about the driving surface, but this

information is limited to lane width, cross-slope, and hydroplaning potential. Many metro sections often have no roadside at all because of the presence of a barrier rail. The barrier rail typically has small slotted openings for the water to drain off of the pavement, but these openings are not easily identified with mobile LiDAR.

In summary, methods for minimal manual interaction to rate rural sections have been developed through this project. These rural sections can consist of travel in both directions or a single direction. Urban and metro sections with curb and gutter or multiple lanes should be evaluated as corridor specific or at the project level. The hydraulic diversity of these types of sections and the need to identify fixed low points such as inlets or barrier openings forces significant data processing interaction and does not lend itself to network-level analysis.

The application of the network-level rating to various roadways is shown in the following sections. Researchers have provided additional descriptions and screenshots to illustrate the application of the rating and to point out potential flaws.

IH 20—ATLANTA DISTRICT

Researchers rated the eastbound direction of IH 20 in the Atlanta District between approximately SH 31 and FM 2199, or reference marker 621 and 624. This portion of IH 20 consists of two eastbound lanes with a narrow inside shoulder and wider outside shoulder. The paved surface appears to be dense grade HMA. Table 23 shows the rating output.

Table 23. IH 20 Surface Drainage Rating Summary.

Begin TRM	End TRM	Section	Alignment Classificaiton	Section Shape	Roadway Surface RT Width Rating	RT Cross Slope Rating	Hydro-planing Rating	RT Roadside Shape	Roadside Surface RT Front Slope Rating	RT Ditch Depth Rating	RT Ditch Slope Rating	Combined Paved Surface Rating	Combined Roadside Rating	Overall Drainage Rating	Overall Rating Normalized to 100
621.0	621.1	1	TANGENT	TANGENT	1.00	1.00	0.90	Primarily FS	1.00	1.00	1.00	0.97	1.00	0.98	98
621.1	621.2	2	TANGENT	TANGENT	1.00	1.00	1.00	Primarily FS	1.00	0.86	1.00	1.00	0.95	0.98	98
621.2	621.3	3	TANGENT	TANGENT	1.00	1.00	1.00	Various Drainage	1.00	1.00	1.00	1.00	1.00	1.00	100
621.3	621.4	4	TANGENT	TANGENT	1.00	1.00	1.00	Primarily Ditch	1.00	0.96	1.00	1.00	0.99	0.99	99
621.4	621.5	5	TANGENT	TANGENT	1.00	1.00	1.00	Primarily Ditch	1.00	0.93	1.00	1.00	0.98	0.99	99
621.5	621.6	6	TANGENT	TANGENT	1.00	1.00	1.00	Primarily Ditch	1.00	0.89	1.00	1.00	0.96	0.98	98
621.6	621.7	7	TANGENT	TANGENT	1.00	1.00	1.00	Primarily Ditch	1.00	0.94	1.00	1.00	0.98	0.99	99
621.7	621.8	8	TANGENT	TANGENT	1.00	1.00	1.00	Primarily Ditch	1.00	0.87	1.00	1.00	0.96	0.98	98
621.8	621.9	9	TANGENT	TANGENT	1.00	1.00	1.00	Primarily Ditch	1.00	0.84	1.00	1.00	0.95	0.97	97
621.9	622.0	10	TANGENT	TANGENT	1.00	1.00	1.00	Primarily Ditch	1.00	0.91	1.00	1.00	0.97	0.99	99
622.0	622.1	11	TANGENT	TANGENT	1.00	1.00	1.00	Primarily Ditch	1.00	0.83	1.00	1.00	0.94	0.97	97
622.1	622.2	12	TANGENT	TANGENT	1.00	1.00	1.00	Primarily Ditch	1.00	0.91	1.00	1.00	0.97	0.98	98
622.2	622.3	13	TANGENT	TANGENT	1.00	1.00	1.00	Primarily Ditch	1.00	0.94	1.00	1.00	0.98	0.99	99
622.3	622.4	14	TANGENT	TANGENT	1.00	1.00	1.00	Primarily Ditch	1.00	0.88	1.00	1.00	0.96	0.98	98
622.4	622.5	15	TANGENT	TANGENT	1.00	1.00	1.00	Primarily Ditch	1.00	0.91	1.00	1.00	0.97	0.98	98
622.5	622.6	16	TANGENT	TANGENT	1.00	1.00	1.00	Primarily Ditch	1.00	0.85	1.00	1.00	0.95	0.98	98
622.6	622.7	17	TANGENT	OUT OF SHAPE	1.00	0.00	1.00	Primarily Ditch	1.00	0.97	1.00	0.67	0.99	0.83	83
622.7	622.8	18	TANGENT	TANGENT	1.00	1.00	1.00	Primarily Ditch	1.00	0.95	1.00	1.00	0.98	0.99	99
622.8	622.9	19	TANGENT	TANGENT	1.00	1.00	1.00	Primarily Ditch	1.00	0.86	1.00	1.00	0.95	0.98	98
622.9	623.0	20	TANGENT	TANGENT	1.00	1.00	1.00	Primarily Ditch	1.00	0.86	1.00	1.00	0.95	0.98	98
623.0	623.1	21	TANGENT	TANGENT	1.00	1.00	1.00	Primarily Ditch	1.00	0.89	1.00	1.00	0.96	0.98	98
623.1	623.2	22	TANGENT	TANGENT	1.00	1.00	1.00	Primarily Ditch	0.99	0.93	1.00	1.00	0.97	0.99	99
623.2	623.3	23	TANGENT	TANGENT	1.00	0.95	1.00	Primarily Ditch	1.00	0.95	1.00	0.98	0.98	0.98	98
623.3	623.4	24	TANGENT	TANGENT	1.00	0.90	1.00	Primarily Ditch	1.00	0.90	1.00	0.97	0.97	0.97	97

This interstate facility has a desired good surface drainage rating. All but one section receives a rating above 90. Section 17 has a rating of 83, driven downward because it was deemed out of shape. The definition of out of shape is the absence of the surface highpoint where it is expected. As described in the Development of Surface Drainage Rating section, researchers use a 50 percent threshold when searching for the location of the highpoint to determine if a section should be classified as out of shape. With 528 cross-sections within a 0.1-mi data collection section, 264 must have the location of the highpoint in the expected location to receive a cross-slope rating.

FM 31—ATLANTA DISTRICT

Data collection for FM 31 began north of IH 20 at reference marker 280 and proceeded southbound. The paved surface ratings reflect the southbound, or K1, lane and the roadside ratings reflect the condition adjacent to the southbound direction of travel. FM 31 consists of one lane in each direction with a partially flushed, seal-coated surface. Table 24 shows the rating summary for FM 31 on 0.1-mi data collection sections with 0.5-mi increments blocked with color changes.

Table 24. FM 31 Surface Drainage Rating Summary.

Begin TRM	End TRM	Section	Alignment Classificaiton	Section Shape	Roadway Surface — RT Width Rating	RT Cross Slope Rating	Hydro-planing Rating	RT Roadside Shape	Roadside Surface — RT Front Slope Rating	RT Ditch Depth Rating	RT Ditch Slope Rating	Combined Paved Surface Rating	Combined Roadside Rating	Overall Drainage Rating	Overall Rating Normalized to 100
280.0	280.1	1	TANGENT	TANGENT	0.86	0.93	1.00	Primarily Ditch	1.00	0.90	1.00	0.93	0.97	0.95	95
280.1	280.2	2	TANGENT	TANGENT	0.86	0.87	1.00	Primarily Ditch	1.00	0.86	1.00	0.91	0.95	0.93	93
280.2	280.3	3	RTCURVE	OUT OF SHAPE	0.85	0.00	1.00	Primarily Ditch	1.00	0.82	1.00	0.62	0.94	0.78	78
280.3	280.4	4	TANGENT	TANGENT	0.84	0.90	1.00	Primarily Ditch	1.00	0.99	1.00	0.91	1.00	0.96	96
280.4	280.5	5	TANGENT	TANGENT	0.86	0.79	1.00	Primarily FS	1.00	0.93	1.00	0.88	0.97	0.93	93
280.5	280.6	6	TANGENT	TANGENT	0.82	0.80	1.00	Primarily FS	1.00	1.00	1.00	0.87	1.00	0.94	94
280.6	280.7	7	TANGENT	TANGENT	0.81	0.67	1.00	Primarily Ditch	0.94	1.00	1.00	0.83	0.98	0.90	90
280.7	280.8	8	TANGENT	TANGENT	0.84	0.76	1.00	Primarily Ditch	1.00	0.72	1.00	0.87	0.91	0.89	89
280.8	280.9	9	TANGENT	OUT OF SHAPE	0.91	0.00	1.00	Primarily Ditch	1.00	0.98	1.00	0.64	0.99	0.82	82
280.9	281.0	10	TANGENT	OUT OF SHAPE	0.81	0.00	1.00	Primarily Ditch	1.00	0.97	1.00	0.60	0.99	0.80	80
281.0	281.1	11	TANGENT	OUT OF SHAPE	0.88	0.00	1.00	Primarily Ditch	1.00	0.87	1.00	0.63	0.96	0.79	79
281.1	281.2	12	TANGENT	OUT OF SHAPE	0.81	0.00	1.00	Primarily Ditch	0.99	0.70	1.00	0.60	0.90	0.75	75
281.2	281.3	13	TANGENT	OUT OF SHAPE	0.85	0.00	1.00	Primarily Ditch	0.99	0.91	1.00	0.62	0.97	0.79	79
281.3	281.4	14	LTCURVE	OUT OF SHAPE	0.88	0.00	1.00	Primarily Ditch	1.00	0.85	1.00	0.63	0.95	0.79	79
281.4	281.5	15	TANGENT	TANGENT	0.90	0.60	1.00	Primarily Ditch	1.00	0.81	0.94	0.83	0.92	0.87	87
281.5	281.6	16	TANGENT	TANGENT	0.95	0.90	1.00	Primarily Ditch	0.99	0.72	1.00	0.95	0.91	0.93	93
281.6	281.7	17	TANGENT	OUT OF SHAPE	0.89	0.00	1.00	Primarily Ditch	1.00	0.92	1.00	0.63	0.97	0.80	80
281.7	281.8	18	TANGENT	TANGENT	0.88	0.83	1.00	Primarily Ditch	0.98	0.97	1.00	0.90	0.98	0.94	94
281.8	281.9	19	TANGENT	OUT OF SHAPE	0.89	0.00	1.00	Primarily Ditch	1.00	0.79	1.00	0.63	0.93	0.78	78
281.9	282.0	20	TANGENT	TANGENT	0.86	0.52	1.00	Primarily Ditch	1.00	0.86	1.00	0.79	0.95	0.87	87
282.0	282.1	21	TANGENT	TANGENT	0.86	0.76	1.00	Primarily Ditch	1.00	0.78	1.00	0.87	0.93	0.90	90
282.1	282.2	22	TANGENT	OUT OF SHAPE	0.86	0.00	1.00	Primarily Ditch	1.00	0.80	0.83	0.62	0.88	0.75	75
282.2	282.3	23	TANGENT	OUT OF SHAPE	0.96	0.00	1.00	Primarily Ditch	0.99	0.78	0.99	0.65	0.92	0.79	79
282.3	282.4	24	TANGENT	OUT OF SHAPE	0.76	0.00	1.00	Primarily Ditch	1.00	0.76	0.83	0.59	0.86	0.73	73
282.4	282.5	25	TANGENT	OUT OF SHAPE	0.83	0.00	1.00	Primarily Ditch	0.99	0.81	0.56	0.61	0.79	0.70	70
282.5	282.6	26	TANGENT	OUT OF SHAPE	0.81	0.00	1.00	Primarily Ditch	0.99	0.71	0.54	0.60	0.75	0.68	68
282.6	282.7	27	TANGENT	OUT OF SHAPE	0.82	0.00	1.00	Primarily Ditch	0.99	0.84	1.00	0.61	0.95	0.78	78
282.7	282.8	28	TANGENT	CURVE TRANS	0.78	0.50	1.00	Primarily Ditch	0.98	0.90	1.00	0.76	0.96	0.86	86
282.8	282.9	29	TANGENT	CURVE TRANS	0.81	0.50	1.00	Primarily Ditch	0.97	0.76	1.00	0.77	0.91	0.84	84
282.9	283.0	30	RTCURVE	RT CURVE	0.70	1.00	1.00	Primarily Ditch	0.99	1.00	1.00	0.90	1.00	0.95	95
283.0	283.1	31	TANGENT	CURVE TRANS	0.72	0.50	1.00	Primarily Ditch	1.00	0.73	1.00	0.74	0.91	0.83	83
283.1	283.2	32	TANGENT	OUT OF SHAPE	0.70	0.00	1.00	Primarily Ditch	1.00	0.90	1.00	0.57	0.97	0.77	77
283.2	283.3	33	TANGENT	CURVE TRANS	0.73	0.50	1.00	Primarily Ditch	1.00	0.77	1.00	0.74	0.92	0.83	83
283.3	283.4	34	LTCURVE	LT CURVE	0.78	1.00	1.00	Primarily Ditch	0.99	0.87	1.00	0.93	0.96	0.94	94
283.4	283.5	35	TANGENT	CURVE TRANS	0.76	0.90	1.00	Primarily Ditch	1.00	0.71	1.00	0.89	0.90	0.89	89
283.5	283.6	36	TANGENT	TANGENT	0.75	0.79	1.00	Primarily Ditch	0.90	1.00	1.00	0.85	0.97	0.91	91
283.6	283.7	37	TANGENT	CURVE TRANS	0.64	0.90	1.00	Primarily Ditch	0.93	0.76	1.00	0.84	0.90	0.87	87
283.7	283.8	38	LTCURVE	LT CURVE	0.72	1.00	1.00	Primarily Ditch	1.00	0.75	1.00	0.91	0.92	0.91	91
283.8	283.9	39	LTCURVE	LT CURVE	0.77	1.00	1.00	Primarily Ditch	0.99	0.92	1.00	0.92	0.97	0.95	95
283.9	284.0	40	TANGENT	CURVE TRANS	0.79	1.00	1.00	Primarily Ditch	0.94	0.62	0.92	0.93	0.83	0.88	88
284.0	284.1	41	TANGENT	CURVE TRANS	0.82	1.00	1.00	Primarily Ditch	0.99	0.98	1.00	0.94	0.99	0.97	97
284.1	284.2	42	TANGENT	CURVE TRANS	0.76	1.00	1.00	Primarily Ditch	0.88	0.76	0.71	0.92	0.78	0.85	85
284.2	284.3	43	TANGENT	CURVE TRANS	0.74	1.00	1.00	Primarily Ditch	1.00	0.87	1.00	0.91	0.96	0.93	93
284.3	284.4	44	RTCURVE	RT CURVE	0.71	1.00	1.00	Primarily Ditch	1.00	0.64	1.00	0.90	0.88	0.89	89
284.4	284.5	45	TANGENT	CURVE TRANS	0.76	0.78	1.00	Primarily Ditch	1.00	0.72	1.00	0.84	0.91	0.88	88
284.5	284.6	46	TANGENT	TANGENT	0.80	0.55	1.00	Primarily Ditch	0.98	0.90	1.00	0.78	0.96	0.87	87
284.6	284.7	47	TANGENT	TANGENT	0.72	0.45	1.00	Primarily Ditch	1.00	0.58	1.00	0.72	0.86	0.79	79
284.7	284.8	48	TANGENT	TANGENT	0.73	0.60	1.00	Primarily Ditch	1.00	0.57	0.54	0.78	0.70	0.74	74
284.8	284.9	49	TANGENT	TANGENT	0.82	0.92	1.00	Primarily Ditch	1.00	0.78	1.00	0.91	0.92	0.92	92
284.9	285.0	50	TANGENT	TANGENT	0.80	0.93	1.00	Primarily Ditch	0.99	0.91	1.00	0.91	0.97	0.94	94
285.0	285.1	51	TANGENT	CURVE TRANS	0.73	0.97	1.00	Primarily Ditch	1.00	0.92	1.00	0.90	0.97	0.93	93
285.1	285.2	52	TANGENT	CURVE TRANS	0.70	0.97	1.00	Primarily Ditch	1.00	0.91	1.00	0.89	0.97	0.93	93
285.2	285.3	53	RTCURVE	RT CURVE	0.70	1.00	1.00	Primarily Ditch	1.00	0.78	1.00	0.90	0.93	0.91	91
285.3	285.4	54	RTCURVE	RT CURVE	0.70	1.00	1.00	Primarily Ditch	1.00	0.81	1.00	0.90	0.94	0.92	92

Data collection for FM 31 began north of IH 20 at reference marker 280 and proceeded southbound. The paved surface ratings reflect the southbound, or K1, lane and the roadside ratings reflect the condition adjacent to the southbound direction of travel. FM 31 consists of one

lane in each direction with a partially flushed, seal-coated surface. Table 24 shows the rating summary for FM 31 on 0.1-mi data collection sections with 0.5-mi increments blocked with color changes.

Table 24 indicates that many of the sections along FM 31 are defined as out of shape. Because of this result, the rating for many of the sections is driven down into the 70s and below. Section 26, at 75 percent, received the lowest roadside drainage rating. The low roadside rating stems from a shallow and flat ditch. Figure 42 is a screenshot from the mobile LiDAR post-processing software, Road Doctor, displaying the shallow and flat ditch in Section 26. Figure 43 represents a digital rendering of the right roadside of Section 26 along FM 31. Researchers created this rendering using the proof of concept code used to apply the network-level rating to large data sets. With a shallow and flat ditch, the expectation would be that the front slope portion of the roadside rating would be high. For Section 26, the front slope receives a 0.99, indicating a steepness slightly steeper than 6H:1V (for front slope rating, see Figure 35)

Figure 42. Section 26 on FM 31.
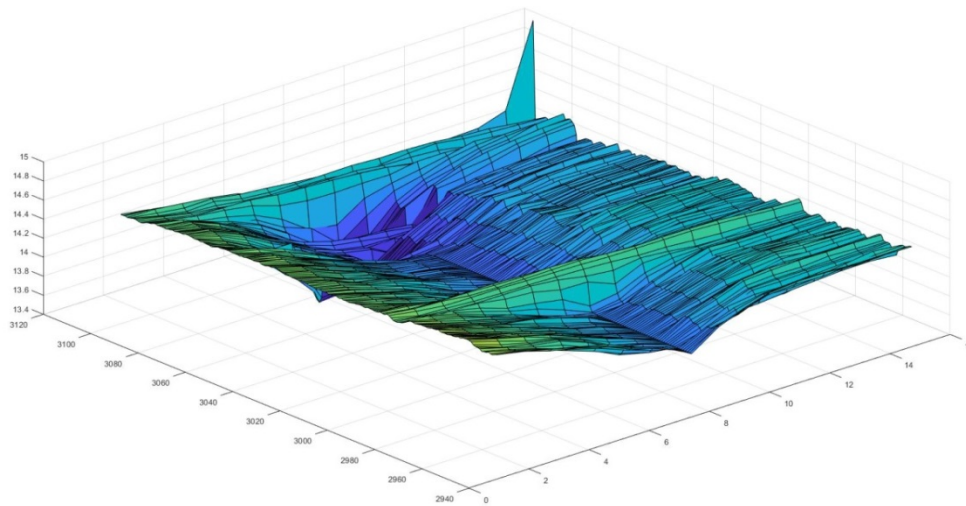
Figure 43. Proof of Concept Code Digital Rendering of Section 26 on FM 31 Right Roadside.

The paved surface rating received additional deductions because of a narrow width. Figure 42 clearly indicates the presence of a well-maintained shoulder beyond the edge stripe. As described in Traveled Way Width rating development, 4R standards were used as the ideal and 3R standards were used as acceptable. Researchers defined acceptable as a passing score of 70 percent, thus any width rating at or above 0.7 indicates a geometric section in compliance with 3R standards. With over 2,500 vehicles per day, FM 31 is required to have 12-ft lanes and 8-ft shoulders to receive a perfect width rating, but can have a 12-ft lane and 2-ft shoulder and receive a width score of 0.7 (see Figure 28 for width rating curves).

The discussion on width and the subsequent rating associated with width illuminates how information within the rating can be drilled down to extract additional information that can be helpful in the management process. Along FM 31, a width change occurs in Section 24, resulting in sections 24 through 54 receiving lower width ratings than sections 1 through 23. The reflectivity data created by Road Doctor clearly display this width change in Figure 44.
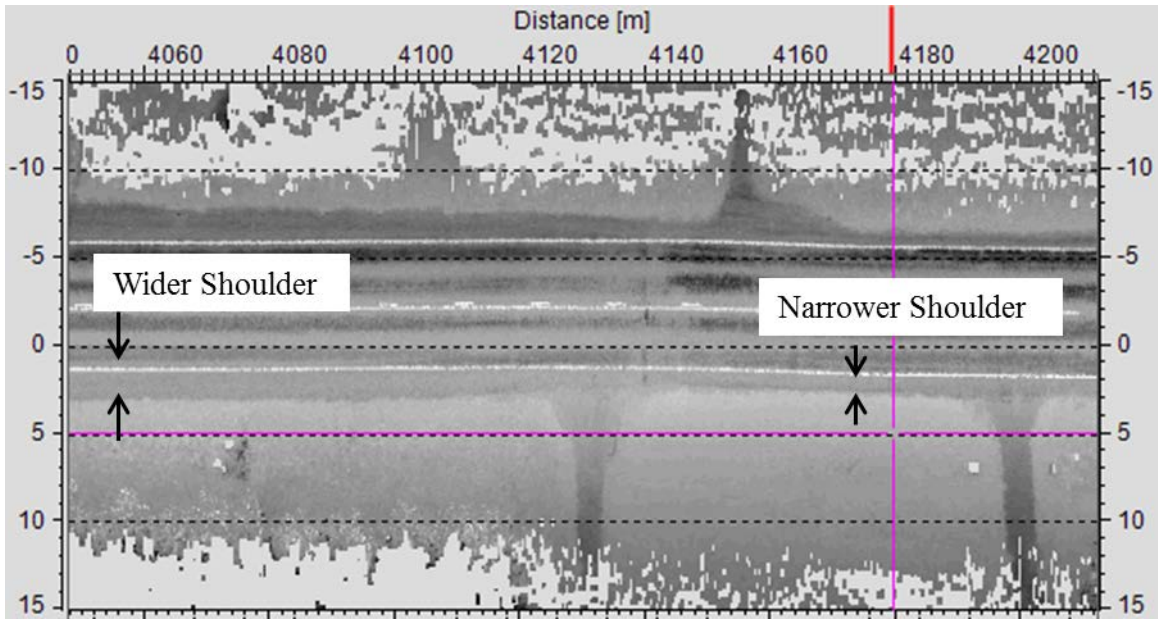
Figure 44. FM 31 Width Transition.

FM 2625—ATLANTA DISTRICT

Researchers collected and rated data on FM 2625 beginning just east of its intersection with US 59. FM 2625 has a partially flushed, seal-coated surface, posted speed limit of 75 mph, and 936 vpd. Table 25 contains the output of the surface drainage rating.

Table 25. FM 2625 Surface Drainage Rating Summary.

Begin TRM	End TRM	Section	Alignment Classificaiton	Section Shape	Roadway Surface RT Width Rating	RT Cross Slope Rating	Hydro-planing Rating	RT Roadside Shape	Roadside Surface RT Front Slope Rating	RT Ditch Depth Rating	RT Ditch Slope Rating	Combined Paved Surface Rating	Combined Roadside Rating	Overall Drainage Rating	Overall Rating Normalized to 100
731.50	731.60	1	LTCURVE	LT CURVE	0.77	1.00	0.70	Primarily Ditch	1.00	1.00	1.00	0.82	1.00	0.91	91
731.60	731.70	2	LTCURVE	LT CURVE	0.80	1.00	0.70	Primarily Ditch	0.97	0.89	1.00	0.83	0.95	0.89	89
731.70	731.80	3	TANGENT	TANGENT	0.86	0.72	0.90	Primarily Ditch	1.00	0.88	1.00	0.83	0.96	0.89	89
731.80	731.90	4	TANGENT	TANGENT	0.80	0.77	0.80	Primarily Ditch	1.00	1.00	1.00	0.79	1.00	0.89	89
731.90	732.00	5	TANGENT	OUT OF SHAPE	0.85	0.00	0.80	Primarily Ditch	1.00	0.99	1.00	0.55	1.00	0.77	77
732.00	732.10	6	TANGENT	TANGENT	0.85	0.72	0.80	Primarily Ditch	1.00	0.93	1.00	0.79	0.98	0.88	88
732.10	732.20	7	TANGENT	TANGENT	0.89	0.81	0.80	Primarily Ditch	0.96	1.00	1.00	0.83	0.99	0.91	91
732.20	732.30	8	RTCURVE	RT CURVE	0.81	1.00	0.80	Primarily Ditch	0.98	1.00	1.00	0.87	0.99	0.93	93
732.30	732.40	9	RTCURVE	CURVE TRANSITION	0.92	0.85	0.90	Primarily Ditch	0.99	0.97	1.00	0.89	0.99	0.94	94
732.40	732.50	10	TANGENT	TANGENT	0.99	0.70	0.70	Primarily Ditch	0.99	0.89	1.00	0.80	0.96	0.88	88
732.50	732.60	11	TANGENT	TANGENT	1.00	0.89	0.80	Primarily Ditch	1.00	0.93	1.00	0.90	0.98	0.94	94
732.60	732.70	12	TANGENT	TANGENT	0.93	0.85	0.80	Primarily Ditch	0.99	1.00	1.00	0.86	1.00	0.93	93
732.70	732.80	13	TANGENT	TANGENT	0.89	0.80	0.70	Primarily Ditch	0.98	0.88	1.00	0.80	0.95	0.87	87
732.80	732.90	14	TANGENT	TANGENT	0.91	0.68	0.70	Primarily Ditch	1.00	0.93	1.00	0.76	0.98	0.87	87
732.90	733.00	15	TANGENT	TANGENT	0.85	0.85	0.80	Primarily Ditch	0.99	0.97	1.00	0.83	0.99	0.91	91
733.00	733.10	16	TANGENT	TANGENT	0.86	0.85	0.80	Primarily Ditch	1.00	0.95	1.00	0.84	0.98	0.91	91
733.10	733.20	17	RTCURVE	OUT OF SHAPE	1.00	0.00	0.80	Primarily Ditch	1.00	0.88	0.73	0.60	0.87	0.73	73
733.20	733.30	18	RTCURVE	OUT OF SHAPE	0.92	0.00	0.80	Primarily Ditch	0.99	0.98	1.00	0.57	0.99	0.78	78
733.30	733.40	19	TANGENT	TANGENT	0.92	0.73	0.80	Primarily Ditch	0.99	0.96	1.00	0.82	0.98	0.90	90
733.40	733.50	20	TANGENT	TANGENT	0.93	0.77	0.80	Primarily Ditch	0.99	0.96	1.00	0.83	0.98	0.91	91
733.50	733.60	21	TANGENT	TANGENT	0.93	0.63	0.80	Primarily FS	0.97	1.00	1.00	0.79	0.99	0.89	89
733.60	733.70	22	TANGENT	TANGENT	0.92	0.56	0.80	Primarily FS	0.96	1.00	1.00	0.76	0.99	0.87	87
733.70	733.80	23	TANGENT	TANGENT	1.00	0.85	0.80	Primarily FS	0.98	1.00	1.00	0.88	0.99	0.94	94
733.80	733.90	24	TANGENT	TANGENT	0.94	0.86	0.80	Primarily Ditch	0.97	1.00	1.00	0.87	0.99	0.93	93
733.90	734.00	25	TANGENT	TANGENT	0.86	0.86	0.70	Primarily Ditch	0.96	0.95	1.00	0.81	0.97	0.89	89
734.00	734.10	26	TANGENT	TANGENT	0.92	0.80	0.70	Primarily Ditch	0.99	0.97	1.00	0.81	0.99	0.90	90
734.10	734.20	27	RTCURVE	RT CURVE	0.94	1.00	0.80	Primarily Ditch	0.98	0.90	1.00	0.91	0.96	0.94	94
734.20	734.30	28	RTCURVE	CURVE TRANSITION	0.94	0.93	0.70	Primarily Ditch	0.97	1.00	1.00	0.86	0.99	0.92	92
734.30	734.40	29	TANGENT	TANGENT	0.96	0.86	0.80	Primarily Ditch	1.00	0.91	0.86	0.87	0.93	0.90	90
734.40	734.50	30	TANGENT	TANGENT	0.98	0.88	0.90	Primarily Ditch	0.99	0.90	1.00	0.92	0.97	0.94	94
734.50	734.60	31	TANGENT	TANGENT	0.92	0.57	0.70	Primarily Ditch	0.97	1.00	1.00	0.73	0.99	0.86	86
734.60	734.70	32	TANGENT	TANGENT	0.88	0.82	0.80	Primarily Ditch	0.98	1.00	0.78	0.84	0.92	0.88	88
734.70	734.80	33	LTCURVE	LT CURVE	0.98	1.00	0.80	Primarily Ditch	0.97	0.96	1.00	0.93	0.98	0.95	95
734.80	734.90	34	LTCURVE	CURVE TRANSITION	1.00	0.90	0.80	Primarily Ditch	0.99	0.92	1.00	0.90	0.97	0.93	93
734.90	735.00	35	TANGENT	TANGENT	0.95	0.79	0.80	Primarily Ditch	0.99	0.94	1.00	0.85	0.98	0.91	91
735.00	735.10	36	TANGENT	TANGENT	0.93	0.68	0.80	Primarily Ditch	0.98	1.00	1.00	0.80	0.99	0.90	90
735.10	735.20	37	TANGENT	TANGENT	0.91	0.74	0.80	Primarily FS	1.00	0.96	1.00	0.82	0.98	0.90	90
735.20	735.30	38	TANGENT	TANGENT	0.86	0.86	0.80	Primarily Ditch	0.98	0.94	1.00	0.84	0.97	0.91	91
735.30	735.40	39	TANGENT	TANGENT	0.82	0.84	0.80	Primarily Ditch	0.99	0.96	1.00	0.82	0.98	0.90	90
735.40	735.50	40	RTCURVE	RT CURVE	0.88	1.00	0.90	Primarily Ditch	1.00	0.91	1.00	0.93	0.97	0.95	95
735.50	735.60	41	RTCURVE	RT CURVE	0.92	1.00	0.70	Primarily Ditch	1.00	0.92	1.00	0.87	0.97	0.92	92
735.60	735.70	42	TANGENT	TANGENT	0.83	0.78	0.80	Primarily Ditch	1.00	0.71	1.00	0.80	0.90	0.85	85
735.70	735.80	43	TANGENT	TANGENT	0.79	0.71	0.70	Primarily Ditch	1.00	0.93	1.00	0.73	0.98	0.85	85
735.80	735.90	44	TANGENT	TANGENT	0.81	0.75	0.70	Primarily Ditch	1.00	0.98	1.00	0.75	0.99	0.87	87
735.90	736.00	45	TANGENT	TANGENT	0.93	0.65	0.80	Primarily Ditch	1.00	0.95	1.00	0.79	0.98	0.89	89
736.00	736.10	46	TANGENT	TANGENT	0.96	0.74	0.80	Primarily FS	1.00	0.96	1.00	0.83	0.99	0.91	91
736.10	736.20	47	TANGENT	TANGENT	0.86	0.85	0.80	Primarily Ditch	1.00	1.00	1.00	0.84	1.00	0.92	92
736.20	736.30	48	TANGENT	TANGENT	0.76	0.85	0.80	Primarily Ditch	0.98	1.00	1.00	0.80	0.99	0.90	90
736.30	736.40	49	TANGENT	OUT OF SHAPE	0.71	0.00	0.70	Primarily Ditch	0.97	0.91	1.00	0.47	0.96	0.71	71
736.40	736.50	50	TANGENT	OUT OF SHAPE	0.95	0.00	0.70	Primarily Ditch	1.00	1.00	1.00	0.55	1.00	0.77	77
736.50	736.60	51	TANGENT	TANGENT	0.93	0.92	0.80	Primarily Ditch	0.93	1.00	1.00	0.88	0.98	0.93	93
736.60	736.70	52	TANGENT	TANGENT	0.88	0.83	0.80	Primarily Ditch	0.99	0.89	1.00	0.84	0.96	0.90	90
736.70	736.80	53	TANGENT	TANGENT	0.80	0.85	0.80	Primarily Ditch	0.98	0.82	1.00	0.82	0.93	0.88	88
736.80	736.90	54	TANGENT	TANGENT	0.82	0.84	0.80	Primarily Ditch	0.98	0.97	1.00	0.82	0.98	0.90	90
736.90	737.00	55	TANGENT	TANGENT	0.81	0.85	0.80	Primarily Ditch	0.99	0.95	1.00	0.82	0.98	0.90	90
737.00	737.10	56	TANGENT	TANGENT	0.79	0.78	0.80	Primarily Ditch	0.99	0.89	1.00	0.79	0.96	0.87	87
737.10	737.20	57	TANGENT	TANGENT	0.78	0.84	0.70	Primarily Ditch	0.99	1.00	1.00	0.77	1.00	0.89	89
737.20	737.30	58	TANGENT	TANGENT	0.82	0.79	0.80	Primarily Ditch	0.98	1.00	1.00	0.80	0.99	0.90	90
737.30	737.40	59	TANGENT	OUT OF SHAPE	0.91	0.00	0.70	Primarily Ditch	0.98	0.92	1.00	0.54	0.97	0.75	75
737.40	737.50	60	TANGENT	TANGENT	0.93	0.77	0.80	Primarily Ditch	1.00	0.90	1.00	0.84	0.97	0.90	90
737.50	737.60	61	TANGENT	TANGENT	0.82	0.80	0.80	Primarily Ditch	0.98	1.00	1.00	0.81	0.99	0.90	90
737.60	737.70	62	TANGENT	TANGENT	0.82	0.92	0.80	Primarily Ditch	1.00	0.92	1.00	0.85	0.97	0.91	91
737.70	737.80	63	TANGENT	TANGENT	0.92	0.86	0.80	Primarily Ditch	1.00	0.94	1.00	0.86	0.98	0.92	92
737.80	737.90	64	TANGENT	TANGENT	0.78	0.85	0.80	Primarily Ditch	1.00	1.00	1.00	0.81	1.00	0.90	90
737.90	738.00	65	TANGENT	TANGENT	0.80	0.93	0.80	Primarily Ditch	1.00	0.93	1.00	0.84	0.98	0.91	91

This portion of FM 2625 has high surface drainage ratings, particularly for the roadside. Only sections deemed as out of shape have ratings in the 70s. Section 17 has the lowest roadside rating and one of the lowest combined ratings. Within Section 17, the roadside rating is 87 percent and the paved surface rating is 60 percent. The paved surface rating is driven downward because the section is out of shape and because it receives a hydroplaning rating of 80 percent. A hydroplaning rating of 80 percent indicates the calculated HPS for this section is between 10 mph and 15 mph below the posted speed limit. For section 17, the HPS was calculated as 59 mph. With a posted speed limit of 70 mph, the 11-mph difference leads to a rating of 0.80. Section 17 also has a ditch depth of 2.4 ft with a flowline slope of 0.73 percent, both below the thresholds to receive a perfect score. Figure 45 is a picture of Section 17. Within Figure 45, it appears the superelevation for the right curve is following the wrong direction toward the left of the screen. Section 17 was identified as out of shape. While Figure 45 looks similar to Figure 42 in terms of roadway width, FM 2625 receives consistently higher ratings associated for width. The reason for this is the difference in average annual daily traffic. FM 2625 has less than 1500 vpd and uses a less punitive width curve than FM 31.
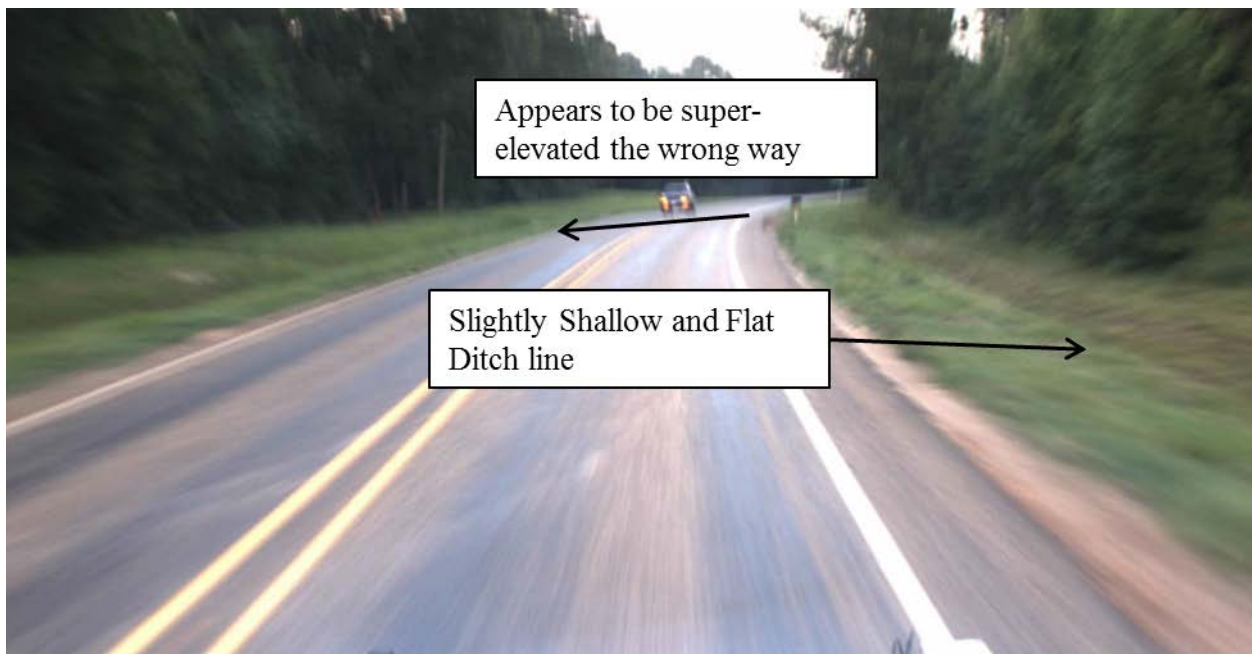
Figure 45. Section 17 on FM 2625.

While Figure 45 displays a curve that is out of shape, other curves along FM 2625 are within shape and receive good ratings. For example, Section 41 is a right curve that is in shape and receives an overall rating of 92. The primary deduction within Section 41 comes from a hydroplaning potential rating of 0.70 due to a posted speed limit of 70 mph and a potential hydroplaning speed of 54 mph. Using mobile LiDAR data and IMU readings, researchers calculated the radius of the curve within Section 41 to be 6,420 ft and the superelevation to be 2.4 percent. Using the calculations described in the Hydroplaning Potential. portion of the report, with the minimum friction factor associated with 80 mph, the required curve radius for Section

41 is 2,308 ft. Therefore, with a radius of over 6,000 ft, this section receives a 1.0 rating for cross-slope.

Figure 46 displays the profile of Section 41 along FM 2625 created using the proof of concept code for network-level applications. Figure 46 indicates that in the direction of travel, the section is in a vertical curve in addition to the horizontal curve described above. The spike shown in Figure 46 comes from the laser striking a passing vehicle. The fact that the section falls within a horizontal and vertical curve helps explain the hydroplaning potential, with the slight superelevation pushing the water from one side of the pavement to the other and the vertical curve assisting in keeping the water on the pavement rather than flowing off of the pavement onto the roadside. Figure 47 was also created within the proof of concept code and shows the cross-section of Section 41, displaying the slight superelevation with the rightward tilt. Finally, Figure 48 was created to show the right roadside. The right roadside receives a rating of 0.97 since the fall in the ditch flowline and the depth of the ditch is easily noticeable in Figure 48.
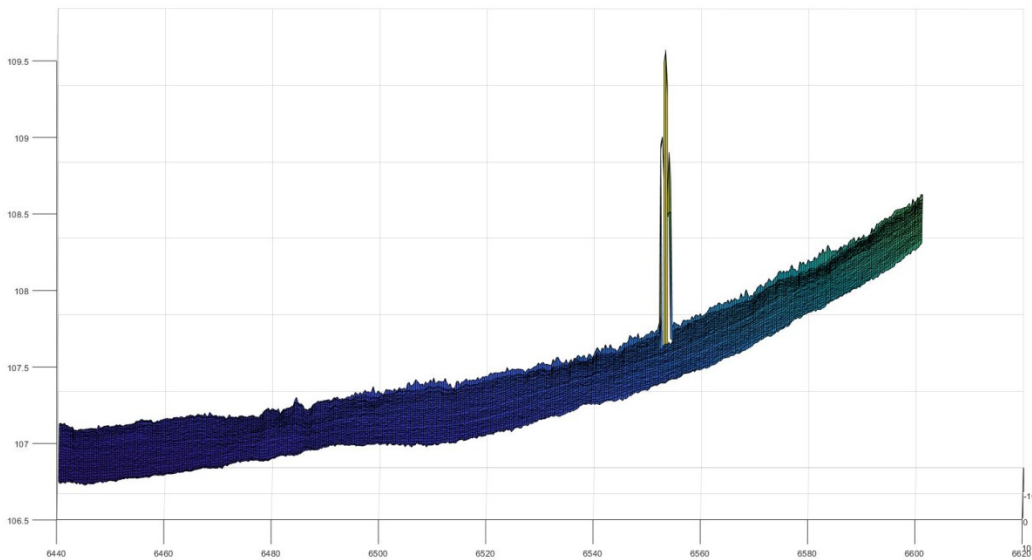
Figure 46. Proof of Concept Code Digital Rendering of Section 41 on FM 2625 Profile.

90
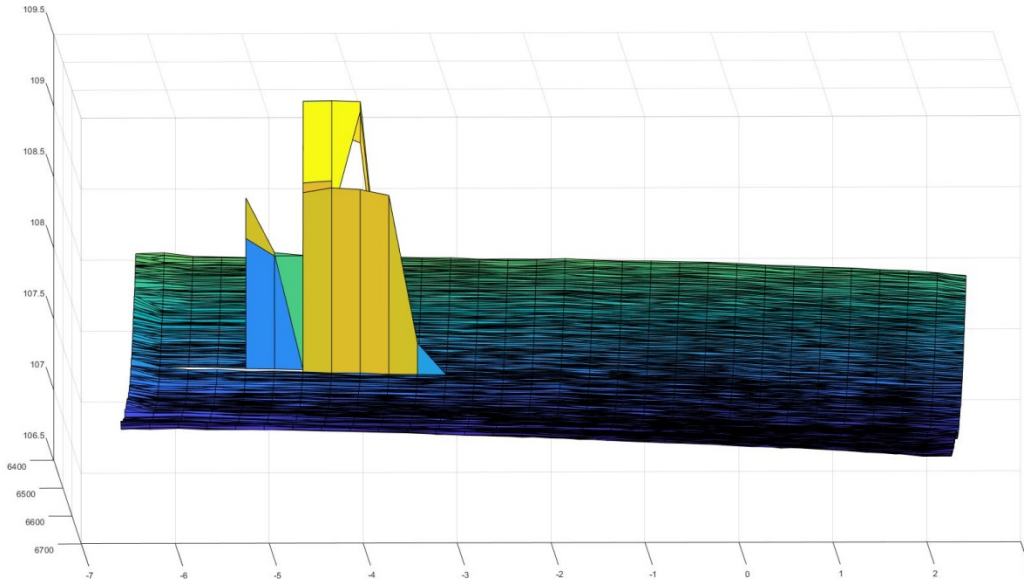
Figure 47. Proof of Concept Code Digital Rendering of Section 41 on FM 2625 Cross-Section.
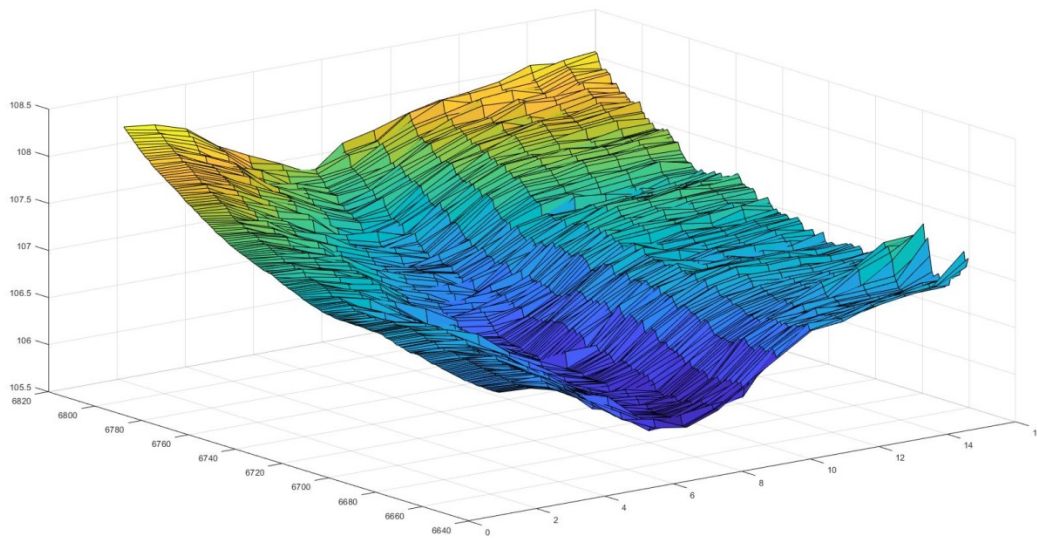
Figure 48. Proof of Concept Code Digital Rendering of Section 41 on FM 2625 Right Roadside.

FM 2983—ATLANTA DISTRICT

FM 2983 is a very short roadway connecting FM 31 and US 59 that essentially runs parallel to US 59, before turning back to intersect with US 59. The roadway only carriers 134 vpd and has a posted speed limit of 55 mph. Table 26 is the network rating output for FM 2983.

Table 26. FM 2983 Surface Drainage Rating Summary.

Begin TRM	End TRM	Section	Alignment Classificaiton	Section Shape	Roadway Surface				Roadside Surface			Combined Paved Surface Rating	Combined Roadside Rating	Overall Drainage Rating	Overall Rating Normalized to 100
					RT Width Rating	RT Cross Slope Rating	Hydro-planing Rating	RT Roadside Shape	RT Front Slope Rating	RT Ditch Depth Rating	RT Ditch Slope Rating				
284.0	284.1	1	RT CURVE	RT CURVE	0.80	0.00	1.00	Primarily Ditch	0.99	0.83	1.00	0.60	0.94	0.77	77
284.1	284.2	2	TANGENT	OUT OF SHAPE	0.88	0.00	1.00	Primarily Ditch	0.99	0.83	1.00	0.63	0.94	0.78	78
284.2	284.3	3	LT CURVE	CURVE TRANSITION	0.84	0.43	1.00	Primarily Ditch	1.00	0.84	1.00	0.76	0.95	0.85	85
284.3	284.4	4	LT CURVE	LT CURVE	1.00	0.86	1.00	Primarily Ditch	1.00	0.83	1.00	0.95	0.94	0.95	95
284.4	284.5	5	LT CURVE	CURVE TRANSITION	0.78	0.43	1.00	Primarily Ditch	0.99	1.00	1.00	0.74	1.00	0.87	87
284.5	284.6	6	RT CURVE	OUT OF SHAPE	0.77	0.00	1.00	Primarily Ditch	0.98	0.88	1.00	0.59	0.95	0.77	77
284.6	284.7	7	TANGENT	TANGENT	0.81	0.78	1.00	Primarily Ditch	1.00	0.68	1.00	0.86	0.89	0.88	88
284.7	284.8	8	RT CURVE	OUT OF SHAPE	0.84	0.00	1.00	Primarily Ditch	0.94	0.61	1.00	0.61	0.85	0.73	73
284.8	284.9	9	TANGENT	CURVE TRANSITION	0.81	0.50	1.00	Primarily Ditch	0.96	0.59	0.58	0.77	0.71	0.74	74
284.9	285.0	10	LT CURVE	LT CURVE	0.98	1.00	1.00	Primarily Ditch	1.00	0.92	1.00	0.99	0.97	0.98	98
285.0	285.1	11	LT CURVE	LT CURVE	0.92	1.00	1.00	Primarily Ditch	0.99	1.00	1.00	0.97	1.00	0.99	99
285.1	285.2	12	TANGENT	CURVE TRANSITION	0.80	1.00	1.00	Primarily Ditch	1.00	1.00	1.00	0.93	1.00	0.97	97
285.2	285.3	13	LT CURVE	LT CURVE	0.82	1.00	1.00	Primarily Ditch	0.91	0.82	1.00	0.94	0.91	0.92	92
285.3	285.4	14	TANGENT	CURVE TRANSITION	0.79	0.50	1.00	Primarily Ditch	0.98	1.00	1.00	0.76	0.99	0.88	88
285.4	285.5	15	LT CURVE	LT CURVE	0.70	0.00	1.00	Primarily Ditch	0.88	1.00	1.00	0.57	0.96	0.76	76

Table 26 provides a rating not yet seen. Both Section 1 and Section 15 are in shape and part of curves, yet the cross-slope rating is 0.0 for each section. When this rating appears within a curve, it implies that the radius of the curve is shorter than the radius required at a 25-mph speed difference using the posted speed limit friction factor. Using mobile LiDAR data, researchers calculated the radius for Section 1 to be 463 ft and the radius for Section 15 to be 377 ft, with minimum required radii of 507 ft and 490 ft, respectively. From this perspective, the calculated radii are not far from the minimum required for a 25-mph differential, so it would possible to mitigate the poor cross-slope rating with curve advisory signs and with speed advisory plaques and chevrons. Figure 49 and Figure 50 display each of these curves and show that no advisory signs or chevrons are installed. It is possible that because each section enters and exits a stop condition with stop advisory signs in place that the speed is low enough that chevrons are not needed on these curves. The surface drainage rating allows engineers and managers to drill down into the rating and make engineering decisions such as that one just described.

Figure 49. Section 1 on FM 2983.

Figure 50. Section 15 on FM 2983.

US 59—ATLANTA DISTRICT

Researchers rated US 59 from just south of the FM 2983 intersection to just north of the FM 1186 intersection. The posted speed limit for US 59 in this area is 75 mph, indicating that hydroplaning speed might be impacted within the rating. Table 27 shows the rating output for US 59. Hydroplaning ratings for each section never exceeds 70 percent, with two sections receiving a rating of 50 percent. The 50 percent hydroplaning speed rating implies that the section can only withstand vehicle speeds between 20 mph and 25 mph below the posted speed

limit. With a posted speed limit of 75 mph, the hydroplaning speed in section 6 and 10 is calculated between 50 mph and 55 mph. The actual calculations are 55 mph and 54 mph, respectively, with corresponding WFTs of 0.16 in. and 0.17 in. A review of Section 10 finds that the water accumulation is wide, at 18 ft, and the flow path contributing to the WFT is approximately 53 ft. Figure 51 is a screen capture of Section 10. Within Figure 51, it appears US 59 is flowing toward the data collection vehicles as it travels up a vertical curve. This situation is indeed the case. With the geometric configuration of both southbound lanes flowing to the right and the additional surface water provided by the turn lane, the WFT increases. With an increase in WFT, the hydroplaning rating decreases.

Table 27. US 59 Surface Drainage Rating Summary.

Begin TRM	End TRM	Section	Alignment Classificaiton	Section Shape	Roadway Surface			RT Roadside Shape	Roadside Surface					Overall Drainage Rating	Overall Rating Normalized to 100
					RT Width Rating	RT Cross Slope Rating	Hydro-planing Rating		RT Front Slope Rating	RT Ditch Depth Rating	RT Ditch Slope Rating	Combined Paved Surface Rating	Combined Roadside Rating		
293.4	293.5	1	TANGENT	TANGENT	1.00	0.25	0.70	Primarily Ditch	0.99	0.97	1.00	0.65	0.99	0.82	82
293.5	293.6	2	TANGENT	TANGENT	1.00	1.00	0.70	Primarily Ditch	0.97	0.86	1.00	0.90	0.94	0.92	92
293.6	293.7	3	TANGENT	TANGENT	1.00	1.00	0.70	Various Drainage	1.00	0.79	1.00	0.90	0.93	0.91	91
293.7	293.8	4	TANGENT	TANGENT	1.00	0.70	0.70	Primarily Ditch	1.00	0.92	1.00	0.80	0.97	0.89	89
293.8	293.9	5	TANGENT	TANGENT	1.00	0.70	0.70	Primarily Ditch	1.00	0.92	1.00	0.80	0.97	0.89	89
293.9	294.0	6	TANGENT	TANGENT	1.00	0.70	0.50	Primarily Ditch	0.90	0.93	1.00	0.73	0.94	0.84	84
294.0	294.1	7	TANGENT	TANGENT	1.00	1.00	0.70	Primarily FS	1.00	0.84	1.00	0.90	0.95	0.92	92
294.1	294.2	8	TANGENT	TANGENT	1.00	0.50	0.70	Primarily FS	1.00	0.83	1.00	0.73	0.94	0.84	84
294.2	294.3	9	TANGENT	TANGENT	1.00	1.00	0.70	Primarily Ditch	0.99	0.87	0.70	0.90	0.86	0.88	88
294.3	294.4	10	TANGENT	TANGENT	1.00	0.50	0.50	Primarily FS	0.91	0.87	1.00	0.67	0.93	0.80	80
294.4	294.5	11	TANGENT	TANGENT	1.00	0.50	0.70	Primarily Ditch	1.00	0.82	1.00	0.73	0.94	0.84	84
294.5	294.6	12	RT CURVE	CURVE TRANSITION	1.00	0.75	0.70	Primarily Ditch	1.00	0.89	1.00	0.82	0.96	0.89	89
294.6	294.7	13	RT CURVE	RT CURVE	1.00	1.00	0.70	Primarily Ditch	1.00	0.98	1.00	0.90	0.99	0.95	95
294.7	294.8	14	RT CURVE	RT CURVE	1.00	1.00	0.70	Primarily Ditch	0.99	0.82	1.00	0.90	0.94	0.92	92
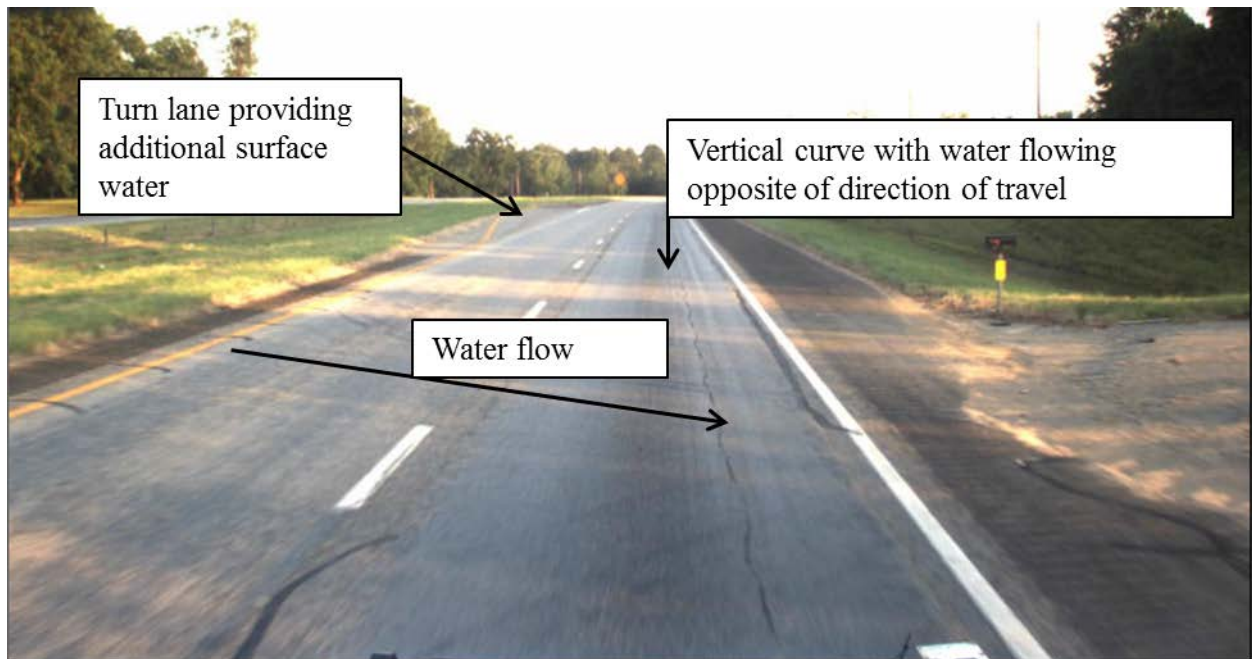
Figure 51. Section 10 on US 59.

FM 1186—ATLANTA DISTRICT

Researchers rated 6.6 mi of FM 1186 between the US 59 intersection and its split with FM 1794, south of the Harrison County line. This portion of FM 1186 has front slopes steeper than 6H:1V, but in most instances front slopes are flatter than 4H:1V. The exception comes in Section 14, where the front slope rating is 74 percent, indicating a steepness between 3.5H:1V and 3H:1V. Shallow and flat ditches appear in sections 63 and 64, with the roadside rating in Section 64 below 70 percent. While isolated roadside conditions affect the rating on FM 1186, the primary driver of low ratings comes from the out-of-shape classification in 32 of the 66 sections. The results for all 66 sections of FM 1186 are shown in Table 28.

Table 28. FM 1186 Surface Drainage Rating Summary.

Begin TRM	End TRM	Section	Alignment Classificaiton	Section Shape	Roadway Surface				Roadside Surface						Overall Rating Normalized to 100
					RT Width Rating	RT Cross Slope Rating	Hydro-planing Rating	RT Roadside Shape	RT Front Slope Rating	RT Ditch Depth Rating	RT Ditch Slope Rating	Combined Surface Rating	Combined Roadside Rating	Overall Drainage Rating	
284	284.1	1	RTCURVE	RT CURVE	1.00	0.47	0.90	Primarily FS	1.00	1.00	1.00	0.79	1.00	0.90	90
284.1	284.2	2	TANGENT	CURVE TRANSITION	0.73	0.55	0.70	Primarily Ditch	0.97	0.68	0.79	0.66	0.81	0.74	74
284.2	284.3	3	TANGENT	TANGENT	0.64	0.63	0.70	Primarily Ditch	1.00	0.94	0.97	0.65	0.97	0.81	81
284.3	284.4	4	TANGENT	TANGENT	0.70	0.79	0.70	Primarily Ditch	0.93	0.85	1.00	0.73	0.93	0.83	83
284.4	284.5	5	TANGENT	OUT OF SHAPE	0.75	0.00	0.80	Primarily Ditch	1.00	0.83	1.00	0.52	0.94	0.73	73
284.5	284.6	6	TANGENT	OUT OF SHAPE	0.75	0.00	0.70	Primarily Ditch	0.99	0.89	1.00	0.48	0.96	0.72	72
284.6	284.7	7	LTCURVE	CURVE TRANSITION	0.98	0.50	0.70	Primarily Ditch	1.00	0.98	1.00	0.73	0.99	0.86	86
284.7	284.8	8	LTCURVE	LT CURVE	0.93	1.00	0.90	Primarily Ditch	1.00	0.91	1.00	0.94	0.97	0.96	96
284.8	284.9	9	LTCURVE	LT CURVE	1.00	1.00	1.00	Primarily FS	1.00	1.00	1.00	1.00	1.00	1.00	100
284.9	285	10	LTCURVE	CURVE TRANSITION	1.00	0.85	0.80	Primarily Ditch	1.00	0.90	1.00	0.88	0.97	0.92	92
285	285.1	11	TANGENT	TANGENT	1.00	0.70	0.80	Primarily Ditch	0.99	0.90	1.00	0.83	0.96	0.90	90
285.1	285.2	12	TANGENT	TANGENT	1.00	0.92	0.70	Primarily Ditch	0.92	1.00	1.00	0.87	0.97	0.92	92
285.2	285.3	13	TANGENT	TANGENT	1.00	0.89	0.70	Primarily Ditch	0.91	1.00	1.00	0.86	0.97	0.92	92
285.3	285.4	14	TANGENT	OUT OF SHAPE	0.65	0.00	0.80	Primarily Ditch	0.74	1.00	1.00	0.48	0.91	0.70	70
285.4	285.5	15	TANGENT	OUT OF SHAPE	1.00	0.00	0.70	Primarily Ditch	0.98	1.00	1.00	0.57	0.99	0.78	78
285.5	285.6	16	TANGENT	OUT OF SHAPE	1.00	0.00	0.70	Primarily Ditch	0.93	1.00	1.00	0.60	0.98	0.79	79
285.6	285.7	17	RTCURVE	CURVE TRANSITION	1.00	0.50	0.90	Primarily Ditch	0.97	1.00	1.00	0.80	0.99	0.89	89
285.7	285.8	18	RTCURVE	RT CURVE	1.00	1.00	0.90	Primarily FS	1.00	1.00	1.00	0.97	1.00	0.98	98
285.8	285.9	19	RTCURVE	CURVE TRANSITION	1.00	0.85	0.90	Primarily FS	1.00	0.99	1.00	0.92	1.00	0.96	96
285.9	286	20	TANGENT	TANGENT	1.00	0.71	0.90	Primarily Ditch	1.00	0.73	1.00	0.87	0.91	0.89	89
286	286.1	21	TANGENT	TANGENT	0.91	0.84	0.80	Primarily Ditch	1.00	0.84	1.00	0.85	0.95	0.90	90
286.1	286.2	22	TANGENT	TANGENT	0.81	0.77	0.80	Primarily Ditch	1.00	0.82	1.00	0.79	0.94	0.87	87
286.2	286.3	23	TANGENT	TANGENT	0.84	0.73	0.80	Primarily Ditch	0.95	1.00	1.00	0.79	0.98	0.89	89
286.3	286.4	24	TANGENT	TANGENT	0.64	0.67	0.80	Primarily Ditch	0.97	1.00	1.00	0.70	0.99	0.85	85
286.4	286.5	25	TANGENT	TANGENT	0.78	0.64	0.70	Primarily Ditch	0.99	0.74	1.00	0.71	0.91	0.81	81
286.5	286.6	26	TANGENT	TANGENT	0.78	0.56	0.70	Primarily Ditch	1.00	0.85	1.00	0.68	0.95	0.81	81
286.6	286.7	27	TANGENT	OUT OF SHAPE	0.69	0.00	0.70	Primarily Ditch	0.97	1.00	1.00	0.46	0.99	0.73	73
286.7	286.8	28	RTCURVE	OUT OF SHAPE	0.66	0.00	0.70	Primarily Ditch	1.00	1.00	1.00	0.45	1.00	0.73	73
286.8	286.9	29	TANGENT	OUT OF SHAPE	0.68	0.00	0.70	Primarily Ditch	1.00	1.00	1.00	0.46	1.00	0.73	73
286.9	287	30	LTCURVE	OUT OF SHAPE	0.73	0.65	0.80	Primarily Ditch	1.00	0.98	1.00	0.72	0.99	0.86	86
287	287.1	31	TANGENT	TANGENT	0.81	0.76	0.70	Primarily Ditch	0.97	0.89	1.00	0.76	0.95	0.85	85
287.1	287.2	32	TANGENT	TANGENT	0.81	0.68	0.70	Primarily Ditch	1.00	0.85	1.00	0.73	0.95	0.84	84
287.2	287.3	33	TANGENT	OUT OF SHAPE	0.82	0.00	0.80	Primarily Ditch	0.98	0.97	1.00	0.54	0.98	0.76	76
287.3	287.4	34	TANGENT	OUT OF SHAPE	0.87	0.00	0.80	Primarily Ditch	0.99	1.00	1.00	0.56	1.00	0.78	78
287.4	287.5	35	LTCURVE	OUT OF SHAPE	0.76	0.00	0.70	Primarily Ditch	1.00	0.94	1.00	0.49	0.98	0.73	73
287.5	287.6	36	LTCURVE	OUT OF SHAPE	0.77	0.00	0.70	Primarily Ditch	1.00	1.00	1.00	0.49	1.00	0.74	74
287.6	287.7	37	LTCURVE	OUT OF SHAPE	0.82	0.00	0.80	Primarily Ditch	0.90	0.94	1.00	0.54	0.95	0.74	74
287.7	287.8	38	TANGENT	OUT OF SHAPE	0.93	0.00	0.80	Primarily Ditch	1.00	0.84	1.00	0.58	0.95	0.76	76
287.8	287.9	39	TANGENT	TANGENT	0.78	0.78	0.70	Primarily Ditch	0.90	0.94	1.00	0.75	0.95	0.85	85
287.9	288	40	TANGENT	OUT OF SHAPE	0.82	0.00	0.80	Primarily Ditch	0.99	0.91	1.00	0.54	0.97	0.75	75
288	288.1	41	RTCURVE	OUT OF SHAPE	0.76	0.00	0.70	Primarily Ditch	1.00	0.90	1.00	0.49	0.97	0.73	73
288.1	288.2	42	TANGENT	OUT OF SHAPE	0.75	0.00	0.80	Primarily Ditch	1.00	0.98	1.00	0.52	0.99	0.76	76
288.2	288.3	43	RTCURVE	OUT OF SHAPE	0.74	0.00	0.80	Primarily Ditch	0.99	0.91	1.00	0.51	0.97	0.74	74
288.3	288.4	44	RTCURVE	OUT OF SHAPE	0.82	0.00	0.90	Primarily Ditch	1.00	0.89	1.00	0.57	0.96	0.77	77
288.4	288.5	45	RTCURVE	OUT OF SHAPE	0.82	0.00	0.80	Primarily Ditch	1.00	0.85	1.00	0.54	0.95	0.74	74
288.5	288.6	46	TANGENT	OUT OF SHAPE	0.74	0.00	0.70	Primarily Ditch	0.97	0.81	1.00	0.48	0.93	0.70	70
288.6	288.7	47	TANGENT	TANGENT	0.72	0.70	0.70	Primarily Ditch	0.92	0.80	1.00	0.71	0.91	0.81	81
288.7	288.8	48	RTCURVE	RT CURVE	0.67	1.00	0.90	Primarily Ditch	0.91	0.72	1.00	0.86	0.87	0.87	87
288.8	288.9	49	RTCURVE	RT CURVE	0.72	1.00	0.90	Primarily Ditch	1.00	0.90	1.00	0.87	0.97	0.92	92
288.9	289	50	TANGENT	CURVE TRANSITION	0.74	0.50	0.70	Primarily Ditch	1.00	0.83	1.00	0.65	0.94	0.79	79
289	289.1	51	TANGENT	OUT OF SHAPE	0.71	0.00	0.80	Primarily Ditch	0.99	0.84	1.00	0.50	0.94	0.72	72
289.1	289.2	52	TANGENT	OUT OF SHAPE	0.59	0.00	0.80	Primarily Ditch	0.91	0.82	1.00	0.46	0.91	0.68	68
289.2	289.3	53	TANGENT	OUT OF SHAPE	0.61	0.00	0.70	Primarily Ditch	1.00	0.90	1.00	0.44	0.97	0.70	70
289.3	289.4	54	TANGENT	TANGENT	0.71	0.84	0.80	Primarily Ditch	1.00	0.78	1.00	0.78	0.93	0.85	85
289.4	289.5	55	TANGENT	OUT OF SHAPE	0.62	0.00	0.80	Primarily Ditch	1.00	0.85	1.00	0.47	0.95	0.71	71
289.5	289.6	56	TANGENT	OUT OF SHAPE	0.62	0.00	0.70	Primarily FS	1.00	0.93	1.00	0.44	0.98	0.71	71
289.6	289.7	57	TANGENT	OUT OF SHAPE	0.81	0.00	0.70	Primarily Ditch	1.00	0.88	1.00	0.50	0.96	0.73	73
289.7	289.8	58	TANGENT	OUT OF SHAPE	0.82	0.00	0.70	Primarily Ditch	1.00	0.94	1.00	0.51	0.98	0.74	74
289.8	289.9	59	TANGENT	OUT OF SHAPE	0.72	0.00	0.70	Primarily Ditch	1.00	0.90	1.00	0.47	0.97	0.72	72
289.9	290	60	TANGENT	OUT OF SHAPE	0.71	0.00	0.80	Primarily Ditch	0.97	1.00	1.00	0.50	0.99	0.75	75
290	290.1	61	LTCURVE	CURVE TRANSITION	0.58	0.50	0.80	Primarily Ditch	1.00	0.88	0.94	0.63	0.94	0.78	78
290.1	290.2	62	LTCURVE	LT CURVE	0.66	1.00	1.00	Primarily Ditch	0.99	0.76	1.00	0.89	0.92	0.90	90
290.2	290.3	63	LTCURVE	CURVE TRANSITION	0.71	0.50	0.80	Primarily Ditch	0.99	0.68	0.74	0.67	0.81	0.74	74
290.3	290.4	64	TANGENT	OUT OF SHAPE	0.79	0.00	0.70	Primarily Ditch	0.93	0.64	0.51	0.50	0.69	0.59	59
290.4	290.5	65	TANGENT	TANGENT	0.70	0.92	0.80	Primarily Ditch	0.98	0.83	0.85	0.81	0.89	0.85	85
290.5	290.6	66	TANGENT	OUT OF SHAPE	0.69	0.00	0.70	Primarily FS	1.00	0.91	1.00	0.46	0.97	0.72	72

In reality, Section 14 falls within a guardrail section protecting a large drainage structure. Researchers chose this section as an example of a potential flaw in network-level ratings. When vast amounts of information need to be processed with little manual intervention, special scenarios might be missed. Presently, this causes little trouble because it allows managers or engineers to investigate the reasonableness of the rating. With video files stored with the LiDAR data, this can be done without a field visit. Figure 52 displays Section 14 and clearly shows the guardrail. A reasonable question is, "How did the rating still provide a rating of 74 percent when there is a vertical drop-off beyond the guardrail?" The vegetation growing in the channel provided a target surface for the laser, and the elevation difference between the roadway surface and the vegetation was such that it appeared a slope was present.

Figure 52. Section 14 on FM 1186.

Figure 53 shows Section 64 along FM 1186. Within Figure 53, the shallow and flat ditch along the right side of the roadway is apparent. The lack of shoulder width speaks to the width rating of 0.70. In fact, the right traveled way width in this section averages 12.04 ft, just wide enough to maintain a passing rating.

Figure 53. Section 64 on FM 1186.

FM 2661—TYLER DISTRICT

FM 2661 in the Tyler District represents the longest continuous section rated within the study. Researchers rated FM 2661 from near the SH 155 intersection north to near the SH 64 intersection for a total of 12.6 mi. FM 2661 is the only roadway rated via counter flow to increasing reference markers. This was done to avoid an obstruction in the southbound lane just south of the SH 31 intersection. Rating FM 2661 was interrupted three times by geometric changes associated with turn lanes or major intersections. These interruptions are similar to the unknown presence of guardrails, as discussed with FM 1186. For FM 2661, these sections were removed from the rating. Table 29 displays the rating output.

Table 29. FM 2661 Surface Drainage Rating Summary.

Begin TRM	End TRM	Section	Alignment Classificaiton	Section Shape	Roadway Surface RT Width Rating	RT Cross Slope Rating	Hydro-planing Rating	RT Roadside Shape	Roadside Surface RT Front Slope Rating	RT Ditch Depth Rating	RT Ditch Slope Rating	Combined Surface Rating	Combined Roadside Rating	Overall Drainage Rating	Overall Rating Normalized to 100
302.7	302.6	1	TANGENT	TANGENT	0.80	0.04	1.00	Primarily Ditch	1.00	0.85	1.00	0.61	0.95	0.78	78
302.6	302.5	2	TANGENT	TANGENT	0.77	0.42	0.90	Primarily Ditch	1.00	0.91	1.00	0.70	0.97	0.83	83
302.5	302.4	3	TANGENT	CURVE TRANSITION	0.76	0.71	1.00	Various Drainage	1.00	0.87	1.00	0.82	0.96	0.89	89
302.4	302.3	4	RTCURVE	RT CURVE	0.76	1.00	1.00	Primarily Ditch	1.00	0.75	0.93	0.92	0.89	0.91	91
302.3	302.2	5	RTCURVE	RT CURVE	0.77	1.00	0.90	Primarily Ditch	1.00	0.75	1.00	0.89	0.92	0.90	90
302.2	302.1	6	TANGENT	CURVE TRANSITION	0.83	0.90	1.00	Primarily FS	1.00	0.86	1.00	0.91	0.95	0.93	93
302.1	302	7	TANGENT	TANGENT	0.79	0.79	0.90	Primarily FS	1.00	1.00	1.00	0.83	1.00	0.91	91
302	301.9	8	RTCURVE	CURVE TRANSITION	0.77	0.90	0.90	Primarily Ditch	0.97	0.77	1.00	0.86	0.91	0.88	88
301.9	301.8	9	RTCURVE	RT CURVE	0.75	1.00	1.00	Primarily FS	0.95	0.93	1.00	0.92	0.96	0.94	94
301.8	301.7	10	RTCURVE	RT CURVE	0.79	1.00	1.00	Primarily Ditch	1.00	0.74	1.00	0.93	0.91	0.92	92
301.7	301.6	11	TANGENT	TANGENT	0.82	0.69	0.90	Primarily FS	0.96	0.79	1.00	0.80	0.92	0.86	86
301.6	301.5	12	TANGENT	TANGENT	0.85	0.57	0.90	Primarily Ditch	0.98	0.77	1.00	0.77	0.92	0.84	84
301.5	301.4	13	TANGENT	TANGENT	0.81	0.59	0.90	Primarily FS	0.92	1.00	1.00	0.77	0.97	0.87	87
301.4	301.3	14	TANGENT	TANGENT	0.76	0.62	0.90	Primarily Ditch	1.00	0.84	1.00	0.76	0.95	0.85	85
301.3	301.2	15	TANGENT	TANGENT	0.75	0.81	0.90	Primarily Ditch	0.97	0.75	1.00	0.82	0.91	0.86	86
301.2	301.1	16	TANGENT	TANGENT	0.75	0.82	0.90	Primarily Ditch	0.99	0.91	1.00	0.82	0.97	0.90	90
301.1	301	17	TANGENT	TANGENT	0.74	0.84	0.90	Primarily FS	0.95	0.23	1.00	0.83	0.73	0.78	78
301	300.9	18	TANGENT	TANGENT	0.77	0.79	0.90	Primarily FS	0.99	0.72	1.00	0.82	0.90	0.86	86
300.9	300.8	19	TANGENT	TANGENT	0.76	0.83	0.90	Primarily FS	0.90	1.00	1.00	0.83	0.96	0.90	90
300.8	300.7	20													
300.7	300.6	21		Turn Lane											
300.6	300.5	22	TANGENT	TANGENT	0.75	0.45	0.90	Primarily Ditch	1.00	0.91	1.00	0.70	0.97	0.84	84
300.5	300.4	23	TANGENT	OUT OF SHAPE	0.79	0.00	0.90	Primarily Ditch	1.00	0.75	1.00	0.56	0.92	0.74	74
300.4	300.3	24	LTCURVE	OUT OF SHAPE	0.78	0.00	1.00	Primarily Ditch	0.97	1.00	1.00	0.59	0.99	0.79	79
300.3	300.2	25	RTCURVE	CURVE TRANSITION	0.79	0.75	1.00	Primarily Ditch	0.94	0.97	1.00	0.85	0.97	0.91	91
300.2	300.1	26	RTCURVE	RT CURVE	0.77	1.00	1.00	Primarily FS	0.92	1.00	1.00	0.92	0.97	0.95	95
300.1	300	27	TANGENT	CURVE TRANSITION	0.77	1.00	0.90	Primarily FS	0.99	0.23	1.00	0.89	0.74	0.82	82
300	299.9	28	LTCURVE	LT CURVE	0.77	1.00	1.00	Primarily FS	0.99	1.00	1.00	0.92	1.00	0.96	96
299.9	299.8	29													
299.8	299.7	30		Turn Lane											
299.7	299.6	31													
299.6	299.5	32													

299.5	299.4	33	TANGENT	TANGENT	0.61	0.53	0.90	Primarily FS	1.00	0.89	0.81	0.68	0.90	0.79	79
299.4	299.3	34	TANGENT	TANGENT	0.50	0.70	1.00	Primarily FS	1.00	1.00	1.00	0.74	1.00	0.87	87
299.3	299.2	35	TANGENT	TANGENT	0.54	0.31	1.00	Primarily Ditch	1.00	0.86	1.00	0.62	0.95	0.79	79
299.2	299.1	36	TANGENT	TANGENT	0.58	0.55	0.90	Primarily FS	1.00	0.88	1.00	0.68	0.96	0.82	82
299.1	299	37	TANGENT	TANGENT	0.53	0.86	0.90	Primarily Ditch	1.00	0.80	1.00	0.77	0.93	0.85	85
299	298.9	38	TANGENT	TANGENT	0.54	0.78	1.00	Primarily Ditch	0.97	1.00	1.00	0.77	0.99	0.88	88
298.9	298.8	39	TANGENT	TANGENT	0.51	0.74	0.90	Primarily Ditch	0.99	0.86	1.00	0.72	0.95	0.84	84
298.8	298.7	40	TANGENT	TANGENT	0.68	0.65	0.90	Primarily Ditch	1.00	0.92	1.00	0.75	0.97	0.86	86
298.7	298.6	41	TANGENT	TANGENT	0.71	0.86	1.00	Various Drainage	0.99	0.99	1.00	0.86	0.99	0.92	92
298.6	298.5	42	TANGENT	TANGENT	0.67	0.36	1.00	Primarily Ditch	1.00	0.88	1.00	0.68	0.96	0.82	82
298.5	298.4	43	TANGENT	TANGENT	0.73	0.09	1.00	Primarily Ditch	0.99	0.91	1.00	0.60	0.97	0.79	79
298.4	298.3	44	TANGENT	TANGENT	0.64	0.13	1.00	Primarily Ditch	1.00	0.82	1.00	0.59	0.94	0.76	76
298.3	298.2	45	TANGENT	TANGENT	0.62	0.42	1.00	Primarily Ditch	1.00	0.91	1.00	0.68	0.97	0.83	83
298.2	298.1	46	TANGENT	TANGENT	0.69	0.65	1.00	Primarily Ditch	1.00	1.00	1.00	0.78	1.00	0.89	89
298.1	298	47	TANGENT	TANGENT	0.62	0.75	1.00	Primarily Ditch	1.00	0.86	1.00	0.79	0.95	0.87	87
298	297.9	48	TANGENT	TANGENT	0.62	0.31	1.00	Primarily Ditch	1.00	0.98	1.00	0.64	0.99	0.82	82
297.9	297.8	49	TANGENT	TANGENT	0.61	0.33	0.90	Primarily Ditch	1.00	0.63	1.00	0.61	0.88	0.74	74
297.8	297.7	50	TANGENT	TANGENT	0.66	0.36	1.00	Primarily Ditch	1.00	0.82	1.00	0.67	0.94	0.81	81
297.7	297.6	51	TANGENT	TANGENT	0.74	0.38	1.00	Primarily Ditch	1.00	0.94	1.00	0.71	0.98	0.84	84
297.6	297.5	52	TANGENT	TANGENT	0.69	0.51	1.00	Primarily Ditch	0.95	1.00	1.00	0.73	0.98	0.86	86
297.5	297.4	53	TANGENT	TANGENT	0.66	0.35	1.00	Primarily Ditch	0.99	0.97	1.00	0.67	0.99	0.83	83
297.4	297.3	54	TANGENT	TANGENT	0.62	0.42	1.00	Primarily Ditch	1.00	0.83	1.00	0.68	0.94	0.81	81
297.3	297.2	55	TANGENT	TANGENT	0.59	0.65	1.00	Primarily Ditch	1.00	0.81	1.00	0.75	0.94	0.84	84
297.2	297.1	56	TANGENT	TANGENT	0.66	0.48	0.90	Primarily Ditch	1.00	0.80	0.95	0.68	0.92	0.80	80
297.1	297	57	TANGENT	TANGENT	0.76	0.86	1.00	Primarily Ditch	0.96	0.85	1.00	0.87	0.94	0.91	91
297	296.9	58	TANGENT	TANGENT	0.72	0.84	1.00	Primarily Ditch	0.99	0.84	1.00	0.85	0.94	0.90	90
296.9	296.8	59	TANGENT	TANGENT	0.60	0.59	1.00	Primarily Ditch	1.00	0.77	0.25	0.73	0.67	0.70	70
296.8	296.7	60	RTCURVE	CURVE TRANSITION	0.61	0.75	1.00	Primarily Ditch	0.99	0.87	1.00	0.79	0.96	0.87	87
296.7	296.6	61	RTCURVE	RT CURVE	0.58	0.90	1.00	Primarily Ditch	0.98	1.00	1.00	0.83	0.99	0.91	91
296.6	296.5	62	RTCURVE	RT CURVE	0.67	0.90	1.00	Primarily Ditch	1.00	0.77	0.58	0.86	0.78	0.82	82
296.5	296.4	63	RTCURVE	CURVE TRANSITION	0.70	0.75	0.90	Primarily Ditch	0.94	0.56	0.58	0.78	0.69	0.74	74
296.4	296.3	64	TANGENT	TANGENT	0.71	0.59	0.90	Primarily Ditch	1.00	0.82	0.90	0.73	0.90	0.82	82
296.3	296.2	65	TANGENT	TANGENT	0.66	0.78	0.90	Primarily Ditch	1.00	0.86	1.00	0.78	0.95	0.87	87
296.2	296.1	66	LTCURVE	CURVE TRANSITION	0.78	0.89	1.00	Primarily Ditch	0.98	1.00	1.00	0.89	0.99	0.94	94
296.1	296	67	LTCURVE	LT CURVE	0.74	0.99	1.00	Primarily FS	0.93	1.00	1.00	0.91	0.98	0.94	94
296	295.9	68	LTCURVE	LT CURVE	0.70	0.99	1.00	Primarily Ditch	0.99	0.94	1.00	0.90	0.98	0.94	94
295.9	295.8	69	LTCURVE	LT CURVE	0.60	0.99	1.00	Primarily Ditch	0.95	0.78	1.00	0.86	0.91	0.89	89
295.8	295.7	70	LTCURVE	CURVE TRANSITION	0.70	0.80	1.00	Primarily Ditch	0.92	0.80	1.00	0.83	0.91	0.87	87
295.7	295.6	71	TANGENT	TANGENT	0.61	0.61	1.00	Primarily Ditch	1.00	0.83	1.00	0.74	0.94	0.84	84
295.6	295.5	72	TANGENT	TANGENT	0.67	0.62	0.90	Primarily Ditch	0.97	0.73	1.00	0.73	0.90	0.82	82
295.5	295.4	73	TANGENT	TANGENT	0.63	0.86	0.90	Primarily Ditch	0.99	0.71	1.00	0.80	0.90	0.85	85
295.4	295.3	74	TANGENT	TANGENT	0.62	0.75	1.00	Primarily FS	0.91	1.00	1.00	0.79	0.97	0.88	88
295.3	295.2	75	TANGENT	TANGENT	0.71	0.82	1.00	Primarily Ditch	0.91	0.75	1.00	0.84	0.89	0.87	87
295.2	295.1	76	TANGENT	OUT OF SHAPE	0.69	0.00	0.90	Primarily Ditch	0.90	0.81	1.00	0.53	0.90	0.72	72
295.1	295	77	RTCURVE	OUT OF SHAPE	0.70	0.00	0.90	Primarily Ditch	0.99	0.86	1.00	0.53	0.95	0.74	74
295	294.9	78	TANGENT	CURVE TRANSITION	0.75	0.50	1.00	Primarily Ditch	1.00	0.98	1.00	0.75	0.99	0.87	87
294.9	294.8	79	LTCURVE	CURVE TRANSITION	0.74	0.50	1.00	Primarily Ditch	0.99	1.00	1.00	0.75	1.00	0.87	87
294.8	294.7	80	LTCURVE	LT CURVE	0.71	1.00	1.00	Primarily Ditch	0.98	1.00	1.00	0.90	0.99	0.95	95
294.7	294.6	81	LTCURVE	LT CURVE	0.72	1.00	0.90	Primarily Ditch	0.98	0.82	0.58	0.87	0.79	0.83	83
294.6	294.5	82	LTCURVE	CURVE TRANSITION	0.66	0.86	1.00	Primarily Ditch	1.00	0.80	1.00	0.84	0.93	0.89	89
294.5	294.4	83	TANGENT	TANGENT	0.71	0.72	1.00	Primarily Ditch	1.00	0.74	1.00	0.81	0.91	0.86	86
294.4	294.3	84	TANGENT	TANGENT	0.75	0.84	1.00	Primarily FS	0.98	1.00	1.00	0.86	0.99	0.93	93
294.3	294.2	85	TANGENT	TANGENT	0.71	0.88	1.00	Primarily FS	0.97	1.00	1.00	0.87	0.99	0.93	93
294.2	294.1	86	RTCURVE	OUT OF SHAPE	0.70	0.00	1.00	Primarily Ditch	0.87	1.00	1.00	0.57	0.96	0.76	76
294.1	294	87	TANGENT	OUT OF SHAPE	0.62	0.00	1.00	Primarily Ditch	0.99	0.97	1.00	0.54	0.99	0.76	76
294	293.9	88	TANGENT	TANGENT	0.62	0.79	1.00	Primarily Ditch	1.00	0.74	1.00	0.81	0.91	0.86	86
293.9	293.8	89	TANGENT	TANGENT	0.63	0.58	1.00	Primarily Ditch	0.99	0.87	1.00	0.74	0.96	0.85	85
293.8	293.7	90	TANGENT	TANGENT	0.73	0.77	0.90	Primarily Ditch	1.00	0.85	1.00	0.80	0.95	0.87	87
293.7	293.6	91	TANGENT	TANGENT	0.74	0.86	1.00	Primarily FS	1.00	0.96	1.00	0.86	0.99	0.93	93
293.6	293.5	92	TANGENT	TANGENT	0.62	0.71	1.00	Primarily FS	1.00	1.00	1.00	0.78	1.00	0.89	89
293.5	293.4	93	TANGENT	TANGENT	0.59	0.55	0.90	Primarily Ditch	0.99	1.00	1.00	0.68	1.00	0.84	84
293.4	293.3	94	TANGENT	TANGENT	0.66	0.76	0.90	Primarily Ditch	1.00	0.96	1.00	0.77	0.99	0.88	88

293.3	293.2	95	SH 31 Intersection												
293.2	293.1	96													
293.1	293	97	TANGENT	TANGENT	0.51	0.82	0.90	Primarily Ditch	1.00	0.78	1.00	0.74	0.93	0.84	84
293	292.9	98	TANGENT	TANGENT	0.54	0.68	0.90	Primarily Ditch	0.95	1.00	1.00	0.71	0.98	0.84	84
292.9	292.8	99	RTCURVE	RT CURVE	0.71	1.00	1.00	Primarily Ditch	0.98	1.00	1.00	0.90	0.99	0.95	95
292.8	292.7	100	RTCURVE	CURVE TRANSITION	0.75	0.88	1.00	Primarily Ditch	0.99	0.79	1.00	0.88	0.93	0.90	90
292.7	292.6	101	TANGENT	TANGENT	0.66	0.77	1.00	Various Drainage	0.99	0.54	1.00	0.81	0.84	0.83	83
292.6	292.5	102	TANGENT	TANGENT	0.65	0.70	1.00	Primarily Ditch	0.94	1.00	1.00	0.78	0.98	0.88	88
292.5	292.4	103	TANGENT	OUT OF SHAPE	0.55	0.00	0.90	Primarily Ditch	1.00	0.96	1.00	0.48	0.98	0.73	73
292.4	292.3	104	TANGENT	CURVE TRANSITION	0.53	0.50	0.90	Primarily Ditch	0.97	0.73	1.00	0.73	0.90	0.81	81
292.3	292.2	105	LTCURVE	LT CURVE	0.60	1.00	0.90	Primarily FS	0.93	1.00	1.00	0.83	0.98	0.90	90
292.2	292.1	106	LTCURVE	LT CURVE	0.43	1.00	1.00	Primarily FS	0.78	1.00	1.00	0.81	0.93	0.87	87
292.1	292	107	LTCURVE	CURVE TRANSITION	0.51	1.00	1.00	Primarily Ditch	0.82	0.85	1.00	0.84	0.89	0.86	86
292	291.9	108	TANGENT	CURVE TRANSITION	0.59	1.00	0.90	Primarily FS	0.96	0.94	1.00	0.83	0.97	0.90	90
291.9	291.8	109	RTCURVE	RT CURVE	0.60	1.00	1.00	Primarily FS	1.00	1.00	1.00	0.87	1.00	0.93	93
291.8	291.7	110	RTCURVE	RT CURVE	0.44	1.00	1.00	Primarily Ditch	1.00	0.92	1.00	0.81	0.97	0.89	89
291.7	291.6	111	TANGENT	TANGENT	0.37	0.89	0.90	Primarily Ditch	1.00	0.99	1.00	0.72	1.00	0.86	86
291.6	291.5	112	RTCURVE	RT CURVE	0.55	1.00	1.00	Primarily Ditch	1.00	0.61	1.00	0.85	0.87	0.86	86
291.5	291.4	113	RTCURVE	RT CURVE	0.58	1.00	1.00	Primarily FS	0.97	1.00	1.00	0.86	0.99	0.92	92
291.4	291.3	114	TANGENT	TANGENT	0.39	0.60	1.00	Primarily Ditch	0.99	0.91	1.00	0.66	0.97	0.82	82
291.3	291.2	115	TANGENT	TANGENT	0.45	0.40	1.00	Primarily FS	0.96	1.00	1.00	0.61	0.99	0.80	80
291.2	291.1	116	TANGENT	TANGENT	0.49	0.84	1.00	Primarily Ditch	0.99	1.00	1.00	0.78	0.99	0.89	89
291.1	291	117	TANGENT	TANGENT	0.45	0.83	0.90	Primarily Ditch	1.00	1.00	1.00	0.73	1.00	0.86	86
291	290.9	118	TANGENT	TANGENT	0.45	0.92	0.90	Primarily Ditch	0.92	1.00	1.00	0.76	0.97	0.87	87
290.9	290.8	119	TANGENT	TANGENT	0.53	0.75	0.90	Primarily Ditch	0.97	0.93	1.00	0.73	0.97	0.85	85
290.8	290.7	120	TANGENT	CURVE TRANSITION	0.35	0.87	0.90	Primarily Ditch	0.98	0.77	1.00	0.71	0.92	0.81	81
290.7	290.6	121	LTCURVE	LT CURVE	0.50	1.00	1.00	Primarily Ditch	0.86	0.63	0.62	0.83	0.70	0.77	77
290.6	290.5	122	LTCURVE	LT CURVE	0.35	1.00	0.90	Primarily Ditch	1.00	0.92	1.00	0.75	0.97	0.86	86
290.5	290.4	123	LTCURVE	LT CURVE	0.55	1.00	1.00	Primarily FS	0.98	1.00	1.00	0.85	0.99	0.92	92
290.4	290.3	124	TANGENT	TANGENT	0.24	0.25	1.00	Primarily FS	0.96	1.00	1.00	0.50	0.99	0.74	74
290.3	290.2	125	TANGENT	TANGENT	0.43	0.69	1.00	Primarily Ditch	0.98	0.83	1.00	0.71	0.94	0.82	82
290.2	290.1	126	TANGENT	TANGENT	0.40	0.54	1.00	Primarily Ditch	0.99	0.71	1.00	0.65	0.90	0.77	77

A consistent reduction in roadway width rating occurs north of the SH 31 intersection. Figure 54 and Figure 55 show the difference in the widened surface north of SH 31, leading to better ratings than south of SH 31. The geometry along FM 2661 appears similar to the geometry on FM roadways in the Atlanta district, yet hydroplaning ratings on FM 2661 are either 0.90 or 1.00. This is not a geometric issue since FM 2661 has sections that are also out of shape; the difference is the posted speed limit. FM 2661 is posted at 60 mph, so while Section 111 has a hydroplaning speed calculation of 54 mph and WFT of 0.22 in., the rating is 0.9 because the comparison of potential hydroplaning speed to posted speed is between 5 mph and 10 mph. In reality, a hydroplaning speed of 54 mph is lower than the 59-mph hydroplaning speed referenced for Section 17 on FM 2625, but Section 17 on FM 2625 receives a lower rating because the posted speed limit is 70 mph. An advantage of the surface drainage rating is the ability to investigate these types of anomalies.

Figure 54. FM 2661 Widened Section North of SH 31.

Figure 55. FM 2661 Non-widened Section South of FM 31.

US 69—TYLER DISTRICT

The portion of US 69 rated within the Tyler District consists of two lanes in each direction with a porous friction course (PFC) surface. The highway is divided with a project crown in the median. The mobile LiDAR data indicate that both southbound lanes flow toward the right EOP except when located in curves. Table 30 shows the overall drainage rating for US 69 was very good.

Table 30. US 69 Surface Drainage Rating Summary.

Begin TRM	End TRM	Section	Alignment Classificaiton	Section Shape	Roadway Surface			RT Roadside Shape	Roadside Surface			Combined Surface Rating	Combined Roadside Rating	Overall Drainage Rating	Overall Rating Normalized to 100
					RT Width Rating	RT Cross Slope Rating	Hydro-planing Rating		RT Front Slope Rating	RT Ditch Depth Rating	RT Ditch Slope Rating				
322.2	322.3	1	TANGENT	TANGENT	1.00	1.00	1.00	Primarily Ditch	1.00	0.78	1.00	1.00	0.93	0.96	96
322.3	322.4	2	RT CURVE	RT CURVE	1.00	1.00	1.00	Primarily FS	0.99	0.87	1.00	1.00	0.95	0.98	98
322.4	322.5	3	TANGENT	TANGENT	1.00	0.95	0.90	Primarily Ditch	1.00	0.72	1.00	0.95	0.91	0.93	93
322.5	322.6	4	LT CURVE	LT CURVE	1.00	1.00	0.90	Primarily FS	0.96	0.79	1.00	0.97	0.92	0.94	94
322.6	322.7	5	LT CURVE	LT CURVE	1.00	1.00	1.00	Primarily FS	0.96	0.23	1.00	1.00	0.73	0.87	87
322.7	322.8	6	TANGENT	TANGENT	1.00	0.95	1.00	Primarily FS	0.99	0.95	1.00	0.98	0.98	0.98	98
322.8	322.9	7	TANGENT	TANGENT	1.00	0.90	1.00	Primarily Ditch	0.90	0.76	1.00	0.97	0.89	0.93	93
322.9	323	8	TANGENT	TANGENT	1.00	0.80	1.00	Primarily Ditch	1.00	0.76	1.00	0.93	0.92	0.93	93
323	323.1	9	TANGENT	TANGENT	1.00	0.90	1.00	Primarily Ditch	1.00	0.90	1.00	0.97	0.97	0.97	97
323.1	323.2	10	TANGENT	TANGENT	1.00	0.95	1.00	Primarily Ditch	1.00	0.87	1.00	0.98	0.96	0.97	97
323.2	323.3	11	TANGENT	TANGENT	1.00	0.90	1.00	Primarily Ditch	1.00	0.73	1.00	0.97	0.91	0.94	94
323.3	323.4	12	TANGENT	TANGENT	0.96	0.80	0.90	Primarily Ditch	1.00	0.88	1.00	0.89	0.96	0.92	92
323.4	323.5	13	LT CURVE	CURVE TRANSITION	1.00	0.90	1.00	Primarily Ditch	0.97	0.99	1.00	0.97	0.99	0.98	98
323.5	323.6	14	LT CURVE	LT CURVE	1.00	1.00	1.00	Primarily FS	0.99	1.00	1.00	1.00	1.00	1.00	100
323.6	323.7	15	LT CURVE	CURVE TRANSITION	1.00	1.00	1.00	Primarily Ditch	1.00	0.83	1.00	1.00	0.94	0.97	97
323.7	323.8	16	TANGENT	CURVE TRANSITION	1.00	1.00	1.00	Primarily Ditch	0.99	0.65	0.89	1.00	0.85	0.92	92
323.8	323.9	17	RT CURVE	RT CURVE	1.00	1.00	1.00	Primarily Ditch	1.00	0.74	1.00	1.00	0.91	0.96	96
323.9	324	18	RT CURVE	RT CURVE	1.00	1.00	1.00	Primarily Ditch	0.99	0.82	1.00	1.00	0.93	0.97	97
324	324.1	19	RT CURVE	RT CURVE	1.00	1.00	1.00	Primarily Ditch	0.99	0.82	1.00	1.00	0.94	0.97	97
324.1	324.2	20	RT CURVE	RT CURVE	1.00	1.00	1.00	Primarily Ditch	1.00	0.82	1.00	1.00	0.94	0.97	97
324.2	324.3	21	TANGENT	TANGENT	1.00	0.90	1.00	Primarily Ditch	0.96	0.98	1.00	0.97	0.98	0.97	97
324.3	324.4	22	TANGENT	TANGENT	1.00	0.90	1.00	Primarily Ditch	0.94	0.85	1.00	0.97	0.93	0.95	95
324.4	324.5	23	TANGENT	TANGENT	1.00	0.95	1.00	Primarily Ditch	0.99	0.86	1.00	0.98	0.95	0.97	97
324.5	324.6	24	TANGENT	TANGENT	1.00	0.90	1.00	Primarily Ditch	0.99	0.81	0.79	0.97	0.86	0.91	91
324.6	324.7	25	TANGENT	TANGENT	1.00	0.90	1.00	Primarily Ditch	0.99	0.84	1.00	0.97	0.94	0.96	96
324.7	324.8	26	TANGENT	TANGENT	1.00	1.00	1.00	Primarily Ditch	1.00	0.70	0.77	1.00	0.83	0.91	91
324.8	324.9	27	TANGENT	TANGENT	1.00	1.00	1.00	Primarily Ditch	0.97	0.82	1.00	1.00	0.93	0.96	96
324.9	325	28	LT CURVE	CURVE TRANSITION	1.00	1.00	1.00	Primarily Ditch	0.97	0.78	0.97	1.00	0.91	0.95	95
325	325.1	29	LT CURVE	LT CURVE	1.00	1.00	1.00	Primarily Ditch	0.91	0.68	1.00	1.00	0.86	0.93	93
325.1	325.2	30	LT CURVE	LT CURVE	1.00	1.00	0.90	Primarily Ditch	0.94	0.86	1.00	0.97	0.93	0.95	95
325.2	325.3	31	TANGENT	TANGENT	1.00	1.00	1.00	Primarily Ditch	0.97	0.98	1.00	1.00	0.98	0.99	99
325.3	325.4	32	TANGENT	TANGENT	1.00	1.00	1.00	Primarily Ditch	1.00	0.92	1.00	1.00	0.97	0.99	99
325.4	325.5	33	TANGENT	TANGENT	1.00	0.95	1.00	Primarily Ditch	1.00	0.81	1.00	0.98	0.94	0.96	96
325.5	325.6	34	RT CURVE	RT CURVE	1.00	1.00	1.00	Primarily Ditch	1.00	0.77	1.00	1.00	0.92	0.96	96
325.6	325.7	35	TANGENT	TANGENT	1.00	1.00	1.00	Primarily Ditch	0.98	0.91	1.00	1.00	0.96	0.98	98
325.7	325.8	36	TANGENT	TANGENT	1.00	0.95	1.00	Primarily Ditch	0.95	0.93	1.00	0.98	0.96	0.97	97
325.8	325.9	37	TANGENT	TANGENT	1.00	0.90	1.00	Primarily Ditch	1.00	0.88	1.00	0.97	0.96	0.96	96
325.9	326	38	TANGENT	TANGENT	1.00	0.90	1.00	Primarily Ditch	1.00	0.92	0.92	0.97	0.95	0.96	96
326	326.1	39	TANGENT	TANGENT	1.00	1.00	1.00	Primarily Ditch	1.00	0.91	1.00	1.00	0.97	0.98	98
326.1	326.2	40	TANGENT	TANGENT	1.00	0.95	1.00	Primarily Ditch	1.00	0.85	0.81	0.98	0.89	0.94	94
326.2	326.3	41	TANGENT	CURVE TRANSITION	1.00	0.98	1.00	Primarily Ditch	0.99	0.94	1.00	0.99	0.98	0.98	98
326.3	326.4	42	LT CURVE	LT CURVE	1.00	1.00	0.90	Various Drainage	0.94	0.97	1.00	0.97	0.97	0.97	97
326.4	326.5	43	LT CURVE	LT CURVE	1.00	1.00	1.00	Primarily Ditch	0.97	0.83	1.00	1.00	0.93	0.97	97
326.5	326.6	44	LT CURVE	LT CURVE	1.00	1.00	0.90	Primarily Ditch	1.00	0.77	1.00	0.97	0.92	0.94	94
326.6	326.7	45	TANGENT	CURVE TRANSITION	1.00	1.00	0.80	Primarily Ditch	1.00	0.75	1.00	0.93	0.91	0.92	92
326.7	326.8	46	TANGENT	TANGENT	1.00	1.00	1.00	Various Drainage	0.99	0.92	1.00	1.00	0.97	0.99	99
326.8	326.9	47	TANGENT	TANGENT	1.00	0.95	0.80	Primarily FS	0.99	0.98	1.00	0.92	0.99	0.95	95
326.9	327	48	RT CURVE	RT CURVE	1.00	1.00	1.00	Primarily Ditch	0.98	0.99	1.00	1.00	0.99	1.00	100
327	327.1	49	RT CURVE	RT CURVE	1.00	1.00	1.00	Primarily Ditch	1.00	0.82	1.00	1.00	0.94	0.97	97
327.1	327.2	50	RT CURVE	RT CURVE	1.00	1.00	1.00	Primarily Ditch	0.99	0.96	1.00	1.00	0.99	0.99	99
327.2	327.3	51	TANGENT	CURVE TRANSITION	1.00	0.98	1.00	Primarily Ditch	1.00	0.86	1.00	0.99	0.95	0.97	97
327.3	327.4	52	TANGENT	TANGENT	1.00	0.95	1.00	Primarily FS	1.00	0.95	1.00	0.98	0.98	0.98	98
327.4	327.5	53	TANGENT	TANGENT	1.00	1.00	1.00	Primarily FS	0.98	1.00	1.00	1.00	0.99	1.00	100
327.5	327.6	54	TANGENT	TANGENT	1.00	1.00	1.00	Primarily Ditch	1.00	0.99	1.00	1.00	1.00	1.00	100
327.6	327.7	55	TANGENT	TANGENT	1.00	0.90	1.00	Primarily Ditch	1.00	0.93	1.00	0.97	0.98	0.97	97
327.7	327.8	56	TANGENT	TANGENT	1.00	95.00	0.90	Primarily Ditch	1.00	0.94	1.00	32.30	0.98	16.64	1664
327.8	327.9	57	TANGENT	TANGENT	1.00	1.00	1.00	Primarily Ditch	1.00	0.92	1.00	1.00	0.92	0.96	96
327.9	328	58	LT CURVE	LT CURVE	1.00	1.00	0.80	Primarily Ditch	1.00	0.96	1.00	0.93	0.99	0.96	96
328	328.1	59	LT CURVE	LT CURVE	1.00	1.00	1.00	Primarily FS	1.00	1.00	1.00	1.00	1.00	1.00	100
328.1	328.2	60	RT CURVE	RT CURVE	1.00	1.00	0.90	Primarily Ditch	0.99	0.94	1.00	0.97	0.98	0.97	97
328.2	328.3	61	RT CURVE	RT CURVE	0.99	1.00	1.00	Primarily Ditch	1.00	0.94	1.00	1.00	0.98	0.99	99
328.3	328.4	62	TANGENT	CURVE TRANSITION	1.00	1.00	1.00	Primarily Ditch	1.00	0.88	1.00	1.00	0.96	0.98	98
328.4	328.5	63	TANGENT	TANGENT	1.00	1.00	1.00	Primarily FS	0.99	0.96	1.00	1.00	0.99	0.99	99
328.5	328.6	64	TANGENT	TANGENT	0.94	1.00	0.90	Primarily FS	1.00	0.92	1.00	0.95	0.97	0.96	96
328.6	328.7	65	RT CURVE	RT CURVE	1.00	1.00	1.00	Primarily FS	0.91	1.00	1.00	1.00	0.97	0.98	98
328.7	328.8	66	RT CURVE	RT CURVE	1.00	1.00	1.00	Primarily FS	1.00	1.00	1.00	1.00	1.00	1.00	100
328.8	328.9	67	TANGENT	CURVE TRANSITION	0.57	1.00	1.00	Primarily Ditch	1.00	0.99	1.00	0.86	1.00	0.93	93

103

Table 30 indicates that potential issues along US 69 might occur with ditch depth because many sections have ratings less than 1.00, and some sections have ratings less than 0.80. All front slopes are at least 4H:1V, with many at 6H:1V or flatter. The front slope conclusion comes from the fact that all front slope ratings are between 0.90 and 1.00. Unfortunately, US 69's traffic volume and speed limit create a desire for as flat of front slopes as possible, so significant ditch deepening might not be feasible. The surface drainage rating presented within this report allows engineers to weigh these options with a new piece of network-level information.

FM 1687—BRYAN DISTRICT

Table 31 shows the network-level surface drainage rating for FM 1687 in the Bryan District.

Table 31. FM 1687 Surface Drainage Rating Summary.

Begin TRM	End TRM	Section	Alignment Classificaiton	Section Shape	RT Width Rating	RT Cross Slope Rating	Hydro-planing Rating	RT Roadside Shape	RT Front Slope Rating	RT Ditch Depth Rating	RT Ditch Slope Rating	Combined Surface Rating	Combined Roadside Rating	Overall Drainage Rating	Overall Rating Normalized to 100
609.9	610.0	1	RTCURVE	RT CURVE	0.87	1.00	0.70	Primarily Ditch	0.96	0.95	1.00	0.86	0.97	0.91	91
610.0	610.1	2	LTCURVE	LT CURVE	0.88	0.98	0.70	Primarily Ditch	0.97	1.00	1.00	0.85	0.99	0.92	92
610.1	610.2	3	TANGENT	TANGENT	0.94	0.66	0.80	Primarily Ditch	0.95	1.00	1.00	0.80	0.98	0.89	89
610.2	610.3	4	TANGENT	TANGENT	0.88	0.61	0.80	Primarily Ditch	0.97	1.00	1.00	0.76	0.99	0.88	88
610.3	610.4	5	LTCURVE	OUT OF SHAPE	0.92	0.00	0.80	Primarily FS	0.96	1.00	1.00	0.57	0.99	0.78	78
610.4	610.5	6	LTCURVE	OUT OF SHAPE	0.88	0.00	0.80	Primarily Ditch	0.92	1.00	1.00	0.56	0.97	0.77	77
610.5	610.6	7	LTCURVE	OUT OF SHAPE	0.92	0.00	0.80	Primarily Ditch	0.94	1.00	1.00	0.57	0.98	0.78	78
610.6	610.7	8	TANGENT	TANGENT	0.88	0.73	0.70	Primarily FS	0.97	1.00	1.00	0.77	0.99	0.88	88
610.7	610.8	9	TANGENT	TANGENT	0.79	0.65	0.90	Primarily Ditch	1.00	0.97	1.00	0.78	0.99	0.88	88
610.8	610.9	10	TANGENT	TANGENT	0.88	0.50	0.80	Primarily Ditch	0.90	1.00	1.00	0.72	0.97	0.85	85
610.9	611.0	11	RTCURVE	RT CURVE	0.84	1.00	0.80	Primarily Ditch	0.97	0.89	1.00	0.88	0.96	0.92	92
611.0	611.1	12	RTCURVE	RT CURVE	0.89	1.00	0.90	Primarily Ditch	0.97	0.90	1.00	0.93	0.96	0.94	94
611.1	611.2	13	RTCURVE	RT CURVE	1.00	1.00	0.70	Primarily Ditch	0.98	0.92	1.00	0.90	0.97	0.93	93
611.2	611.3	14	RTCURVE	RT CURVE	1.00	1.00	0.70	Primarily Ditch	0.95	1.00	1.00	0.90	0.98	0.94	94
611.3	611.4	15	RTCURVE	RT CURVE	0.91	1.00	0.90	Primarily Ditch	0.96	1.00	1.00	0.94	0.99	0.96	96
611.4	611.5	16	TANGENT	CURVE TRANSITION	0.87	0.84	0.80	Primarily Ditch	0.96	1.00	1.00	0.84	0.99	0.91	91
611.5	611.6	17	TANGENT	TANGENT	0.88	0.68	0.80	Primarily Ditch	0.97	1.00	1.00	0.79	0.99	0.89	89
611.6	611.7	18	TANGENT	TANGENT	0.82	0.73	0.70	Primarily Ditch	1.00	0.93	1.00	0.75	0.98	0.86	86
611.7	611.8	19	TANGENT	TANGENT	0.78	0.74	0.80	Primarily Ditch	1.00	0.94	1.00	0.77	0.98	0.88	88
611.8	611.9	20	TANGENT	TANGENT	0.82	0.19	0.90	Primarily Ditch	1.00	0.85	0.78	0.64	0.88	0.76	76
611.9	612.0	21	TANGENT	TANGENT	0.74	0.19	0.90	Primarily Ditch	1.00	0.92	1.00	0.61	0.97	0.79	79
612.0	612.1	22	TANGENT	CURVE TRANSITION	0.91	0.59	0.80	Primarily Ditch	1.00	0.97	1.00	0.77	0.99	0.88	88
612.1	612.2	23	RTCURVE	RT CURVE	0.81	1.00	0.80	Primarily Ditch	1.00	0.96	1.00	0.87	0.99	0.93	93
612.2	612.3	24	RTCURVE	RT CURVE	0.83	1.00	0.90	Primarily Ditch	1.00	0.88	1.00	0.91	0.96	0.93	93
612.3	612.4	25	RTCURVE	CURVE TRANSITION	0.81	0.46	0.80	Primarily Ditch	1.00	0.93	1.00	0.69	0.98	0.83	83
612.4	612.5	26	TANGENT	OUT OF SHAPE	0.92	0.00	0.70	Primarily Ditch	1.00	0.93	0.64	0.54	0.86	0.70	70
612.5	612.6	27	TANGENT	OUT OF SHAPE	0.87	0.00	0.80	Primarily Ditch	1.00	0.92	0.90	0.56	0.94	0.75	75
612.6	612.7	28	RTCURVE	CURVE TRANSITION	0.88	0.41	0.80	Primarily Ditch	0.99	1.00	1.00	0.69	1.00	0.85	85
612.7	612.8	29	RTCURVE	RT CURVE	0.88	0.81	0.90	Primarily Ditch	1.00	0.78	1.00	0.86	0.93	0.89	89
612.8	612.9	30	RTCURVE	CURVE TRANSITION	0.78	0.41	0.80	Primarily Ditch	1.00	0.74	0.68	0.66	0.81	0.73	73
612.9	613.0	31	TANGENT	OUT OF SHAPE	0.71	0.00	0.90	Primarily Ditch	1.00	0.83	0.99	0.54	0.94	0.74	74
613.0	613.1	32	LTCURVE	OUT OF SHAPE	0.74	0.00	0.90	Primarily Ditch	1.00	0.76	1.00	0.55	0.92	0.73	73
613.1	613.2	33	LTCURVE	OUT OF SHAPE	0.74	0.00	0.80	Primarily Ditch	0.99	0.80	1.00	0.51	0.93	0.72	72
613.2	613.3	34	TANGENT	TANGENT	0.76	0.60	0.90	Primarily FS	1.00	0.92	1.00	0.75	0.97	0.86	86
613.3	613.4	35	TANGENT	TANGENT	0.75	0.45	0.70	Primarily FS	1.00	0.93	1.00	0.63	0.98	0.81	81
613.4	613.5	36	TANGENT	TANGENT	0.73	0.22	0.70	Primarily Ditch	1.00	0.71	1.00	0.55	0.90	0.73	73
613.5	613.6	37	TANGENT	OUT OF SHAPE	0.72	0.00	0.80	Primarily Ditch	0.99	0.87	1.00	0.51	0.95	0.73	73
613.6	613.7	38	TANGENT	CURVE TRANSITION	0.71	0.00	0.80	Primarily Ditch	0.98	0.73	1.00	0.50	0.90	0.70	70
613.7	613.8	39	LTCURVE	LT CURVE	0.71	0.92	1.00	Primarily Ditch	0.96	1.00	1.00	0.88	0.99	0.93	93
613.8	613.9	40	LTCURVE	CURVE TRANSITION	0.76	0.82	0.70	Primarily Ditch	0.98	1.00	1.00	0.76	0.99	0.88	88
613.9	614.0	41	TANGENT	CURVE TRANSITION	0.68	0.82	0.80	Primarily Ditch	0.97	0.97	1.00	0.77	0.98	0.87	87
614.0	614.1	42	LTCURVE	LT CURVE	0.68	0.72	0.80	Primarily Ditch	0.95	0.81	1.00	0.73	0.92	0.83	83
614.1	614.2	43	LTCURVE	LT CURVE	0.71	0.72	0.90	Primarily Ditch	0.94	0.94	1.00	0.78	0.96	0.87	87
614.2	614.3	44	LTCURVE	LT CURVE	0.75	0.72	1.00	Primarily Ditch	1.00	0.98	1.00	0.82	0.99	0.91	91
614.3	614.4	45	TANGENT	TANGENT	0.65	0.80	0.70	Primarily Ditch	1.00	0.80	1.00	0.72	0.93	0.82	82

Section 26 along FM 1687 has the lowest rating of 70. Section 26 is plagued by being out of shape, with a 0.70 hydroplaning rating, and a flat ditch line. The measurements that lead to the rating indicate the roadside slope in Section 26 is approximately 0.6 percent and the hydroplaning speed is 53 mph. Again, the deduction in hydroplaning speed is based on the posted speed limit of 70 mph along FM 1687. Figure 56 displays Section 26.

Figure 56. Section 26 on FM 1687.

FM 2818—BRYAN DISTRICT

Table 32 presents the rating results for FM 2818 in the Bryan District. Additional drill-down techniques similar to those described with the previous sections can be performed.

Table 32. FM 2818 Surface Drainage Rating Summary.

					Roadway Surface				Roadside Surface						Overall Rating Normalized to 100
Begin TRM	End TRM	Section	Alignment Classificaiton	Section Shape	RT Width Rating	RT Cross Slope Rating	Hydro-planing Rating	RT Roadside Shape	RT Front Slope Rating	RT Ditch Depth Rating	RT Ditch Slope Rating	Combined Surface Rating	Combined Roadside Rating	Overall Drainage Rating	
409.3	409.4	1	TANGENT	TANGENT	0.50	0.30	1.00	Primarily Ditch	1.00	1.00	1.00	0.60	1.00	0.80	80
409.4	409.5	2	TANGENT	TANGENT	0.38	0.34	1.00	Primarily Ditch	1.00	0.99	1.00	0.58	1.00	0.79	79
409.5	409.6	3	TANGENT	TANGENT	0.99	0.25	1.00	Primarily Ditch	0.99	1.00	1.00	0.75	1.00	0.87	87
409.6	409.7	4	TANGENT	TANGENT	1.00	0.49	1.00	Primarily Ditch	1.00	0.94	1.00	0.83	0.98	0.90	90
409.7	409.8	5	TANGENT	TANGENT	0.93	0.50	1.00	Primarily Ditch	1.00	0.96	1.00	0.81	0.99	0.90	90
409.8	409.9	6	TANGENT	TANGENT	0.96	0.78	1.00	Primarily FS	0.96	1.00	1.00	0.91	0.99	0.95	95
409.9	410.0	7	RT CURVE	CURVE TRANSITION	0.95	0.89	1.00	Primarily FS	0.95	0.23	1.00	0.94	0.73	0.84	84
410.0	410.1	8	RT CURVE	RT CURVE	0.57	1.00	1.00	Primarily Ditch	1.00	1.00	1.00	0.86	1.00	0.93	93
410.1	410.2	9	RT CURVE	RT CURVE	0.36	1.00	1.00	Primarily FS	0.99	1.00	1.00	0.79	1.00	0.89	89
410.2	410.3	10	RT CURVE	RT CURVE	0.38	1.00	1.00	Primarily FS	0.99	1.00	1.00	0.79	1.00	0.90	90
410.3	410.4	11	RT CURVE	RT CURVE	0.39	1.00	1.00	Primarily Ditch	1.00	1.00	1.00	0.80	1.00	0.90	90
410.4	410.5	12	RT CURVE	RT CURVE	0.49	1.00	1.00	Primarily Ditch	1.00	1.00	1.00	0.83	1.00	0.92	92
410.5	410.6	13	TANGENT	TANGENT	0.43	0.95	1.00	Primarily Ditch	1.00	1.00	1.00	0.79	1.00	0.90	90
410.6	410.7	14	TANGENT	TANGENT	0.97	0.90	1.00	Primarily Ditch	0.99	0.96	1.00	0.96	0.98	0.97	97
410.7	410.8	15	TANGENT	TANGENT	0.52	0.90	1.00	Primarily FS	1.00	0.84	1.00	0.81	0.95	0.88	88
410.8	410.9	16	TANGENT	TANGENT	0.42	0.90	1.00	Primarily Ditch	1.00	0.99	1.00	0.77	1.00	0.88	88
410.9	411.0	17	TANGENT	TANGENT	0.52	0.90	1.00	Primarily Ditch	1.00	0.99	0.99	0.81	0.99	0.90	90
411.0	411.1	18	TANGENT	TANGENT	0.57	1.00	1.00	Primarily Ditch	1.00	1.00	1.00	0.86	1.00	0.93	93
411.1	411.2	19	TANGENT	TANGENT	0.55	1.00	1.00	Primarily Ditch	1.00	1.00	1.00	0.85	1.00	0.93	93
411.2	411.3	20	LT CURVE	OUT OF SHAPE	0.57	0.00	1.00	Primarily Ditch	0.99	1.00	1.00	0.52	1.00	0.76	76
411.3	411.4	21	TANGENT	TANGENT	0.48	1.00	1.00	Primarily Ditch	1.00	1.00	1.00	0.83	1.00	0.91	91
411.4	411.5	22	LT CURVE	CURVE TRANSITION	0.44	1.00	1.00	Primarily FS	0.97	1.00	1.00	0.81	0.99	0.90	90
411.5	411.6	23	LT CURVE	LT CURVE	0.47	1.00	1.00	Primarily FS	0.94	0.23	1.00	0.82	0.73	0.77	77

106

SH 30—BRYAN DISTRICT

Table 33 presents the rating results for SH 30 in the Bryan District.

Table 33. SH 30 Surface Drainage Rating Summary.

| | | | | | Roadway Surface | | | | Roadside Surface | | | | | | |
Begin TRM	End TRM	Section	Alignment Classificaiton	Section Shape	RT Width Rating	RT Cross Slope Rating	Hydro-planing Rating	RT Roadside Shape	RT Front Slope Rating	RT Ditch Depth Rating	RT Ditch Slope Rating	Combined Surface Rating	Combined Roadside Rating	Overall Drainage Rating	Overall Rating Normalized to 100
624.8	624.9	1	TANGENT	TANGENT	0.55	0.53	1.00	Primarily Ditch	1.00	1.00	0.91	0.69	0.97	0.83	83
624.9	625.0	2	TANGENT	TANGENT	0.55	0.64	1.00	Primarily Ditch	1.00	1.00	0.93	0.73	0.98	0.85	85
625.0	625.1	3	TANGENT	TANGENT	0.70	0.91	1.00	Primarily FS	1.00	1.00	1.00	0.87	1.00	0.94	94
625.1	625.2	4	TANGENT	TANGENT	0.65	0.87	1.00	Primarily Ditch	1.00	1.00	0.93	0.84	0.98	0.91	91
625.2	625.3	5	TANGENT	OUT OF SHAPE	0.53	0.00	1.00	Primarily Ditch	1.00	1.00	0.92	0.51	0.97	0.74	74
625.3	625.4	6	TANGENT	TANGENT	0.56	0.84	1.00	Primarily Ditch	1.00	1.00	0.92	0.80	0.97	0.89	89
625.4	625.5	7	TANGENT	TANGENT	0.55	0.82	1.00	Primarily Ditch	1.00	1.00	0.96	0.79	0.99	0.89	89

FM 136—CORPUS CHRISTI DISTRICT

Table 34 presents the results for FM 136 in the Corpus Christi District. Along FM 136, from approximately Section 24 to Section 41, the roadway has been widened. The traveled way width ratings clearly indicate this change since the ratings for sections before and after these sections are well below 0.7 but are often at 1.0 through the widened sections. FM 136 was plagued by out-of-shape sections with flat ditch lines. Flat ditches are to be expected in the Corpus Christi District as the terrain flattens through the coastal plains. Front slope ratings are typically 1.0, indicating front slopes are at least as flat as 6H:1V and implying that some ditch deepening could be performed without compromising safety. A detailed analysis of this can be done at the project level and is discussed in significant detail in the US 75—Paris District project level application section.

Table 34. FM 136 Surface Drainage Rating Summary.

Begin TRM	End TRM	Section	Alignment Classificaiton	Section Shape	Roadway Surface			RT Roadside Shape	Roadside Surface			Combined Surface Rating	Combined Roadside Rating	Overall Drainage Rating	Overall Rating Normalized to 100
					RT Width Rating	RT Cross Slope Rating	Hydro-planing Rating		RT Front Slope Rating	RT Ditch Depth Rating	RT Ditch Slope Rating				
581.0	581.1	1	TANGENT	TANGENT	0.57	0.77	0.90	Primarily Ditch	1.00	0.94	1.00	0.75	0.98	0.86	86
581.1	581.2	2	TANGENT	TANGENT	0.60	0.50	0.90	Primarily Ditch	1.00	0.92	1.00	0.67	0.97	0.82	82
581.2	581.3	3	TANGENT	TANGENT	0.60	0.34	0.90	Primarily Ditch	1.00	0.92	1.00	0.61	0.97	0.79	79
581.3	581.4	4	TANGENT	TANGENT	0.61	0.61	0.80	Primarily Ditch	1.00	0.94	1.00	0.67	0.98	0.83	83
581.4	581.5	5	TANGENT	TANGENT	0.63	0.36	0.90	Primarily Ditch	1.00	0.93	1.00	0.63	0.98	0.80	80
581.5	581.6	6	TANGENT	TANGENT	0.60	0.65	0.90	Primarily Ditch	1.00	0.91	1.00	0.71	0.97	0.84	84
581.6	581.7	7	TANGENT	TANGENT	0.50	0.63	0.90	Primarily Ditch	1.00	0.85	1.00	0.68	0.95	0.81	81
581.7	581.8	8	TANGENT	OUT OF SHAPE	0.52	0.00	0.70	Primarily Ditch	1.00	0.88	1.00	0.41	0.96	0.68	68
581.8	581.9	9	TANGENT	OUT OF SHAPE	0.40	0.00	0.70	Primarily Ditch	1.00	0.85	0.63	0.37	0.83	0.60	60
581.9	582.0	10	TANGENT	TANGENT	0.30	0.54	0.70	Primarily Ditch	1.00	0.91	0.57	0.51	0.83	0.67	67
582.0	582.1	11	RTCURVE	OUT OF SHAPE	0.52	0.00	1.00	Primarily Ditch	1.00	0.91	0.42	0.51	0.77	0.64	64
582.1	582.2	12	RTCURVE	OUT OF SHAPE	0.57	0.00	0.80	Primarily Ditch	1.00	0.89	0.46	0.46	0.78	0.62	62
582.2	582.3	13	TANGENT	TANGENT	0.53	0.36	0.90	Primarily Ditch	1.00	0.93	0.81	0.60	0.91	0.75	75
582.3	582.4	14	TANGENT	OUT OF SHAPE	0.55	0.00	0.90	Primarily Ditch	1.00	0.92	1.00	0.48	0.97	0.73	73
582.4	582.5	15	TANGENT	OUT OF SHAPE	0.50	0.00	0.80	Primarily Ditch	1.00	0.95	1.00	0.43	0.98	0.71	71
582.5	582.6	16	TANGENT	TANGENT	0.36	0.83	0.80	Primarily Ditch	1.00	0.97	0.87	0.66	0.95	0.81	81
582.6	582.7	17	TANGENT	TANGENT	0.51	0.79	0.80	Primarily Ditch	1.00	0.96	1.00	0.70	0.99	0.84	84
582.7	582.8	18	TANGENT	TANGENT	0.35	0.63	0.80	Primarily Ditch	1.00	0.95	0.89	0.59	0.95	0.77	77
582.8	582.9	19	TANGENT	TANGENT	0.50	0.66	0.80	Primarily Ditch	1.00	0.85	0.84	0.65	0.90	0.78	78
582.9	583.0	20	TANGENT	TANGENT	0.08	0.82	0.70	Primarily Ditch	1.00	0.85	1.00	0.53	0.95	0.74	74
583.0	583.1	21	TANGENT	TANGENT	0.00	0.61	0.80	Primarily Ditch	1.00	0.92	1.00	0.47	0.97	0.72	72
583.1	583.2	22	TANGENT	OUT OF SHAPE	0.00	0.00	0.70	Primarily Ditch	1.00	0.87	1.00	0.23	0.96	0.59	59
583.2	583.3	23	TANGENT	TANGENT	0.24	0.57	0.80	Primarily Ditch	1.00	0.75	1.00	0.54	0.92	0.73	73
583.3	583.4	24	TANGENT	TANGENT	1.00	0.78	0.80	Primarily Ditch	0.96	0.88	1.00	0.86	0.95	0.90	90
583.4	583.5	25	TANGENT	TANGENT	1.00	0.83	0.50	Various Drainage	0.90	1.00	1.00	0.78	0.97	0.87	87
583.5	583.6	26	TANGENT	TANGENT	1.00	0.88	0.70	Primarily Ditch	0.84	1.00	1.00	0.86	0.95	0.90	90
583.6	583.7	27	TANGENT	TANGENT	1.00	0.80	0.70	Primarily Ditch	0.90	1.00	1.00	0.83	0.97	0.90	90
583.7	583.8	28	TANGENT	TANGENT	1.00	0.68	0.50	Primarily Ditch	0.99	0.89	1.00	0.73	0.96	0.84	84
583.8	583.9	29	TANGENT	TANGENT	0.88	0.51	0.70	Primarily Ditch	0.98	1.00	0.99	0.70	0.99	0.84	84
583.9	584.0	30	TANGENT	TANGENT	1.00	0.86	0.50	Primarily Ditch	0.99	0.98	0.55	0.79	0.84	0.81	81
584.0	584.1	31	LTCURVE	OUT OF SHAPE	0.82	0.00	0.70	Primarily Ditch	1.00	0.98	1.00	0.51	0.99	0.75	75
584.1	584.2	32	LTCURVE	OUT OF SHAPE	0.70	0.00	0.90	Primarily FS	1.00	1.00	1.00	0.53	1.00	0.77	77
584.2	584.3	33	TANGENT	TANGENT	0.98	0.81	0.50	Primarily Ditch	1.00	1.00	1.00	0.77	1.00	0.88	88
584.3	584.4	34	TANGENT	TANGENT	1.00	0.81	0.70	Primarily Ditch	1.00	0.93	1.00	0.84	0.98	0.91	91
584.4	584.5	35	TANGENT	TANGENT	1.00	0.83	0.50	Primarily Ditch	1.00	0.91	0.99	0.78	0.96	0.87	87
584.5	584.6	36	TANGENT	TANGENT	0.95	0.84	0.70	Primarily Ditch	1.00	0.83	0.87	0.83	0.90	0.87	87
584.6	584.7	37	TANGENT	TANGENT	1.00	0.71	0.70	Primarily Ditch	0.99	0.95	1.00	0.80	0.98	0.89	89
584.7	584.8	38	TANGENT	TANGENT	1.00	0.88	0.70	Primarily Ditch	0.94	1.00	1.00	0.86	0.98	0.92	92
584.8	584.9	39	TANGENT	TANGENT	0.94	0.91	0.80	Primarily Ditch	0.70	1.00	1.00	0.88	0.90	0.89	89
584.9	585.0	40	TANGENT	TANGENT	0.93	0.81	0.70	Primarily Ditch	0.97	1.00	1.00	0.81	0.99	0.90	90
585.0	585.1	41	TANGENT	TANGENT	0.89	0.85	0.70	Primarily Ditch	0.99	0.96	1.00	0.81	0.98	0.90	90
585.1	585.2	42	TANGENT	TANGENT	0.73	0.55	0.70	Primarily Ditch	1.00	0.83	0.69	0.66	0.84	0.75	75
585.2	585.3	43	TANGENT	OUT OF SHAPE	0.73	0.00	0.70	Primarily Ditch	0.94	0.86	0.87	0.48	0.89	0.68	68
585.3	585.4	44	TANGENT	TANGENT	0.71	0.82	0.70	Primarily Ditch	0.84	0.41	0.52	0.74	0.59	0.66	66
585.4	585.5	45	RTCURVE	OUT OF SHAPE	0.62	0.00	0.50	Primarily Ditch	1.00	0.77	0.53	0.37	0.77	0.57	57
585.5	585.6	46	RTCURVE	OUT OF SHAPE	0.73	0.00	0.90	Primarily Ditch	1.00	0.85	0.54	0.54	0.80	0.67	67
585.6	585.7	47	RTCURVE	OUT OF SHAPE	0.54	0.00	0.50	Primarily Ditch	1.00	0.90	1.00	0.35	0.97	0.66	66
585.7	585.8	48	TANGENT	TANGENT	0.81	0.86	0.50	Primarily Ditch	1.00	0.81	0.17	0.72	0.66	0.69	69
585.8	585.9	49	TANGENT	TANGENT	0.57	0.57	0.50	Primarily Ditch	1.00	0.77	0.27	0.55	0.68	0.61	61
585.9	586.0	50	LTCURVE	CURVE TRANSITION	0.75	0.66	0.50	Primarily Ditch	1.00	0.78	0.67	0.64	0.81	0.72	72

108

586.0	586.1	51	LTCURVE	LT CURVE	0.55	0.74	0.90	Primarily Ditch	1.00	0.89	1.00	0.73	0.96	0.85	85
586.1	586.2	52	TANGENT	TANGENT	0.82	0.67	0.70	Primarily Ditch	1.00	0.92	0.56	0.73	0.83	0.78	78
586.2	586.3	53	TANGENT	OUT OF SHAPE	0.81	0.00	0.70	Primarily Ditch	1.00	0.96	0.82	0.50	0.93	0.72	72
586.3	586.4	54	TANGENT	OUT OF SHAPE	0.78	0.00	0.70	Primarily Ditch	1.00	1.00	1.00	0.49	1.00	0.75	75
586.4	586.5	55	TANGENT	TANGENT	0.63	0.79	0.80	Primarily FS	1.00	0.76	0.59	0.74	0.78	0.76	76
586.5	586.6	56	TANGENT	OUT OF SHAPE	0.71	0.00	0.50	Primarily Ditch	0.99	0.89	0.94	0.40	0.94	0.67	67
586.6	586.7	57	TANGENT	OUT OF SHAPE	0.70	0.00	0.70	Primarily Ditch	1.00	0.77	1.00	0.47	0.92	0.70	70
586.7	586.8	58	TANGENT	TANGENT	0.53	0.81	0.70	Primarily Ditch	1.00	0.88	1.00	0.68	0.96	0.82	82
586.8	586.9	59	TANGENT	OUT OF SHAPE	0.50	0.00	0.70	Primarily Ditch	1.00	0.96	1.00	0.40	0.99	0.69	69
586.9	587.0	60	TANGENT	OUT OF SHAPE	0.68	0.00	0.80	Primarily Ditch	1.00	0.94	0.67	0.49	0.87	0.68	68
587.0	587.1	61	TANGENT	TANGENT	0.72	0.71	1.00	Primarily Ditch	1.00	0.91	0.46	0.81	0.79	0.80	80
587.1	587.2	62	TANGENT	TANGENT	0.70	0.45	0.80	Primarily Ditch	1.00	0.90	1.00	0.65	0.97	0.81	81
587.2	587.3	63	TANGENT	TANGENT	0.72	0.17	1.00	Primarily Ditch	1.00	0.91	0.71	0.63	0.87	0.75	75
587.3	587.4	64	TANGENT	TANGENT	0.71	0.39	0.80	Primarily Ditch	1.00	0.91	0.80	0.63	0.90	0.77	77
587.4	587.5	65	TANGENT	TANGENT	0.73	0.55	0.90	Primarily Ditch	1.00	0.93	0.77	0.73	0.90	0.81	81
587.5	587.6	66	TANGENT	TANGENT	0.71	0.24	0.70	Primarily Ditch	1.00	0.83	1.00	0.55	0.94	0.75	75
587.6	587.7	67	TANGENT	OUT OF SHAPE	0.70	0.00	0.80	Primarily Ditch	1.00	0.88	1.00	0.50	0.96	0.73	73
587.7	587.8	68	TANGENT	OUT OF SHAPE	0.56	0.00	0.70	Primarily Ditch	1.00	0.87	1.00	0.42	0.96	0.69	69
587.8	587.9	69	TANGENT	OUT OF SHAPE	0.71	0.00	0.70	Primarily Ditch	0.98	0.90	1.00	0.47	0.96	0.71	71
587.9	588.0	70	TANGENT	OUT OF SHAPE	0.71	0.00	0.70	Primarily Ditch	1.00	0.92	0.73	0.47	0.88	0.68	68
588.0	588.1	71	TANGENT	TANGENT	0.63	0.63	0.70	Primarily Ditch	1.00	0.91	0.70	0.65	0.87	0.76	76
588.1	588.2	72	TANGENT	TANGENT	0.25	0.84	0.70	Primarily Ditch	1.00	1.00	1.00	0.60	1.00	0.80	80
588.2	588.3	73	TANGENT	TANGENT	0.26	0.82	0.70	Primarily Ditch	1.00	1.00	1.00	0.59	1.00	0.80	80
588.3	588.4	74	TANGENT	TANGENT	0.53	0.78	0.70	Primarily Ditch	1.00	0.93	1.00	0.67	0.98	0.82	82
588.4	588.5	75	RTCURVE	OUT OF SHAPE	0.89	0.00	0.90	Primarily Ditch	1.00	0.78	1.00	0.60	0.93	0.76	76
588.5	588.6	76	RTCURVE	OUT OF SHAPE	0.73	0.00	0.70	Primarily Ditch	1.00	0.76	0.55	0.48	0.77	0.62	62
588.6	588.7	77	TANGENT	TANGENT	0.78	0.82	0.50	Primarily Ditch	1.00	0.88	1.00	0.70	0.96	0.83	83
588.7	588.8	78	TANGENT	OUT OF SHAPE	0.77	0.00	0.70	Primarily Ditch	1.00	0.91	0.47	0.49	0.79	0.64	64
588.8	588.9	79	TANGENT	OUT OF SHAPE	0.63	0.00	0.70	Primarily Ditch	1.00	0.92	1.00	0.44	0.97	0.71	71
588.9	589.0	80	TANGENT	OUT OF SHAPE	0.67	0.00	0.80	Primarily Ditch	1.00	0.92	1.00	0.49	0.97	0.73	73
589.0	589.1	81	TANGENT	TANGENT	0.72	0.30	0.50	Primarily Ditch	1.00	0.92	1.00	0.51	0.97	0.74	74
589.1	589.2	82	TANGENT	TANGENT	0.55	0.00	0.70	Primarily Ditch	1.00	0.94	1.00	0.42	0.98	0.70	70
589.2	589.3	83	TANGENT	TANGENT	0.00	0.25	0.80	Primarily Ditch	1.00	0.92	1.00	0.35	0.97	0.66	66
589.3	589.4	84	LTCURVE	CURVE TRANSITION	0.00	0.13	0.80	Primarily Ditch	1.00	0.92	0.64	0.31	0.85	0.58	58
589.4	589.5	85	LTCURVE	LT CURVE	0.38	0.00	1.00	Primarily FS	1.00	0.96	1.00	0.46	0.99	0.72	72
589.5	589.6	86	LTCURVE	LT CURVE	0.76	0.00	0.90	Primarily Ditch	1.00	0.94	1.00	0.55	0.98	0.77	77
589.6	589.7	87	TANGENT	CURVE TRANSITION	0.77	0.00	0.70	Primarily FS	1.00	0.86	0.77	0.49	0.88	0.68	68
589.7	589.8	88	TANGENT	OUT OF SHAPE	0.71	0.00	0.90	Primarily FS	1.00	0.91	1.00	0.54	0.97	0.75	75
589.8	589.9	89	TANGENT	TANGENT	0.64	0.58	0.70	Primarily FS	1.00	0.90	0.56	0.64	0.82	0.73	73
589.9	590.0	90	TANGENT	TANGENT	0.73	0.56	0.70	Primarily Ditch	1.00	0.78	0.74	0.66	0.84	0.75	75
590.0	590.1	91	TANGENT	TANGENT	0.76	0.73	0.50	Primarily Ditch	1.00	0.83	0.93	0.66	0.92	0.79	79
590.1	590.2	92	TANGENT	TANGENT	0.78	0.52	1.00	Primarily Ditch	1.00	0.86	0.08	0.77	0.65	0.71	71
590.2	590.3	93	TANGENT	TANGENT	0.77	0.82	0.80	Primarily Ditch	1.00	0.86	0.69	0.80	0.85	0.82	82
590.3	590.4	94	TANGENT	TANGENT	0.77	0.83	0.80	Primarily Ditch	1.00	0.78	1.00	0.80	0.93	0.86	86
590.4	590.5	95	TANGENT	TANGENT	0.76	0.69	0.70	Primarily Ditch	1.00	0.85	0.96	0.72	0.94	0.83	83
590.5	590.6	96	TANGENT	TANGENT	0.84	0.47	0.80	Primarily Ditch	1.00	0.81	1.00	0.70	0.94	0.82	82
590.6	590.7	97	TANGENT	TANGENT	0.75	0.79	0.70	Primarily Ditch	1.00	0.83	0.32	0.75	0.72	0.73	73
590.7	590.8	98	TANGENT	TANGENT	0.76	0.54	0.70	Primarily Ditch	1.00	0.80	0.51	0.67	0.77	0.72	72
590.8	590.9	99	TANGENT	OUT OF SHAPE	0.80	0.00	0.50	Primarily Ditch	1.00	0.81	1.00	0.43	0.94	0.69	69
590.9	591.0	100	TANGENT	OUT OF SHAPE	0.75	0.00	0.70	Primarily Ditch	1.00	0.84	0.61	0.48	0.81	0.65	65
591.0	591.1	101	TANGENT	TANGENT	0.78	0.41	0.70	Primarily Ditch	1.00	0.81	1.00	0.63	0.94	0.78	78
591.1	591.2	102	TANGENT	TANGENT	0.71	0.36	0.70	Primarily Ditch	1.00	0.86	1.00	0.59	0.95	0.77	77
591.2	591.3	103	TANGENT	TANGENT	0.62	0.56	1.00	Primarily Ditch	1.00	0.92	1.00	0.73	0.97	0.85	85
591.3	591.4	104	TANGENT	TANGENT	0.71	0.34	0.80	Primarily Ditch	1.00	0.94	1.00	0.62	0.98	0.80	80
591.4	591.5	105	TANGENT	TANGENT	0.66	0.62	0.50	Primarily Ditch	1.00	0.91	0.60	0.59	0.84	0.72	72
591.5	591.6	106	TANGENT	TANGENT	0.76	0.48	0.90	Primarily Ditch	1.00	0.89	0.00	0.71	0.63	0.67	67
591.6	591.7	107	TANGENT	OUT OF SHAPE	0.78	0.00	0.70	Primarily Ditch	1.00	0.92	0.89	0.49	0.94	0.71	71
591.7	591.8	108	TANGENT	TANGENT	0.71	0.37	0.50	Primarily Ditch	0.99	0.91	0.47	0.53	0.79	0.66	66
591.8	591.9	109	TANGENT	TANGENT	0.79	0.21	0.70	Primarily Ditch	1.00	0.94	0.86	0.56	0.93	0.75	75

Section 10 along FM 136 receives an overall drainage rating of 67. A major reduction comes because of the width calculation. Figure 57 is a screenshot of Section 10 and clearly displays the narrowness of the roadway with no edge striping. Additional drainage reductions come with the flatness of the roadway and the flatness of the ditch flowline. Figure 58 is a digital rendering of the right roadside created within the proof of concept code. Within this rendering, the same elements noted in Figure 57 can be seen. The flowline of the ditch steepens as it approaches the

cross-culvert, but the ditch flowline approaching that point is flat enough to present a sedimentation or potential ponding issue. The ditch flowline slope in this area is approximately 0.6 percent. Figure 59 represents the digital rendering of the paved surface. The spike in Figure 59 represents the laser measuring the passing truck, seen in Figure 57.
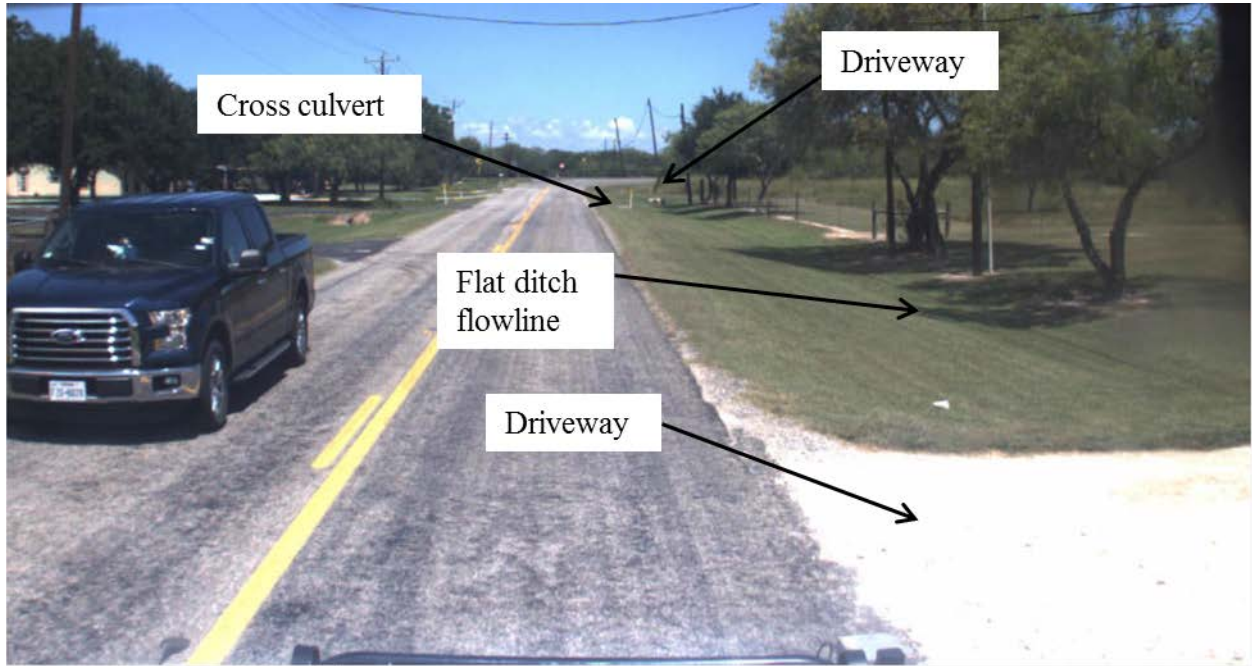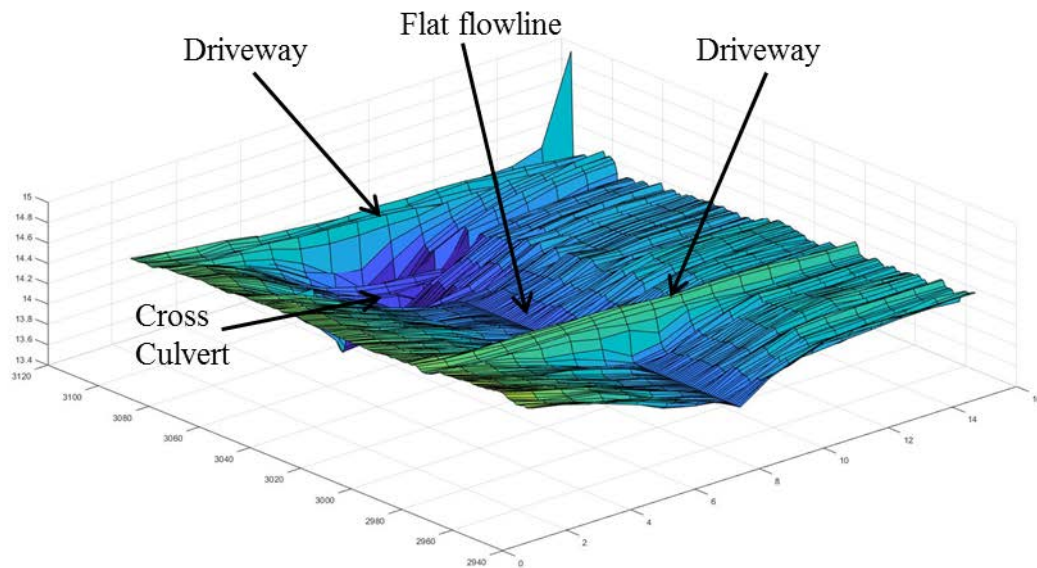

Figure 57. Section 10 along FM 136.

Figure 58. Section 10 along FM 136 Proof of Concept Code Right Roadside Image.
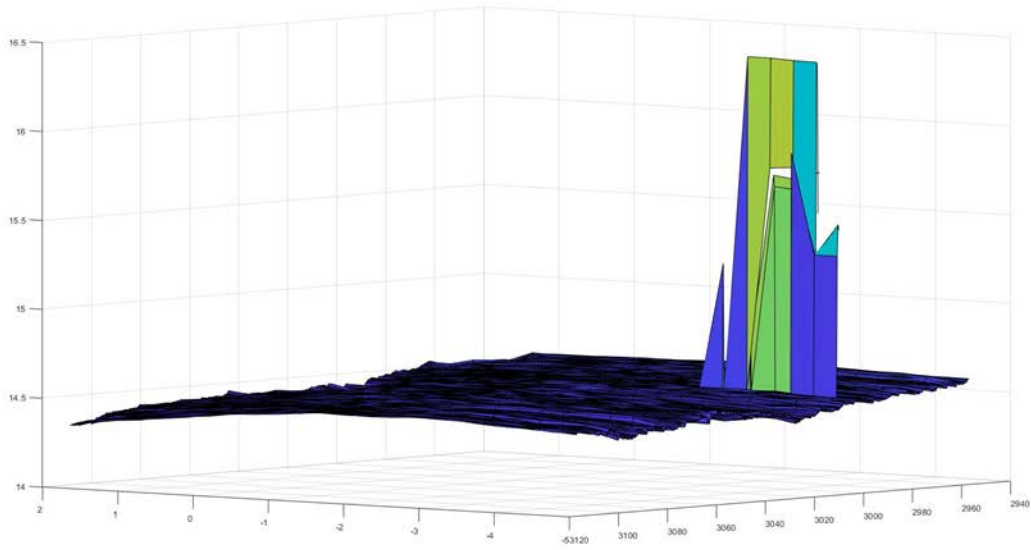
Figure 59. Section 10 along FM 136 Proof of Concept Code Paved Surface Image.

FM 2678—CORPUS CHRISTI DISTRICT

Table 35 presents the network-level results for FM 2678 in the Corpus Christi District.

Table 35. FM 2678 Surface Drainage Rating Summary.

Begin TRM	End TRM	Section	Alignment Classificaiton	Section Shape	Roadway Surface			RT Roadside Shape	Roadside Surface			Combined Surface Rating	Combined Roadside Rating	Overall Drainage Rating	Overall Rating Normalized to 100
					RT Width Rating	RT Cross Slope Rating	Hydro-planing Rating		RT Front Slope Rating	RT Ditch Depth Rating	RT Ditch Slope Rating				
576.0	576.1	1	LTCURVE	LT CURVE	0.62	1.00	0.80	Primarily Ditch	1.00	0.97	0.65	0.81	0.87	0.84	84
576.1	576.2	2	LTCURVE	LT CURVE	0.59	1.00	0.70	Primarily Ditch	1.00	0.95	1.00	0.76	0.98	0.87	87
576.2	576.3	3	LTCURVE	LT CURVE	1.00	1.00	0.70	Primarily Ditch	1.00	0.97	0.81	0.90	0.92	0.91	91
576.3	576.4	4	TANGENT	CURVE TRANSITION	1.00	0.96	0.80	Primarily Ditch	1.00	0.96	1.00	0.92	0.98	0.95	95
576.4	576.5	5	TANGENT	TANGENT	1.00	0.93	0.80	Primarily Ditch	1.00	0.90	0.79	0.91	0.90	0.90	90
576.5	576.6	6	TANGENT	TANGENT	0.95	0.84	0.90	Primarily Ditch	1.00	0.90	0.95	0.89	0.95	0.92	92
576.6	576.7	7	TANGENT	TANGENT	1.00	0.79	0.80	Primarily Ditch	1.00	0.95	0.88	0.86	0.94	0.90	90
576.7	576.8	8	TANGENT	TANGENT	1.00	0.97	0.80	Primarily Ditch	1.00	1.00	0.88	0.92	0.96	0.94	94
576.8	576.9	9	RTCURVE	CURVE TRANSITION	1.00	0.98	0.80	Primarily Ditch	1.00	1.00	1.00	0.93	1.00	0.96	96
576.9	577.0	10	RTCURVE	RT CURVE	0.89	1.00	0.70	Primarily Ditch	1.00	0.99	1.00	0.86	1.00	0.93	93
577.0	577.1	11	RTCURVE	CURVE TRANSITION	1.00	0.96	0.70	Primarily Ditch	1.00	0.90	1.00	0.89	0.97	0.93	93
577.1	577.2	12	TANGENT	TANGENT	1.00	0.92	0.90	Primarily Ditch	1.00	0.91	0.86	0.94	0.92	0.93	93
577.2	577.3	13	TANGENT	TANGENT	1.00	0.88	0.90	Primarily Ditch	0.97	0.88	0.52	0.93	0.79	0.86	86
577.3	577.4	14	TANGENT	TANGENT	1.00	0.86	0.90	Primarily Ditch	1.00	0.88	0.64	0.92	0.84	0.88	88
577.4	577.5	15	TANGENT	TANGENT	1.00	0.94	0.80	Primarily Ditch	1.00	0.92	0.55	0.91	0.83	0.87	87
577.5	577.6	16	TANGENT	TANGENT	1.00	0.95	0.90	Primarily Ditch	1.00	0.93	0.53	0.95	0.82	0.88	88
577.6	577.7	17	TANGENT	TANGENT	1.00	0.85	0.70	Primarily Ditch	1.00	0.90	1.00	0.85	0.97	0.91	91
577.7	577.8	18	LTCURVE	OUT OF SHAPE	0.99	0.00	0.70	Primarily Ditch	1.00	0.92	0.86	0.56	0.93	0.75	75
577.8	577.9	19	TANGENT	TANGENT	1.00	0.85	0.90	Primarily Ditch	1.00	0.92	0.97	0.88	0.96	0.92	92
577.9	578.0	20	TANGENT	TANGENT	1.00	0.86	0.90	Primarily Ditch	1.00	0.98	1.00	0.92	0.99	0.96	96
578.0	578.1	21	TANGENT	TANGENT	1.00	0.76	0.80	Primarily Ditch	1.00	0.94	1.00	0.85	0.98	0.92	92
578.1	578.2	22	TANGENT	TANGENT	1.00	0.92	0.80	Primarily Ditch	1.00	0.89	0.63	0.91	0.84	0.87	87
578.2	578.3	23	LTCURVE	CURVE TRANSITION	1.00	0.96	0.50	Primarily Ditch	1.00	0.75	0.53	0.82	0.76	0.79	79
578.3	578.4	24	LTCURVE	LT CURVE	1.00	1.00	0.70	Primarily Ditch	1.00	0.82	0.54	0.90	0.79	0.84	84
578.4	578.5	25	LTCURVE	LT CURVE	1.00	1.00	0.50	Primarily Ditch	1.00	0.97	0.87	0.83	0.95	0.89	89
578.5	578.6	26	LTCURVE	LT CURVE	1.00	1.00	0.80	Primarily Ditch	0.99	1.00	1.00	0.93	1.00	0.97	97
578.6	578.7	27	LTCURVE	LT CURVE	1.00	1.00	0.80	Primarily Ditch	0.99	1.00	1.00	0.93	1.00	0.96	96
578.7	578.8	28	LTCURVE	LT CURVE	1.00	1.00	0.80	Primarily Ditch	1.00	0.99	1.00	0.93	1.00	0.97	97
578.8	578.9	29	LTCURVE	LT CURVE	1.00	1.00	0.80	Primarily Ditch	1.00	1.00	1.00	0.93	1.00	0.97	97
578.9	579.0	30	TANGENT	CURVE TRANSITION	1.00	0.50	0.70	Primarily Ditch	1.00	0.92	0.76	0.73	0.90	0.81	81
579.0	579.1	31	TANGENT	OUT OF SHAPE	0.78	0.00	0.70	Primarily Ditch	1.00	0.92	1.00	0.49	0.97	0.73	73
579.1	579.2	32	TANGENT	OUT OF SHAPE	0.74	0.00	0.80	Primarily Ditch	1.00	0.91	0.46	0.51	0.79	0.65	65
579.2	579.3	33	TANGENT	TANGENT	0.74	0.71	0.70	Primarily Ditch	1.00	0.99	1.00	0.72	1.00	0.86	86
579.3	579.4	34	TANGENT	OUT OF SHAPE	0.96	0.00	0.70	Primarily Ditch	1.00	1.00	1.00	0.55	1.00	0.78	78
579.4	579.5	35	TANGENT	OUT OF SHAPE	0.77	0.00	0.70	Primarily FS	0.99	1.00	1.00	0.49	1.00	0.74	74
579.5	579.6	36	TANGENT	OUT OF SHAPE	0.67	0.00	0.70	Primarily Ditch	1.00	1.00	1.00	0.46	1.00	0.73	73
579.6	579.7	37	TANGENT	OUT OF SHAPE	0.72	0.00	0.70	Primarily Ditch	1.00	0.93	0.60	0.47	0.84	0.66	66
579.7	579.8	38	TANGENT	TANGENT	0.78	0.78	0.80	Primarily Ditch	1.00	0.90	0.53	0.79	0.81	0.80	80
579.8	579.9	39	TANGENT	TANGENT	0.78	0.82	0.70	Primarily Ditch	1.00	0.90	0.53	0.77	0.81	0.79	79
579.9	580.0	40	TANGENT	TANGENT	0.78	0.86	0.80	Primarily Ditch	1.00	0.90	1.00	0.81	0.97	0.89	89
580.0	580.1	41	TANGENT	OUT OF SHAPE	0.68	0.00	0.80	Primarily Ditch	1.00	0.91	0.67	0.49	0.86	0.68	68
580.1	580.2	42	TANGENT	OUT OF SHAPE	0.78	0.00	0.80	Primarily Ditch	1.00	0.94	0.64	0.53	0.86	0.69	69
580.2	580.3	43	TANGENT	OUT OF SHAPE	0.86	0.00	0.80	Primarily Ditch	1.00	0.94	1.00	0.55	0.98	0.77	77
580.3	580.4	44	TANGENT	OUT OF SHAPE	0.86	0.00	0.80	Primarily Ditch	1.00	0.96	1.00	0.55	0.99	0.77	77
580.4	580.5	45	LTCURVE	CURVE TRANSITION	0.80	1.00	0.50	Primarily Ditch	1.00	1.00	1.00	0.60	1.00	0.80	80
580.5	580.6	46	LTCURVE	LT CURVE	0.77	1.00	0.70	Primarily Ditch	1.00	1.00	1.00	0.82	1.00	0.91	91
580.6	580.7	47	LTCURVE	LT CURVE	1.00	1.00	0.70	Primarily Ditch	1.00	1.00	0.81	0.90	0.94	0.92	92
580.7	580.8	48	LTCURVE	LT CURVE	0.72	1.00	0.70	Primarily Ditch	1.00	1.00	0.64	0.81	0.88	0.84	84
580.8	580.9	49	LTCURVE	LT CURVE	0.53	1.00	0.90	Primarily Ditch	1.00	0.95	1.00	0.81	0.98	0.90	90
580.9	581.0	50	LTCURVE	LT CURVE	0.64	1.00	0.90	Primarily Ditch	1.00	1.00	1.00	0.85	1.00	0.92	92

581.0	581.1	51	LTCURVE	LT CURVE	0.99	0.85	0.50	Primarily Ditch	1.00	0.95	1.00	0.78	0.98	0.88	88
581.1	581.2	52	TANGENT	TANGENT	0.60	0.71	0.70	Primarily Ditch	1.00	0.96	1.00	0.67	0.99	0.83	83
581.2	581.3	53	TANGENT	TANGENT	0.73	0.00	0.70	Primarily Ditch	1.00	0.94	1.00	0.48	0.98	0.73	73
581.3	581.4	54	TANGENT	TANGENT	0.55	0.93	0.70	Primarily Ditch	1.00	0.92	1.00	0.72	0.97	0.85	85
581.4	581.5	55	RTCURVE	RT CURVE	0.53	1.00	0.80	Primarily Ditch	1.00	0.93	1.00	0.78	0.98	0.88	88
581.5	581.6	56	RTCURVE	RT CURVE	0.72	1.00	0.80	Primarily Ditch	1.00	0.92	0.90	0.84	0.94	0.89	89
581.6	581.7	57	RTCURVE	RT CURVE	0.72	1.00	0.80	Primarily Ditch	1.00	0.84	0.83	0.84	0.89	0.86	86
581.7	581.8	58	RTCURVE	RT CURVE	0.73	1.00	0.80	Primarily Ditch	1.00	0.81	0.54	0.84	0.78	0.81	81
581.8	581.9	59	RTCURVE	RT CURVE	0.76	1.00	0.80	Primarily Ditch	1.00	0.86	0.19	0.85	0.68	0.77	77
581.9	582.0	60	RTCURVE	RT CURVE	0.72	1.00	0.70	Primarily Ditch	1.00	0.88	0.73	0.81	0.87	0.84	84
582.0	582.1	61	RTCURVE	RT CURVE	1.00	1.00	0.80	Primarily Ditch	1.00	0.96	1.00	0.93	0.99	0.96	96
582.1	582.2	62	RTCURVE	RT CURVE	1.00	1.00	0.70	Primarily Ditch	1.00	1.00	1.00	0.90	1.00	0.95	95
582.2	582.3	63	RTCURVE	RT CURVE	1.00	1.00	0.80	Primarily Ditch	1.00	0.79	1.00	0.93	0.93	0.93	93
582.3	582.4	64	RTCURVE	RT CURVE	1.00	1.00	0.50	Primarily Ditch	1.00	0.88	0.81	0.83	0.90	0.86	86
582.4	582.5	65	TANGENT	TANGENT	1.00	0.89	0.50	Primarily Ditch	1.00	0.94	0.60	0.80	0.85	0.82	82
582.5	582.6	66	TANGENT	TANGENT	1.00	0.88	0.80	Primarily Ditch	1.00	0.93	0.64	0.89	0.85	0.87	87
582.6	582.7	67	TANGENT	TANGENT	1.00	0.92	0.80	Primarily FS	1.00	0.97	1.00	0.91	0.99	0.95	95
582.7	582.8	68	TANGENT	TANGENT	1.00	0.62	0.70	Primarily Ditch	1.00	0.92	1.00	0.77	0.97	0.87	87
582.8	582.9	69	TANGENT	TANGENT	1.00	0.82	0.70	Primarily Ditch	1.00	0.82	1.00	0.84	0.94	0.89	89
582.9	583.0	70	TANGENT	TANGENT	1.00	0.95	0.90	Primarily Ditch	1.00	0.87	0.66	0.95	0.84	0.90	90
583.0	583.1	71	TANGENT	TANGENT	1.00	0.98	0.80	Primarily FS	1.00	0.97	1.00	0.93	0.99	0.96	96
583.1	583.2	72	TANGENT	TANGENT	1.00	0.81	0.80	Primarily FS	0.99	0.96	1.00	0.87	0.99	0.93	93
583.2	583.3	73	TANGENT	TANGENT	1.00	0.75	0.70	Primarily Ditch	0.98	0.93	0.69	0.82	0.87	0.84	84
583.3	583.4	74	TANGENT	TANGENT	1.00	0.66	0.70	Primarily Ditch	0.95	0.99	1.00	0.79	0.98	0.88	88
583.4	583.5	75	TANGENT	TANGENT	1.00	0.27	0.90	Primarily Ditch	0.96	0.99	1.00	0.72	0.99	0.85	85
583.5	583.6	76	TANGENT	TANGENT	1.00	0.62	0.70	Primarily Ditch	0.95	0.98	1.00	0.77	0.98	0.87	87
583.6	583.7	77	TANGENT	TANGENT	1.00	0.34	0.70	Primarily Edge Drain	0.14	1.00	1.00	0.68	0.71	0.70	70
583.7	583.8	78	TANGENT	TANGENT	1.00	0.38	0.70	Various Drainage	0.63	1.00	1.00	0.69	0.88	0.79	79
583.8	583.9	79	TANGENT	TANGENT	1.00	0.67	0.70	Primarily Ditch	0.91	1.00	1.00	0.79	0.97	0.88	88
583.9	584.0	80	TANGENT	TANGENT	1.00	0.93	0.80	Primarily Ditch	0.96	0.98	1.00	0.91	0.98	0.94	94
584.0	584.1	81	TANGENT	TANGENT	1.00	0.91	0.70	Primarily Ditch	0.97	0.99	1.00	0.87	0.99	0.93	93
584.1	584.2	82	TANGENT	TANGENT	1.00	0.46	0.50	Primarily Ditch	0.96	1.00	1.00	0.65	0.99	0.82	82
584.2	584.3	83	TANGENT	TANGENT	1.00	0.31	0.70	Various Drainage	0.51	1.00	1.00	0.67	0.84	0.75	75
584.3	584.4	84	TANGENT	OUT OF SHAPE	1.00	0.00	0.70	Primarily Ditch	0.94	1.00	1.00	0.57	0.98	0.77	77
584.4	584.5	85	TANGENT	TANGENT	1.00	0.52	0.70	Various Drainage	0.66	1.00	1.00	0.74	0.89	0.81	81
584.5	584.6	86	TANGENT	TANGENT	1.00	0.85	0.70	Primarily Ditch	0.98	0.94	1.00	0.85	0.97	0.91	91
584.6	584.7	87	TANGENT	TANGENT	1.00	0.96	1.00	Primarily FS	0.99	1.00	1.00	0.99	1.00	0.99	99
584.7	584.8	88	TANGENT	TANGENT	1.00	0.54	0.70	Primarily FS	1.00	1.00	1.00	0.75	1.00	0.87	87
584.8	584.9	89	TANGENT	TANGENT	1.00	0.64	0.70	Primarily Ditch	1.00	0.97	1.00	0.78	0.99	0.89	89
584.9	585.0	90	TANGENT	TANGENT	1.00	0.26	0.70	Primarily Ditch	0.95	0.97	1.00	0.65	0.97	0.81	81

Section 33 on FM 2678 in the Corpus Christi district represents a tangent section with an overall rating of 86. This section has a roadside rating of 1.0 and a paved surface rating of 0.72. The paved surface rating is impacted by reductions in width, cross-slope, and hydroplaning potential ratings. This section is chosen as an example because in reality the width rating should equal 1.0, increasing the overall rating to 0.90. The width rating fails because the algorithm classifies the EOP too close to the edgeline stripe. Seal-coated roadways can create this issue at the network level. FM 2678 consists of a seal-coated surface where the precoated rock has begun to display the aggregate surface below the precoat, as shown in Figure 60. The EOP algorithm looks for reflectivity changes to determine the offset to the pavement's edge, and the exposed aggregate face can trick the algorithm into believing it has reached the EOP. Overall, the algorithm is highly effective at finding the EOP. Width transitions and the effectiveness in capturing these transitions has been previously discussed with FM 31 in the Atlanta District and FM 2661 in the Tyler District. Across 260 seal-coated sections on FM 2661, FM 31, and FM 2678, the algorithm accurately measures the width 234 times, while in only 26 it finds a narrower width than actual field conditions.

Figure 60. Section 33 along FM 2678 in the Corpus Christi District.

Additional analysis of Section 33 along FM 2678 reveals that the cross-slope rating receives a reduction because the data collection lane cross-slope has flatness issues. The average data collection lane cross-slope within Section 33 is 1.3 percent. Figure 61 displays the flatness of the cross-slope as generated within a cross-section of the mobile LiDAR processing software, Road Doctor. Figure 62 is a figure that can be extracted from the proof of concept code that creates a digital portrait of each section within the analysis. In particular, Figure 62 displays the paved surface of Section 33 along FM 2678. The approximate location of the crown, near the −2 offset line, can be seen in Figure 62. The dimensions within Figure 62 are in metric units and the −2 represents 2 m left of the plumb location of the laser. To the right of the −2 m offset line, the flatness of the data collection lane is easily seen, particularly when compared with the slope of the adjacent. As a point of reference, the average slope of the adjacent lane is approximately 1.8 percent over the 0.1-mi data collection section.
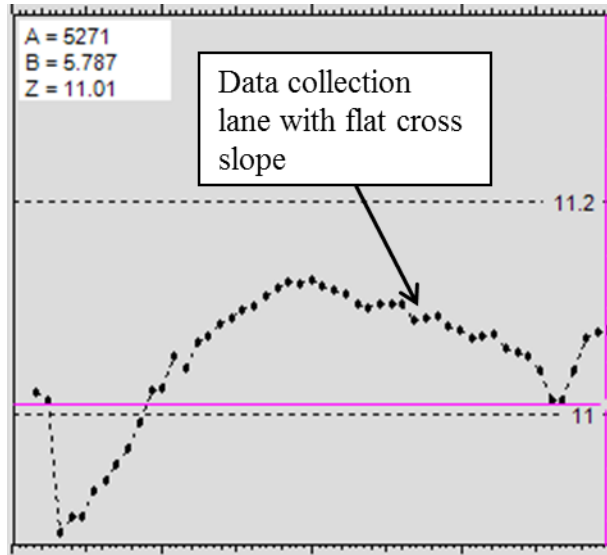
Figure 61. Flat Cross-Slope within Section 33 of FM 2678.
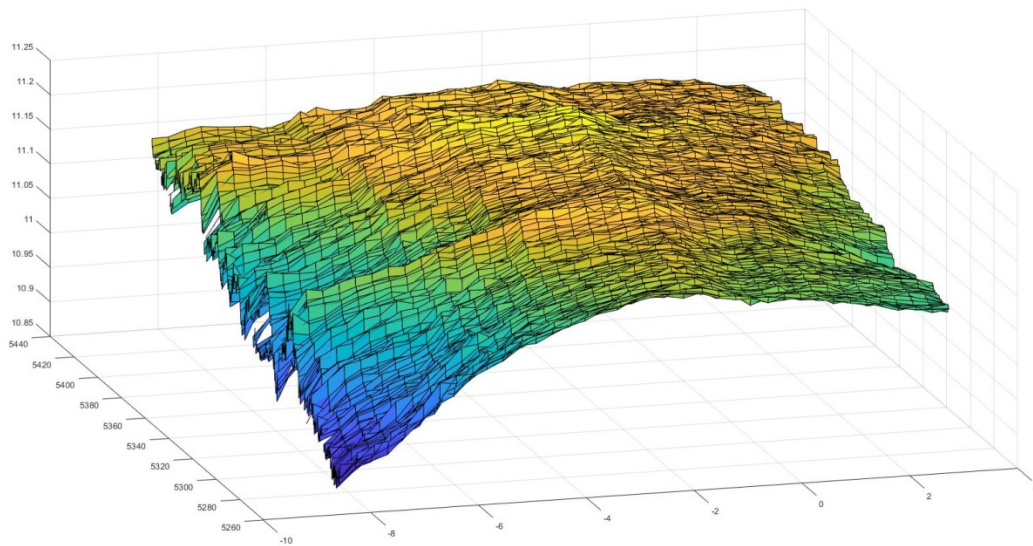

Figure 62. Proof of Concept Code Paved Surface for Section 33 on FM 2678.

Section 33 receives an additional reduction due to hydroplaning potential. As per the Monte Carlo simulation, the hydroplaning speed calculation is 59 mph, but because of a posted speed limit of 75 mph, a rating of 0.7 results.

US 77—CORPUS CHRISTI DISTRICT

Table 36 presents the network-level results for US 77 in the Corpus Christi District.

Table 36. US 77 Surface Drainage Rating Summary.

Begin TRM	End TRM	Section	Alignment Classificaiton	Section Shape	Roadway Surface RT Width Rating	RT Cross Slope Rating	Hydro-planing Rating	RT Roadside Shape	Roadside Surface RT Front Slope Rating	RT Ditch Depth Rating	RT Ditch Slope Rating	Combined Surface Rating	Combined Roadside Rating	Overall Drainage Rating	Overall Rating Normalized to 100
622.7	622.8	1	LT CURVE	LT CURVE	0.36	1.00	0.70	Primarily Ditch	1.00	1.00	1.00	0.69	1.00	0.84	84
622.8	622.9	2	TANGENT	CURVE TRANSITION	1.00	1.00	0.50	Primarily Ditch	1.00	1.00	0.99	0.83	0.99	0.91	91
622.9	623.0	3	RT CURVE	RT CURVE	1.00	1.00	0.70	Primarily Ditch	1.00	1.00	1.00	0.90	1.00	0.95	95
623.0	623.1	4	RT CURVE	RT CURVE	1.00	1.00	0.70	Primarily FS	0.96	1.00	1.00	0.90	0.99	0.94	94
623.1	623.2	5	TANGENT	TANGENT	0.58	0.35	0.50	Primarily Ditch	1.00	1.00	1.00	0.48	1.00	0.74	74
623.2	623.3	6	LT CURVE	CURVE TRANSITION	0.61	0.68	0.50	Primarily Ditch	1.00	1.00	1.00	0.59	1.00	0.80	80
623.3	623.4	7	LT CURVE	LT CURVE	1.00	1.00	0.90	Primarily Ditch	1.00	1.00	0.80	0.97	0.93	0.95	95
623.4	623.5	8	LT CURVE	LT CURVE	0.53	1.00	0.90	Primarily Ditch	1.00	1.00	0.97	0.81	0.99	0.90	90
623.5	623.6	9	LT CURVE	LT CURVE	0.51	1.00	0.90	Primarily Ditch	1.00	1.00	1.00	0.80	1.00	0.90	90
623.6	623.7	10	LT CURVE	LT CURVE	0.76	1.00	0.90	Primarily FS	1.00	0.72	1.00	0.89	0.91	0.90	90
623.7	623.8	11	TANGENT	TANGENT	0.97	0.36	0.70	Primarily Ditch	1.00	0.95	1.00	0.68	0.98	0.83	83
623.8	623.9	12	TANGENT	TANGENT	1.00	0.77	0.70	Primarily Ditch	1.00	0.93	0.95	0.82	0.96	0.89	89
623.9	624.0	13	TANGENT	TANGENT	1.00	0.63	0.70	Primarily Ditch	1.00	0.94	1.00	0.78	0.98	0.88	88
624.0	624.1	14	TANGENT	TANGENT	1.00	0.73	0.70	Primarily Ditch	1.00	0.96	1.00	0.81	0.99	0.90	90
624.1	624.2	15	LT CURVE	CURVE TRANSITION	1.00	0.86	0.70	Primarily Ditch	1.00	1.00	1.00	0.85	1.00	0.93	93
624.2	624.3	16	LT CURVE	LT CURVE	1.00	1.00	0.70	Primarily FS	1.00	1.00	1.00	0.90	1.00	0.95	95
624.3	624.4	17	RT CURVE	CURVE TRANSITION	1.00	1.00	0.70	Primarily Ditch	1.00	1.00	1.00	0.90	1.00	0.95	95
624.4	624.5	18	RT CURVE	RT CURVE	0.55	1.00	0.70	Primarily Ditch	1.00	1.00	1.00	0.75	1.00	0.87	87
624.5	624.6	19	TANGENT	TANGENT	1.00	0.74	0.70	Primarily FS	0.96	1.00	1.00	0.81	0.99	0.90	90
624.6	624.7	20	TANGENT	TANGENT	1.00	0.82	0.70	Primarily Ditch	0.99	1.00	1.00	0.84	1.00	0.92	92
624.7	624.8	21	TANGENT	TANGENT	1.00	0.93	0.70	Primarily Ditch	1.00	1.00	1.00	0.88	1.00	0.94	94
624.8	624.9	22	TANGENT	TANGENT	1.00	0.84	0.70	Primarily Ditch	1.00	1.00	1.00	0.85	1.00	0.92	92
624.9	625.0	23	TANGENT	TANGENT	1.00	0.66	0.70	Primarily FS	0.90	1.00	1.00	0.79	0.97	0.88	88
625.0	625.1	24	TANGENT	TANGENT	1.00	0.82	0.70	Primarily Ditch	0.97	1.00	1.00	0.84	0.99	0.91	91
625.1	625.2	25	TANGENT	TANGENT	1.00	0.93	0.70	Primarily Ditch	1.00	1.00	1.00	0.88	1.00	0.94	94
625.2	625.3	26	TANGENT	TANGENT	1.00	0.96	0.70	Primarily Ditch	1.00	1.00	0.70	0.89	0.90	0.89	89
625.3	625.4	27	TANGENT	TANGENT	1.00	0.91	0.80	Primarily Ditch	1.00	0.98	1.00	0.90	0.99	0.95	95
625.4	625.5	28	TANGENT	TANGENT	1.00	0.92	0.70	Primarily Ditch	1.00	1.00	1.00	0.87	1.00	0.94	94
625.5	625.6	29	TANGENT	TANGENT	1.00	0.91	0.80	Primarily FS	0.98	1.00	1.00	0.90	0.99	0.95	95
625.6	625.7	30	TANGENT	TANGENT	1.00	0.92	0.70	Primarily Ditch	0.99	1.00	1.00	0.87	1.00	0.93	93

URBAN AND METRO SECTIONS

Urban and metro sections present differently than rural sections. The roadway to roadside interaction differs significantly and often varies throughout these types of sections. Metro sections are often too wide to accurately capture the entire surface of interest in a single data collection run. For example, approximately 13 mi of IH 45 within the Houston District was analyzed within this study.

This portion of IH 45 initially consisted of five southbound lanes before a travel lane dropped off, resulting in only four southbound lanes. With the combination of a wide inside shoulder and multiple merge and exit lanes, the overall paved surface width can exceed 75 ft. Data were collected in the far outside lane and then collected in one of the more interior lanes. Data collection in the outside lane impacts the ability to accurately measure paved surface elements far to the left but still within travel lanes. Data collection in the outside lane provides little in the way of information regarding the roadside because often no roadside exists due to concrete barriers flanking both the inside and outside. Using data collected from the inside lane, the portion of IH 45 was treated similar to a project level analysis. The 13 mi of data were subdivided into 0.1-mi data collection sections, similar to the approach taken for the network-

116

level analysis. Within each data collection section, each lane width, lane cross-slope, and hydroplaning potential was calculated. These results are shown in Table 37.

Table 37. IH 45 Southbound Results.

Length (mi)	Section No.	Alignment Classification	Lane 1 Width	Lane 1 Cross Slope	Lane 2 Width	Lane 2 Cross Slope	Lane 3 Width	Lane 3 Cross Slope	Lane 4 Width	Lane 4 Cross Slope	Lane 5 Width	Lane 5 Cross Slope	Tot. Avg. Cross Slope	Hydro-planing Speed	Radius
0.1	1	TANGENT	11.98	2.32%	12.11	2.07%	11.93	1.64%	12.05	1.82%	12.40	1.86%	1.94%	56.8	
0.2	2	TANGENT	11.99	2.34%	12.11	2.07%	11.95	1.58%	12.09	1.68%	12.57	1.78%	1.89%	56.1	
0.3	3	TANGENT	12.29	1.79%	12.30	1.62%	11.85	1.87%	12.15	1.74%	12.58	1.81%	1.77%	54.5	
0.4	4	TANGENT	11.94	1.68%	12.16	1.99%	12.01	2.07%	12.28	1.40%	12.35	1.50%	1.73%	54.5	
0.5	5	TANGENT	11.87	1.75%	12.02	1.98%	12.00	1.80%	12.23	1.47%	12.58	1.86%	1.77%	56.2	
0.6	6	TANGENT	12.20	1.39%	12.03	1.93%	11.91	1.41%	12.21	1.65%	12.27	1.42%	1.56%	54.2	
0.7	7	TANGENT	11.84	1.53%	12.10	2.02%	11.89	1.50%	12.34	2.05%	12.45	1.84%	1.79%	54.1	
0.8	8	TANGENT	11.82	1.48%	12.06	2.00%	11.85	1.64%	12.28	1.86%	12.43	1.69%	1.73%	54.3	
0.9	9	TANGENT	11.90	1.71%	12.19	2.04%	11.06	1.92%	13.16	1.94%	12.63	1.86%	1.89%	55.8	
1	10	TANGENT	11.99	1.98%	12.13	1.96%	12.04	2.06%	12.10	1.97%	13.77	1.77%	1.95%	57.1	
1.1	11	TANGENT	11.97	1.85%	12.03	1.66%	12.20	1.31%	11.94		11.88	1.96%	1.70%	55.7	
1.2	12	TANGENT	12.15	1.40%	11.99	1.58%	12.19	1.37%	12.32	2.32%	12.25	1.90%	1.71%	55.2	
1.3	13	TANGENT	12.10	1.54%	11.96	1.56%	12.20	1.33%	12.06	2.09%	12.53	2.24%	1.75%	55.5	
1.4	14	TANGENT	12.20	1.92%	11.97	1.74%	12.00	1.64%	12.07	1.65%	12.54	2.43%	1.88%	53.5	
1.5	15	TANGENT	12.23	2.16%	12.01	1.92%	11.99	1.77%	11.97	1.76%	12.63	2.08%	1.94%	54.0	
1.6	16	TANGENT	12.04	2.30%	12.07	2.03%	11.93	1.52%	12.00		12.66	1.75%	1.90%	53.7	
1.7	17	TANGENT	12.22	2.24%	11.92	2.04%	12.10	1.57%	12.16	1.43%	12.42	1.28%	1.71%	54.0	
1.8	18	TANGENT	12.01	2.51%	11.97	2.16%	12.06	1.76%	12.22	1.55%	12.44	1.90%	1.98%	53.8	
1.9	19	TANGENT	11.85	2.64%	11.95	2.12%	12.22	1.84%	12.06	1.70%	12.68	1.83%	2.02%	56.5	
2	20	TANGENT	11.96	2.16%	12.09	1.94%	12.11	1.50%	12.11	2.01%	12.39	1.67%	1.86%	55.6	
2.1	21	TANGENT	11.92	2.13%	12.06	1.86%	11.94	1.94%	12.01	1.92%	12.56	2.38%	2.05%	56.4	
2.2	22	TANGENT	11.92	1.98%	12.03	1.73%	11.86	2.07%	12.03	1.62%	12.54	2.17%	1.92%	56.3	
2.3	23	TANGENT	11.90	1.83%	12.42	1.92%	11.47	2.22%	12.45	1.86%	12.20	2.20%	2.00%	55.6	
2.4	24	TANGENT	11.89	1.65%	12.18	1.80%	11.88	1.73%	12.18	1.61%	12.52	2.17%	1.79%	55.7	
2.5	25	TANGENT	11.59	1.89%	12.10	1.90%	12.08	1.53%	12.16	2.03%	12.51	2.13%	1.90%	56.1	
2.6	26	TANGENT	11.80	2.27%	12.15	1.90%	12.09	1.60%	12.15	2.11%	12.96	2.37%	2.05%	54.1	
2.7	27	TANGENT	11.84	1.96%	12.05	1.85%	12.19		12.09		12.62	2.17%	1.99%	54.6	
2.8	28	TANGENT	11.97	2.57%	12.36	2.06%	12.09	2.09%	12.06		12.56	2.63%	2.34%	56.3	
2.9	29	RT CURVE	12.12	3.66%	12.46	2.96%	11.69	3.20%	12.87	2.86%	12.31	3.25%	3.19%	55.9	5462
3	30	RT CURVE	12.43	3.59%	12.25	2.90%	11.87	2.99%	12.13	2.59%	12.47	3.39%	3.09%	56.0	
3.1	31	TANGENT	11.93	2.39%	12.12	2.06%	12.04	2.12%	12.05	1.09%	12.53	2.52%	2.04%	55.6	
3.2	32	TANGENT	12.19	2.08%	11.98	1.87%	12.13	2.20%	12.04		12.81	2.00%	2.04%	55.6	
3.3	33	LT CURVE	12.00	2.36%	12.05	2.10%	12.10	2.09%	11.96		13.00	1.88%	2.11%	56.1	17091
3.4	34	LT CURVE	12.04	2.51%	12.00	1.82%	11.95	1.72%	11.97	1.14%	13.16	2.13%	1.86%	56.1	
3.5	35	TANGENT	11.79	2.83%	12.00	1.61%	12.08	1.91%	12.16	1.09%	12.79	2.01%	1.89%	55.8	
3.6	36	LT CURVE TRANS.	11.10	0.82%	12.25	-0.28%	11.96	-0.37%	11.90		12.77	0.90%	0.27%	55.0	6214
3.7	37	LT CURVE	12.04	-2.57%	12.04	-3.18%	11.95	-3.41%	11.79	-1.67%	13.13	-3.29%	-2.83%	55.3	
3.8	38	LT CURVE	12.31	-2.47%	11.64	-2.95%	12.37	-2.79%	12.84		11.71	-3.08%	-2.82%	53.6	
3.9	39	LT CURVE TRANS.	11.72	0.97%	11.89	0.62%	12.21	0.79%	12.56	0.30%	11.65	-1.28%	0.28%	56.4	
4	40	TANGENT	11.02	2.39%	11.98	2.12%	12.32	1.73%	12.60		11.79	0.30%	1.64%	54.7	
4.1	41	TANGENT	12.41	2.02%	12.03	1.97%	12.16		13.01			NA	2.00%	54.8	
4.2	42	TANGENT	12.15	2.34%	12.05	1.88%	12.10	2.07%	12.97	1.17%		NA	1.87%	56.3	
4.3	43	TANGENT	12.42	2.24%	12.01	1.64%	12.14	2.14%	12.99	1.17%		NA	1.80%	56.6	
4.4	44	TANGENT	11.98	2.30%	12.03	1.83%	12.10	2.06%	12.95	1.10%		NA	1.82%	55.3	
4.5	45	TANGENT	11.93	2.14%	11.98	2.01%	11.92	2.06%	13.32	1.15%		NA	1.84%	55.5	
4.6	46	TANGENT	12.10	2.31%	11.97	2.11%	11.69	2.11%	14.30	1.78%		NA	2.08%	54.3	
4.7	47	TANGENT	12.07	2.12%	12.18	2.06%	11.89	2.30%	13.13			NA	2.16%	56.4	

4.8	48	RT CURVE	12.17	2.76%	12.18	2.27%	11.94	2.02%	12.78		NA	2.35%	55.6	
4.9	49	RT CURVE	12.66	2.66%	12.26	2.25%	12.04	1.95%	13.01		NA	2.28%	55.7	
5	50	RT CURVE	12.37	2.74%	12.24	2.44%	12.11	2.00%	11.89		NA	2.39%	55.5	9442
5.1	51	RT CURVE	12.30	2.20%	12.15	2.02%	12.02	2.06%	11.65	1.80%	NA	2.02%	55.0	
5.2	52	RT CURVE	11.76	2.04%	12.29	1.86%	11.73	1.84%	12.26	2.26%	NA	2.00%	54.6	
5.3	53	RT CURVE	11.31	2.13%	11.80	2.02%	11.44	2.01%	12.51	2.25%	NA	2.10%	55.1	
5.4	54	TANGENT	12.03	1.71%	11.25	1.42%	10.90		11.73	1.88%	NA	1.67%	55.6	
5.5	55	TANGENT	12.46	1.26%	11.10	1.14%	10.91	1.42%	11.02	1.56%	NA	1.35%	56.1	
5.6	56	TANGENT	10.95	1.31%	11.06		10.93	1.47%	11.07	1.54%	NA	1.44%	55.3	
5.7	57	TANGENT	10.84	1.35%	11.08	1.26%	10.87	1.13%	11.04	1.54%	NA	1.32%	55.7	
5.8	58	TANGENT	10.90	1.34%	11.08	1.23%	10.89	1.14%	11.08	1.77%	NA	1.37%	56.0	
5.9	59	TANGENT	10.82		11.08	1.30%	10.89		11.15	1.41%	NA	1.35%	55.8	
6	60	TANGENT	10.94	1.51%	11.06	1.40%	10.89	1.34%	11.12	1.62%	NA	1.47%	56.6	
6.1	61	LT CURVE	10.93	1.21%	11.01	1.18%	11.14	1.47%	10.99	1.62%	NA	1.37%	55.6	10407
6.2	62	TANGENT	10.95		11.01		11.26	1.10%	11.08	1.45%	NA	1.27%	53.2	
6.3	63	TANGENT	11.08		10.97		11.01	1.11%	11.10	1.44%	NA	1.28%	54.3	
6.4	64	TANGENT	10.97		11.09		11.09	1.17%	11.00	1.51%	NA	1.34%	53.2	
6.5	65	TANGENT	10.94	1.30%	11.05		11.06		11.13	1.53%	NA	1.41%	55.6	
6.6	66	TANGENT	10.98	1.37%	10.97	1.26%	11.02	1.18%	11.09	1.35%	NA	1.29%	57.6	
6.7	67	TANGENT	11.04	1.54%	10.97	1.13%	11.00		10.95		NA	1.34%	57.1	
6.8	68	TANGENT	10.93	1.70%	10.98		11.07	1.18%	10.89		NA	1.44%	58.1	
6.9	69	TANGENT	10.92	1.52%	11.08	1.23%	11.08	1.29%	11.09	1.39%	NA	1.36%	58.3	
7	70	TANGENT	11.03	1.48%	11.09	1.21%	11.00	1.24%	11.05	1.30%	NA	1.31%	57.0	
7.1	71	TANGENT	11.01	1.42%	11.11	1.28%	10.93	1.18%	11.17		NA	1.29%	57.8	
7.2	72	TANGENT	11.15	1.67%	11.23	1.30%	11.00	1.26%	11.04	1.13%	NA	1.34%	57.4	
7.3	73	TANGENT	11.17	1.44%	11.15	1.26%	10.93	1.20%	11.35		NA	1.30%	55.5	
7.4	74	TANGENT	10.95	1.27%	11.26	1.15%	11.05	1.17%	11.19	1.61%	NA	1.30%	53.9	
7.5	75	TANGENT	10.99	1.30%	11.11	1.14%	11.06	1.22%	11.15	1.48%	NA	1.28%	54.7	
7.6	76	TANGENT	10.95	1.65%	11.14		11.08	1.16%	11.22	1.17%	NA	1.33%	53.7	
7.7	77	TANGENT	10.95	1.34%	11.33	1.15%	10.86		11.02	1.37%	NA	1.29%	57.2	
7.8	78	TANGENT	10.77	1.22%	11.23		10.98	1.28%	11.16	1.18%	NA	1.23%	56.7	
7.9	79	TANGENT	10.78	1.43%	11.37	1.25%	10.98		11.12	1.26%	NA	1.32%	56.9	
8	80	TANGENT	10.83	1.37%	11.23	1.29%	10.91	1.45%	11.19	1.65%	NA	1.44%	56.0	
8.1	81	TANGENT	11.22		10.83		11.17	1.16%	11.31	1.62%	NA	1.39%	56.7	
8.2	82	TANGENT	11.16		10.82	1.12%	11.02		11.26	1.55%	NA	1.33%	54.5	
8.3	83	TANGENT	11.18		10.91		11.02	1.22%	11.23	1.23%	NA	1.23%	56.9	
8.4	84	TANGENT	11.17		10.84	1.26%	11.05	1.31%	11.46		NA	1.28%	56.9	
8.5	85	TANGENT	11.00		10.98	1.30%	10.95	1.32%	11.53	1.39%	NA	1.34%	57.1	
8.6	86	TANGENT	11.11	1.15%	10.89	1.37%	11.13	1.36%	11.58	1.18%	NA	1.26%	56.6	
8.7	87	RT CURVE	10.94	1.08%	11.08		10.93	1.27%	11.63		NA	1.18%	56.1	11333
8.8	88	LT CURVE	10.96		10.93	-1.70%	10.90	-1.07%	11.39	-0.55%	NA	-1.11%	12.6	
8.9	89	LT CURVE	10.59	-2.74%	11.40		10.97	-3.95%	11.50		NA	-3.35%	12.6	3634
9	90	LT CURVE	10.94	-2.78%	11.05		10.93		11.66		NA	-2.78%	12.6	
9.1	91	LT CURVE TRANS.	11.14		11.00	-2.42%	10.90		11.45		NA	-2.42%	12.6	
9.2	92	TANGENT	11.04		11.04		10.99		11.89	1.68%	NA	1.68%	55.8	
9.3	93	TANGENT	11.22	1.83%	11.03	1.76%	11.06	1.73%	12.24	1.74%	NA	1.77%	56.9	
9.4	94	RT CURVE	11.11	1.32%	11.52	1.29%	10.81	1.26%	11.95	1.28%	NA	1.29%	52.6	6603
9.5	95	TANGENT	11.08	1.19%	11.12	1.18%	10.96	1.19%	12.09	1.18%	NA	1.19%	52.6	
9.6	96	TANGENT	11.17	1.21%	11.36	1.14%	10.63		12.09		NA	1.18%	54.1	
9.7	97	TANGENT	11.11	1.39%	11.35		10.74		12.29	1.21%	NA	1.30%	57.3	
9.8	98	TANGENT	11.15	1.39%	11.55	1.34%	10.74	1.26%	11.92	1.23%	NA	1.31%	55.4	
9.9	99	TANGENT	11.03	1.58%	11.06	1.57%	11.33	1.45%	11.97	1.40%	NA	1.50%	56.0	
10	100	TANGENT	11.06	1.31%	10.99	1.32%	10.98	1.26%	12.13	1.22%	NA	1.28%	54.7	

10.1	101	TANGENT	11.13	1.39%	10.68	1.37%	11.36	1.30%	12.00	1.29%		NA	1.34%	55.6	
10.2	102	TANGENT	10.93	1.31%	10.90	1.27%	11.05	1.26%	13.33	1.26%		NA	1.28%	52.9	
10.3	103	LT CURVE	11.10	1.31%	11.21	1.27%	10.67		12.38	1.25%		NA	1.28%	53.8	8104
10.4	104	LT CURVE	11.00	1.66%	11.09	1.55%	10.92	1.48%	12.05	1.46%		NA	1.54%	54.7	
10.5	105	TANGENT	11.07	1.27%	10.91	1.25%	11.18		12.25			NA	1.26%	55.5	
10.6	106	TANGENT	10.98	1.34%	11.05	1.32%	10.56	1.22%	12.68	1.19%		NA	1.27%	54.9	
10.7	107	TANGENT	10.92	1.26%	11.07	1.25%	11.10		11.99			NA	1.26%	54.8	
10.8	108	TANGENT	10.99	1.34%	11.19	1.26%	11.24	1.18%	11.70	1.17%		NA	1.24%	55.9	
10.9	109	TANGENT	10.95	1.35%	11.35	1.23%	10.84	1.20%	11.93	1.18%		NA	1.24%	56.3	
11	110	TANGENT	10.88	1.66%	11.09	1.52%	11.02	1.48%	12.02	1.44%		NA	1.53%	55.7	
11.1	111	TANGENT	11.05	1.68%	11.07	1.51%	11.01	1.48%	12.14	1.48%		NA	1.54%	55.8	
11.2	112	TANGENT	11.01	1.27%	11.07	1.23%	11.03	1.16%	11.95			NA	1.22%	55.4	
11.3	113	TANGENT	11.00	1.34%	11.13		10.97		12.35			NA	1.34%	52.9	
11.4	114	TANGENT	11.01		10.96		11.10	1.21%	12.44			NA	1.21%	53.2	
11.5	115	RT CURVE	11.10	1.28%	11.17	1.24%	10.87	1.21%	12.05			NA	1.25%	53.7	16747
11.6	116	TANGENT	11.15	1.47%	11.24	1.37%	10.86	1.33%	12.01	1.32%		NA	1.37%	56.3	
11.7	117	TANGENT	11.03	1.47%	11.39	1.44%	10.90	1.33%	12.24	1.32%		NA	1.39%	55.6	
11.8	118	TANGENT	11.04	1.64%	11.18	1.57%	10.91	1.53%	12.16	1.49%		NA	1.56%	56.0	
11.9	119	TANGENT	11.01	1.64%	11.07	1.55%	10.97	1.49%	12.02	1.45%		NA	1.53%	53.9	
12	120	TANGENT	11.15	1.46%	11.08	1.38%	11.00	1.35%	11.93	1.33%		NA	1.38%	55.8	
12.1	121	TANGENT	11.20	1.88%	11.20	1.80%	10.90	1.79%	12.12	1.75%		NA	1.80%	55.0	
12.2	122	LT CURVE	10.94	1.55%	11.23	1.64%	11.01	1.68%	12.07	1.70%		NA	1.64%	54.8	7558
12.3	123	TANGENT	10.89	1.28%	11.21	1.26%	11.09	1.27%	11.76	1.26%		NA	1.27%	53.2	
12.4	124	TANGENT	10.99	1.25%	11.10	1.19%	11.64	1.20%	11.42	1.18%		NA	1.20%	53.4	
12.5	125	TANGENT	11.02		10.92	1.49%	11.45	1.42%	11.58	1.37%		NA	1.43%	52.8	
12.6	126	RT CURVE	10.93	1.63%	11.08	1.58%	11.33	1.59%	11.39	1.54%		NA	1.58%	55.5	
12.7	127	RT CURVE	11.04	3.18%	11.14	3.17%	11.40	3.15%	11.23	3.11%		NA	3.15%	55.9	3908
12.8	128	RT CURVE	11.21	2.93%	11.20	2.98%	11.51	2.98%	11.30	2.99%		NA	2.97%	55.2	
12.9	129	TANGENT	11.03	1.48%	11.34	1.49%	11.27	1.46%	11.30	1.36%		NA	1.45%	54.3	
13	130	TANGENT	10.90	1.55%	11.43	1.52%	11.14	1.50%	11.43	1.44%		NA	1.50%	54.0	

Section 89 along IH 45 consists of a left curve with a radius calculation of 3,634 ft and a superelevation of 2.74 percent falling to the left. Figure 63 displays Section 89 during the data collection.

Figure 63. Section 89 along IH 45.

Similarly, Section 38 consists of a left curve with a radius of 6,214 ft with an average superelevation to the left, or inside of IH 45, of 2.82 percent. This dynamic creates a potential hydroplaning speed of 53.6 mph on a roadway with a posted speed limit of 60 mph. This section consists of five southbound lanes approximately 12 ft in width. Figure 64 displays a screen shot from the night of collection, and Figure 65 displays a digital rendering developed with the proof of concept code. The 1-ft × 1-ft grid discussed in other parts of the report can be seen in the rendering. The elevation information contained in these grids helps in calculating cross-slopes, hydroplaning speed, and other elevation-dependent parameters. However, Figure 65 also shows the challenges associated with data collection on metro sections. Gaps are clearly seen to the far right of the gridded data. This same challenge exists to the far left when collecting data on rural sections, but the larger issue on metro sections is that these gaps occur in the direction of data collection. This discrepancy is one of the primary reasons metro sections should be treated more like project level analysis.

Figure 64. Section 38 along IH 45.
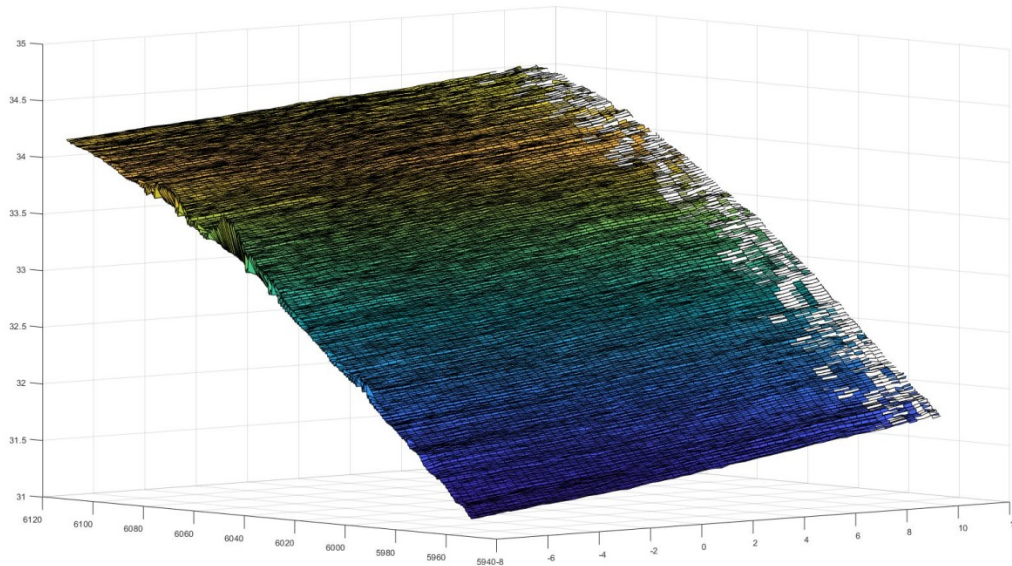
Figure 65. Section 38 along IH 45 Proof of Concept Code Rendering.

Urban curb and gutter sections also present specific points of analysis that are better evaluated from a project level perspective. Figure 66 shows a curb and gutter section along SH 30 (Harvey Rd.) in the Bryan District. Data were collected during daytime hours, and traffic is easily visible in Figure 66. Traffic to the left of the data collection vehicle presents a target for the laser to impact prior to making contact with the roadway surface. Traffic impacts occur during rural data collection as well, but on two-lane facilities the analysis focuses on the data collection lane and the adjacent roadside, limiting the impacts of passing traffic. Also, in the rural environment, the volume of traffic causes fewer problems, and the algorithms used to develop the ratings filters out the erroneous points created by the laser measuring passing vehicles. The filter threshold allows for ratings when 50 percent measurement occurs. Figure 67 consists of the reflectivity data generated in the Road Doctor post-processing software that displays 0.1-mi of data with a truck obscuring a significant amount of data collection to the left of the data collection lane. Figure 67 was created from data collected along SH 30 (Harvey Rd.) in the Bryan District.

Figure 66. Urban Curb and Gutter Section Example.
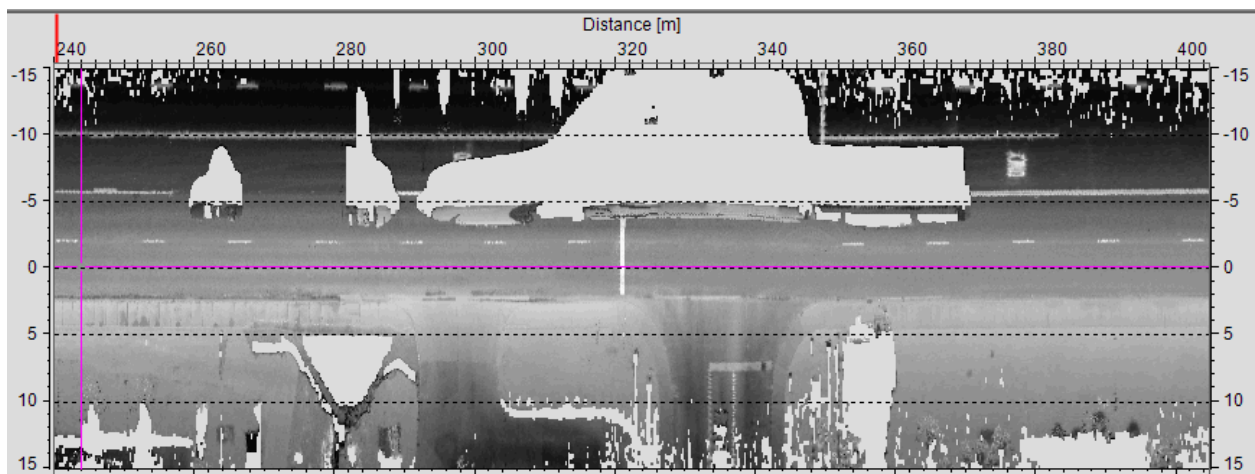
Figure 67. Passing Traffic Impacting Data Collection in a Curb and Gutter Section.

While traffic components and changes in geometry, such as the addition of turn lanes and intersection elements, impact the ability to rate urban sections in a network-level fashion, data can be measured that provides valuable information to decision makers. For example, Figure 68 displays a 1-ft × 1-ft digital rendering of SH 30. Within this rendering, the location of the inlets and outlets for surface water can be seen. Creating this rendering with gridded data allows for the determination of drainage basins along the data collection section. Knowing the drainage basin size allows for additional hydraulic calculations for inlet sizing and outside lane ponding that capitalize on mobile LiDAR-measured, existing drainage conditions. For most hydraulic calculation, design values are used, but mobile LiDAR now presents an opportunity to use actual field measurements to redesign or make adjustments.

Figure 69 consists of two cross-sections generated in the Road Doctor post-processing software. One of the cross-sections displays the elevation jump that occurs at the curb. Within this 0.1-mi data collection section, different analyses can be performed regarding features such as curb height and driveway locations and size. Figure 70 consists of a 0.1-mi data collection section in an urban environment with multiple driveways. The measurements taken with mobile LiDAR help in distinguishing the location and size of driveways. The lengths with heights between 6 in. and 7 in. represent full curb and gutter lengths. Spikes in the data come from the laser impacting tall objects near the back of curb, such as a vehicle sitting in the driveway, a utility pole, or vegetation.
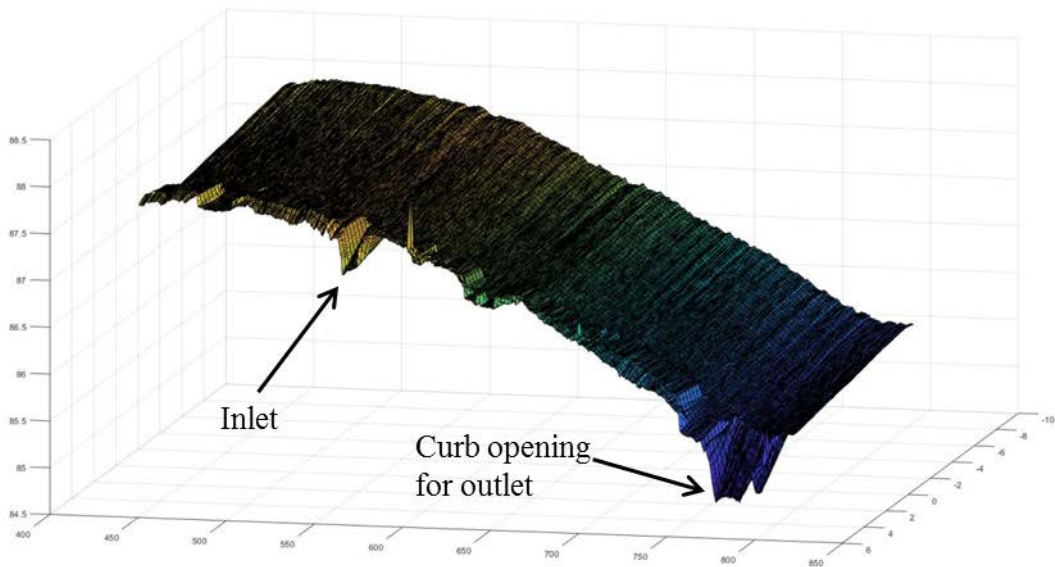
Figure 68. Proof of Concept Code Rendering of a Curb and Gutter Section.
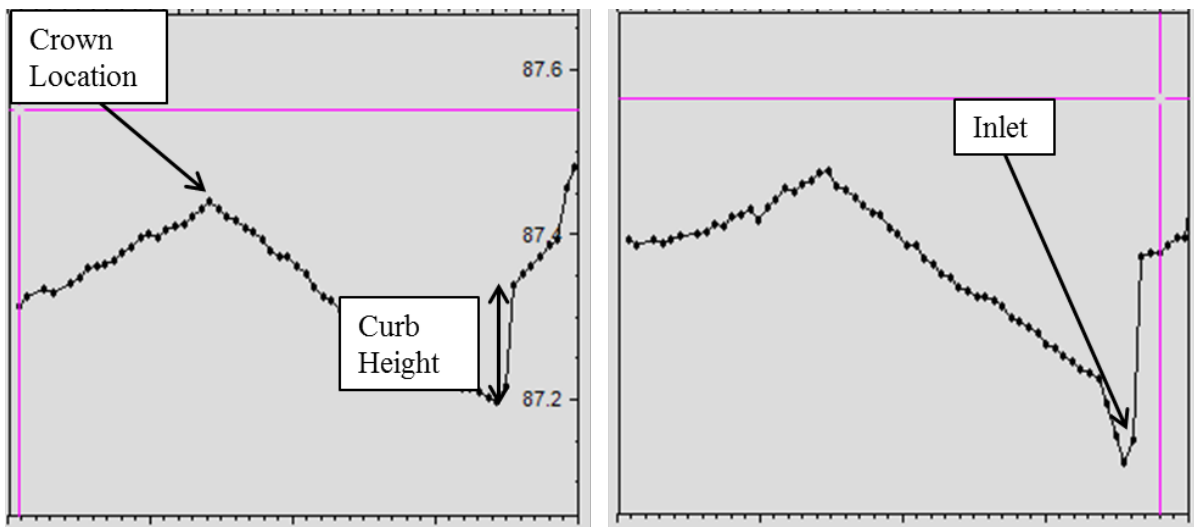
Figure 69. Road Doctor Processing Software Cross-Section of a Curb and Gutter Section.
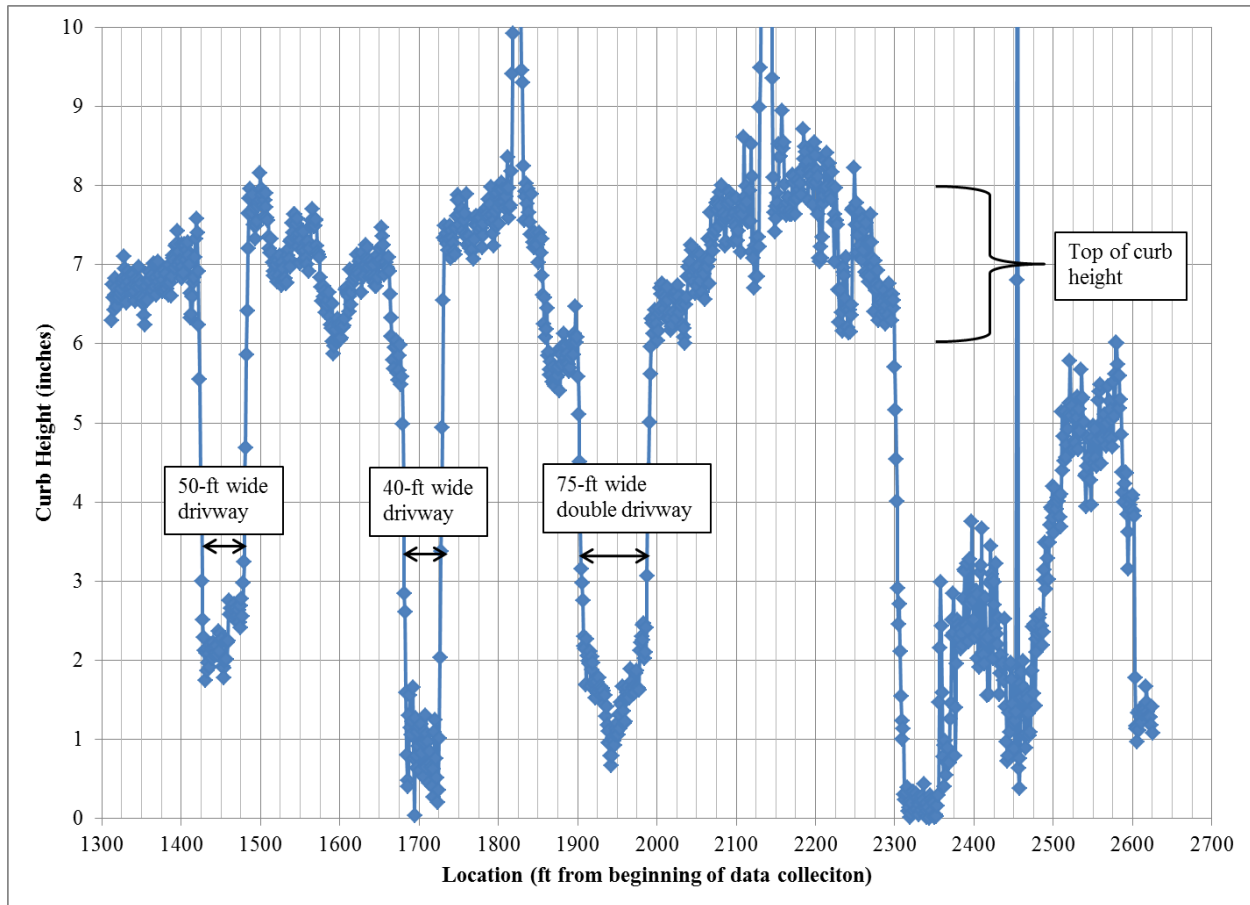
Figure 70. Curb and Gutter Section Analysis.

While difficult to perform at the network level, curb and gutter sections can be evaluated for a variety of elements that might assist in decision making. Figure 70 provides information that might be helpful in terms of access management analysis, providing decision makers with information on driveway size and spacing. If this situation existed within an urban section with a raised median, an additional data collection could be performed on the inside lane to capture median opening spacing. By using the information collected on median openings and driveway spacing, additional evaluation could be performed on access management optimization. Obviously, this type of analysis more needs to occur at a project level.

Furthermore, collecting data in the outside lane facilitates an evaluation of curb height, particularly if the gutter pan has hot-mix in it. For specific projects, such as mill and fill in an urban environment, mobile LiDAR measurements can be used to estimate the thickness of hot-mix currently in the gutter pan. Other more typical analyses can be performed, such as lane width, cross-slope, and hydroplaning, if desired.

Mobile LiDAR provides a tool to capture vast amounts of data that can be converted to information for urban curb and gutter sections and multi-lane metro sections. Unlike rural highways with roadway and roadside features, urban and metro sections have various geometric

124

features that hamper the ability to rate at the network level. Unlike pavement distress that allows for a particular evaluation in a lane, surface geometry moves beyond the lane and must capture impacts from other lanes, the roadside, and other asset features such as curb and gutter and inlets. While algorithms and proof of concept code allow for more rapid processing of LiDAR data with little manual analysis, they were developed for typical rural environments, and urban and metro sections present many exceptions. In fact, a generalized network-level algorithm for rural and metro areas was deemed infeasible because more work must be performed to develop algorithms and proof of concept code for the exceptions than for the basic generalized code.

Typical measurements on lane width and cross-slope can easily be obtained, but beyond these simple elements, researchers discovered that detailed inputs of what might help the decision maker were required to extract the proper data for analysis. Due to the large number of exceptions within these types of pavement sections, researchers were unable to settle on exact elements to include in a surface drainage rating. Rather, researchers recommend using mobile LiDAR techniques within these types of sections to evaluate specific points of concern. In summary, comparing the surface drainage in a rural area with metro and urban areas is not comparing apples to apples. Rural areas allow for the creation of network-level tools, while urban and metro areas contain many exceptions to the rules, thereby essentially forcing the transition to a more project level review.

DRAINAGE RATING APPLICATION SUMMARY

The surface drainage rating was successfully applied to 73.5 miles of roadway. The rating consists of three paved surface elements, each contributing 33 percent to the overall paved surface rating and 16.7 percent to the overall drainage rating. Three additional roadside elements were rated and contributed 33 percent to the roadside rating and 16.7 percent to the overall rating. A paved surface rating was equally combined with the roadside rating to generate the overall rating.

Many low ratings resulted from sections classified as out of shape. Out-of-shape sections received a rating of 0.0 for cross-slope. Surface ratings were also impacted by hydroplaning speed calculations. Some of the rural roadways have a posted speed limit of 70 mph or 75 mph, but the hydroplaning speed calculation indicates hydroplaning potential at less than 60 mph. It is likely that the design speed for the roadway is less than 70 mph based on the age of the facilities; nonetheless, the rating was developed based on posted speed in an attempt to capture motorist behavior.

Roadside ratings were often higher than the paved surface rating. When roadsides received deductions, it was typically due to either shallow ditches or flat flowlines. Often, front slopes received perfect ratings, while depth or flowlines received deductions. When this is the case, it might be possible to deepen and steepen ditches without creating too-steep front slopes and thereby impacting safety. The paradox between safety and drainage weaves its way through the

rating. The rating system was developed to acquiesce to safety requirements and then fit drainage needs within those boundaries. For this reason, the roadside can receive a high rating for the front slope and a low rating for the ditch depth because these features often counterbalance each other. In reality, designers and engineers perform the same balancing act. The network-level surface drainage rating allows engineers to have a performance metric that accounts for both safety and drainage.

Within the study, proof of concept code was developed for application of the drainage rating. Significant effort was expended to develop this proof of concept code to deal with the vast amount of data collected with mobile LiDAR. It is impractical to think that the amount of data and size of TxDOT's network can be manually processed; therefore, researchers developed a proof of concept code to generate network-level ratings. In future implementation projects, this code can be improved for efficiency, but it presently presents the proof that for rural networks vast amounts of data can be collected and processed to provide metrics to describe surface drainage.

Urban and metro sections present several problems in the development of the proof of concept code. The geometry within these sections varies, and the contribution of the roadside is sometimes completely nonexistent. These types of sections do not compare to the same roadway and roadside contributions seen on rural sections. Throughout the course of the project and the development of proof of concept code, researchers found that extensive work was required to capture the exceptions that must be accounted for with urban and metro sections. Researchers concluded that urban and metro sections should be treated more similarly to project level analyses rather than network-level analyses. Project level analyses can be highly effective with manual processing, as described in the next section.

PROJECT LEVEL APPLICATIONS OF MOBILE LIDAR MEASUREMENTS

The primary objective within this task was to perform project level analyses using mobile LiDAR and develop recommendations based on that data. Project level analyses were performed on:

- US 75 in the Paris District.
- RM 652 in the Odessa District.
- US 77 in the Austin District.
- IH 30 in the Atlanta District.

On the US 75 analysis for the Paris District, mobile LiDAR measurements were used to develop a roadside ditch grading plan and to design an underdrain system. Originally, it was believed that these drainage improvements would be used to move the water out from under the concrete pavement to allow for rubblization. The Paris District decided not to pursue rubblization; nonetheless, mobile LiDAR data were used to perform ditch grading. The underdrain design is also included in this task report.

The RM 652 analysis included developing a roadside drainage design and new profile design for a 2-mi portion of the roadway. This roadway potentially sits atop gypsum deposits, making it necessary to ensure water moves away from the pavement structures as efficiently as possible. RM 652 has a narrow 100-ft ROW with a 36-ft wide roadway. Mobile LiDAR assisted in the design of ditches where ditches were not originally present. The narrowness of ROW forced a detailed analysis of front slope conditions. This analysis was facilitated by the near continuous nature of mobile LiDAR measurements.

Mobile LiDAR analysis was used on US 77 to identify rutted locations and provide this information to district maintenance forces to help make decisions on where to perform maintenance work. Using mobile LiDAR, rut maps were created on approximately 5 mi of US 77. In addition to identifying rutted locations, LiDAR data were used to evaluate the roadside and make recommendations on where drainage improvements were needed.

IH 30, through Titus County in the Atlanta District, was evaluated for rutting using mobile LiDAR. This portion of IH 30 experienced premature distress. The mobile LiDAR analysis identified areas of rutting deeper than 0.5 in. in both wheel paths in each outside lane. Areas of deep rutting were then cross-referenced using the accompanying video to determine if deep rutting and striping were occurring at the same location.

This task report includes many figures to display LiDAR measurements and design recommendations produced by LiDAR analysis. Many of these figures include elevations. These elevations are only as accurate as the GPS on the MLS. Designs are based on locating a tie-point

and assuming measurements are relative from that location. The relative assumption provides accurate measurements for preliminary design development in relation to the actual project. Additionally, the design is accurate enough to move forward with detailed design based on the scope and details generated in the mobile LiDAR analysis.

US 75—PARIS DISTRICT

Background Information

A project level evaluation occurred on US 75 on the north side of Sherman, Texas, within the Paris District. This case study evaluated a 700 m (0.4 mi) segment of US 75 in northern Texas that has persistent drainage related failures and distresses. Annual maintenance costs for this section exceed $500,000, with many treatments lasting less than one year. The primary culprit appears to be water under and within the pavement structure. When water becomes entrapped within the pavement structure, the strength of unbound layers and subgrade soils is greatly reduced. Pumping begins to occur that can lead to faulting, cracking, and shoulder deterioration. Loading a pavement with wet sublayers results in moving the fines out of those layers, leading to a loss of support (*58*). Figure 71 shows an example of this type of pumping and faulting from the case study area.

Figure 71. Water Pumping through Pavement and Shoulder Faulting at Project Site.

For any maintenance or rehabilitation technique to perform adequately, the water must be captured and moved away from the pavement structure. Concrete rubblization, followed by an overlay, was being considered as a rehabilitation tactic. Prior to rubblization, the base and subgrade must be dried with the installation of an underdrain system. The underdrain system

must be constructed in a way that efficiently moves water to the roadside, and the roadside must be graded to ensure positive drainage continues away from the pavement.

The project site is located on US 75 on the north side of Sherman, Texas, within the TxDOT Paris District. US 75 is a divided highway traveling north and south, with two lanes in each direction separated by a large grass median. The pavement structure consists of 0.25 m (10 in.) of jointed plain concrete pavement over 0.15 m (6 in.) of flexible base, constructed in the early 1980s. The section originally consisted of flexible shoulders and was replaced in 1998 with 0.25 m (10 in.) jointed plain concrete shoulders. Each direction of travel consists of a 1.22 m (4 ft) inside shoulder, two 3.66 m (12 ft) travel lanes, and a 3.05 m (10 ft) outside shoulder. The most recent traffic data from 2016 indicated an average annual daily traffic of 54,544 vpd.

An internal TxDOT report from 2012 noted poor drainage at multiple locations along the corridor. The report indicated that long after rain events, water can be seen standing in ditches, and there is clear evidence of water pumping through pavement joints (*59*). Site visits conducted in 2016 verified these observations. Figure 72 shows the site with water pumping through the joints and literally squirting up as a truck passes over the pavement.
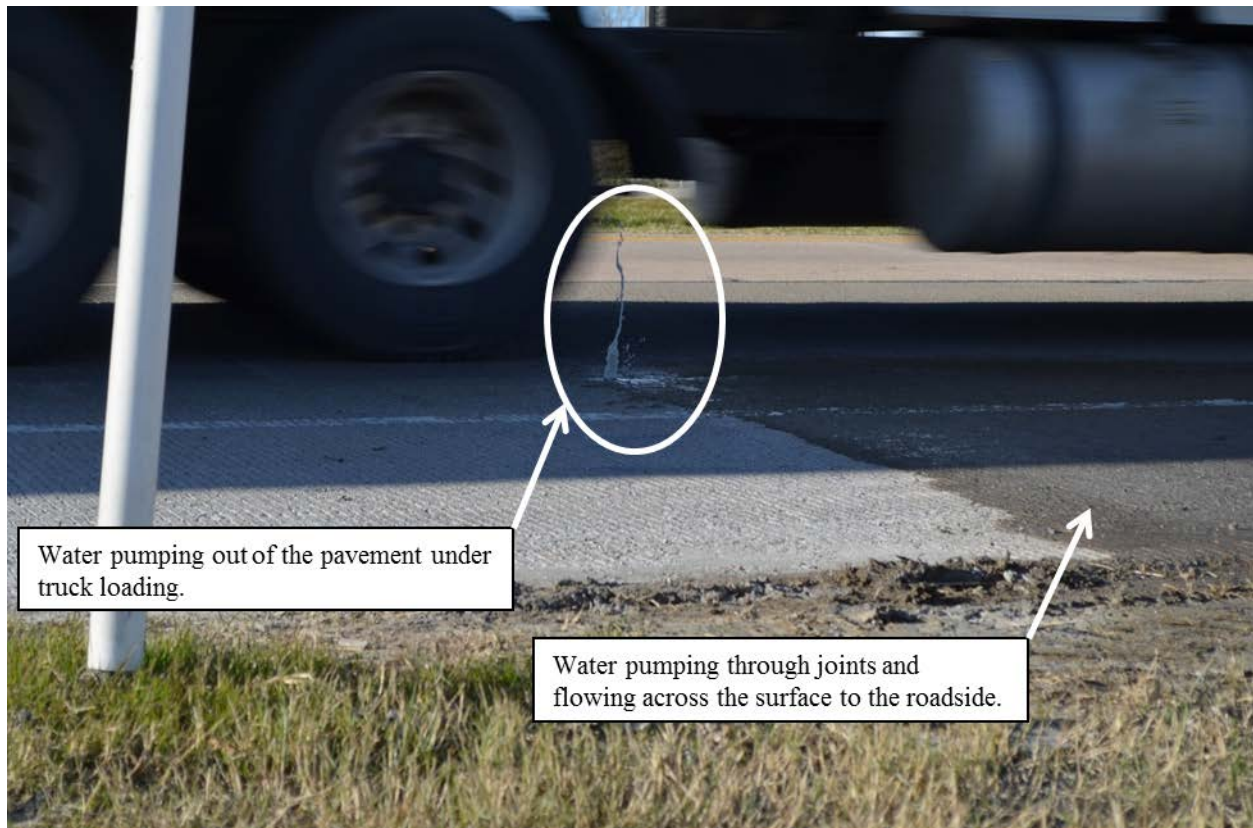
Figure 72. Water Pumping during Truck Traffic Loading.

Water is clearly under the concrete pavement, but another issue is a shallow ditch with its flowline near the EOP that does not drain well. Figure 73 shows this ditch with water standing

over a week after the last rain event. At this location, the frontage road rises above the mainlanes, creating a front slope off of the frontage road that drives the ditch flowline toward the mainlanes. This presents a significant challenge within the project level analysis.
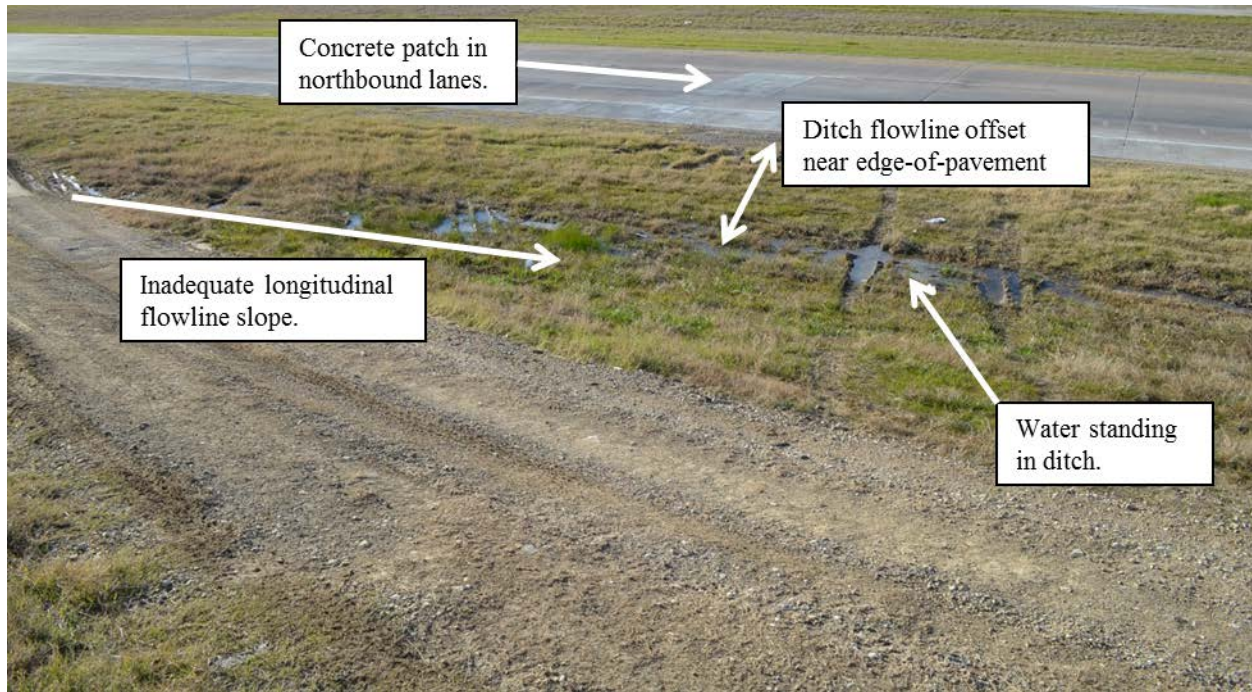
Figure 73. Flat and Shallow Ditch along US 75.

Potential Project Scope and Design Constraints

Mobile LiDAR was used to collect surface geometry to determine how roadside drainage could be improved and also to determine how and where a longitudinal underdrain should be placed. In the plan view, the underdrain should be placed longitudinally along the joint between the mainlanes and shoulder, ensuring that water under the traveled way is captured and moved out. To move the water out, underdrain lateral lines must be constructed to convey the water from the longitudinal line to the roadside.

Many design constraints exist within this project. First, the area in question is in a speed zone transition leaving town. The speed limit increases within the project limits to 75 mph. At this speed limit, the front slope off of the mainlane shoulder must remain as flat as possible. The flowline of the ditch must be lowered below the bottom of the pavement structure and have positive drainage. The cut required in the ditch must not compromise slope steepness. To obtain the required cut and maintain a flat front slope off of the mainlanes, it would be easiest to move the flowline of the ditch horizontally toward the frontage road. Unfortunately, this cannot be done without creating too steep of a frontage road front slope. The existing front slope along the northbound frontage road is as steep as 4.2H:1V, with a prolonged slope (~230 ft) of steeper than 5H:1V, all measured with mobile LiDAR. Using LiDAR data, it is known that the height of the

front slope is between 14 ft and 15 ft, and steepening it creates slope stability concerns. During project level analysis, the frontage road front slope is kept as flat as possible, with flatter than 3.5H:1V desirable.

Project Level Analysis and Design

The primary area of interest discussed in this study is a section along the northbound lanes, near a ramp merge point with a shallow, flat ditch along the roadside. Figure 74 shows this location.
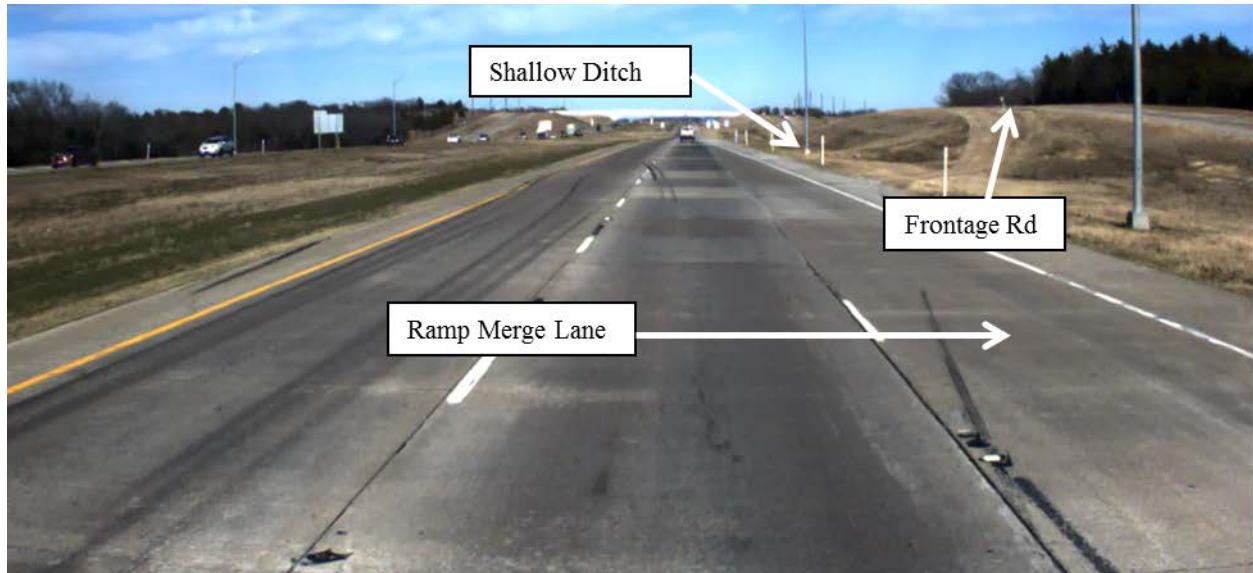
Figure 74. Project Level Location.

The following design questions were addressed using data collected with mobile LiDAR:

1. What are the limits of the drainage issue along the outside EOP?
2. How shallow is the outside ditch in relation to the pavement structure?
3. What cut is required in the ditch flowline to achieve positive drainage while ensuring both mainlane and frontage road front slopes do not exceed design tolerance?
4. What are the anticipated front slopes on the mainlanes and frontage road after rubblization and overlay?
5. With these cuts, where are the flowline daylight points?
6. How does the ditch flowline coordinate with the underdrain flowline to ensure water is moved out from under the mainlanes?
7. What is the fall and suggested spacing for the underdrain laterals?

During data processing, the data grid was built on 2-ft transverse and longitudinal increments. Additionally, raw reflection data were used to determine the location of lane striping and the EOP. Figure 75 displays the area of interest using LiDAR reflection data.
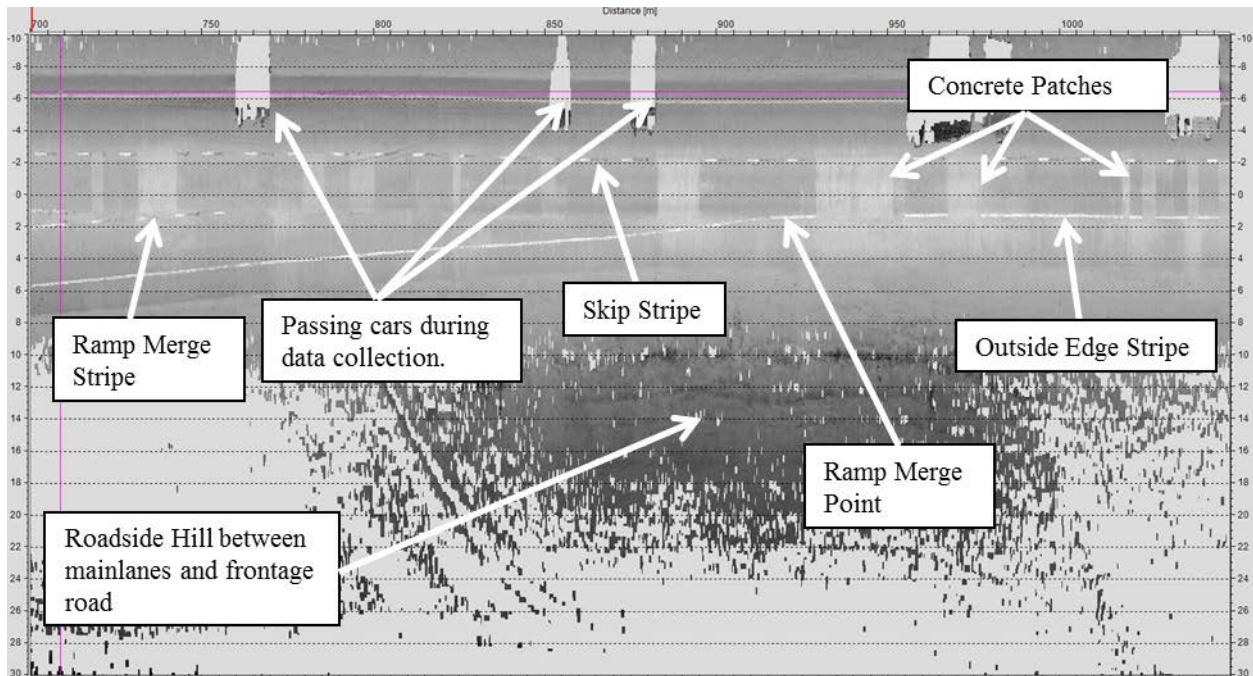
Figure 75. Project Plan View Displayed with Reflection Data.

All dimensions in Figure 75 are in meters. The reflection data clearly illustrate the pavement striping. The ramp completes its merge near the 915-m location in the longitudinal direction. The extent of the hill between the mainlanes and frontage road is also clear from approximately 800 m to almost 1000 m. Concrete patches are also easily visible in the reflection data.

To answer the design questions above, the existing highpoint of the ditch must be found, and the future highpoint of the ditch must be determined. This highpoint will dictate the limits of the drainage problem. Using LiDAR data, it is known that the existing ditch highpoint is located near 810 m. The flowline at this point is higher than the bottom of the pavement structure. From the highpoint, the existing ditch flows to the north with an approximate slope of 0.6 percent. The flatness of the slope keeps the flowline above the bottom of the pavement structure for over 200 m (650 ft).

To visualize the problem and potential solution, Figure 76 displays the current bottom of pavement structure elevation compared with the existing ditch flowline elevation and the proposed ditch flowline elevation. These elevations were generated from LiDAR-collected data. The longitudinal reference in Figure 76 matches that in Figure 75 and travels parallel to the northbound mainlane centerline. Existing conditions are built upon LiDAR data, which collects a measurement each time it encounters a target object. This can make the data look noisy, but it provides significantly more information to develop a preliminary design than traditional techniques.
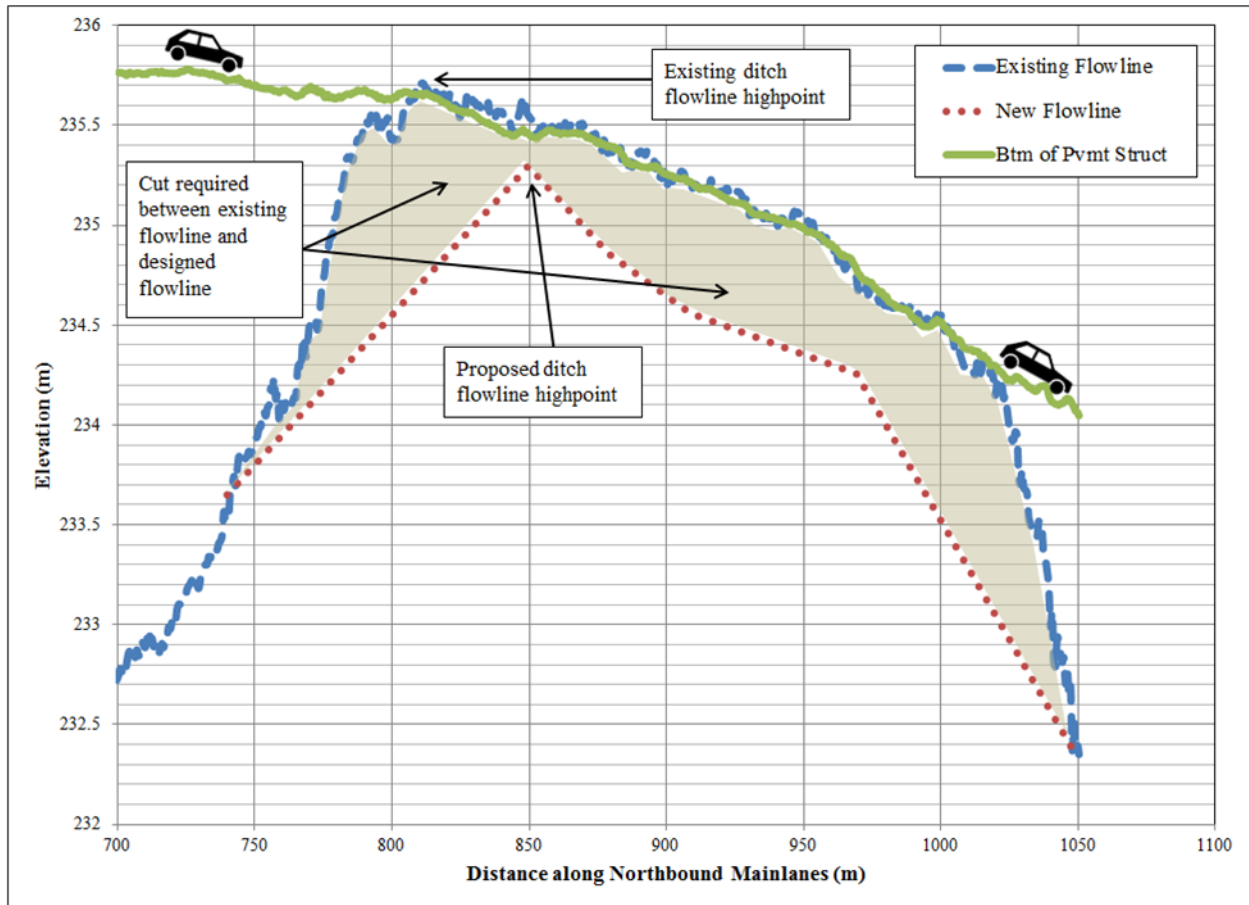
Figure 76. Existing and Proposed Elevations.

The current flowline of the ditch is at or near the bottom of the pavement structure elevation from the 800-m mark to approximately 1025 m. The highpoint of the existing ditch near 810 m is also clear in Figure 76. The proposed highpoint was moved to 850 m. This location was fixed after multiple iterations for design. The elevation of the highpoint was also set to 0.15 m (6 in.) below the bottom of the pavement structure. This value was selected so that a 0.15 m (6 in.) underdrain pipe could be installed below the existing pavement structure. From this point, moving both north and south, the goal is to lower the flowline of the ditch to provide adequate outfall slope for the underdrain. To lower the flowline to the bottom of the pavement structure, a cut of 0.24 m (0.78 ft) is required. The new front slope adjacent to the mainlanes will be 8.27H:1V. From this point, the ditch should be graded at a 1.5 percent fall to the south. Following the existing horizontal flowline of the ditch, daylight should be achieved approximately 110 m (360 ft) to the south. Using the existing ditch alignment, daylight should occur approximately 15.5 m (50.5 ft) from the edge of the ramp, measuring perpendicular to the mainlanes. Moving back to the highpoint, the ditch should be graded to drain to the north at 1.5 percent for 30.5 m (100 ft). At this point, the cut should be approximately 0.51 m (1.68 ft), creating a front slope approximately 5.3:1 after final pavement construction. After grading at 1.5 percent for 30.5 m (100 ft), the grade of the ditch should be flattened to 1 percent to the north

and held for another 30.5 m (100 ft). At this point, the cut is likely to be just above 0.61 m (2 ft), creating a 4.8H:1V front slope. Again, the flowline slope should be flattened to 0.5 percent to the north and held for 59 m (195 ft), where the cut will be approximately 0.43 m (1.4 ft) and the front slope will be 6.4H:1V. Finally, at this point, the flowline should be steepened to 2.4 percent to the north and held until daylight. Daylight is expected to occur an additional 79.25 m (260 ft) to the north. As with drainage to the south, drainage to the north should follow the existing horizontal offset of the flowline.

Figure 76 and the associated descriptions answer the first five questions raised in the preceding section. The questions, with answers, are relisted below:

1. What are the limits of the drainage issue along the outside EOP? Using the existing horizontal flowline offset, daylight is expected near 740 m and 1050 m. The amount of ditch grading required is expected to be approximately 310 m (1015 ft).
2. How shallow is the outside ditch in relation to the pavement structure? The existing flowline is above the bottom of the pavement structure for over 225 m (735 ft).
3. What cut is required in the ditch flowline to achieve positive drainage while ensuring both mainlane and frontage road front slopes do not exceed design tolerance? The cuts and front slopes are variable. Table 38 displays cut information provided to the TxDOT district and ultimately to a ditch grading contractor. This cut information formed the basis for actual field construction. These cuts were developed completely from LiDAR data. Figure 77 displays the expected future front slope.
4. What are the anticipated front slopes on the mainlanes and frontage roads after rubblization and overlay? Figure 77 provides information on the expected front slope for the mainlanes and frontage road.
5. With these cuts, where are the flowline daylight points? These points are listed in the answer to question 1, where the limits of construction are defined.

Table 38. Designed Ditch Cuts and Slopes.

Location (m)	Approx. FL Offset (m)	Depth of cut (m)	Ditch Flowline Slope
-110	15.4	0	-1.50%
-91	14.1	0.144	-1.50%
-76	14.5	0.56	-1.50%
-61	12.7	1.12	-1.50%
-46	7.1	0.973	-1.50%
-31	7.3	0.774	-1.50%
-16	5.7	0.547	-1.50%
Highpoint	**4.6**	**0.239**	
16	4.6	0.42	-1.50%
31	4.6	0.513	-1.50%
46	4.9	0.629	-1.00%
61	4.9	0.646	-1.00%
76	5.5	0.695	-0.50%
91	5.5	0.626	-0.50%
106	5.5	0.633	-0.50%
120	6.1	0.462	-0.50%
137	6.1	0.726	-2.40%
152	7.3	1.03	-2.40%
167	11.6	1.102	-2.40%
182	13.4	0.868	-2.40%
197	24.4	0.251	-2.40%
200	24.4	0	-2.40%
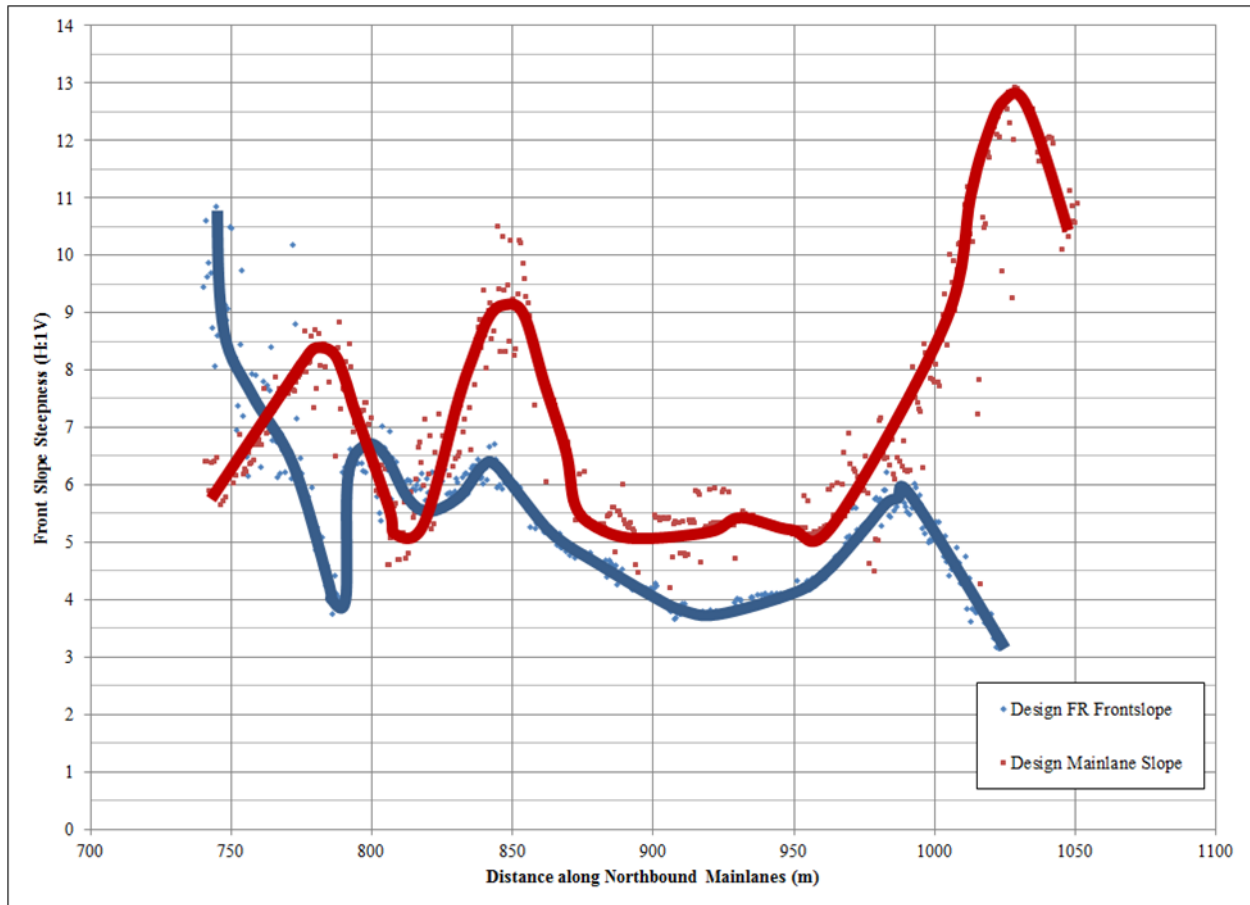
Figure 77. Mainlane and Frontage Road Design Front Slope Steepness.

Figure 77 indicates frontage front slopes remain at or near 4H:1V except for a short section between 900 m and 950 m. Even within this section, the frontage front slope maximum steepness is 3.78H:1V, a steepness that assuages slope stability concerns. Mainlane front slopes will become steeper than 6H:1V, specifically in the area where the current ditch is shallow and closest to the EOP. For the most part, final mainlane front slope steepness—that is, after rubblization and overlay—will be near 5H:1V. The use of LiDAR in this design presents engineers with the unique ability to completely understand the front slopes and how different techniques may affect those slopes. Ultimately, a more informed design decision is made.

While solving the roadside drainage issue is integral, it will only be effective if it is done in a way that provides positive drainage to the underdrain system. Mobile LiDAR measurements provided accurate surface data on US 75. The surface of US 75, within the area of interest, has 0.5 percent fall toward the north. With a flat profile grade, minimizing the cut to the underdrain flowline becomes challenging. Using a 0.15 m (6 in.) diameter underdrain pipe, the minimum cut from the pavement surface is 0.56 m (22 in.). This cut is required to get below the pavement structure of 0.41 m (16 in.) and account for the 0.15 m (6 in.) diameter pipe. Figure 78 displays two underdrain options, along with the preliminary longitudinal underdrain design provided to TxDOT.

136

Option 1 in Figure 78 sets the underdrain highpoint at the ditch flowline highpoint and provides 2 percent fall in each direction. With this option, by the 1050 m mark, the cut below the pavement surface exceeds 3 m (9.8 ft). Option 2 moves the underdrain highpoint to the 740-m location and places the flowline at the minimum cut of 0.56 m. One percent fall is provided to the north to 1050 m. Even with a flatter flowline slope, the cut at 1050 m exceeds 2 m (6.6 ft). Using the LiDAR data for design, it is clear that the longitudinal underdrain must be placed with a very flat flowline slope. Through multiple iterations, a design was provided placing the underdrain highpoint at 740 m with the minimum cut of 0.56 m. The design underdrain passes through the 850-m mark with a flowline elevation equal to the new roadside ditch flowline elevation. This flat spot is overcome by designing lateral underdrain lines to have adequate fall on each side of the flat spot.
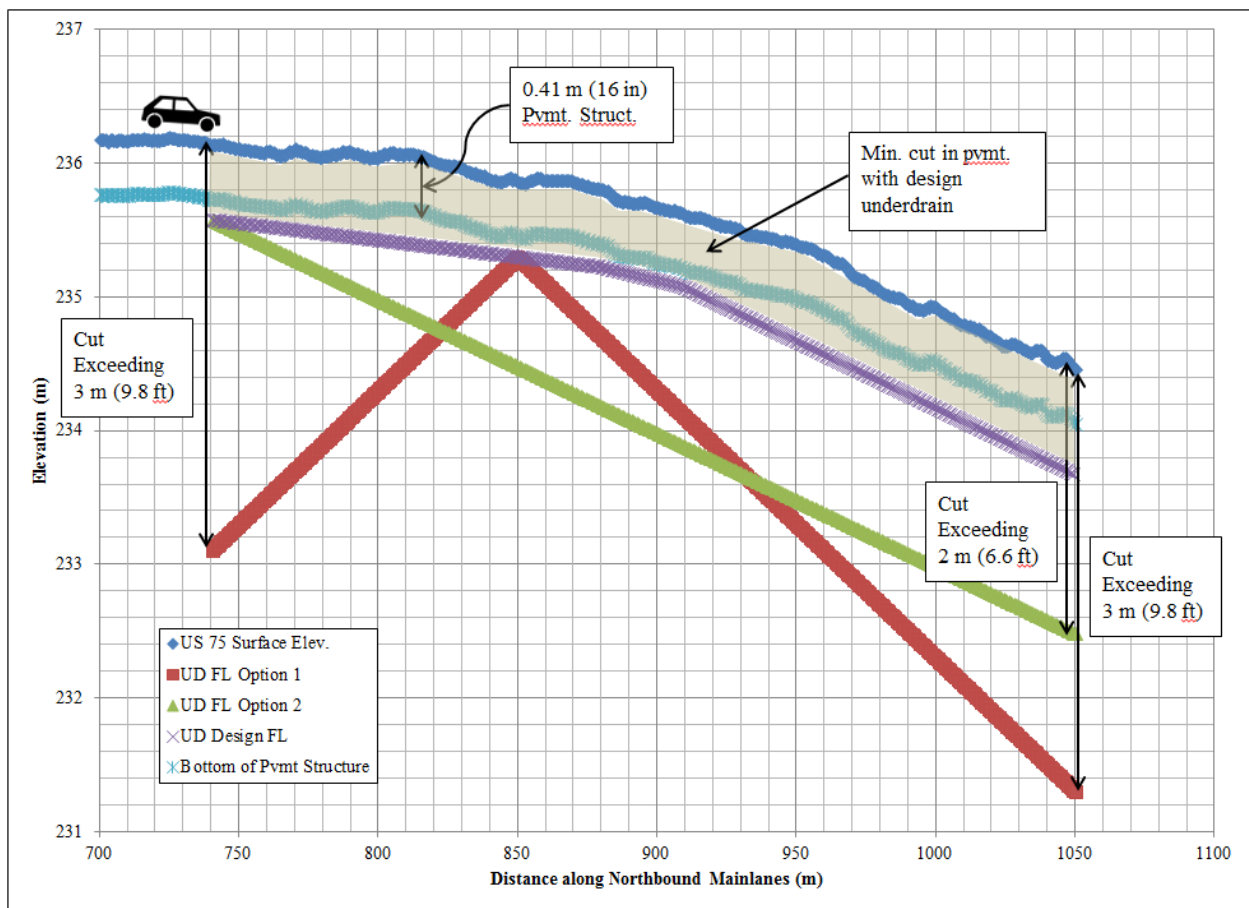
Figure 78. Longitudinal Underdrain Path Options.

The description above makes it clear that the lateral underdrain lines will be required to move the water out from under the pavement structure. The longitudinal underdrain flowline designed in Figure 78 was done to create a flat spot at the ditch highpoint but allow for lateral pipes with at least 2 percent fall within 15.24 m (50 ft) of the flat spot. Figure 79 shows potential design slopes for lateral underdrain pipes. Lateral outfall pipes should be placed at spacings to meet many design considerations. A primary consideration is moving the water out in a relatively flat area.

Additionally, lateral spacing should be close enough to allow for periodic clean-out of the longitudinal pipe. Figure 79 allows engineers to adjust lateral spacing with an understanding of how steep the flowlines can become. The flat spot is clearly visible at 850 m, but within 10 m (33 ft) on either side, lateral lines can be placed with 2 percent fall. The longitudinal underdrain at this location has 0.25 percent fall to the north. The initial underdrain design provided to TxDOT recommends placing lateral lines at 30 m (100 ft) spacings to ensure water is efficiently moved out from under the pavement with lateral lines.
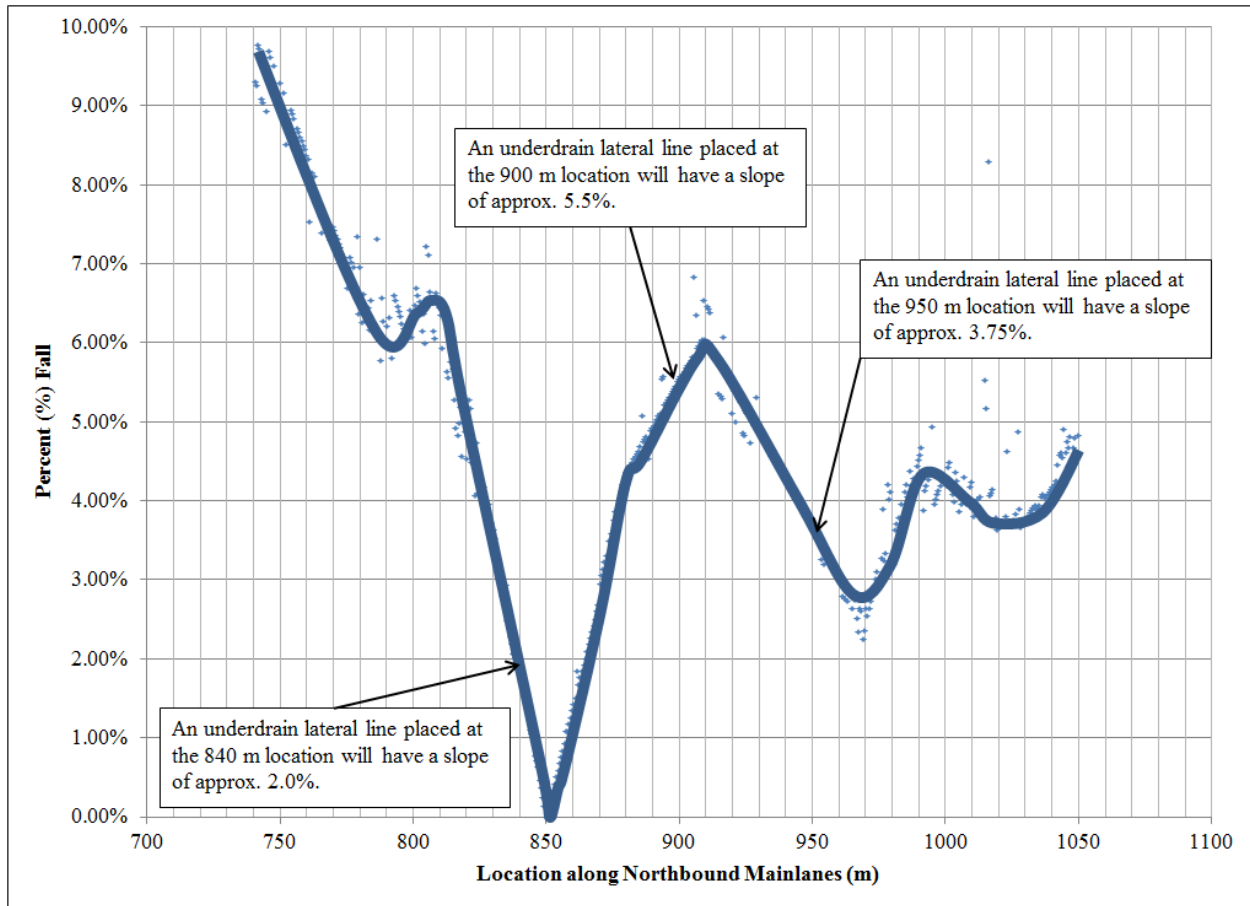
Figure 79. Potential Lateral Underdrain Pipe Slopes.

Figure 79 and the descriptions associated with it help answer the final two design questions:

6. How does the ditch flowline coordinate with the underdrain flowline to ensure water is moved out from under the mainlanes? Figure 78 and Figure 79 illustrate the answer to this question. In summary, the new flowline of the ditch is low enough to provide adequate water outfall from the underdrain flowline, which is necessarily flat to avoid excessive cut within the pavement. The roadside is regraded in such a way to continue to move water away from the pavement.

7. What is the fall and suggested spacing for the underdrain laterals? Figure 79 provides information on percent fall potential for lateral lines. The critical point is near the 850-m location where the ditch flowline and underdrain flowline are designed at the same elevation. The ditch is graded to begin to provide lateral fall as quickly as possible without increasing the cut too much to exceed front slope design constraints. Table 39 is a small portion of a design table provided to TxDOT. This table combines ditch, longitudinal, and lateral underdrain information. Arrows within the table indicate additional data are available within the master table.

Table 39. Flowline Design Table.

Location (m)	Design Ditch FL Elev. (m)	Ditch FL Long. Slope (%)	UD FL Elev. (m)	UD Long. Slope (%)	Offset from UD to Ditch (m)	UD Lateral Slope (%)	New Mainlane Front-slope (#H:1V)
↑	↑	↑	↑	↑	↑	↑	↑
832.638	235.031	1.50%	235.341	-0.25%	9.736	3.18%	7.1
833.247	235.040	1.50%	235.340	-0.25%	10.346	2.89%	8.0
833.857	235.049	1.50%	235.338	-0.25%	10.346	2.79%	8.0
834.467	235.059	1.50%	235.336	-0.25%	9.736	2.85%	7.4
835.076	235.068	1.50%	235.335	-0.25%	9.126	2.93%	6.6
↓	↓	↓	↓	↓	↓	↓	↓
845.439	235.223	1.50%	235.309	-0.25%	8.517	1.00%	8.3
846.049	235.232	1.50%	235.307	-0.25%	9.736	0.77%	10.3
846.659	235.241	1.50%	235.306	-0.25%	9.126	0.70%	9.4
847.268	235.251	1.50%	235.304	-0.25%	8.517	0.63%	8.3
↓	↓	↓	↓	↓	↓	↓	↓
850.316	235.296	1.50%	235.296	-0.25%	7.907	0.00%	8.3
850.926	235.287	-1.50%	235.295	-0.25%	7.907	0.10%	8.4
851.535	235.278	-1.50%	235.293	-0.25%	8.517	0.18%	9.3
↓	↓	↓	↓	↓	↓	↓	↓
855.193	235.223	-1.50%	235.284	-0.25%	9.126	0.67%	9.2
↓	↓	↓	↓	↓	↓	↓	↓
864.947	235.077	-1.50%	235.260	-0.25%	9.126	2.00%	7.4
↓	↓	↓	↓	↓	↓	↓	↓
869.214	235.013	-1.50%	235.249	-0.25%	9.126	2.59%	6.8
869.823	235.004	-1.50%	235.248	-0.25%	9.126	2.67%	6.6
870.433	234.995	-1.50%	235.246	-0.25%	8.517	2.95%	5.8
↓	↓	↓	↓	↓	↓	↓	↓

US 75 Project Level Analysis Conclusions

The study described in this article demonstrates how LiDAR data can be used to develop a preliminary design for the improvement of roadside drainage and installation of underdrain. This design is vital to the implementation of a permanent rehabilitation strategy for a portion of US 75

in northern Texas. No rehabilitation strategy will work without removing the water from the pavement structure. The location in the case study proved challenging because of a shallow and flat ditch near the mainlanes. The flowline offset of this ditch was controlled by slope stability concerns of the front slope along the frontage road and mainlane front slope steepness.

Data collected using mobile LiDAR provided the information to develop a preliminary design that will improve roadside drainage by lowering the ditch flowline below the bottom of the pavement structure. A grading plan was developed to ensure longitudinal fall of the new ditch. The design of the ditch works in coordination with the design of an underdrain system to be constructed at the joint between the mainlanes and shoulder. LiDAR provided the data to design the underdrain by controlling the depth of cut below the pavement surface while ensuring adequate lateral fall between the longitudinal underdrain and the ditch flowline. A flat profile grade along US 75 controlled the allowable fall in the longitudinal pipe to a substantially flat design. In working through the design flowline of the ditch and coordinating it with the design flowline of the longitudinal pipe, underdrain lateral pipes were designed to be equipped with at least 2 percent fall except in a small window near the ditch highpoint.

Cut data and preliminary design information were provided to the TxDOT Paris District. TTI personnel met with TxDOT and its ditch grading contractor to perform preliminary ditch cleaning work. This work was deemed advantageous by the district regardless of the ultimate outcome of the rubblization. TTI worked on site with the ditch cleaning contractor and provided specific locations to begin ditch cleaning and estimated cut depths. Several weeks after ditch grading, TxDOT personnel indicated the ditch was still dry, empirically performing better than prior to the ditch cleaning. Figure 80 shows ditch cleaning work.

Figure 80. Ditch Grading Work along US 75.

Finally, TTI provided three detail sheets to be included in the final plan set used in the rubblization contract. These plan sheets are provided in the Appendix. Ultimately, the Paris District decided not to pursue the construction of a 1000-ft rubblized test section.

RM 652—EL PASO DISTRICT

Background Information

A project level surface drainage study might seem out of place in a region that receives less than 1 ft of annual rainfall, but improving the surface geometry along RM 652 is critical to addressing its needs. RM 652 was identified as a roadway that might be vulnerable to gyp-sink. Using nondestructive testing, TTI identified locations with high deflections, indicating the potential for a structural problem. Mobile LiDAR was collected on RM 652 to determine if the locations with high deflections exhibited profile deviations and to determine if roadside improvements could be made to ensure water drains efficiently. The primary area of interest and the analysis within focuses on RM 652 between reference markers 142 and 144.

An initial review of the roadway profile generated using LiDAR data indicated unusual dips. These dips corresponded to locations with high deflections that had no ditch depth to facilitate drainage. While the dips appeared abnormal, the geometry of the dips seemed uniform rather than chaotic, as would be expected with a sinkhole. Original plan sets were requested and provided by the El Paso District. Plan sets indicate RM 652 originally consisted of a 24-ft crown with an 18-ft paved surface within a 100-ft ROW. In or around 1970, the crown was widened to 36 ft within the existing 100-ft ROW. Reference marker 142 corresponds to STA 145+00 from old plan sets. Within this area, several water crossing dips were constructed within the original RM 652 profile. Figure 81 shows that these dips exist in the current roadway profile, as measured using mobile LiDAR.
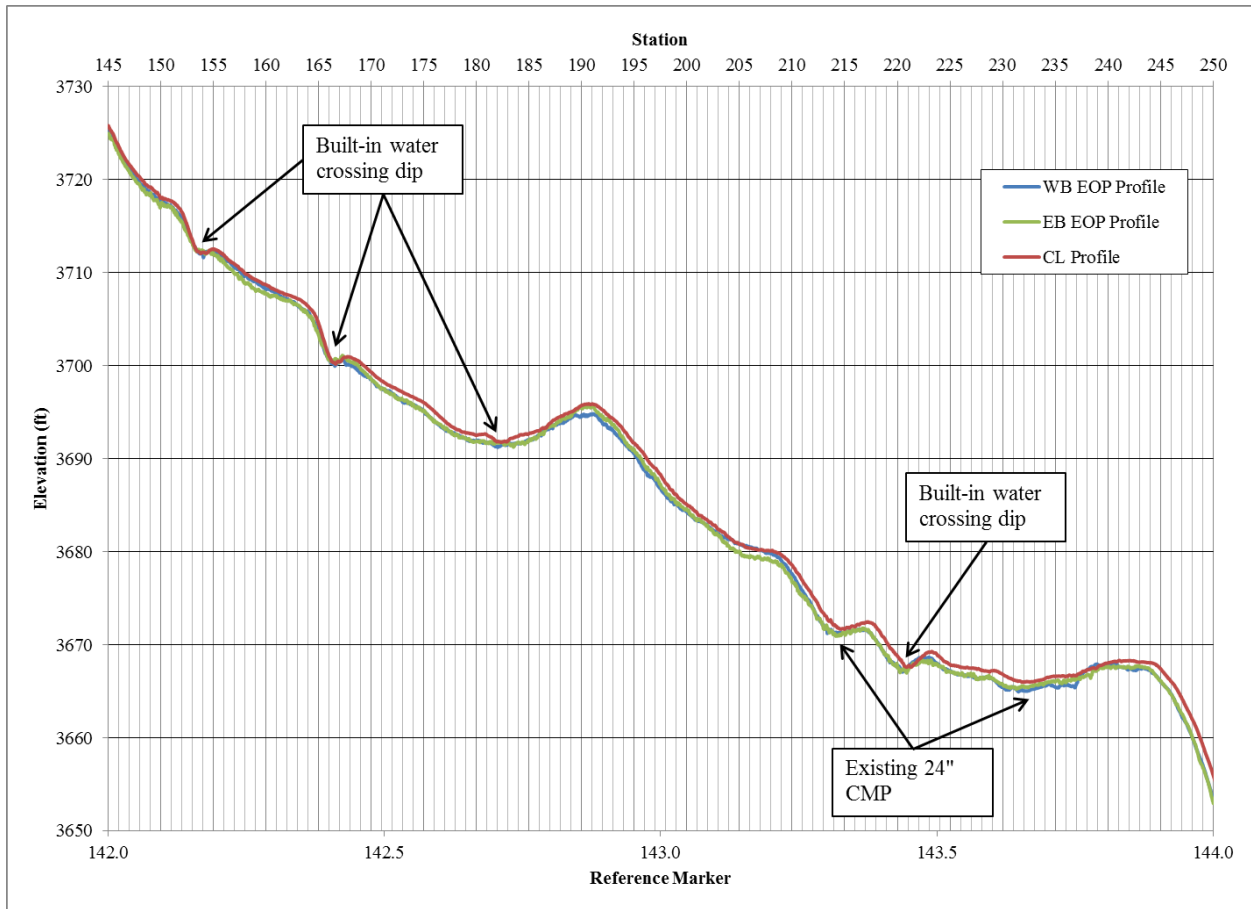
Figure 81. Existing Pavement Profiles.

Ensuring adequate drainage along the roadside is critical in mitigating potential gyp-sink along the corridor. Between reference markers 142 and 144, the natural flow path is to the north roadside. Figure 82 and Figure 83 are 1970 plan details for the culverts at STA 214+25 and STA 231+70, displaying flow from right to left, or from the south side of RM 652 to the north side. Within the 2-mi area of interest, these are the only culverts; all other water crossings occur through dips constructed in the pavement profile. From this point forward, figures include station numbers rather than reference markers to correspond with potential plan development.
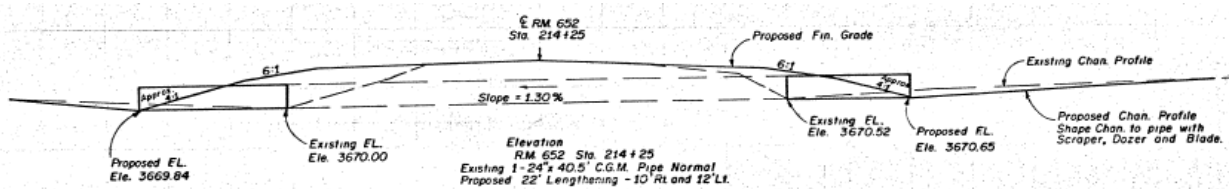
Figure 82. 1970 Plan Detail for Culvert at STA 214+25.
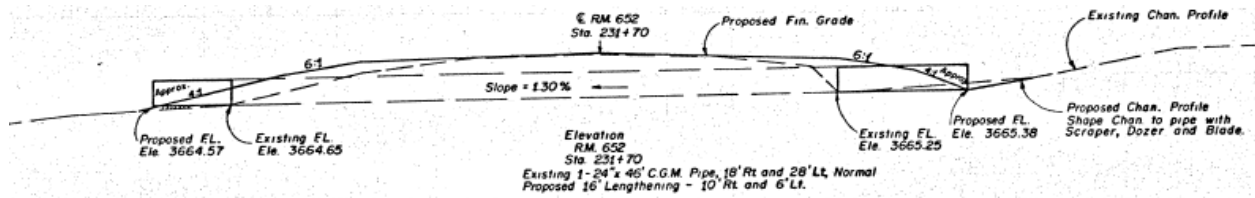
Figure 83. 1970 Plan Detail for Culvert at STA 231+70.

The north side of RM 652 is adjacent to the westbound direction of travel, so new design recommendations begin by addressing the low side, which is the westbound side of RM 652. Figure 82 and Figure 83 also show the culvert extension required in 1970 to widen RM 652 to a 36-ft crown. The widening of RM 652 presents additional drainage challenges because there is a need to create ditches, but the width of the roadside is limited by the 100-ft ROW. In an area receiving little rainfall, as is the case along RM 652, this would not typically cause problems. However, with the need to improve drainage, the narrow ROW and wide pavement can present front slope steepness issues, often a controlling factor.

Current Site Conditions

Figure 84 through Figure 87 consist of centerline profile grades with the minimum north roadside elevation over 3000-ft sections. The northern roadside represents the low point; it is chosen as the primary point of analysis, allowing for design to proceed upstream. The minimum elevation offset is graphed using a secondary vertical axis. Minimum elevation offsets less than 20 ft from the EOP indicate the existence of a ditch. When minimum elevation offsets begin to exceed 20 ft from the EOP, water is trying to leave the ROW, creating a front-slope-only condition. The built-in dips clearly transition to front-slope-only sections where water wants to leave the ROW on the north side of the roadway. It is also clear that when a ditch is present, it is often within 15 ft of the EOP, with a typical distance of 12 ft.
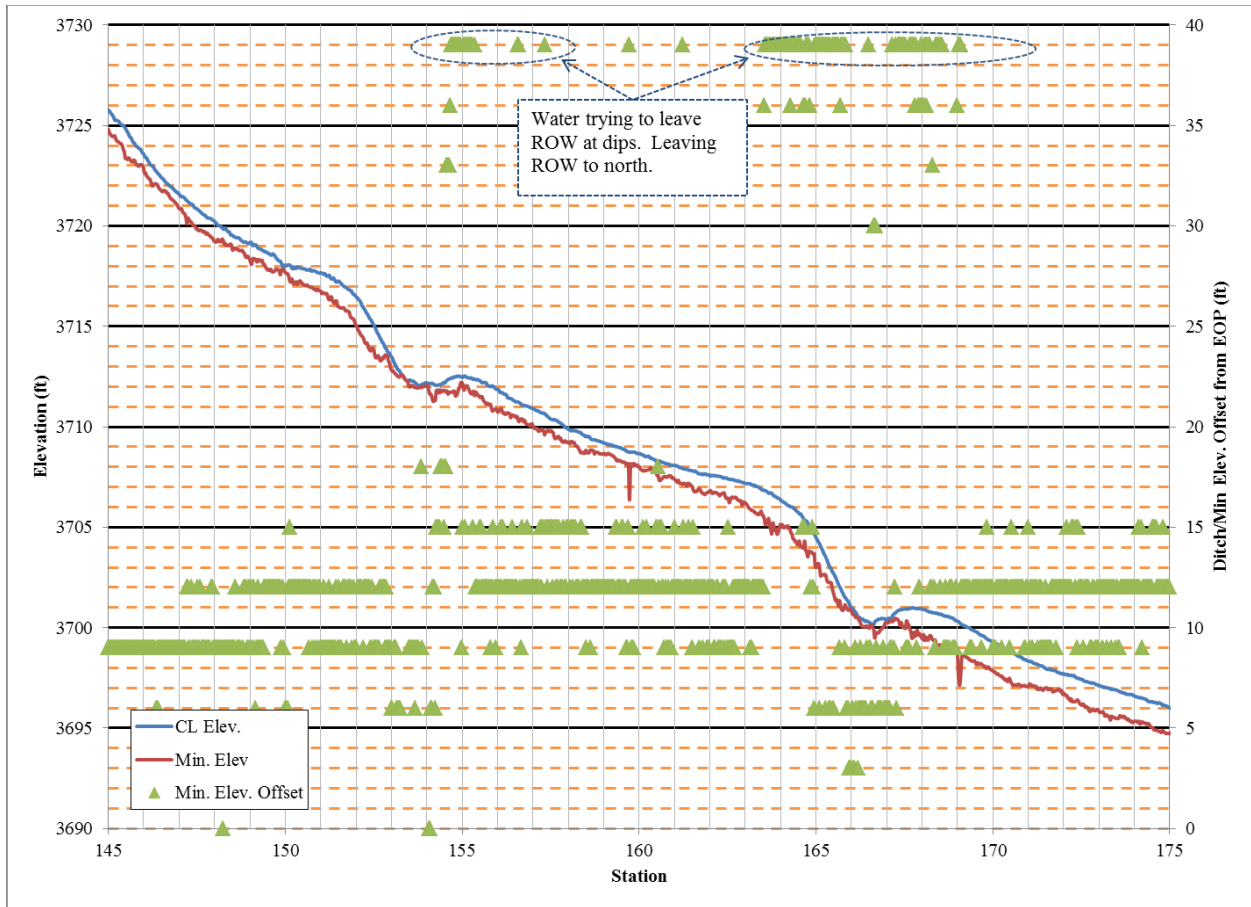
Figure 84. Pavement Profile, Roadside Minimum Elevation Profile, and Minimum Elevation Offset (145+00 to 175+00).
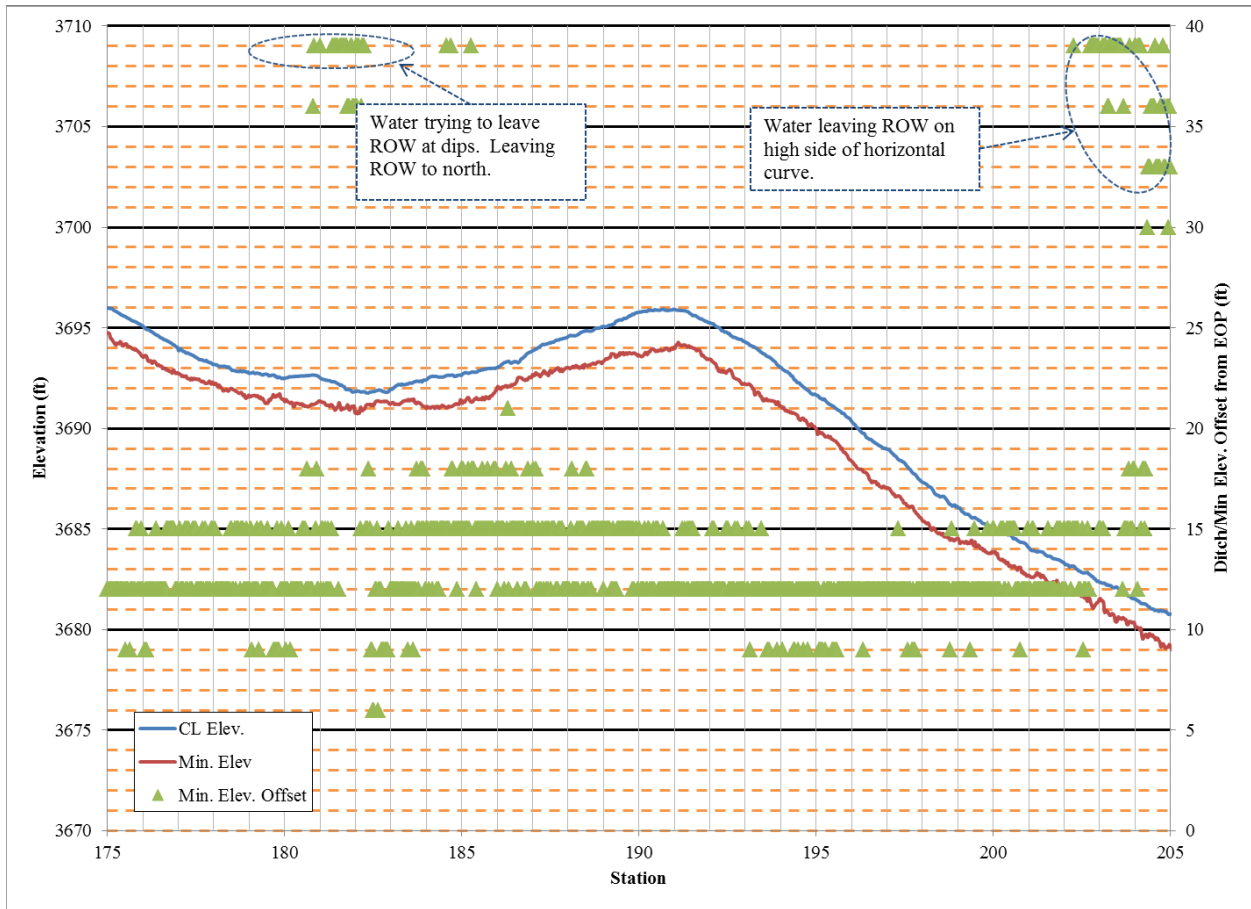
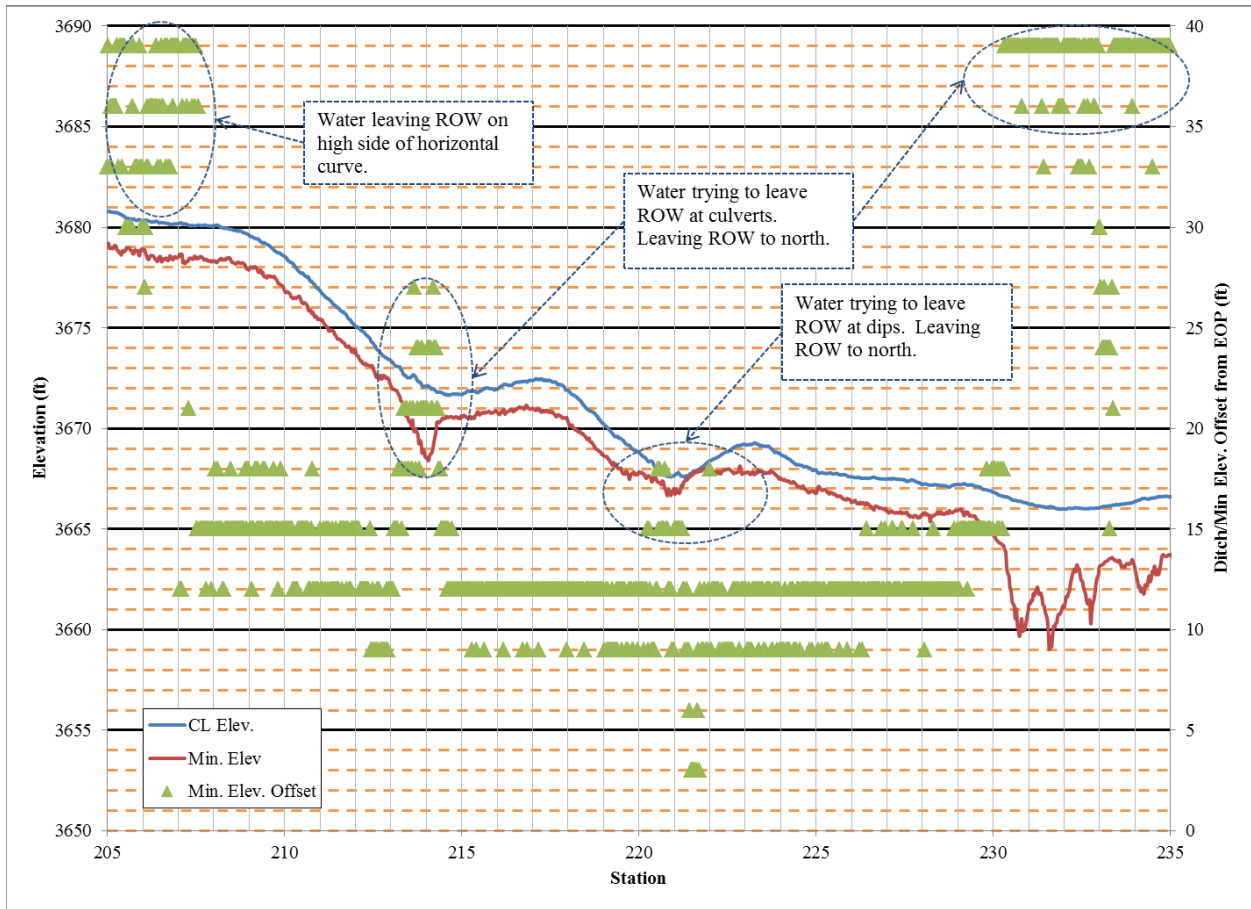**Figure 85. Pavement Profile, Roadside Minimum Elevation Profile, and Minimum Elevation Offset (175+00 to 205+00).**

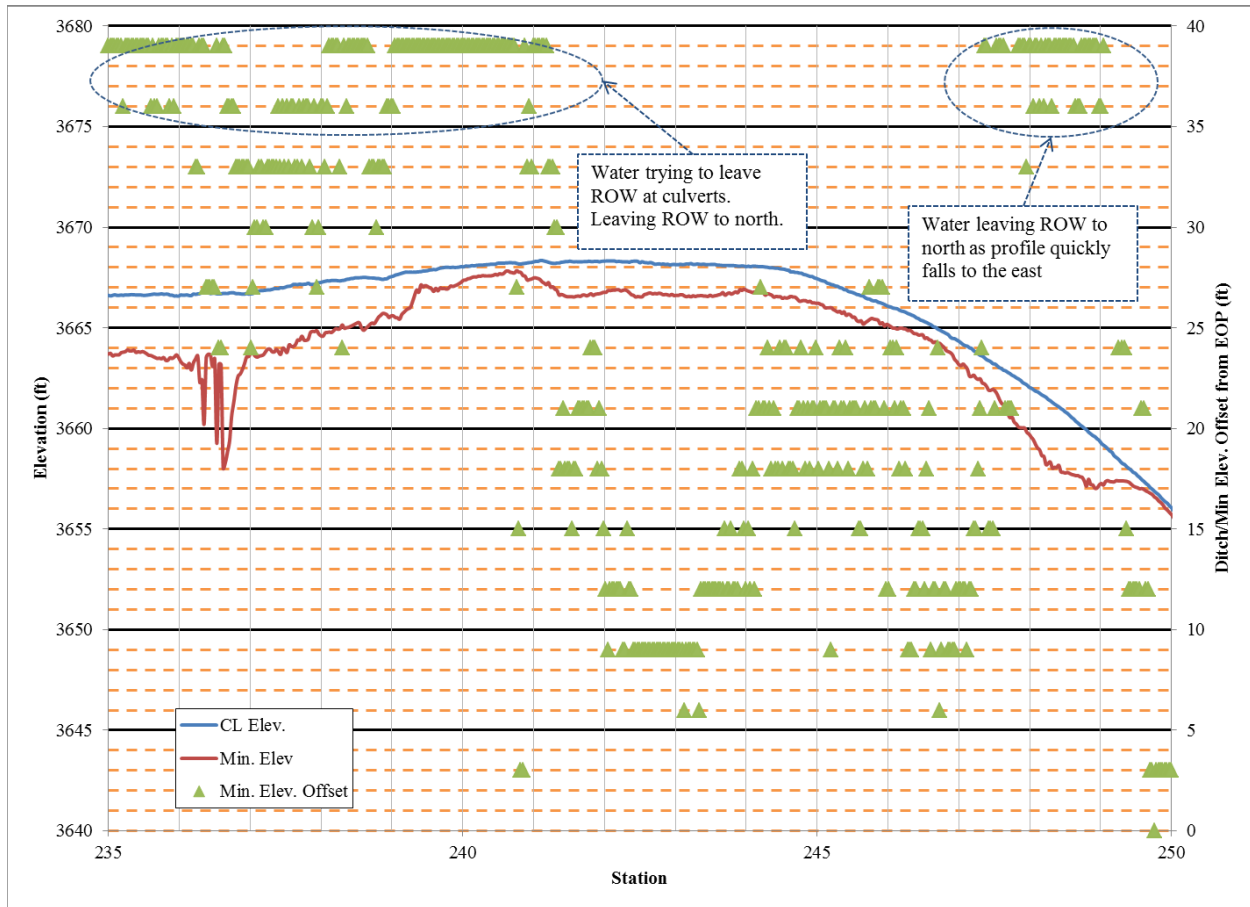**Figure 86. Pavement Profile, Roadside Minimum Elevation Profile, and Minimum Elevation Offset (205+00 to 235+00).**

146

Figure 87. Pavement Profile, Roadside Minimum Elevation Profile, and Minimum Elevation Offset (235+00 to 250+00).

With a typical ditch offset of 12 ft, ditch depths of greater than 2 ft produce front slopes steeper than 6:1, while 4-ft deep ditches generate critically steep front slopes of 3:1. Figure 88 and Figure 89 show current ditch depths. Ditch depths represented in these figures are actually the minimum elevation along the roadside, so in a front-slope-only section the minimum elevation exists near the ROW line. Figure 84 through Figure 87 show the location of the minimum elevation in relation to the EOP.
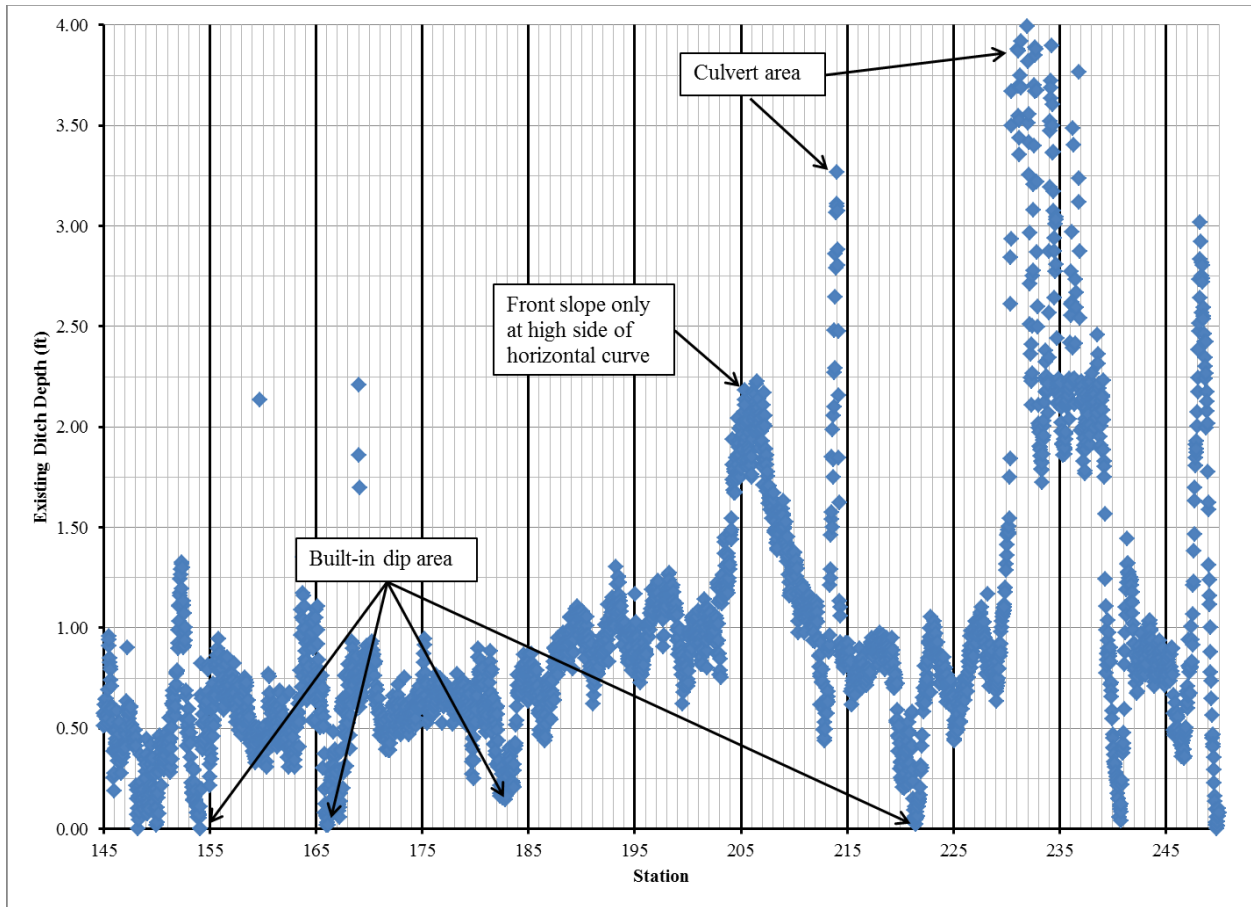
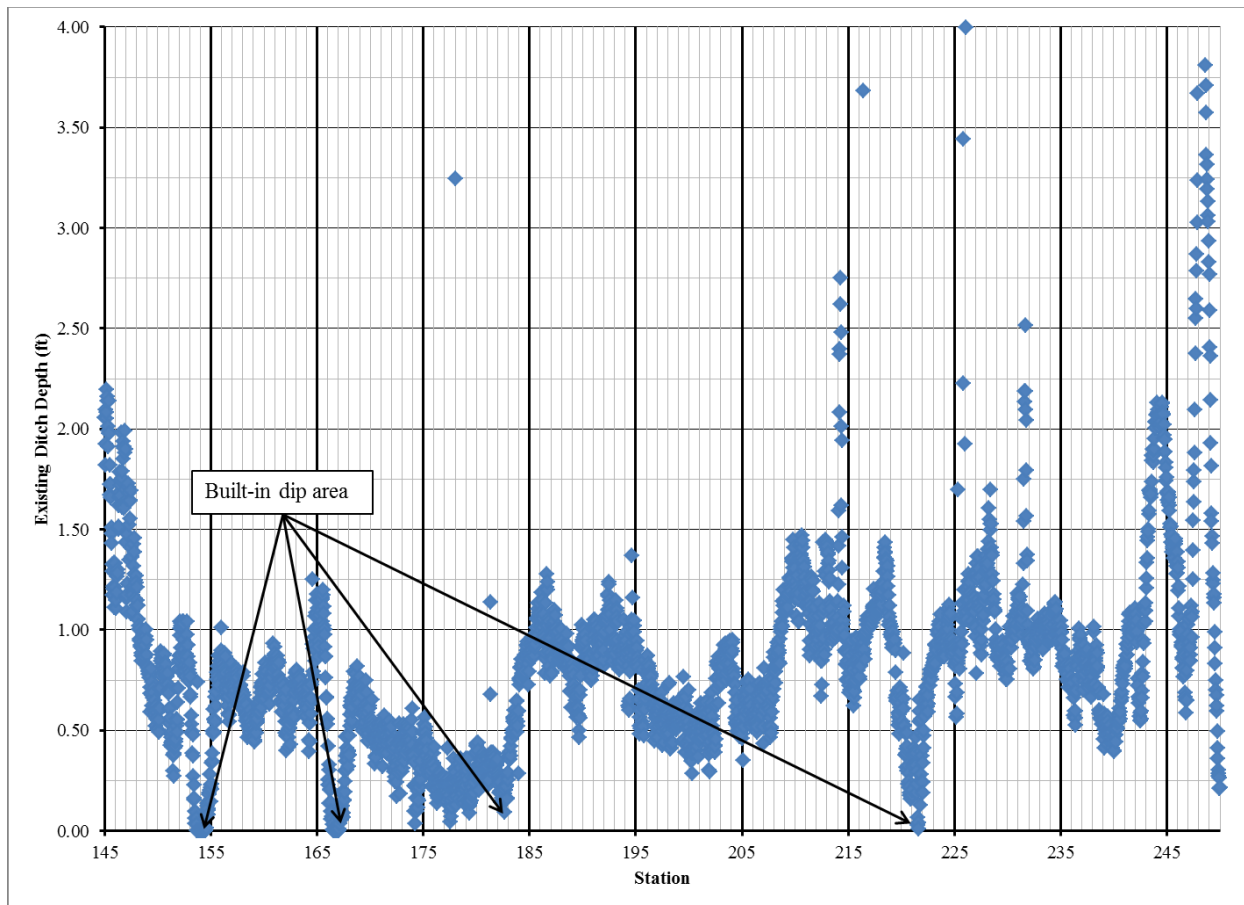**Figure 88. Existing North Roadside (Adjacent to Westbound) Ditch Depth.**

Figure 89. Existing South Roadside (Adjacent to Eastbound) Ditch Depth.

As expected, the built-in dip areas have no ditch depth. These areas are designed to allow the water to spill over the roadway from south to north. Therefore, while rainfall in this region is less than other parts of the state, improving the drainage features along the roadside is critical to the success of RM 652. Design suggestions are developed with the intent to lower the flow of water as much as possible in relation to the pavement structure and ensure positive flow when water is traveling in ditches along the ROW.

LiDAR-Based Design

A potential design strategy to improve drainage within this 2-mi section, along with rehabilitating the roadway, requires the installation of cross-culverts at the built-in dips. Installation of a cross-culvert requires raising the roadway profile grade and in turn increasing the steepness of the front slope. Figure 90 through Figure 93 show a designed westbound EOP profile compared with the existing westbound EOP profile. These figures also show a designed ditch flowline elevation. On a secondary vertical axis, the front slope steepness created with the new design elevations is charted along with the critical steepness of 3H:1V and a desired steepness of 6H:1V. The front slope steepness assumes that the ditch flowline offset is located

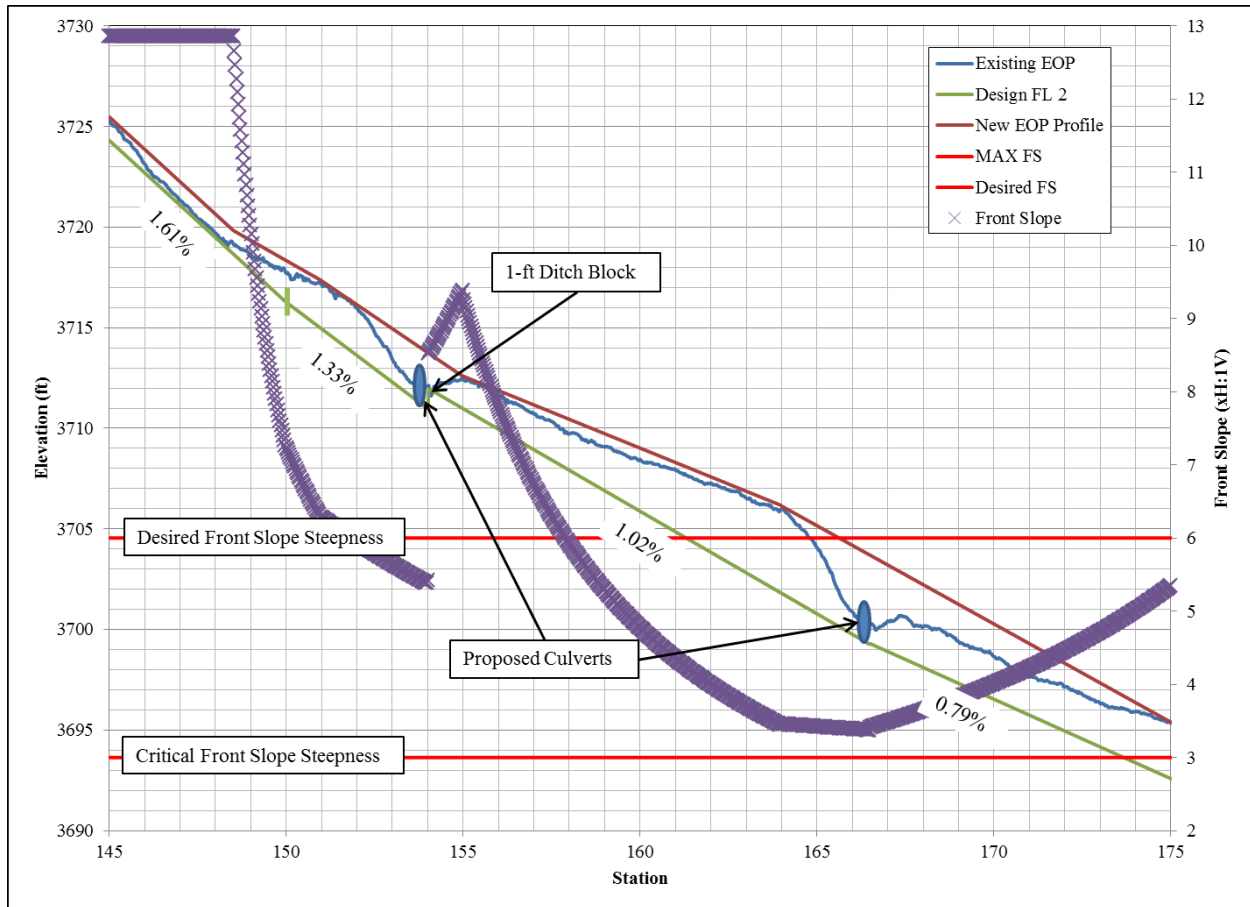15 ft from the EOP. Below each figure is a discussion of the design elements within the respective stations.

Figure 90. STA 145+00 to STA 175+00 Design Westbound EOP and Ditch Flowline with Front Slope Steepness.

Figure 90 shows two proposed culverts at the existing built-in dip locations near STA 154+00 and STA 166+50. On the downstream side of the proposed culvert at STA 154+00 is a 1-ft ditch block to immediately raise the ditch flowline before beginning to fall eastward again. Culvert diameters of 24 in. are assumed. This placement is the downstream side of the cross-culverts. There is a proposed flowline slope adjustment near STA 150+00 where the flowline should flatten from 1.61 percent fall to 1.33 percent fall. Flattening is required to maintain a reasonable amount of fall on the downstream side of the proposed culvert and ditch block at STA 154+00. If the culvert at STA 154+00 is placed too deeply, adequate fall cannot be maintained to the culvert at STA 166+50 without creating a front slope steeper than 3H:1V. The roadside adjacent to the westbound direction of travel begins to steepen as the new profile grade is raised to span the built-in dip near STA 165+00. At the location of the culvert, the front slope approaches but does not exceed 3H:1V since the fill required in the dip exceeds 3 ft. The blue line represents the current EOP and provides a visual tool to indicate that the installation of culverts at built-in dip locations requires raising the profile of the roadway.
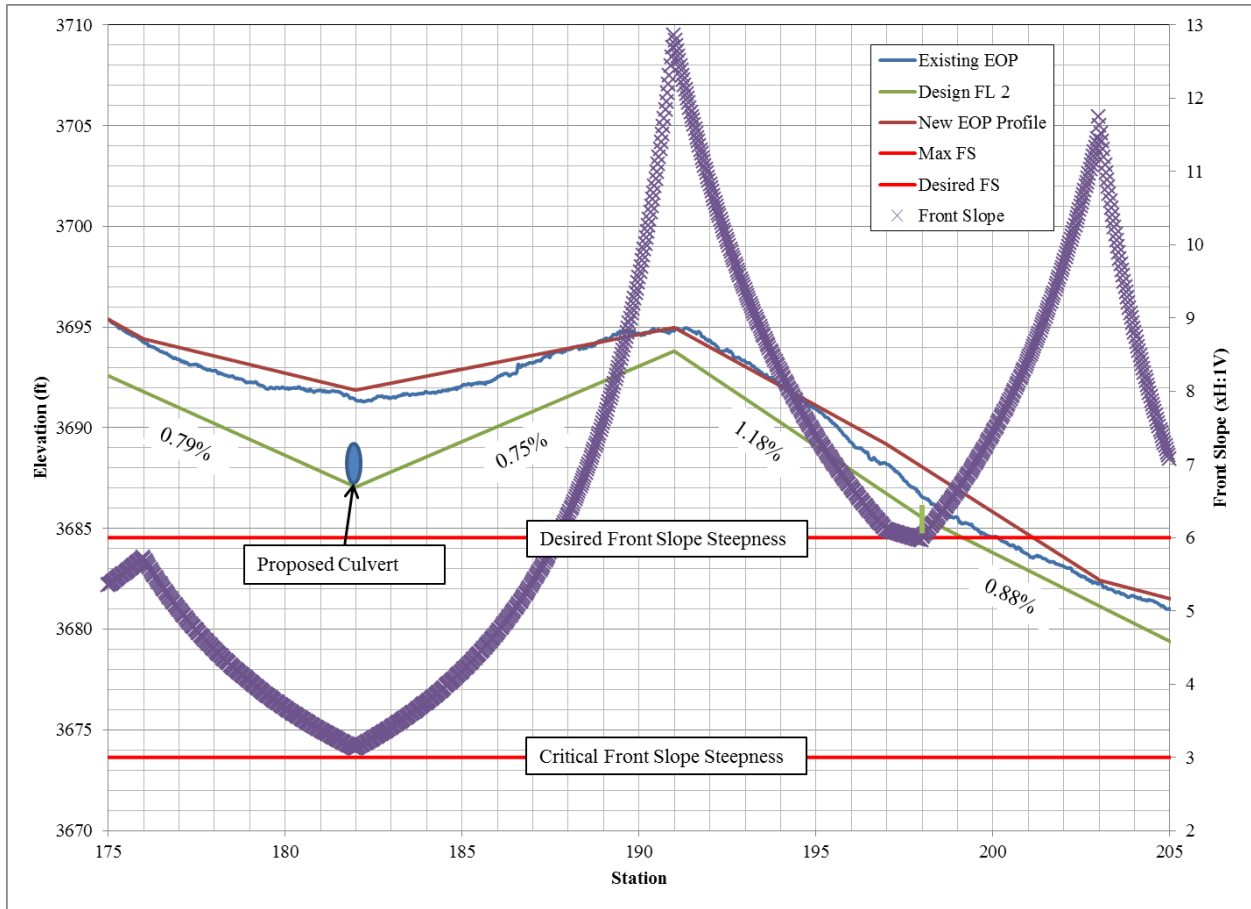
Figure 91. STA 175+00 to STA 205+00 Design Westbound EOP and Ditch Flowline with Front Slope Steepness.

Figure 91 shows a proposed culvert at the existing dip location near STA 182+00. In an effort to maintain adequate longitudinal flowline fall over long runs, the culvert at STA 182+00 is placed deep in the ground. This is the only proposed culvert that can be placed without raising the profile of the road. The depth of culvert at this location increases front slope steepness to almost the critical level of 3H:1V. A ditch flowline grade break is proposed at STA 198+00. At this point, the flowline flattens from 1.18 percent to 0.88 percent to help mitigate front slope steepening that occurs by filling the built-in dip at STA 214+00.
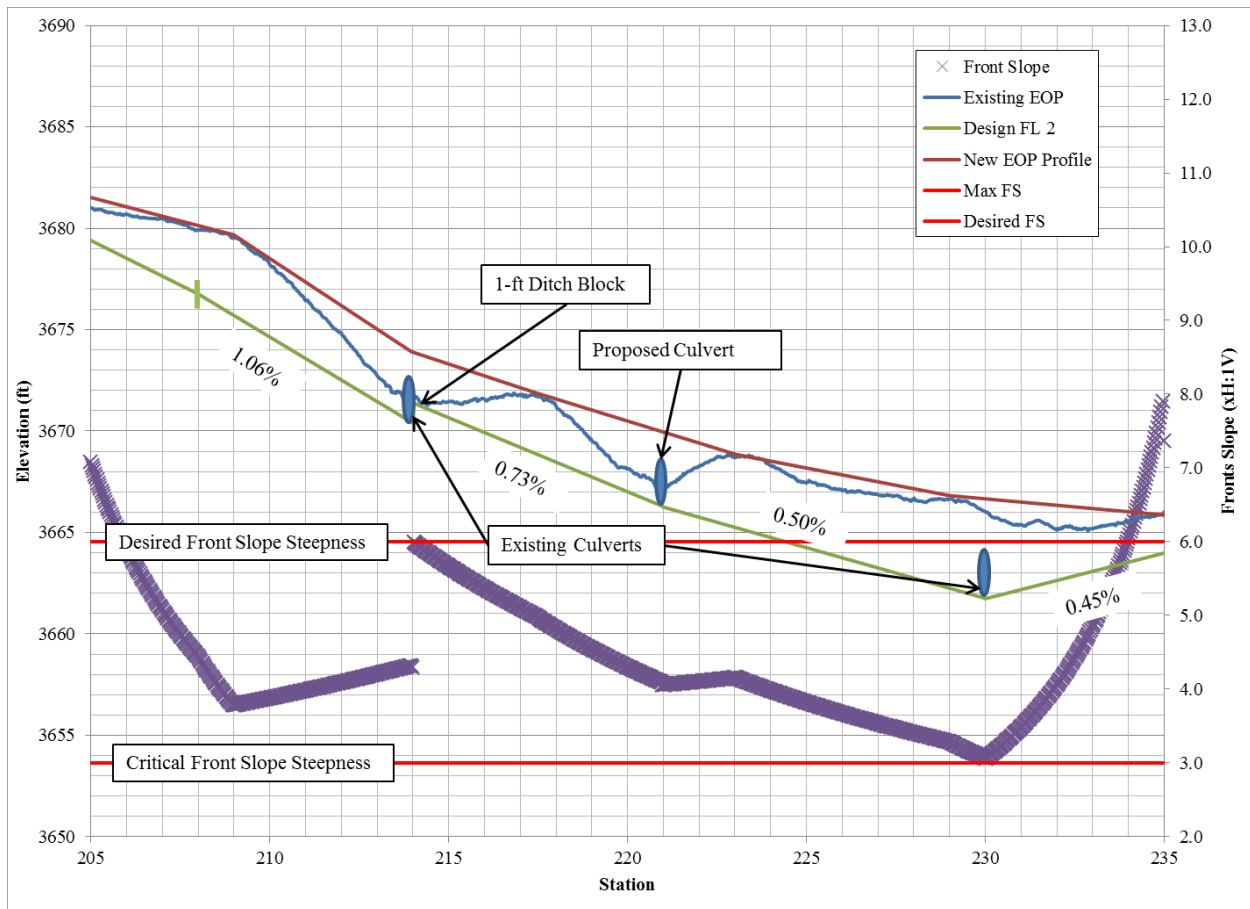
Figure 92. STA 205+00 to STA 235+00 Design Westbound EOP and Ditch Flowline with Front Slope Steepness.

Figure 92 consists of the two existing culvert locations near STA 214+00 and STA 230+00. Each of these existing culverts will need to be replaced to match the proposed design. Prior to reaching the culvert near STA 214+00, a flowline grade break is proposed near STA 208+00. At this location, the flowline steepens from 0.88 percent to 1.06 percent. The flowline grade becomes fairly flat between the culverts, so care should be taken to maintain eastward fall. The culvert at STA 214+00 includes a 1-ft ditch block immediately downstream to increase the flowline elevation before continuing eastwardly flow. This ditch block is required to raise the ditch flowline for adequate fall between culverts. A new culvert should be installed at the built-in dip near STA 221+00. A culvert is recommended at this location only to facilitate a water crossing, as originally designed. From a profile grade and ditch flowline perspective, no culvert is required between the two existing culverts. A more thorough hydraulic study would be required to ensure the downstream culvert at STA 230+00 would not be overwhelmed without making provision for water to cross at STA 221+00. At the proposed EOP profile and new ditch flowline, the 3000-ft section shown in Figure 92 has the steepest continuous front slope. For almost the entire 3000 ft, the steepness is between 6H:1V and the critical steepness of 3H:1V. The steepest location is found at the culvert at STA 230+00, where the front slope becomes almost 3H:1V.
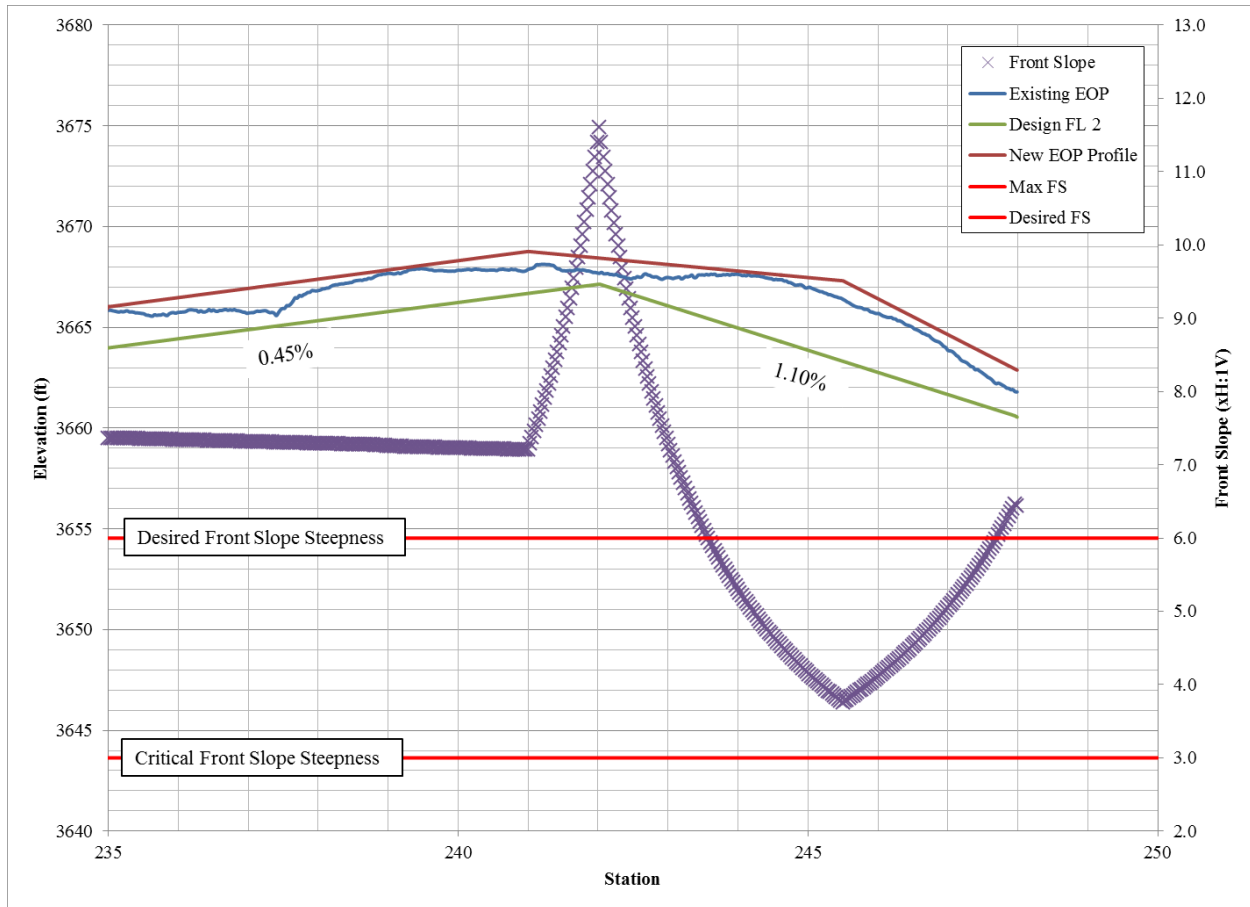
152

Figure 93. STA 235+00 to STA 250+00 Design Westbound EOP and Ditch Flowline with Front Slope Steepness.

Figure 93 is the eastern end of this 2-mi section. Beginning near STA 242+00, the profile grade of RM 652 begins to fall quickly to the east toward a significant low spot where water crosses and flows back to the south. The uphill flowline grade leaving the culvert at STA 230+00 is the flattest proposed flowline within the 2-mi section.

As previously stated, within this 2-mi section the north roadside serves as the downstream side in relation to the south roadside, so design profiles are based on tying in to ditch flowline elevations shown in Figure 90 through Figure 93. Assuming a 1.5 percent crown and accounting for two horizontal curves requiring superelevation, a centerline profile and right EOP profile (adjacent to eastbound traffic) were developed. With a new right EOP, a ditch flowline profile for the south side of the roadways was designed. Figure 94 shows the design profiles for both ditch flowlines, both edges of pavement, and the centerline.
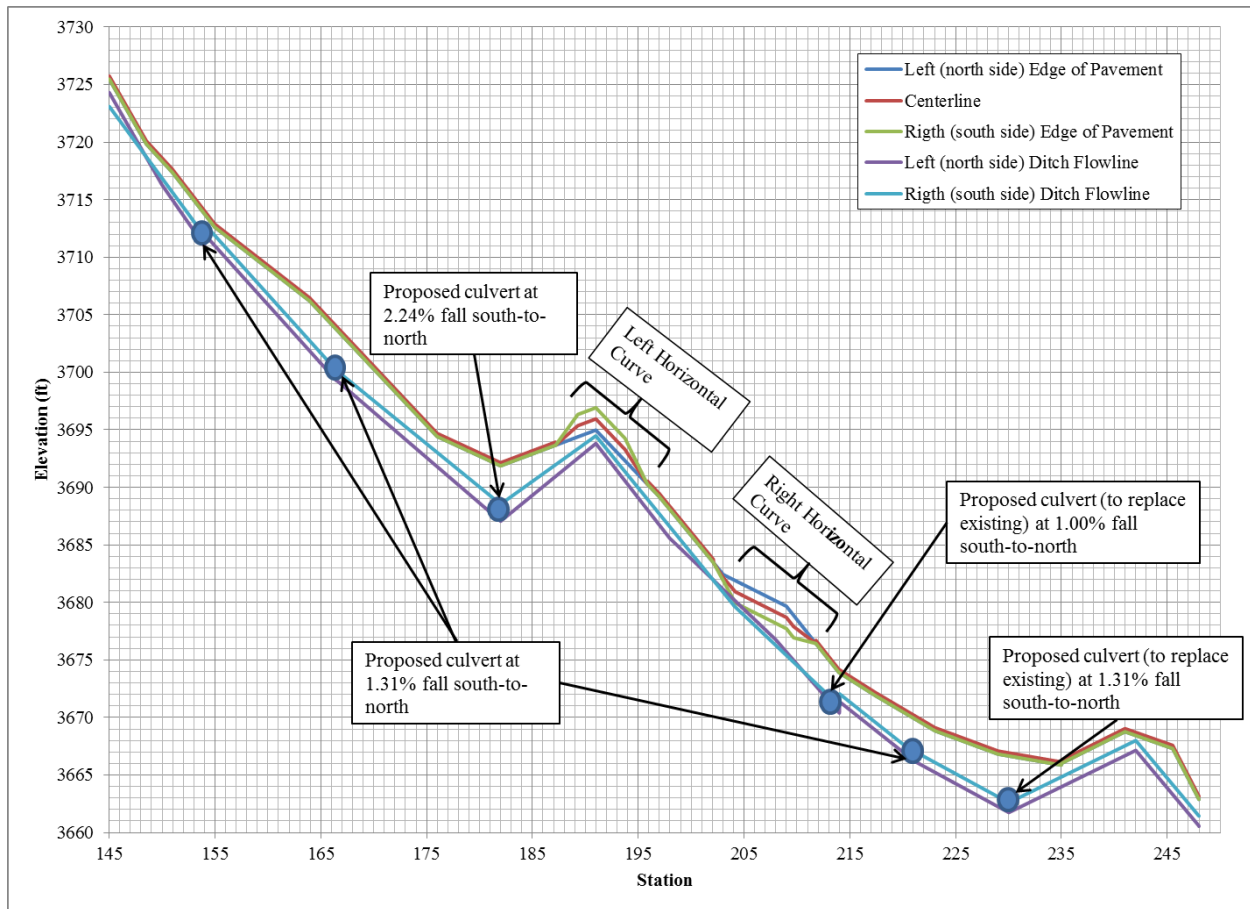
Figure 94. Design Profiles from STA 145+00 to STA 250+00.

One of the primary objectives of the new design is to move surface water away from the pavement structure. By creating longitudinal fall in the ditch flowline and coupling this fall with increased ditch depth, water will move away from the pavement quicker and does so at an added depth. The increase in ditch depth gained in the proposed design is shown for the north roadside in Figure 95 and for the south roadside in Figure 96. Figure 95 indicates that under the proposed design, the north roadside ditch depth will always exceed 1 ft, a depth rarely achieved under current conditions. The depth begins to approach 1 ft between STA 185+00 and STA 195+00 where the roadway enters a left horizontal curve, placing the north roadside on the low side of the curve. Care should be taken in this area to deal with water approaching the pavement structure. A potential mitigation strategy would be to pour a concrete flume on the low side of the curve in this area. As for the south roadside, Figure 96 displays the ditch depth. The ditch depth on the south side is less than 1 ft in three locations. The first location near STA 154+00 occurs because of the ditch block immediately located downstream of the proposed culvert. This ditch block shallows the ditch depth only briefly as the longitudinal fall creates more depth, but the ditch block helps ensure front slope steepness remains flatter than critical as ditch depth increases. Near STA 205+00, where ditch depth becomes shallowest, the south roadside finds itself on the low side of a horizontal curve. Once again, because water encroaches on the

154

pavement structure in this location, a concrete flume to prevent infiltration might be necessary. The final location of the shallow ditch occurs near the top of hill at the end of the project, just before the profile grade falls sharply to the east. Figure 95 and Figure 96 illustrate the increase ditch depth on both roadsides with the proposed design. These depths are obtained while limiting front slope steepness to not steeper than 3H:1V. Figure 97 shows the front slope steepness created by the proposed design. These steepness values assume that when a ditch is present, it is located 15 ft from the EOP. In many locations, this will require shifting the ditch toward the ROW line.
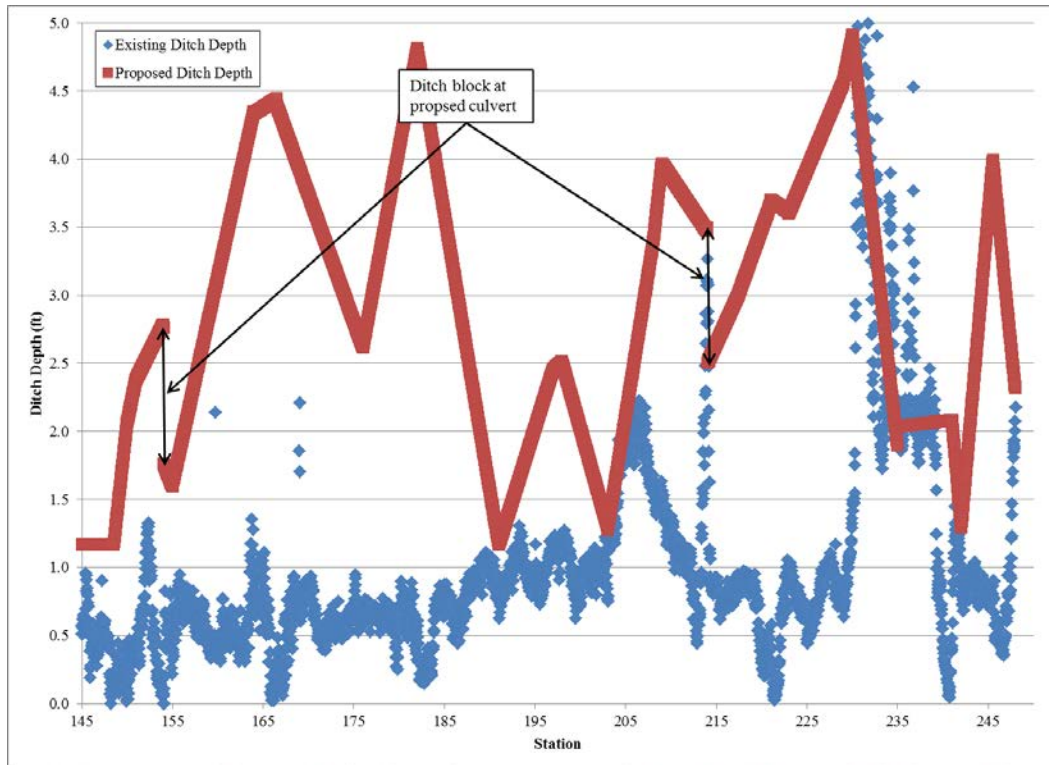

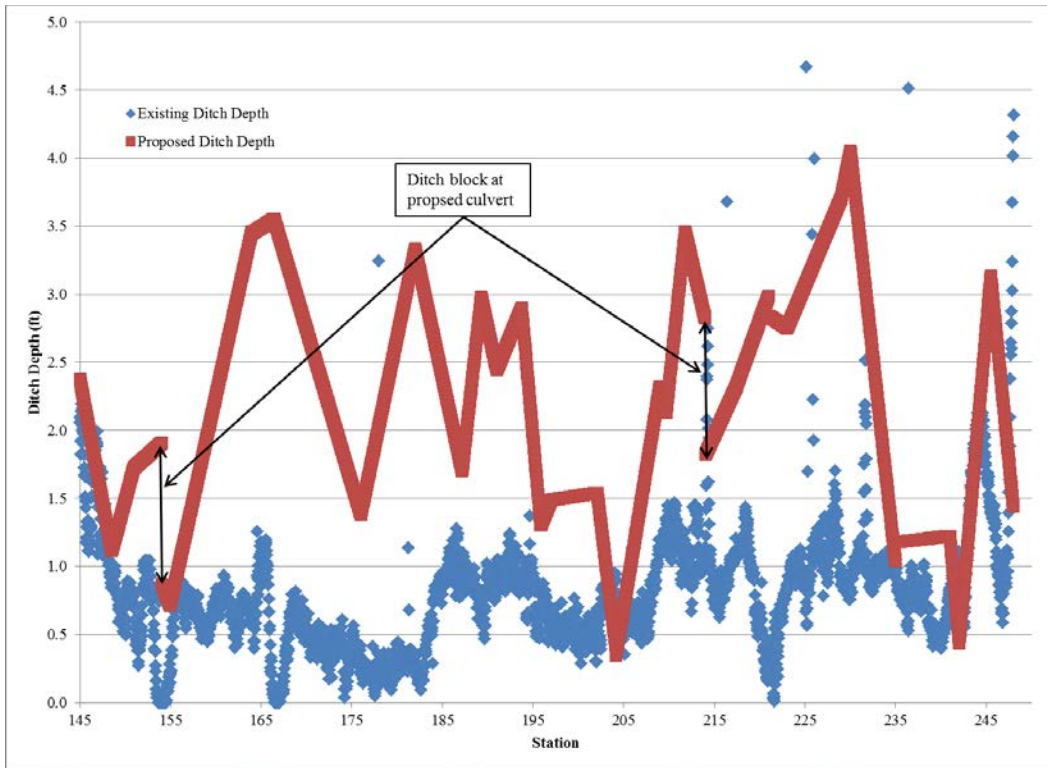**Figure 95. North Roadside Proposed Ditch Depth Compared with Existing Ditch Depth.**

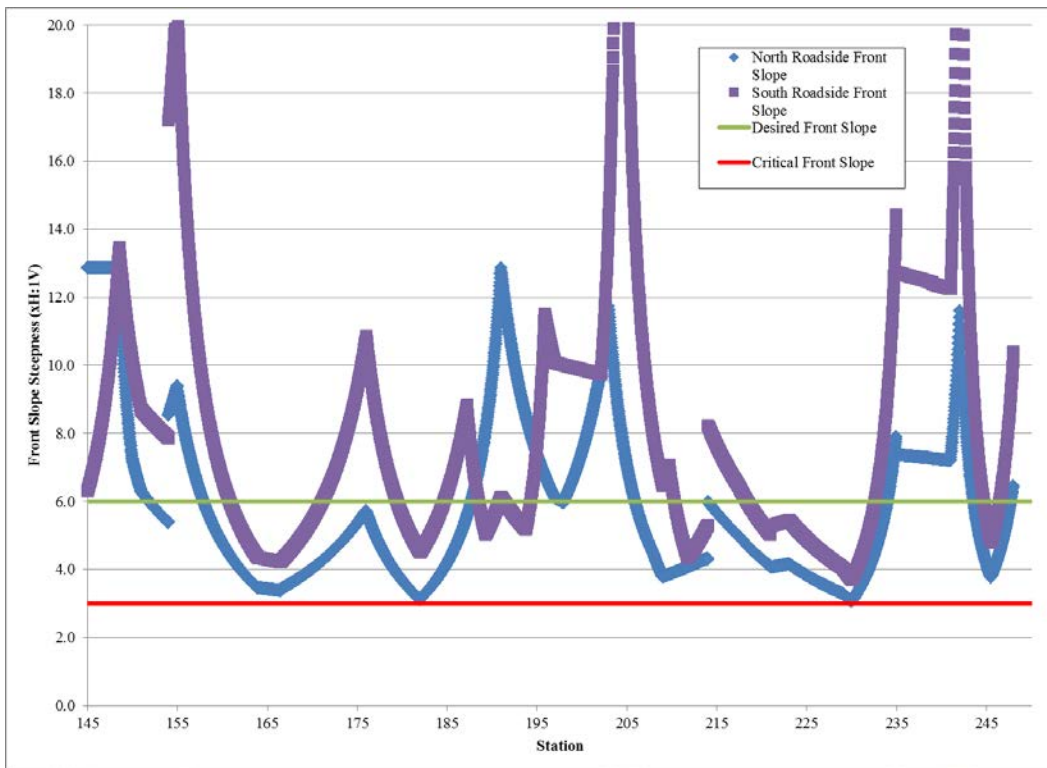**Figure 96. South Roadside Proposed Ditch Depth Compared with Existing Ditch Depth.**

Figure 97. Design Front Slope Steepness.

The previous discussion focused on a complete reconstruction of RM 652 between reference markers 142 and 144. With four built-in dip locations within these 2 mi, isolating a repair becomes challenging. With the design ditch depths as deep as or deeper than the existing ditch depth and the fact that the design front slope does not exceed critical steepness despite an increase in profile elevation, the ditch design can be implemented as long as proposed culverts are installed. The proposed culverts eliminate the built-in dip locations and offer the potential to isolate work actions.

Installation of the culvert near STA 154+00 requires paving work to begin near STA 151+00 and tie-in near STA 155+00. Within this 400 ft, the built-in dip will be filled to cover the proposed culvert. For the culvert installation near STA 166+50, pavement work must begin near STA 164+00 and can tie in near STA 175+00. While a tie in is possible near STA 175+00, additional pavement work is required beginning near STA 176+00 to cover the proposed culvert at STA 182+00. Pavement profile work is required to approximately STA 188+00 to install the culvert at STA 182+00. Replacement of the culvert at STA 214+00 and installation of a new culvert near STA 221+00 requires pavement work from STA 209+00 to STA 223+00. The existing culvert at STA 230+00 can be lowered without pavement work beyond the installation of new pipe.

In summary, the minimum pavement work required from reference marker 142 to 144 will impact 4,100 ft. Within this 2-mi section of RM 652, approximately 0.8 mi of pavement reconstruction and profile grade changes is required to install the necessary culverts and improve roadside drainage. By eliminating profile grade changes outside of this 4,100 ft, ditch depths will not increase as much as if the entire 2-mi section was rebuilt.

Table 40 summarizes the proposed flowline design.

Table 40. Ditch Flowline Design Summary.

From STA	To STA	LT (north side) Ditch Grade	RT (south side) Ditch Grade	LT (north side) Flowline Elev.	RT (south side) Flowline Elev.
145+00	150+00	−1.61%	−1.25%		
150+00	154+00	−1.33%	−1.02%		
154+00				3711.00	3711.86
154+00	166+50	−1.02%	−1.02%		
166+50				3699.29	3700.15
166+50	182+00	−0.79%	-0.75%		
182+00				3687.06	3688.54
182+00	191+00	0.75%	0.66%		
191+00	198+00	−1.18%	−1.13%		
198+00	204+00	−0.88%	−1.13%		
204+00	208+00	−0.88%	−0.87%		
208+00	214+00	−1.06%	−0.87%		
214+00				3670.39	3671.05
214+00	221+00	−0.73%	−0.73%		
221+00				3666.26	3667.12
221+00	230+00	−0.50%	−0.50%		
230+00				3661.75	3662.60
230+00	242+00	0.45%	0.45%		
242+00	248+00	−1.10%	−1.10%		

RM 652 Project Level Analysis Conclusions

RM 652 consisted of a unique geometric situation where the roadway functioned as the conduit for water to pass from one side of the roadway to the other. In the original design of RM 652 in the early 1950s, low water crossings were built into the pavement profile. Unfortunately, these locations provide an area for water infiltration into the pavement structure, proving detrimental because of the presence of gypsum. Using Mobile LiDAR, a new design was developed that addresses roadside drainage and the pavement profile. The design includes the installation of culverts and the placement of overburden in the existing dips. Using mobile LiDAR, flowline grades were developed on the north ROW as the controlling line within the design. Transitioning these flowline grades to an EOP for westbound traffic was controlled by front slope steepness. An effort was made on both roadsides to minimize front slope steepness while maintaining at least 0.50 percent fall in the ditch and maximizing ditch depth.

US 77—AUSTIN DISTRICT

Background Information

An analysis was performed on US 77 from the City Limits of Giddings to the Fayette County line. This analysis was performed to provide the Austin District with information on where best to perform maintenance work to mitigate rutting. In addition to rut identification, roadside ditches were reviewed to evaluate drainage adequacy. Overall, this portion of US 77 has extensive bleeding, rutting (particularly in the outside wheel path), and poor roadside drainage. The typical section of US 77 within these limits is a four-lane roadway, two lanes in each direction, with no median. From LiDAR measurements, it is known that each lane is approximately 11-ft wide, and 1-ft shoulders exist adjacent to each direction of travel. In summary, four lanes of travel exist in approximately a 46-ft footprint. Figure 98 shows LiDAR reflectivity data, showing the lane markings and width of traveled way and width of paved area.
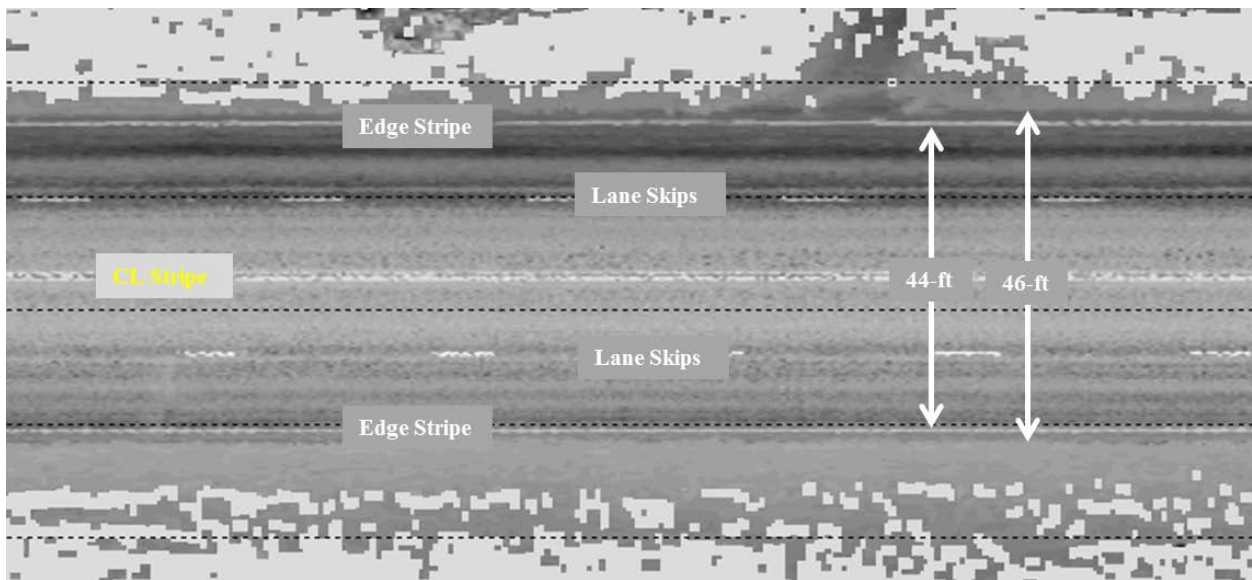
Figure 98. US 77 Width.

LiDAR Analysis

The outside lanes in both directions were evaluated for rutting. All rutting measurements, regardless of direction are referenced from the pavement change near reference marker 476+1.831. At this location, the pavement changes from a recent HMA to seal coat, which is shown in Figure 99. The analysis ends near the county line where US 77 transitions from two lanes in each direction with no median to one lane in each direction, near reference marker 482+0.996.

Figure 99. Pavement Used as Reference Point on US 77.

The length of the analysis spanned just over 27,000 ft (approx. 5.11 mi). Both the outside north and southbound lanes contain long lengths of 0.5-in. or deeper rutting. Table 41 lists the length of rutting 0.5-in. or deeper in both outside lanes and in each wheel path. This is further illustrated in the 0.5-mi section breakdowns located in the Appendix. These breakdowns provide a visualization of where pavement sections are rutted for long runs.

Table 41. Length of Wheel Path Rutting.

Lane	Wheel Path	Length of Rutting ≥ ½" (ft)
Outside Southbound	Inside	5,276
Outside Southbound	Outside	11,296
Outside Northbound	Inside	6,769
Outside Northbound	Outside	6,815

The outside southbound lane clearly has more rutting in the outside wheel path. Table 42 provides the suggested areas requiring rut fill. These areas are also labeled on the breakdowns in the Appendix. Care was taken to develop realistic lengths of rut fill and to avoid assigning work to short increments. During the actual rut fill operations, it is likely that areas will be extended or shortened to feather the material into and out of the rut. All displacement measurements in the repair location table are referenced from the pavement change near TRM 476+1.831.

Table 42. Rut Fill Locations.

Section No.	Location No.	Begin Disp.	End Disp.	Lane	Wheel Path	Length (ft)
1	SB1	200	475	Outside SB	Outside	275
	SB2	875	980	Outside SB	Both	105
	SB3	2135	2575	Outside SB	Inside	440
	NB1	370	1750	Outside NB	Both	1380
	NB2	2270	2675	Outside NB	Inside	405
2	SB4	2625	2805	Outside SB	Both	180
3	SB 5	6235	6490	Outside SB	Outside	255
	NB 3	6530	6700	Outside NB	Outside	170
4	NB 4	8630	9510	Outside NB	Outside	880
	SB 6	8670	9030	Outside SB	Outside	360
	SB 7	9700	10360	Outside SB	Outside	660
5	SB 8	10825	11125	Outside SB	Outside	300
	SB 9	11680	11820	Outside SB	Both	140
	SB 10	12330	12535	Outside SB	Outside	205
	NB 5	11075	11200	Outside NB	Both	125
	NB 6	11655	11955	Outside NB	Inside	300
	NB 7	12300	12395	Outside NB	Outside	95
6	SB 11	13130	13420	Outside SB	Outside	290
	SB 12	13775	13850	Outside SB	Outside	75
	NB 8	13130	13740	Outside NB	Outside	610
	NB 9	14060	14185	Outside NB	Outside	125
7	SB 13	16175	16295	Outside SB	Outside	120
	SB 14	17550	18235	Outside SB	Both	685
8	SB 15	18375	18495	Outside SB	Outside	120
	SB 16	19505	24145	Outside SB	Outside	4640
	NB 10	19235	19465	Outside NB	Outside	230
	NB 11	20075	21005	Outside NB	Outside	930
9	NB 12	21200	22000	Outside NB	Both	800
	NB 13	22505	23050	Outside NB	Inside	545
	SB 17	21440	21685	Outside SB	Inside	245
10	SB 18	24450	27115	Outside SB	Both	2665
	NB 14	26035	27000	Outside NB	Outside	965

Because LiDAR data indicated more rutting in the outside wheel path than the inside wheel path, particularly in the southbound direction, additional LiDAR analysis was performed on the roadside. The roadside analysis was performed to determine if roadside improvements can be done to lengthen the life of pavement repairs. Unfortunately, many of the existing cross-culverts are not deep enough to significantly improve roadside drainage. For example, Section 4 has shallow ditches, but the cross-culvert within this section is too shallow to gain any significant

depth along the roadside. Even though depth cannot be created in this section, ditch cleaning to ensure contiguous positive drainage is advisable. The analysis was performed by identifying locations where the flowline of the ditch is within 2 ft of the EOP elevation as measured using mobile LiDAR. Potential work locations were developed based on this criterion and the ability to improve positive drainage by working upstream from a deep cross-culvert or an area where water exists at a TxDOT ROW. Figure 100 shows an example. Table 43 shows suggested roadside ditch cleaning locations and limits. The begin location is referenced from the pavement change at the north end of the project. The locations are shown visually in the charts in the Appendix. While no work is shown in Section 4, Section 6, and Section 7, these 0.5-mi sections have shallow ditches that might need to be deepened, but the cross-culverts are not deep enough to provide significant cut in the ditch line. Section 7 along the southbound roadside appears to have a birdbath where the water does not drain either north or south. Also, the TxDOT stockpile location along the southbound roadside holds water, contributing to rutting in the area.
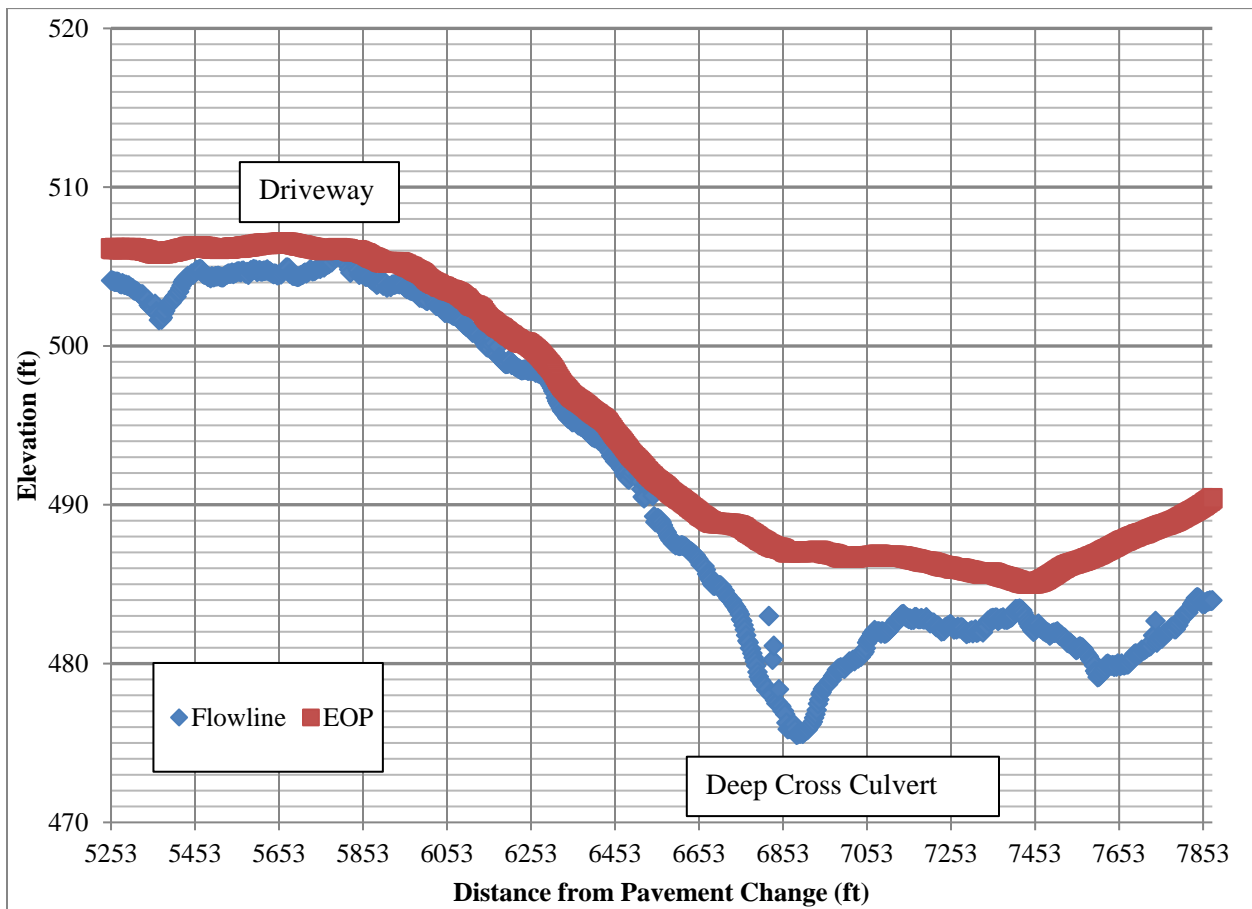

Figure 100. Shallow Ditch Depth in Relation to EOP Elevation.

Table 43. Ditch Cleaning and Grading Locations.

Grading Location	Roadside	Section	Downstream Point Description	Begin Work Dist. (ft)	End Work Dist. (ft)	Flow Direction	Length of Ditch Cleaning
1	Southbound	2	Front-Slope-Only Area Where Water Exits ROW	2925 (just south of driveway)	3700 (ROW transitions to front slope only)	South at approx. 1.85% fall	775
2	Southbound	3	Deep Cross-Culvert	5850 (just south of driveway)	6850 (at cross-culvert)	South at approx. 2.85% fall	1000
3	Southbound	5	Cross-Culvert	11050	12135	South at approx. 1.80% fall	1085
4	Southbound	8	Large Cross-Culvert	18680 (just south of small cross-culvert	20335 (at large cross-culvert)	South at approx. 1.3% fall	1655
5	Southbound	9	Shallow Cross-Culvert	21140 (rutter area on ROW)	22215 (at small cross-culvert)	South at approx. 0.5% fall	75
6	Southbound	10	Cross-Culvert	23940 (at cross-culvert)	24520	North at approx. 1.50% fall	580
7	Southbound	10	Cross-Culvert	24520	25100 (at cross-culvert)	South at approx. 2.10% fall	580
8	Southbound	10	Low Spot Approaching Bridge	25100	26060	South at approx. 1.30% fall	960

US 77 Project Level Analysis Conclusions

The rut data generated by mobile LiDAR measurements was used by the district to plan maintenance paving work to mitigate rutting. Spot maintenance overlays were performed in areas with the most significant rutting. Figure 101 shows an example of a spot overlay within the analyzed area. Roadside drainage work has not yet been performed. For this analysis, mobile LiDAR measurements proved beneficial in identifying the most concerning areas in terms of rutting and linking those areas with potential roadside improvements.

Figure 101. Spot Overlay on US 77.

IH 30—ATLANTA DISTRICT

Background Information

A rutting analysis using mobile LiDAR measurements was conducted on IH 30 in the Atlanta District through all of Titus County, to Morris County, to the Sulphur River. The analysis included approximately 28 mi of data in the outside eastbound and outside westbound lanes. Because mobile LiDAR data accompanied video data, data collection was broken up into approximately 4-mi sections to minimize the file size. The Atlanta District is experiencing rutting and stripping issues along IH 30.

Mobile LiDAR Analysis

The primary purpose of this analysis was to provide the district with information on where rutting exceeded 0.5 in. Using mobile LiDAR data, this information was provided in the left (inside) and right (outside) wheel paths. Figure 102 shows rutting in the westbound direction, and Figure 103 shows rutting in the eastbound direction. Reference markers are depicted by the x-axis. Mobile LiDAR provided almost continuous rutting measurements. For this analysis, 1-ft increments were used with transverse measurements across the wheel paths taken on 2-in. increments.
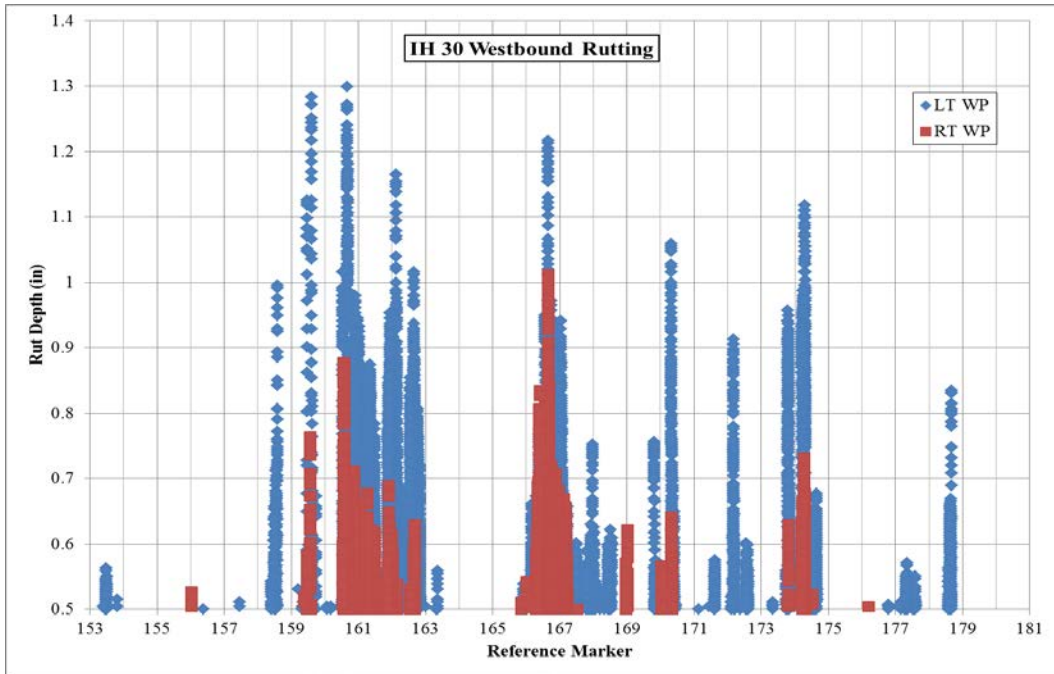
Figure 102. IH 30 Westbound Wheel Path Rutting.
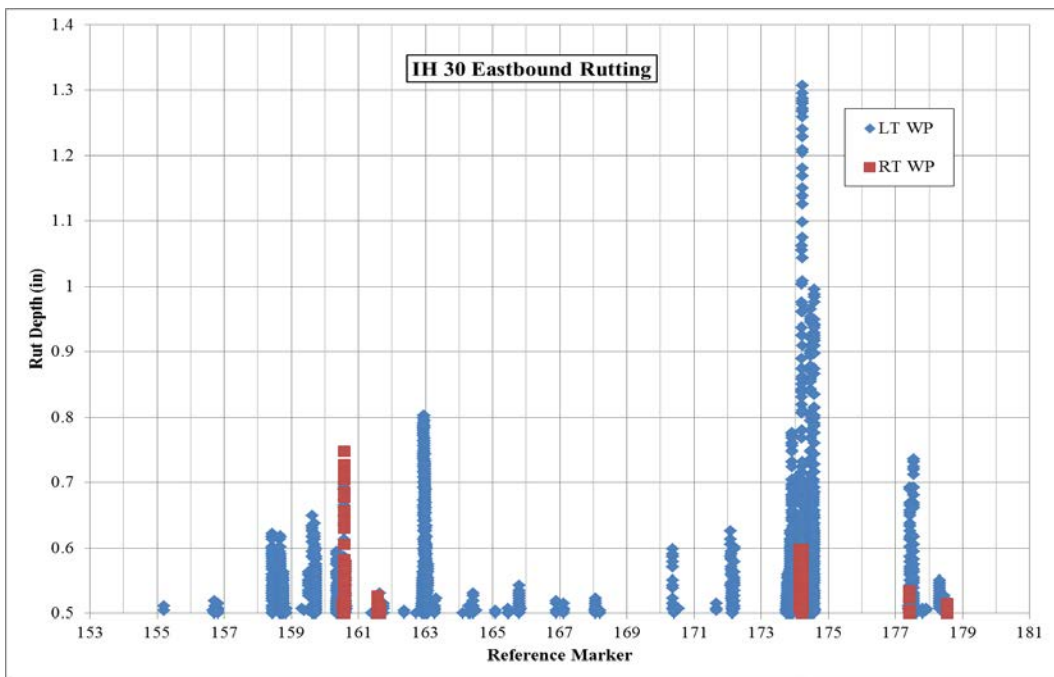
Figure 103. IH 30 Eastbound Wheel Path Rutting.

Figure 102, near reference marker 167, depicts rutting in the left wheel path that exceeds 1 in. and approaches 1 in. in the right wheel path. Unfortunately, this rutting occurs in an area of newer construction, as shown in Figure 104.

Figure 104. IH 30 Westbound Area with Deep Rutting.

While Figure 104 does not display visible signs of distress, other areas in the westbound direction experiencing deep rutting also display signs of potential striping. Figure 105 displays an image near reference marker 163 in the westbound direction. Left wheel path rutting in this area begins to exceed 1 in. Figure 105 shows material coming to the surface in both the left and right wheel path, potentially indicating striping.

Figure 105. IH 30 Westbound Location with Deep Rutting and Potential Striping.

Figure 102 and Figure 103 were provided to the district along with a table of rut depths on 1-ft increments. This information was presented in a conference call, along with a visual presentation using post-processing software. During the presentation, rut maps and corresponding video were used to convey results to district staff. According to district staff, the areas identified as deep rutting with mobile LiDAR were filed verified.

SUMMARY, CONCLUSIONS, AND RECOMMENDATIONS

Mobile LiDAR provides an effective tool to measure various surface geometric features at highway speeds. Mobile LiDAR techniques are rapidly penetrating industry, but the ability to process and make sense of the vast amount of data created continues to create challenges. The use of mobile LiDAR data to generate network-level tools and information is essentially nonexistent across other state DOTs. The network-level tool created within this research project presents an opportunity to add to TxDOT's overall asset management system with a surface drainage rating. The surface drainage rating developed through this project includes paved surface attributes and roadside attributes measured exclusively with a mobile LiDAR device and processed in bulk with limited manual intervention.

While the initial goal of the project was the development of a surface drainage rating, the project evolved into a surface rating that captures drainage-related elements. The impetus of this evolution was the historical tradition of roadway design balancing many design elements. Often, roadway design requires geometric features that are not as hydraulically efficient as desired but are required to maintain safety. In order to hold safety paramount, the surface drainage rating evaluated design compliance of surface elements measured with mobile LiDAR. For example, while the location of the roadway to roadside interface is important to delineate where to begin roadside analysis, define the edge for hydroplaning evaluation, and set an elevation to determine ditch depth, it also allows for the calculation of traveled way width. Traveled way width is an important safety parameter, and the need to widen a roadway can ultimately impact the roadside drainage. Therefore, the traveled way width was rated based on design standards and included in the paved surface rating.

Researchers provide a paved and roadside rating only in the direction of travel. The accuracy of the data and the density of the point cloud from which to draw information creates the need to focus the rating in the direction of data collection. As the target surface gets farther from the laser, the point density decreases. In an effort to limit interpolation between measurements and improve overall accuracy, researchers chose to only provide a rating in the direction of travel of the data collection vehicle. For all but one roadway rated, ratings were done in the K1 direction (i.e., the direction of increasing reference markers). Rating in a single direction also offers temporal consistency for implementation of the process.

Within this research project, proof of concept code was successfully developed to process vast amounts of mobile LiDAR data and convert data into a surface drainage rating. The rating developed specifically applies to rural roadway sections with an unconfined edge. For roadways such as these, the data are collected on the following elements:

- Traveled way width.
- Data collection lane cross-slope.
- Hydroplaning speed.

- Right roadside front slope.
- Right roadside ditch depth.
- Right roadside flowline slope.

The first three elements impact the rating of the paved surface, while the last three impact the rating on the roadside. In addition to creating a sub-rating for each of these elements to feed the overall rating, a descriptor is provided for the paved surface and the roadside. Using alignment information from the IMU associated with the mobile LiDAR unit, the alignment of each 0.1-mi data collection section is defined as either tangent, right curve, or left curve. Subsequently, processed mobile LiDAR elevation data are used to determine if the roadway is in shape relative to the expected location of the highpoint on the surface. Roadside drainage receives a descriptive note of either primarily ditch, primarily front slope, or various drainage that might occur in front slope to ditch transitions.

Using network-level information generated from mobile LiDAR measurements and developed within the report, roadway managers and engineers can evaluate roadway and roadside surfaces for needs. For example, if a data collection section falls within a geometric curve, a cross-slope rating of less than 1.0 indicates the radius of that curve is shorter than ideal, given the current superelevation. As the cross-slope rating decreases, the difference in speed at which a motorist can safely navigate the curve and the posted speed limit increases. A low rating might result, but the local manager might know or be able to check the video and determine that the proper advisory sign(s) and/or chevrons are in place. Other investigative techniques provide an understanding of not only an element within the rating but also if improvements can be made to that particular geometric element.

The project described within the report produced a rating for 73.5 miles of roadway within four districts and performed a project level analysis on four different projects. The project level analyses included providing detailed design for proposed work on US 75 in the Paris District and RM 653 in the El Paso District. Each of these project level applications required coordinating between the paved surface and the roadside. A project level analysis was also performed on IH 30 in the Atlanta District and US 77 in the Austin District. The primary output for each of these analyses were rut maps for maintenance decision making.

The current surface drainage rating is limited to rural sections. This limitation comes from the desire to automate as much of the network-level processing as possible as well as geometric limitations on urban and metro sections. Urban and metro sections have little to no roadside that contributes to the overall drainage rating. Also, for the water to exit the roadway in these sections, inlets or barrier openings must be identified. The ability to identify these at the network level with minimal manual processing is not feasible. Presently, researchers recommend treating urban and metro sections like project level analyses.

Researchers recommend selecting a single district to implement the rating across the entire rural network. A review of wet weather crashes should take place during the complete implementation to validate hydroplaning speed output. Also, by implementing the rating across a district, additional study can be performed on potential drainage impacts on pavement performance. The US 77 project level analysis seems to indicate that ditch depth and outside wheel path rutting could be related. The rating system was applied to FM 1660 in the Austin District and FM 1696 in the Bryan District. These results were not discussed within, but each of these sections were scheduled for rehab work. Both roadways were determined to be significantly out of shape, but no other obvious drainage-related issues were present. A lack of temporal surface measurement information limits this analysis, but casting a wider net across an entire district could help better determine the relationship between drainage performance and pavement performance.

REFERENCES

1. Park, H., W. Robert, and K. Lawrence. *2013 Transportation Asset Management Peer Exchange.* FHWA-HIF-13-069, Federal Highway Administration (FHWA) through Spy Pond Partners, LLC, Washington, DC, 2013.

2. Federal Highway Administration (FHWA). Transportation Asset Management Plans. 2015. http://www.fhwa.dot.gov/asset/plans.cfm, 2015.

3. Schraven, D. Effectiveness of Infrastructure Asset Management: Challenges for Public Agencies. *Built Environment Project and Asset Management*, Vol. 1, No. 1, 2011, pp. 61-74.

4. Hawkins, N. *Use of Transportation Asset Management Principles in State Highway Agencies.* NCHRP Synthesis 439, Transportation Research Board, Washington, DC, 2013.

5. Texas Department of Transportation (TxDOT). *What is PMIS?* Materials and Pavements Section of the Construction Division, Austin, TX, 2009.

6. ———. *Condition of Texas Pavements: PMIS Annual Report FY 2006-2009.* Materials and Pavements Section of the Construction Division, Austin, TX, 2009.

7. ———. *Highway Bridge Program—Improving the Safety of Texas Bridges.* TxDOT Bridge Division, Austin, TX, 2014.

8. ———. *Pocket Facts—FY 2013.* TxDOT, Austin, TX, 2014.

9. Gao, L., S. Chi, J. Prozzi, Y. Yildirim, Z. Zhang, C. Centurion, and M. Murphy. *Per State Assessment of TxDOT Maintenance Program and Practices—Workshop and Road Rally Findings.* FHWA/TX-11/0-6664-1, Texas Department of Transportation through Center for Transportation Research, Austin, TX, 2011.

10. Hui, W., Z. Zhang, and A. S. Qazi. Evaluation of Texas Condition Assessment Program and Recommendations for Improvement. In *TRB 2013 Annual Meeting*, Transportation Research Board, Washington, DC, 2013.

11. Chang, J. C., D. J. Findley, C. M. Cunningham, and M. K. Tsai. Considerations for Effective Lidar Deployment by Transportation Agencies. *Transportation Research Record: Journal of the Transportation Research Board*, No. 2440, 2014, pp. 1-8.

12. Tsai, Y. C., and F. Li. Critical Assessment of Detecting Asphalt Pavement Cracks Under Different Lighting and Low Intensity Contrast Conditions using Emerging 3D Laser Technology. *Journal of Transportation Engineering*, Vol. 138, No. 5, 2012, pp. 649-656.

13. Tsai, Y. C., C. B. Ai, Z. H. Wang, and E. Pitts. Mobile Cross-Slope Measurement Method using Lidar Technology. *Transportation Research Record*, No. 2367, 2013, pp. 53-59.

14. Findley, D., C. Cunningham, and J. Hummer. Comparison of Mobile and Manual Data Collection for Roadway Components. *Transportation Research.Part C, Emerging Technologies*, Vol. 19, No. 3, 2011, pp. 521-540.

15. Olsen, M. J., G. V. Roe, C. Glennis, F. Persi, M. Reedy, D. Hurwitz, K. Williams, H. Tuss, A. Squellati, and M. Knodler. *Guidelines for the use of Mobile LIDAR in Transportation Applications.* NCHRP Report 748, Transportation Research Board, Washington, DC, 2013.

16. Cook, A. A., M. Saito, and G. G. Schultz. Heuristic Approach to Identifying Horizontal Curves and their Parameters Given Lidar Point Cloud Data. *Transportation Research Record*, No. 2521, 2015, pp. 22-30.

17. Cazorzi, F., G. Dalla Fontana, A. De Luca, G. Sofia, and P. Tarolli. Drainage Network Detection and Assessment of Network Storage Capacity in Agrarian Landscape. *Hydrological Processes*, Vol. 27, No. 4, 2013, pp. 541-553.

18. Lantieri, C. Mobile Laser Scanning System for Assessment of the Rainwater Runoff and Drainage Conditions on Road Pavements. *International Journal of Pavement Research and Technology*, Vol. 8, No. 1, 2015, pp. 1-9.

19. Mraz, A., and A. Nazef. Innovative Techniques with a Multipurpose Survey Vehicle for Automated Analysis of Cross-Slope Data. *Transportation Research Record*, No. 2068, 2008, pp. 32-38.

20. Kashani, A. G., M. J. Olsen, C. E. Parrish, and N. Wilson. A Review of LIDAR Radiometric Processing: From Ad Hoc Intensity Correction to Rigorous Radiometric Calibration. *Sensors (Basel, Switzerland)*, Vol. 15, No. 11, 2015, pp. 28099-28128.

21. Hans, Z., R. Tenges, S. Hallmark, R. Souleyrette, and S. Pattnaik. Use of LiDAR-Based Elevation Data for Highway Drainage Analysis: A Qualitative Assessment. In *2003 Mid-Continent Transportation Research Symposium*, Iowa State University, Ames, Iowa, 2003, pp. 1-19.

22. Puente, I., H. González Jorge, J. Martínez Sánchez, and P. Arias. Review of Mobile Mapping and Surveying Technologies. *Measurement*, Vol. 46, No. 7, 2013, pp. 2127-2145.

23. O'Callaghan, J. F., and D. M. Mark. The Extraction of Drainage Networks from Digital Elevation Data. *Computer Vision, Graphics and Image Processing*, Vol. 28, 1984, pp. 323-344.

24. Choi, Y., H. Yi, and H. Park. A New Algorithm for Grid-Based Hydrologic Analysis by Incorporating Stormwater Infrastructure. *Computers and Geosciences*, No. 37, 2011, pp. 1035-1044.

25. Schwanghart, W. Short Communication: TopoToolbox 2-MATLAB-Based Software for Topographic Analysis and Modeling in Earth Surface Sciences. *Earth Surface Dynamics*, Vol. 2, No. 1, 2014, pp. 1-7.

26. Schwanghart, W. TopoToolbox: A Set of Matlab Functions for Topographic Analysis. *Environmental Modelling & Software*, Vol. 25, No. 6, 2010, pp. 770-781.

27. Gallaway, B. M., D. L. Ivey, G. Hayes, W. B. Ledbetter, R. M. Olson, D. L. Woods, and R. F. Schiller Jr. *Pavement and Geometric Design Criteria for Minimizing Hydroplaning.* FHWA-RD-79-31, Texas Transportation Institiute for FHWA, College Station, TX, 1979.

28. Ong, G. P., and T. F. Fwa. Prediction of Wet-Pavement Skid Resistance and Hydroplaning Potential. *Transportation Research Record*, No. 2005, 2007, pp. 160-171.

29. Luo, W., K. C. P. Wang, and L. Li. Hydroplaning on Sloping Pavements Based on Inertial Measurement Unit (IMU) and 1mm 3D Laser Imaging Data. *Periodica Polytechnica.Transportation Engineering*, Vol. 44, No. 1, 2016, pp. 42-49.

30. Luo, W., K. C. P. Wang, L. Li, Q. J. Li, and M. Moravec. Surface Drainage Evaluation for Rigid Pavements using an Inertial Measurement Unit and 1-mm Three-Dimensional Texture Data. *Transportation Research Record*, Vol. 2457, 2014, pp. 121-128.

31. Anderson, D. A., R. S. Huebner, J. R. Reed, J. C. Warner, and J. J. Henry. *Improved Surface Drainage of Pavements.* PTI 9825, National Cooperative Highway Research Program Transportation Research Board, Washington D.C., 1998.

32. Yassin, M., W. Jayasooriya, and M. Gunaratne. Assessment of the Reliability of Predicting Hydroplaning Risk Based on Past Hydroplaning Accident Data on the Florida Interstate System. *Transportation Research Record*, Vol. 2369, 2013, pp. 104-113.

33. Gallaway, B. M., R. E. Schiller, and J. G. Rose. *The Effects of Rainfall Intensity, Pavement Cross Slope, Surface Texture, and Drainage Length on Pavement Water Depths. by Bob M. Gallaway, Robert E. Schiller, and Jerry G. Rose.* College Station: Texas Transportation Institute, Texas A & M University, 1971, 1971.

34. Huebner, R. S., D. A. Anderson, J. C. Warner, and J. R. Reed. PAVDRN Computer Model for Predicting Water Film Thickness and Potential for Hydroplaning on New and Reconditioned Pavements. *Transportation Research Record*, Vol. 1599, No. 1, 1997, pp. 128-131.

35. Gunaratne, M., Q. Lu, J. Yang, J. Metz, W. Jayasooriya, M. Yassin, and S. Amarasiri. *Hydroplaning on Multi Lane Facilities.* BDK84 977-14, Florida Department of Transportaion by University of South Florida, Tampa, FL, 2012.

36. Rai, R. K., A. Upadhyay, and V. P. Singh. Effect of Variable Roughness on Runoff. *Journal of Hydrology*, Vol. 382, 2010, pp. 115-127.

37. Isidoro, J., and J. de Lima. Analytical Closed-Form Solution for 1D Linear Kinematic Overland Flow Under Moving Rainstorms. *Journal of Hydrologic Engineering*, Vol. 18, No. 9, 2013, pp. 1148-1156.

38. Tisdale, T. S., J. M. Hamrick, and S. L. Yu. Kinematic Wave Analysis of Sheet Flow using Topography Fitted Coordinates. *Journal of Hydrologic Engineering*, Vol. 4, No. 4, 1999, pp. 367.

39. Reed, J. Hydraulic Resistance of Pavement Surfaces. *Journal of Transportation Engineering*, Vol. 109, No. 2, 1983, pp. 286-296.

40. American Association of State Highway and Transportation Officials (AASHTO). *Highway Drainage Guidelines. 4th Ed.* Washington, D.C., 2007.

41. Escarameia, M., Y. Gasowski, R. W. P. May, and L. Bergamini. Estimation of Runoff Depths on Paved Areas. *Urban Water Journal*, Vol. 3, No. 4, 2006, pp. 185-197.

42. Texas Department of Transportation (TxDOT). *Hydrualic Design Manual.* Texas Department of Transportation (TxDOT), Austin, TX, 2014 (Rev. 2015).

43. Roadscanners. Roadscanners - Beyond the Surface. 2016. http://www.roadscanners.fi/company/, Accessed March 16, 2016.

44. SICK: Sensor Intelligence. *Detection and Ranging Solutions Laser Measurment Technology—Components and Application Packages.* Product Catalog 2012/2013, SICK, Waldkirch, Germany, 2011.

45. Texas Department of Transportation (TxDOT). Standard Specifications for Construction and Maintenance of Highways, Streets, and Bridges
Item 6 Control of Materials
300 Items Surface Courses and Pavements. , 2014.

46. TireRack. Tire Tech
Tire Specs Explained: Tread Depth. 2017.
https://www.tirerack.com/tires/tiretech/techpage.jsp?techid=197, Accessed October 5, 2017.

47. ———. Tire Tech
Air Pressure, Time Fluctations. 2017.
https://www.tirerack.com/tires/tiretech/techpage.jsp?techid=74, Accessed October 5, 2017.

48. Asquith, W. H., and M. C. Roussel. *Atlas of Depth-Duration Frequency of Precipitation Annual Maxima for Texas. by William H. Asquith and Meghan C. Roussel.* Austin, Tex. : U.S. Dept. of the Interior, U.S. Geological Survey, Water Resources Division, 2004], 2004.

49. Gallaway, B. M., and J. G. Rose. *Macro-Texture, Friction, Cross Slope and Wheel Track Depression Measurements on 41 Typical Texas Highway Pavements. by Bob M. Gallaway and Jerry G. Rose.* College Station : Texas Transportation Institute, Texas A & M University, 1970, 1970.

50. American Association of State Highway and Transportation Officials (AASHTO). *Roadside Design Guide. 4th Ed.* Washington, D.C., 2011.

51. Texas Department of Transportation (TxDOT). *Roadway Design Manual.* Texas Department of Transportation, Austin, TX, 2014.

52. Matintupa, A., and T. Saarenketo. *New Survey Techniques in Drainage Evaluation: Laser Scanner and Thermal Camera.* Task D1, ROADEX Network, Rovaniemi, Finland, 2012.

53. Iowa Department of Transportation. Design Manual. , No. 3G-1, 2012.

54. New York State Department of Transportation. *Highway Design Manual.* , Albany, NY, 2016.

55. Illinois Department of Transportation. *Drainage Design.* Bureau of Local Roads and Streets, Springfield, IL, 2006.

56. Washington State Department of Transportation. *Hydraulics Manual.* Hydraulics Office, Olympia, WA, 2017.

57. Michigan Department of Transportation. *Drainage Manual.* , Lansing, MI, 2006.

58. Huang, Y. H. *Pavement Analysis and Design. 2nd Ed.* Upper Saddle River, NJ : Pearson/Prentice Hall, 2004; 2nd ed, 2004.

59. Mackey, R., D. Selman, N. Paramanantham, and W. Blackmon. Pavement Report US 75. *TxDOT Paris District Internal Report*, 2012.

APPENDIX

SURFACE DRAINAGE RATING PSEUDOCODE

<u>Legend</u>
Bold font represents a descriptor for an entire data collection section
X_{RS} = Right edge stripe offset
X_{REOP} = Right edge of pavement offset
X_{LS} = Left edge stripe offset
X_{LEOP} = Left edge of pavement offset
X_{CL} = Centerline stripe offset (to first stripe left of the data collection vehicle)
W_{RTLN} = Width of right lane
W_{RTSHLD} = Width of right shoulder
W_{LTLN} = Width of left lane
W_{LTSHLD} = Width of left shoulder
j = point in analysis
j+1 = values with larger α than j, therefore j+1 exists to the left of j in the physical world, but to the right in the scanner data table.
j−1 = values with smaller α than j, therefore j−1 exists to the right of j in the physical world, but to the left in the scanner data table.
XS_{1x1} = any cross-section taken from the 1-ft × 1-ft grid
XS_{3x3} = any cross-section taken from the 3-ft × 3-ft grid
E_{max} = maximum elevation from within a cross-section or transverse string of data
E_{min} = minimum elevation from within a cross-section or transverse string of data
OS_{max} = horizontal offset to maximum elevation point
OS_{min} = horizontal offset to minimum elevation point
OS_{maxadj} = offset with maximum frequency adjacent to either of the two highest frequency offsets
OS_{HP} = average paved highpoint offset within a data collection section
$OS_{between}$ = offset between the two highest frequency offsets for either maximum elevation or minimum elevation
OS_{mid} = horizontal offset to the middle of the paved surface
E_{mid} = elevation of the middle of the paved surface
OS_{RTmax} = maximum right offset within analysis area
OS_{LTmax} = maximum left offset within analysis area
OS_{First} = the first transverse offset beyond the edge of pavement used in 3-ft × 3-ft grids
E_{first} = elevation associated with the first transverse offset beyond the edge of pavement in 3-ft × 3-ft grids
LOC_{PC} = longitudinal location at a point of curvature
LOC_{PT} = longitudinal location at a point of tangency
Az_{PC} = Azimuth from IMU table at point of curvature
Az_{PT} = Azimuth from IMU table at point of tangency
E_{PC}, E_{PT}, N_{PC}, N_{PT} = easting and northing from IMU table for point of curvature and point of tangency
LC = length of chord for a horizontal curve
I = angle between the intersection of the projection of Az_{PC} and Az_{PT}
R = curve radius

General Information
- Need a prompt to input:
  - TxDOT District.
  - Posted speed limit (0 mph as minimum and 85 mph as maximum).
  - Surface type, surface options are listed below.
    - Concrete—"CONC."
    - Dense graded hot-mix asphalt—"HMA."
    - Open graded surface—"OGC."
    - Good condition seal coat—"ST."
    - Flushed or shelled seal coat—"FST."
    - Unknown asphaltic surface—"ASPH."
  - Daily traffic (0 is the minimum limit and 1,000,000 the maximum).

Surface Extraction
Surface extraction requires the rawest form of data. These data consist of a reflectivity value and straight-line distance from the laser to the target object at each location.

<u>Find right edge stripe.</u>
- Evaluate each transverse string of data within the data collection section.
- For $25° ≤ α ≤ 75°$.
  - If $225 ≤ R ≤ 254$ output $α$, distance, and "Stripe Found" for the transverse string being analyzed.
    - Elseif R is never between 225 and 254, output "No Stripe."
  - If "Stripe Found" frequency < 35 percent of all transverse strings, output "**No Stripe in this Section.**"
  - If "Stripe Found" frequency ≥ 35 percent.
    - Find 5 most common $α$ values ($α_{XS}$, $α_S$, $α_M$, $α_L$, $α_{XL}$).
      - If $α_{XL} – α_{XS} ≤ 9.5°$ (increased to 5 most common and 9.5° to account for up to 2' wander in the striping).
        - And $Σ$ $α_{XS}$, $α_S$, $α_M$, $α_L$, $α_{XL} ≥ 35$ percent of "Stripe Found" count, calculate the associated average $α$ and distance. Use the average values to calculate an offset to the right edge stripe, X_{RS}.
        - X_{RS} is calculated using the following geometry:
          - If $α<90°$, $X_{RS} = Distance*sin(90° − α)$.
          - For the right side, $α$ will always be less than 90°.
        - Output, "**Right Edge Stripe at X$_{RS}$ distance.**"
    - Elseif, "Stripe Found" frequency ≥ 35 percent, but the other conditions are not met, output "**Error.**"

<u>Find right edge of pavement.</u>

- If the section was defined as "**Right Edge Stripe at X$_{RS}$ distance,**" cut the data and only use transverse strings that contain stripe. Each transverse string where stripe was found will be analyzed.
  - o For $30° \leq \alpha \leq \alpha_{stripe}$ and subscript j represents the point of analysis.
    - ▪ If $R_{j-1} - R_j \geq 20$ (Jump 20 rule where smaller α should have larger R value. The opposite cannot meet the jump rule.).
      - Average R_{j+1}, R_{j+2}, $R_{j+3} = R_{javg}$
      - If $R_{j-1} - R_{javg} \geq 10$, output and store the α, distance associated with R_j and note "RT Edge Found" for the transverse string.
        - o Elseif, the jump and average check are not found, output "RT Edge Not Found" for the transverse string.
      - If Σ(RT Edge Found) > 35 percent frequency,
        - o Find the 4 most common α values (α_S, α_M, α_L, α_{XL}).
          - ▪ If $\alpha_{XL} - \alpha_S \leq 9°$.
          - ▪ Or $\alpha_L - \alpha_S \leq 9°$.
          - ▪ Or $\alpha_{XL} - \alpha_M \leq 9°$.
          - ▪ And Σ(α within $9°$) ≥ 35 percent frequency.
            - Average α and distance. Use the average values to calculate an offset to the right edge of pavement, X$_{REOP}$.
            - X$_{REOP}$ is calculated using the following geometry:
            - If $\alpha < 90°$, X$_{REOP}$ = Distance*sin($90° - \alpha$).
            - Output, "**Right edge of pavement at X$_{REOP}$ distance.**"
      - Else, output "**RT Edge Not Found.**"
- If the section was defined as "**No stripe in this section,**" use on transverse strings with no stripe to look for the EOP.
  - o For $45° \leq \alpha \leq 70°$.
    - ▪ If $R_{j-1} - R_j \geq 20$ (Jump 20 rule where smaller α should have larger R value. The opposite cannot meet the jump rule.).
      - Average R_{j+1}, R_{j+2}, $R_{j+3} = R_{javg}$.
      - If $R_{j-1} - R_{javg} \geq 10$, output and store the α, distance associated with R_j and note "RT Edge Found" for the transverse string.
        - o Elseif, the jump and average check are not found, output "RT Edge Not Found" for the transverse string.
      - If Σ(RT Edge Found) > 35 percent frequency,
        - o Find the 4 most common α values (α_S, α_M, α_L, α_{XL}).
          - ▪ If $\alpha_{XL} - \alpha_S \leq 9°$.

- - - Or $\alpha_L - \alpha_S \leq 9°$.
    - Or $\alpha_{XL} - \alpha_M \leq 9°$.
    - And $\Sigma(\alpha$ within $9°) \geq 35$ percent frequency.
      - Average α and distance. Use the average values to calculate an offset to the right edge of pavement, X_{REOP}.
      - X_{REOP} is calculated using the following geometry:
      - If $\alpha < 90°$, $X_{REOP} = Distance*sin(90° - \alpha)$.
      - For the right side, α will always be less than $90°$.
      - Output, "**Right edge of pavement at X_{REOP} distance.**"
  - Else, output "**RT Edge Not Found.**"

Find right shoulder.
- If the section was defined as "**No stripe in this section,**" output "**No Right Shoulder.**"
- If the section was defined as "**Right Edge Stripe at X_{RS} distance,**" cut the data and only use transverse strings that contain stripe. Each transverse string where stripe was found will be analyzed.
  - R_j = location of stripe with corresponding α_j.
  - For R_{j-1}, R_{j-2}, R_{j-3}, average R values = R_{RTAvg} (this is the average of the 3 R values to the right of the right edge stripe, thus smaller α values).
  - For R_{j+4}, R_{j+5}, R_{j+6}, average R values = R_{LTAvg} (this is the average of the 3 R values to the left of the right edge stripe. By using R_{j+4}, it adds $2.6668°$ to R_j to make sure it is left of the right edge stripe).
  - If abs($R_{RTAvg} - R_{LTAvg}) \leq 10$, output "SHLD" for that transverse string of data
    - If Σ(SHLD Count) ≥ 35 percent,
      - And, "**Right Edge Stripe at X_{RS} distance**" and "**Right edge of pavement at X_{REOP} distance**" output "**Right Shoulder.**"
        - Elseif the section was defined as "**Right Edge Stripe at X_{RS} distance**" and "**RT Edge Not Found,**" output "**Unknown.**" (This accounts for those sections where stripe and shoulder are found, but the edge cannot be defined.)
    - Elseif the section was defined as "**Right Edge Stripe at X_{RS} distance**" and "**RT Edge Not Found,**" output "**No Shoulder, EOP at Edge Stripe**" (this accounts for those sections where stripe is found, but shoulder and edge are not).

- o When "**No Shoulder, EOP at Edge Stripe**" is the descriptor for the data collection section, output "**Right edge of pavement at X_{RS} distance.**"

<u>Find the left edge stripe.</u>
- Evaluate each transverse string of data within the data collection section.
- For $140° \leq \alpha \leq 165°$
  - o If $170 \leq R_j$
    - And $(R_j - R_{j-1}) \geq 15$ output α, distance, and "Stripe Found" for the transverse string being analyzed.
    - Else output "No Stripe."
  - o If "Stripe Found" frequency < 25 percent of all transverse strings, output "**No Stripe in this Section.**"
  - o If "Stripe Found" frequency $\geq$ 25 percent.
    - Find 2 most common α values (α_S, α_L).
      - If $\alpha_L - \alpha_S \leq 3°$.
        - o And Σ $\alpha_S, \alpha_L \geq 40$ percent of "Stripe Found" count, calculate the associated average α and distance. Use the average values to calculate an offset to the left edge stripe, X_{LS}.
        - o X_{LS} is calculated using the following geometry:
          - On the left side, α will always be greater than 90°.
          - If $\alpha > 90°$, $X_{LS} = \text{Distance} * \sin(\alpha - 90°)$.
        - o Output, "**Left Edge Stripe at $-X_{LS}$ distance.**"
    - Elseif, "Stripe Found" frequency $\geq$ 25 percent, but the other conditions are not met, output "**Error.**"

<u>Find left edge of pavement.</u>
- If the section was defined as "**Left Edge Stripe at $-X_{LS}$ distance,**" cut the data and only use transverse strings that contain stripe. Each transverse string where stripe was found will be analyzed.
  - o For $(\alpha_{stripe} + 2 \, \alpha \text{ increment})° \leq \alpha \leq 165°$.
    - If $R_{j+1} - R_j \geq 15$ (Jump 15 rule where larger α should have larger R value).
      - Average R_{j+2}, R_{j+3}, $R_{j+4} = R_{javg}$.
      - If $R_{javg} - R_j \geq 10$, output and store the α, distance associated with R_j and note "LT Edge Found" for the transverse string.
        - o Elseif, the jump and average check are not found, output "LT Edge Not Found" for the transverse string.
      - If Σ(LT Edge Found) < 35 percent frequency, output "**LT Edge Not Found.**"
        - o Else, find the 2 most common α values (α_S, α_L).

- - - Or $\alpha_L - \alpha_S \leq 4°$.
    - And $\Sigma(\alpha$ within $4°) \geq 25$ percent frequency.
      - Average α and distance. Use the average values to calculate an offset to the right edge of pavement, X_{LEOP}.
      - X_{LEOP} is calculated using the following geometry:
    - For the left side, α will always be greater than 90°.
    - If $\alpha > 90°$, $X_{LEOP} = Distance*sin(\alpha - 90°)$.
    - Output, "**Left edge of pavement at –X$_{LEOP}$ distance.**"
  - Else, output "**LT Edge Not Found.**"
- If the section was defined as "**No stripe in this section,**" use only transverse strings with no stripe to look for the edge of pavement.
  - For $135° \leq \alpha \leq 155°$.
    - If $R_{j+1} - R_j \geq 15$ (Jump 15 rule where larger α should have larger R value).
      - Average $R_{j+2}, R_{j+3}, R_{j+4} = R_{javg}$.
      - If $R_{javg} - R_j \geq 10$, output and store the α, distance associated with R_j and note "LT Edge Found" for the transverse string.
        - Elseif, the jump and average check are not found, output "LT Edge Not Found" for the transverse string.
      - If Σ(LT Edge Found) < 35 percent frequency, output "**LT Edge Not Found.**"
        - Else, find the 2 most common α values (α_S, α_L).
          - Or $\alpha_L - \alpha_S \leq 4°$.
          - And $\Sigma(\alpha$ within $4°) \geq 25$ percent frequency.
            - Average α and distance. Use the average values to calculate an offset to the right edge of pavement, X_{LEOP}.
            - X_{LEOP} is calculated using the following geometry:
          - For the left side, α will always be greater than 90°.
          - If $\alpha > 90°$, $X_{LEOP} = Distance*sin(\alpha - 90°)$.
          - Output, "**Left edge of pavement at –X$_{LEOP}$ distance.**"
      - Else, output "**LT Edge Not Found.**"

Find the center stripe.
- Evaluate each transverse string of data within the data collection section.
- For $90° \leq \alpha \leq 140°$.

- o If $225 \leq R_j \leq 254$ output α_{Stripe}, distance, and "Stripe Found" for the transverse string being analyzed.
  - ▪ If "Stripe Found,"
    - For $\alpha_{Stripe} + 3° \leq \alpha \leq \alpha_{Stripe} + 12°$.
      - o If $215 \leq R_j \leq 254$, output "Double Stripe,"
        - ▪ Else, output "Single Stripe."
  - ▪ Elseif R is never between 225 and 254, output "No Stripe."
- • Find the 3 most common α_{Stripe} ($\alpha_{Stripe1}$, $\alpha_{Stripe2}$, $\alpha_{Stripe3}$).
  - o If $abs(\alpha_{Stripe1} - \alpha_{Stripe2}) \leq 8°$.
  - o And $abs(\alpha_{Stripe1} - \alpha_{Stripe3}) \leq 8°$.
  - o And $abs(\alpha_{Stripe2} - \alpha_{Stripe3}) \leq 8°$.
  - o And Σ frequency($\alpha_{Stripe1}$, $\alpha_{Stripe2}$, $\alpha_{Stripe3}$) > 40 percent Σ frequency(all α_{Stripe}).
    - ▪ Average ($\alpha_{Stripe1}$, $\alpha_{Stripe2}$, $\alpha_{Stripe3}$) and ($d_{Stripe1}$, $d_{Stripe2}$, $d_{Stripe3}$).
    - ▪ Calculate a stripe offset.
      - $X_{CL} = d_{avgStripe}*sin(\alpha_{avgStripe} - 90°)$.
      - Output, "**Centerline stripe at –X_{CL} distance.**"
  - o Else, output "**Centerline stripe not found.**"

Average to fill in gaps.
- • If the offset to edge stripe or EOP is not found within a data collection section, but is found in other data collection sections.
  - o Average the offsets for those data collection sections where it is found and assign the average as the relevant offset to those data collection sections with missing offsets.

Calculate width of interest.
- • If X_{RS} and X_{CL} are defined.
  - o $W_{RTLN} = (X_{RS} - X_{CL})$.
    - ▪ Output "**Right lane W_{RTLN} wide.**"
  - o Elseif X_{CL} is defined, no right stripe (no X_{RS}), and X_{REOP} is defined (accounts for roadways with no edge stripe).
    - ▪ $W_{RTLN} = (X_{REOP} - X_{CL})$.
    - ▪ Output "**Right lane W_{RTLN} wide.**"
      - Elseif X_{CL} unknown.
        - o Output "**Right lane width unknown.**"
- • If X_{LS} and X_{CL} are defined.
  - o $W_{LTLN} = (X_{CL} - X_{LS})$.
    - ▪ Output "**Left lane W_{LTLN} wide.**"
  - o Elseif X_{CL} is defined, no left stripe (no X_{LS}), and X_{LEOP} is defined (accounts for roadways with no edge stripe).
    - ▪ $W_{LTLN} = (X_{LEOP} - X_{CL})$.

- - - - ▪ Output "**Left lane W_{LTLN} wide.**"
- - - - - Elseif X_{LS} or X_{CL} unknown.
- - - - - - ○ Output "**Left lane width unknown.**"
- - If $X_{RS} \neq X_{REOP}$ and X_{RS} and X_{REOP} are defined.
- - - ○ $W_{RTSHLD} = (X_{REOP} - X_{RS})$.
- - - ○ Elseif $X_{RS} = X_{REOP}$.
- - - - ▪ $W_{RTSHLD} = 0$.
- - - - ▪ Output "**Right shoulder width W_{RTSHLD} wide.**"
- - - ○ Elseif X_{RS} and X_{REOP} are unknown.
- - - - ▪ Output "**Right shoulder width unknown.**"
- - If $X_{LS} \neq X_{LEOP}$ and X_{LS} and X_{LEOP} are defined.
- - - ○ $W_{LTSHLD} = (X_{LS} - X_{LEOP})$.
- - - ○ Elseif $X_{LS} = X_{LEOP}$.
- - - - ▪ $W_{LTSHLD} = 0$.
- - - - ▪ Output "**Left shoulder width W_{LTSHLD} wide.**"
- - - ○ Elseif X_{LS} and X_{LEOP} are unknown.
- - - - ▪ Output "**Left shoulder width unknown.**"

Rate the lane widths.
- Note: The rating is the same for both the right and left lane widths.
- - ○ Calculate rated width, W_{LTRate} (or W_{RTRate}).
- - - ▪ $W_{LTRate} = W_{LTLN} + 0.5* W_{LTSHLD}$.
- - - ▪ $W_{RTRate} = W_{RTLN} + 0.5* W_{RTSHLD}$.
- - - - - If W_{LTRate} (or W_{RTRate}) ≥ 12.
- - - - - - ○ LNRating = 1.0.
- - - - - If $11 \leq W_{LTRate}$ (or W_{RTRate}) < 12.
- - - - - - ○ LNRating = $0.1*(W_{LTRate}$ (or W_{RTRate})) $- 0.2$.
- - - - - If $9 \leq W_{LTRate}$ (or W_{RTRate}) < 11.
- - - - - - ○ LNRating = $0.2*((W_{LTRate}$ (or W_{RTRate})) -1.3.
- - - - - If $8 < W_{LTRate}$ (or W_{RTRate}) < 9.
- - - - - - ○ LNRating = $0.5*((W_{LTRate}$ (or W_{RTRate})) $- 4$.
- - - - - If W_{LTRate} (or W_{RTRate}) ≤ 8.
- - - - - - ○ LNRating = 0.0.
- - ○ Else
- - - ▪ LNRating = Unknown.
- - ○ **Output LNRating for each lane with a data collection section.**

Paved Geometry Calculation
Geometric calculation requires a transition from raw data to gridded data on 1-ft $\times$ 1-ft grids. The gridded data are formatted with row descriptors associated with longitudinal location parallel

with the direction of travel, while the column descriptors represent horizontal offsets moving transversely across the pavement. In the transverse direction, the location of the laser represents the zero point, not the roadway centerline. The matrix is populated with elevation values corresponding to a longitudinal and transverse point.

Extract the paved surface.
- Call X_{RS}, X_{REOP}, X_{LS}, X_{LEOP}, X_{CL}.
- Chunk the data into 161 m (0.1-mi) data collection sections that match the sections associated with raw data.
- If edge striping was found.
  - Extract the paved surface from each chunk of data by selecting offset values inside X_{RS} and X_{LS}.
  - If edge striping was not found.
    - Extract the paved surface from each chunk of data by selecting offset values inside X_{REOP} and X_{LEOP}.

Find the highpoint and its offset.
- For each XS_{1x1}.
  - Find maximum elevation, E_{max}, and
  - Find offset, OS_{max}, to maximum elevation.
- Determine the frequency distribution of OS_{max}.
- Find the two most common OS_{max} (OS_{max1}, OS_{max2}) from the frequency distribution
  - If abs($OS_{max1} - OS_{max2}$) < 0.31.
    - Σ frequency(OS_{max1}, OS_{max2}, Highest OS_{maxadj}).
      - If Σ frequency(OS_{max1}, OS_{max2}, Highest OS_{maxadj}) ≥ 50 percent.
        - Average(OS_{max1}, OS_{max2}, OS_{maxadj}) = OS_{HP}.
          - Output "**Pavement highpoint offset = OS_{HP}.**"
  - Or Else abs($OS_{max1} - OS_{max2}$) < 0.61.
    - Σ frequency(OS_{max1}, OS_{max2}, $OS_{between}$).
      - If Σ frequency(OS_{max1}, OS_{max2}, $OS_{between}$) ≥ 50 percent.
  - Else output "**Pavement highpoint offset unknown.**"

Classify the section.
- If the OS_{HP} is defined above.
  - Define the offset of the middle of the paved area and its elevation.
    - OS_{mid} = nearest gridded offset value to X_{CL}.
    - E_{mid} = elevation at OS_{mid}.
  - If (min(OS_{max1}, OS_{max2}, OS_{maxadj}) − 0.31) < OS_{mid} < (max(OS_{max1}, OS_{max2}, OS_{maxadj}) + 0.31).
    - Or

- If $(\min(OS_{max1}, OS_{max2}, OS_{between}) - 0.31) < OS_{mid} < (\max(OS_{max1}, OS_{max2}, OS_{between}) + 0.31)$.
    - Output "**Tangent.**"
- Elseif $(\max(OS_{max1}, OS_{max2}, OS_{between}) + 0.31) > OS_{HP} \geq OS_{LTmax}$.
    - Or
        - Elseif $(\max(OS_{max1}, OS_{max2}, OS_{maxadj}) - 0.31) > OS_{HP} \geq OS_{LTmax}$.
            - Output "**RT Curve.**"
- Elseif $(\min(OS_{max1}, OS_{max2}, OS_{between}) - 0.31) < OS_{HP} \leq OS_{RTmax}$.
    - Or
        - Elseif $(\min(OS_{max1}, OS_{max2}, OS_{maxadj}) - 0.31) < OS_{HP} \leq OS_{RTmax}$.
            - Output "**LT Curve.**"
- If the OS_{HP} is not defined above.
    - If the preceding data collection section = "Tangent."
    - And
    - If the succeeding data collection section = "RT Curve" or "LT Curve."
    - Or
    - If the preceding data collection section = "RT Curve" or "LT Curve."
    - And
    - If the succeeding data collection section = "Tangent."
        - Output "**Curve Transition.**"
- Else.
    - Output "**Out of shape.**"

<u>Calculate the LT and RT cross-slopes.</u>
- Only use cross-sections used to classify the section within this analysis (at least 50 percent of the original 528). Includes the three most common offset values.
- If the cross-section is classified as "Out of Shape" leave blanks for the cross-slope.
- Else, extract offsets for left and right stripe.
    - Find nearest 1-ft transverse offset inside of X_{RS} and X_{LS} (or if striping is not found the nearest 1-ft transverse offset inside of X_{REOP} and X_{LEOP}).
    - Use $X_{RS1Grid}$ and $X_{LS1Grid}$ to represent the 1-ft transverse offsets.
    - And
    - Use $E_{RS1Grid}$ and $E_{LS1Grid}$ to represent the elevations corresponding with $X_{RS1Grid}$ and $X_{LS1Grid}$.
- If the section is classified as "Tangent."
    - $CS_{RT} = (E_{max} - E_{RS1Grid})/(OS_{HPEach} - X_{RS1Grid})$
    - $CS_{LT} = (E_{max} - E_{LS1Grid})/(OS_{HPEach} - X_{LS1Grid})$
    - Or
        - If the section is classified as "Right Curve," calculate the superelevation for the entire roadway.

- - - $CS_{LT} = CS_{RT} = (E_{max} - E_{RS1Grid})/(OS_{HP} - X_{RS1Grid})$.
  - ■ Or
    - • If the section is classified as "Left Curve."
      - ○ $CS_{LT} = CS_{RT} = (E_{max} - E_{LS1Grid})/(OS_{HP} - X_{LS1Grid})$.
        - ■ Output "**Right Cross-Slope = CS_{RT}.**"
        - ■ Output "**Left Cross-Slope = CS_{LT}.**"

Rate each left and right cross-slope.
- • Only transverse strings of data with a highpoint that matches its classification should be used in the rating. All transverse strings with highpoints at other locations should be discarded.
- • If the section is defined as "Tangent."
  - ○ Note: The calculation is the same for both the left and right cross-slope. Both the left and right cross-slope must have a rating.
  - ○ For a <u>wet</u> climate.
    - ■ If $0.0185 \leq CS_{RT}$ (or CS_{LT}) ≤ 0.0265.
      - • $CS_{RT}Rating = 1.0$.
      - • Elseif $0.0165 \leq CS_{RT}$ (or CS_{LT}) < 0.0185.
        - ○ $CS_{RT}Rating = 0.95$.
      - • Elseif $0.0135 \leq CS_{RT}$ (or CS_{LT}) < 0.0165.
        - ○ $CS_{RT}Rating = 0.90$.
      - • Elseif $0.0115 \leq CS_{RT}$ (or CS_{LT}) < 0.0135.
        - ○ $CS_{RT}Rating = 0.80$.
      - • Elseif $0.0085 \leq CS_{RT}$ (or CS_{LT}) < 0.0115.
        - ○ $CS_{RT}Rating = 0.70$.
      - • Elseif $0.0065 \leq CS_{RT}$ (or CS_{LT}) < 0.0085.
        - ○ $CS_{RT}Rating = 0.60$.
      - • Elseif $0.0035 \leq CS_{RT}$ (or CS_{LT}) < 0.0065.
        - ○ $CS_{RT}Rating = 0.50$.
      - • Elseif $0.0015 \leq CS_{RT}$ (or CS_{LT}) < 0.0035.
        - ○ $CS_{RT}Rating = 0.25$.
      - • Elseif CS_{RT} (or CS_{LT}) < 0.0015.
        - ○ $CS_{RT}Rating = 0$.
      - • Elseif $0.0265 < CS_{RT}$ (or CS_{LT}) ≤ 0.0285.
        - ○ $CS_{RT}Rating = 0.70$.
      - • Elseif $0.0285 < CS_{RT}$ (or CS_{LT}) ≤ 0.0335.
        - ○ $CS_{RT}Rating = 0.50$.
      - • Elseif $0.0335 < CS_{RT}$ (or CS_{LT}) ≤ 0.04.
        - ○ $CS_{RT}Rating = 0.25$.
      - • Elseif $0.04 < CS_{RT}$ (or CS_{LT}).

- o $CS_{RT}Rating = 0.0$.
- o For a <u>dry</u> climate.
    - ▪ If $0.0135 \leq CS_{RT}$ (or CS_{LT}) ≤ 0.0215.
        - • $CS_{RT}Rating = 1.0$.
        - • Elseif $0.0115 \leq CS_{RT}$ (or CS_{LT}) < 0.0135.
            - o $CS_{RT}Rating = 0.90$.
        - • Elseif $0.0085 \leq CS_{RT}$ (or CS_{LT}) < 0.0115.
            - o $CS_{RT}Rating = 0.80$.
        - • Elseif $0.0065 \leq CS_{RT}$ (or CS_{LT}) < 0.0085.
            - o $CS_{RT}Rating = 0.70$.
        - • Elseif $0.0035 \leq CS_{RT}$ (or CS_{LT}) < 0.0065.
            - o $CS_{RT}Rating = 0.60$.
        - • Elseif $0.0015 \leq CS_{RT}$ (or CS_{LT}) < 0.0035.
            - o $CS_{RT}Rating = 0.25$.
        - • Elseif CS_{RT} (or CS_{LT}) < 0.0015.
            - o $CS_{RT}Rating = 0$.
        - • Elseif $0.0215 < CS_{RT}$ (or CS_{LT}) ≤ 0.0235.
            - o $CS_{RT}Rating = 0.95$.
        - • Elseif $0.0235 < CS_{RT}$ (or CS_{LT}) ≤ 0.0265.
            - o $CS_{RT}Rating = 0.90$.
        - • Elseif $0.0265 < CS_{RT}$ (or CS_{LT}) ≤ 0.0285.
            - o $CS_{RT}Rating = 0.70$.
        - • Elseif $0.0285 < CS_{RT}$ (or CS_{LT}) ≤ 0.0335.
            - o $CS_{RT}Rating = 0.50$.
        - • Elseif $0.0335 < CS_{RT}$ (or CS_{LT}) ≤ 0.04.
            - o $CS_{RT}Rating = 0.25$.
        - • Elseif $0.04 < CS_{RT}$ (or CS_{LT}).
            - o $CS_{RT}Rating = 0.0$.
- • When a section is reached that is classified as "RT Curve," "LT Curve," or "Curve Transition."
    - o Identify the first LOC (LOC_{PC}) value where the highpoint is located within an area to define a curve or the preceding section.
    - o Evaluate the classification of the following sections to find the last adjacent section that is not classified as either "RT Curve," "LT Curve," or "Curve Transition." The end of the curve will fall in this section.
    - o Using the final data collection section where the end of the curve is located, identify the last LOC (LOC_{PT}) value where the highpoint is located within an area to define a curve.
    - o Access the IMU Table.

- Acquire the northing, easting, and azimuth for the beginning LOC (LOC$_{PC}$) value and ending LOC (LOC$_{PT}$) value identified above.
    - Calculate LC using the northing and easting values.
        - LC = sqrt((E$_{PT}$ – E$_{PC}$)^2 + (N$_{PT}$ – N$_{PC}$)^2).
    - Calculate the intersecting angel, I.
        - If "LT Curve," I = Az$_1$ – Az$_2$.
        - If "RT Curve," I = Az$_2$ – Az$_1$.
    - Calculate the radius, R.
        - R = (LC/(2*sin(I/2)))/0.3048.
- All sections described as "Curve Transition" will receive a cross-slope rating the same as the curve.
- If a section is described as "RT Curve" or "LT Curve," the posted speed must be known for rating purposes.

Average the cross-slopes.
- For "Tangent" sections, only use the transverse strings that met the highpoint requirement for a tangent section within the data collection section.
    - For CS$_{RT}$ that exist within a data collection section.
        - Σ CS$_{RT}$/(No. of CS$_{RT}$).
            - **Output average CS$_{RT}$ value for data collection section.**
    - For CS$_{LT}$ that exist within a data collection section.
        - Σ CS$_{LT}$/(No. of CS$_{LT}$).
            - **Output average CS$_{LT}$ value for data collection section.**
- For "Curve Transition" and "Out of Shape" sections, calculate the average cross-slope for each lane use each transverse string of data.
    - In the right lane, the calculation for each string of data is:
        - CS$_{RT}$ = (E$_{Rcenter}$ – E$_{RS1Grid}$)/(X$_{Rcenter}$ – X$_{RS1Grid}$).
            - Where the Rcenter subscript represents the elevation and offset one transverse string to the right of the center of the pavement.
                - **Output average CS$_{RT}$ value for data collection section.**
    - In the left lane, the calculation for each string of data is:
        - CS$_{LT}$ = (E$_{Lcenter}$ – E$_{LS1Grid}$)/(X$_{Lcenter}$ – X$_{LS1Grid}$).
            - Where the Lcenter subscript represents the elevation and offset one transverse string to the left of the center of the pavement.
                - **Output average CS$_{LT}$ value for data collection section.**

Consolidate the cross-slope ratings—this rates each string before averaging.
- For CS$_{RT}$ that exist within a data collection section.
- ΣRating/(No. of CS$_{RT}$).
- For CS$_{LT}$ that exist within a data collection section.

- ΣRating/(No. of CS_{LT}).
    - **Output the "CS_{RT}Rating" and "CS_{LT}Rating" for each data collection section.**

Rate the difference between cross-slopes.
- This rating can be applied to all sections, regardless of classification. No changes need to be made for specific classifications.
- If $0 \leq abs(CS_{RT} - CS_{LT}) \leq 0.04$.
    - $\Delta Rating = 1.0$.
- If $0.08 < abs(CS_{RT} - CS_{LT})$.
    - $\Delta Rating = 0.0$.
- If $0.04 < abs(CS_{RT} - CS_{LT}) \leq 0.08$.
    - $\Delta Rating = -(1/4)*abs(CS_{RT} - CS_{LT})+2$.
        - **Output the ΔRating for each data collection section.**

Hydroplaning Potential Calculation
Hydroplaning potential is calculated using the 1-ft × 1-ft grids, but the first grid point beyond the EOP must be the limiting transverse point rather than the first grid point inside of the EOP. TopoToolbox is required to perform these calculations.

Extract the surface.
- Call X_{RS}, X_{REOP}, X_{LS}, X_{LEOP}, X_{CL}.
- Chunk the data into 161 m (0.1-mi) data collection sections that match the sections associated with raw data.
- Extract the surface from each chunk of data by selecting the first offset values outside X_{REOP} and X_{LEOP}.
- For TopoToolbox to move in the proper direction, the data must be sorted from the largest (last) Loc value to the smallest (first) Loc value.
    - Within the extracted data, count the number of columns and the number of rows that contain elevation data.
    - Place the gridded data into a text file with 6 rows of header data:
        - ncols # (number of columns with elevation data).
        - nrows # (number of rows with elevation data).
        - xllcorner # (left most offset value in the gridded data).
        - yllcorner # (smallest (first) Loc value). With the data sorted, this should be the bottom Loc value in the spreadsheet.
        - Cell_size 0.3048 (or the proper cell size).
        - NODATA_Value 0.0000.

Extract the largest drainage basin within each data collection section (using TopoToolbox).
- Extract maximum flow accumulation from the data collection section FL_{max}.

- o Store the x, y, z coordinates for FL_{max}.
- Extract drainage basins between X_{RS} and X_{LS}.
- Find the Euclidean distance from the low point used in the analysis to each cell within the drainage basin.
- Find the slope to each cell within the drainage basin.
- Calculate the drainage basin area in English units.
- Calculate the average width of the drainage basin in English units.
  - o The average is calculated based on each width at each cross-section.
- Based on the TxDOT District, assign a rainfall intensity value, I (in./hr).
  - o The TxDOT District will either by Atlanta, Bryan, Corpus Christi, Houston, or Tyler depending on the user input.
    - ▪ I values for each of these districts can be called from the *HPS variables* spreadsheet under the *I values for hydro calcs* tab.
      - The I value should be taken from the 50 year – 15 minute Intensity (in/hr) column. This should be Column E.
- Based on user input of the surface type, calculate discharge, Q_{DB} (ft^3/s).
  - o Calculate discharge, Q_{DB} (ft^3/s).
    - ▪ If surface type is CONC, HMA, ST, FST, OR ASPH.
      - $Q_{DB} = I* A_{DB}$.
  - o Calculate unit discharge, q_{DB} (ft^3/s-ft).
    - ▪ $q_{DB} = Q_{DB}/ W_{DB}$.
- Determine what Manning's *n* should be used and label it n_{man}.
  - o n_{man} should be the smaller value between an n value from the table and a calculated n value.
  - o Calculate Reynold's number: $Re = q_{DB}/(1.052*10^{-5})$.
    - ▪ If surface type = HMA, ST, FST, OR ASPH.
      - $n_{calc} = 0.0823*Re^{-0.174}$.
    - ▪ If surface type = CONC.
      - If Re ≥ 1000.
        - o $n_{calc} = 0.017$.
      - If 500 ≤ Re < 1000.
        - o $n_{calc} = 0.319/Re^{0.480}$.
      - If Re < 500.
        - o $n_{calc} = 0.345/Re^{0.502}$.
  - o n_{table} is a Manning's *n* value taken from the *HPS variables* workbook located in the *Texture and n values* worksheet and in the TxDOT Manning's *n* column (Column D).
  - o $n_{man} = min(n_{calc}, n_{table})$.
- Calculate the total depth of water.
  - o depth = $((q_{DB}/((1.49/n_{man})*DB_{slope}^{(1/2)}))^{(3/5)})*12$.

- ▪ Multiplying by 12 at the end is required to move the depth into inches.
        - ▪ Note: DB_{slope} must be a percentage, that is 3 percent must be 0.03 in the calculations.
- Check that the time of concentration does not exceed 15 minutes.
    - ○ toc = $DB_{Length}/(3600*(1.49/n_{man})*depth^{(2/3)}*DB_{slope}^{(1/2)})$.
        - ▪ For DB_{Length}, use the maximum Euclidean distance.
        - ▪ For DB_{slope}, use the slope associated with the maximum Euclidean distance.
    - ○ If toc > 15, stop and output "ERROR."
    - ○ Else continue with calculations.
- In order to calculate the WFT, the MTD must be called from the *HPS variables* workbook under the *Texture and n values* worksheet from the MTD (in) column (Column C).
    - ○ WFT = depth – MTD.
- Calculate an HPS using a Monte Carlo simulation using the daily traffic count as the number of simulations.
    - ○ Two HPS will be calculated, the Galloway speed (GHPS) and the finite element speed (FEMHPS).
    - ○ Monte Carlo code has been provided as *HydroMonteCarlo_update.m.*
- Rate the section for both GHPS and FEMHPS (both referred to generically as HPS in the rating calculations.
    - ○ If HPS ≥ (Posted Speed – 5).
        - ▪ Rate section as 1.0.
    - ○ If (Posted Speed – 5) > HPS ≥ (Posted Speed − 10).
        - ▪ Rate Section as 0.9.
    - ○ If (Posted Speed −10) > HPS ≥ (Posted Speed – 15)
        - ▪ Rate section as 0.8.
    - ○ If (Posted speed −15) > HPS ≥ (Posted Speed −20).
        - ▪ Rate section as 0.7.
    - ○ If (Posted speed −20) > HPS ≥ (Posted Speed – 25).
        - ▪ Rate section as 0.5.
    - ○ If (Posted speed – 25) > HPS ≥ (Posted Speed – 30).
        - ▪ Rate section as 0.25.
    - ○ If (Posted Speed – 30) > HPS.
        - ▪ Rate section as 0.0.

Roadside Geometry Calculation
Roadside geometric evaluation requires a transition from raw data to 3-ft × 3-ft gridded data. The gridded data are formatted with row descriptors associated with longitudinal location parallel with the direction of travel, while the column descriptors represent horizontal offsets moving transversely across the pavement. In the transverse direction, the location of the laser represents

the zero point, not the roadway centerline. The matrix is populated with elevation values corresponding to a longitudinal and transverse point.

Extract the surface.
- Call X_{REOP} and X_{LEOP}.
- Chunk the data into 161 m (0.5-mi) data collection sections that match the sections associated with raw data.
- 176 cross-sections will initially be created.
- Extract the left and right roadside surfaces from each chunk of data by selecting the first offset values ~~outside~~ inside X_{REOP} and X_{LEOP} for each data collection section.
- The left and right roadside surfaces will be evaluated independently.

Find the minimum roadside elevation.
- Note: These extractions and evaluations are the same for both right and left roadsides. For clarity, when possible only right roadside pseudocode is shown.
- For the right roadside at each cross-section (i.e., transverse string on 3-ft spacing).
  - Find E_{min} and corresponding OS_{min}.
    - If $(OS_{RTmax} - 1.83) < OS_{min} \leq OS_{RTmax}$.
      - Label cross-section as "FS."
      - Elseif $(OS_{RTFirst} + 1.83) < OS_{min} \leq (OS_{RTmax} - 1.83)$.
        - Label cross-section as "Ditch."
        - Else.
          - Label cross-section as "Edge Drain"
- For the left roadside at each cross-section (i.e., transverse string on 3-ft spacing).
  - Find E_{min} and corresponding OS_{min}.
    - If $(OS_{LTmax} + 1.83) > OS_{min} \geq OS_{LTmax}$ (b/c left roadside has negative offsets).
      - Label cross-section as "FS."
      - Elseif $(OS_{LTFirst} - \times 1.83) > OS_{min} \geq (OS_{LTmax} + 1.83)$.
        - Label cross-section as "Ditch."
        - Else.
          - Label cross-section as "Edge Drain."

Classify the section.
- Check the offset frequency.
  - If Σfrequency(FS) > 50 percent.
    - Output "**Primarily FS**" for data collection section.
    - Elseif Σfrequency(Ditch) > 50 percent.
      - Output "**Primarily Ditch**" for data collection section.
      - Elseif Σfrequency(Edge Drain) > 50 percent.
        - Output "Primarily Edge Drain" for data collection section.

- o Else.
  - ▪ "Various Drainage" for data collection section (this accounts for section where no geometric type reaches 50 percent frequency.

Calculate front slope steepness, rate each cross-section, and consolidate ratings.

- Calculate the front slope for each cross-section (each string of data) labeled either "FS" or "Ditch" and average the front slope steepness for the entire data collection section.
  - o For the right roadside at each cross-section.
    - ▪ $FS_{RT} = (OS_{min} - OS_{First})/(E_{first} - E_{min})$.
      - $FS_{RTAvg} = \Sigma FS_{RT}/No.$ of cross-sections.
  - o For the left roadside at each cross-section.
    - ▪ $FS_{LT} = (OS_{First} - OS_{min})/(E_{first} - E_{min})$.
      - $FS_{LTAvg} = \Sigma FS_{LT}/No.$ of cross-sections.
  - o **Output the "FS_{RTAvg}" and "FS_{LTAvg}" for each data collection section.**
- Rate each cross-section (each string) and then average each rating within the data collection section to provide a rating for the data collection section (same for both roadsides).
  - o If $FS_{RT} \geq 6.0$.
    - ▪ $FS_{RT}Rating = 1.0$.
  - o Elseif $4.0 \leq FS_{RT} < 6.0$.
    - ▪ $FS_{RT}Rating = 0.05* FS_{RT} +0.7$.
  - o Elseif $3.0 \leq FS_{RT} < 4.0$.
    - ▪ $FS_{RT}Rating = 0.2* FS_{RT} + 0.1$.
  - o Elseif $2.0 \leq FS_{RT} < 3.0$.
    - ▪ $FS_{RT}Rating = 0.7* FS_{RT} - 1.4$.
  - o Elseif $FS_{RT} < 2.0$.
    - ▪ $FS_{RT}Rating = 0.0$.
      - $\Sigma FS_{RT}Rating/No.$ of cross-sections.
        - o Output the "$FS_{RT}Rating$" and "$FS_{LT}Rating$" for each data collection section.

Calculate ditch depth and ditch offset.
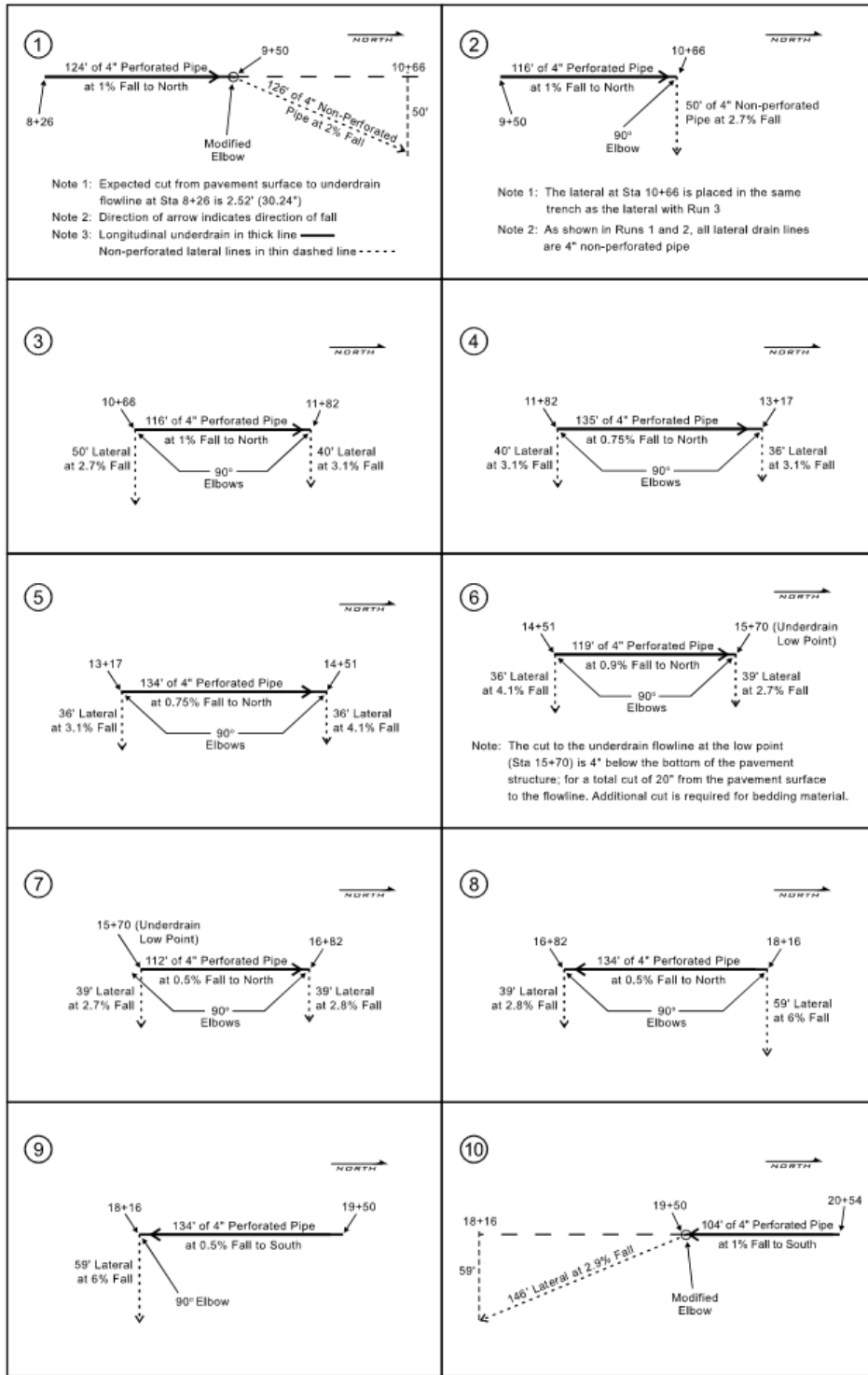Roadside analysis begins at one offset value inside of the EOP.

- For each cross-section (each string of data) labeled "Ditch":
  - o $Depth_{RT (or LT)} = (E_{First} - E_{min})$.
  - o $DOS_{RT} = (OS_{min} - OS_{First})$ or $DOS_{LT} = (OS_{First} - OS_{min})$.
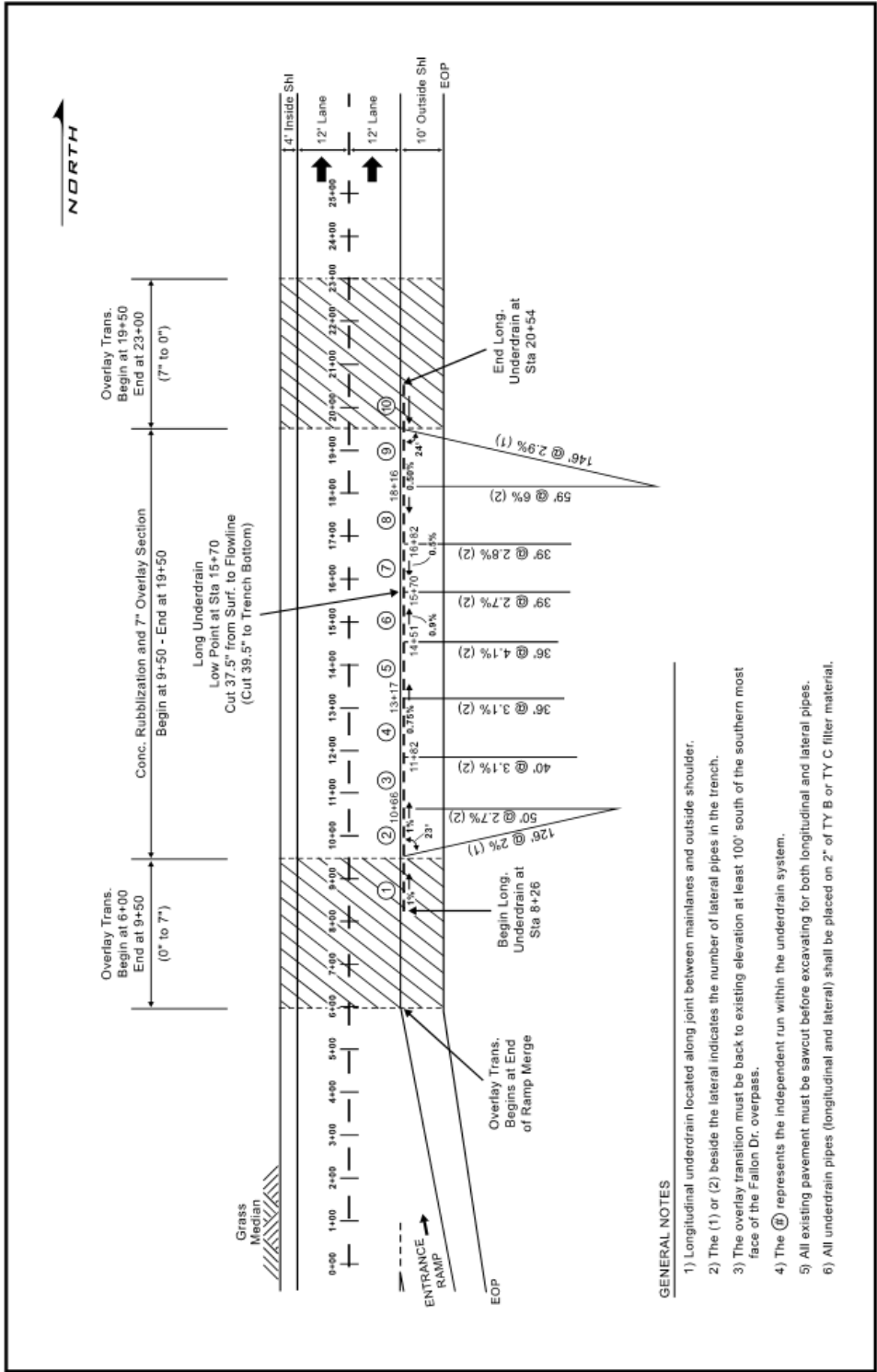 - o This will take place for both the left and right roadside.

- Average the depth and offset within each data collection section (this should take place regardless of whether or not the data collection section is labeled as "Primarily Ditch"). This takes place for both the right and left roadside.
    - $Depth_{RTAvg} = \Sigma Depth_{RT}/No.$ of cross-sections (same for left side).
    - $DOS_{RTAVG} = \Sigma DOS_{RT}/No.$ of cross-sections (same for left side).

Calculate the slope for the largest roadside drainage basin.
- Use TopoToolbox to find the drainage basins on the right and left roadside.
    - Identify the drainage basin with the largest accumulation.
        - Find the beginning point and ending point associated with this drainage basin.
            - Determine the length of the drainage basin and the associated elevation fall within the drainage basin.
                - Calculate the slope of the drainage basin.

# US 75—PARIS DISTRICT PROJECT LEVEL ANALYSIS PLAN SHEETS

NORTH

Grass Median

ENTRANCE RAMP

EOP

Overlay Trans. Begin at 6+00 End at 9+50 (0" to 7')

Conc. Rubblization and 7" Overlay Section
Begin at 9+50 - End at 19+50

Overlay Trans. Begin at 19+50 End at 23+00 (7" to 0")

Long Underdrain
Low Point at Sta 15+70
Cut 37.5" from Surf. to Flowline
(Cut 39.5" to Trench Bottom)

4' Inside Shl
12' Lane
12' Lane
10' Outside Shl
EOP

End Long. Underdrain at Sta 20+54

Begin Long. Underdrain at Sta 8+26

Overlay Trans. Begins at End of Ramp Merge

146' @ 2.9% (1)
59' @ 6% (2)
39' @ 2.8% (2)
39' @ 2.7% (2)
36' @ 4.1% (2)
36' @ 3.1% (2)
40' @ 3.1% (2)
50' @ 2.7% (2)
126' @ 2% (1)

GENERAL NOTES

1) Longitudinal underdrain located along joint between mainlanes and outside shoulder.

2) The (1) or (2) beside the lateral indicates the number of lateral pipes in the trench.

3) The overlay transition must be back to existing elevation at least 100' south of the southern most face of the Fallon Dr. overpass.

4) The (#) represents the independent run within the underdrain system.

5) All existing pavement must be sawcut before excavating for both longitudinal and lateral pipes.

6) All underdrain pipes (longitudinal and lateral) shall be placed on 2" of TY B or TY C filter material.

197

EDGE OF LANE

FLOW*

4" PIPE UNDERDRAIN

PVC SCHEDULE 40 CONDUIT 90° SWEEP OR EQUAL (TYPICAL)

4" PVC PIPE LATERALS (NON-PERFORATED)

*See Layout for Direction and Slope for Flow

FLOW

4" PIPE UNDERDRAIN

OUTLET
OUTLET
8"

FLOW

4" PIPE UNDERDRAIN

GLUED CONNECTION (TYPICAL)

See Layout for Spacing

FLOW

4" PIPE UNDERDRAIN

CLEAN OUT

OUTLET
8"

PVC SCHEDULE 40 CONDUIT 90° SWEEP OR EQUAL (TYPICAL)

4" PVC PIPE LATERALS (NON-PERFORATED)

A
A

PLAN DETAIL OF PIPE UNDERDRAIN LATERALS

Outlet Detail (typ)
(Removable Rodent Screen Not Shown)

VARIES

PERFORATED PIPE (4")
(SLOPE VARIES)

3" TY D HMA

9" CRUSHED CONC.

TYPE B OR C FILTER MATERIAL (DEPTH VARIES)

SECTION A-A

ROW

LANE SKIP

VARIES

12' LANE   10' SHLDR

VARIES

3'

NON-PERFORATED PIPE (4")
VAR. SLOPE

RIPRAP (CONC.) (CL B) (4")
See Note 5

ELEVATION

1" MIN. FOR SINGLE LATERAL
1.33' MIN. FOR DOUBLE LATERAL

3" TY D HMA

EXISTING MATERIAL (NOTE 6)

NON-PERFORATED PIPE (4")

2" DEPTH
TY B OR C FILTER MATERIAL

SECTION B-B

PIPE UNDERDRAIN DETAIL

PVC PIPE (4")
VAR. SLOPE

SAW CUT PAVEMENT

VARIES

12' LANE   10' SHLDR

PERFORATED PIPE (4")
VAR. SLOPE

SAW CUT PAVEMENT AT JOINT

PERFORATED PIPE (4")
VAR. SLOPE

PARTIAL PLAN VIEW

GENERAL NOTE:

1. Saw cut existing pavement
2. Remove material and place pipe underdrain. No edge condition shall be left overnight. Trench will be filled to existing surface per section A-A and B-B by the end of each day.
3. All materials and procedures according to TxDOT Specification Item 556 unless otherwise noted.
4) All underdrain pipes (longitudinal and lateral) shall be placed on 2" of TY B or TY C filter material.
5) Place 3' X 2' x4" CLB concrete riprap and OM-2Z. Match existing front slope.
6) Lateral pipe trenches may be backfilled with existing excavated materials.
7) TY B or C backfill may be substituted with an approved alternate material.

US 77—AUSTIN DISTRICT PROJECT LEVEL RUTTING DETAILS

Rutting Sections

Rutting color scale for Sections 1 thru 11.
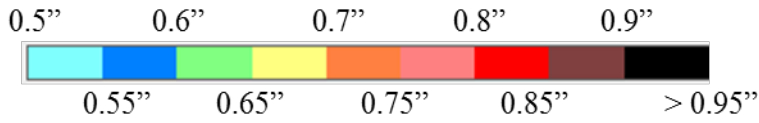
Section 1: TRM 476+1.831 to 478+0.331 (pavement change to + ½-mile)
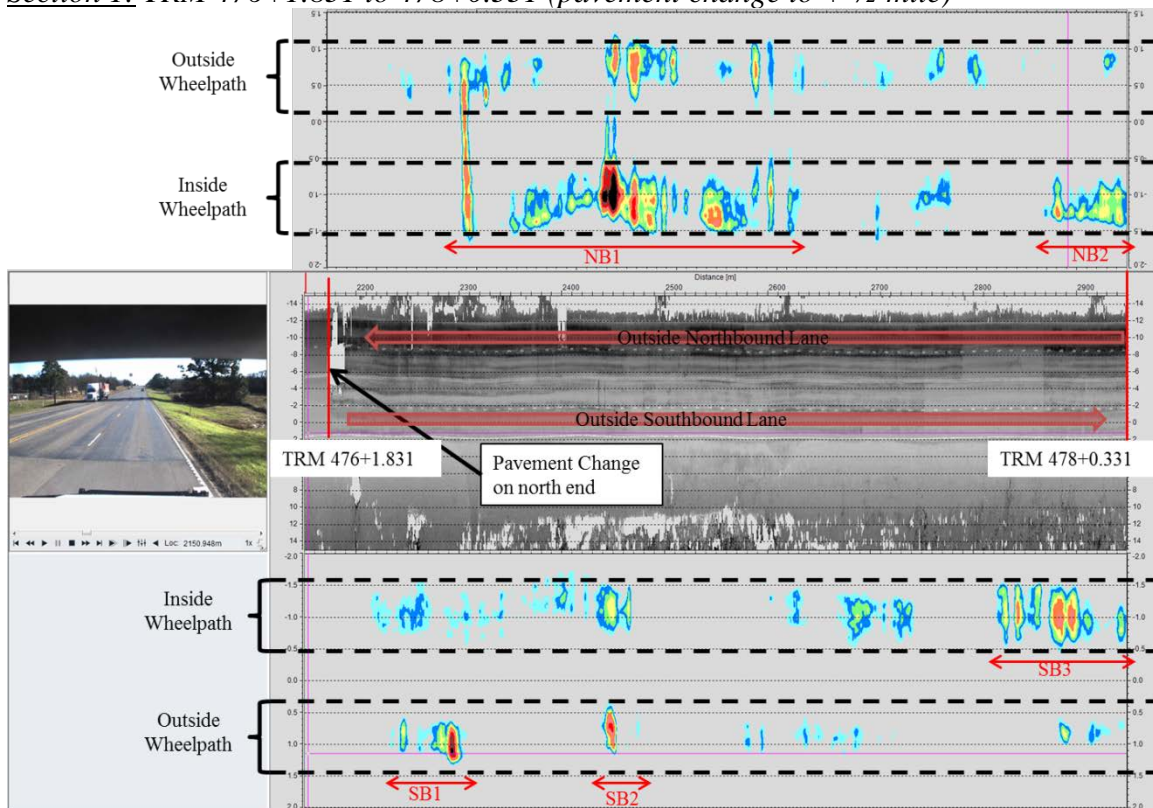
Section 2: *TRM 478+0.331 to 478+0.831*
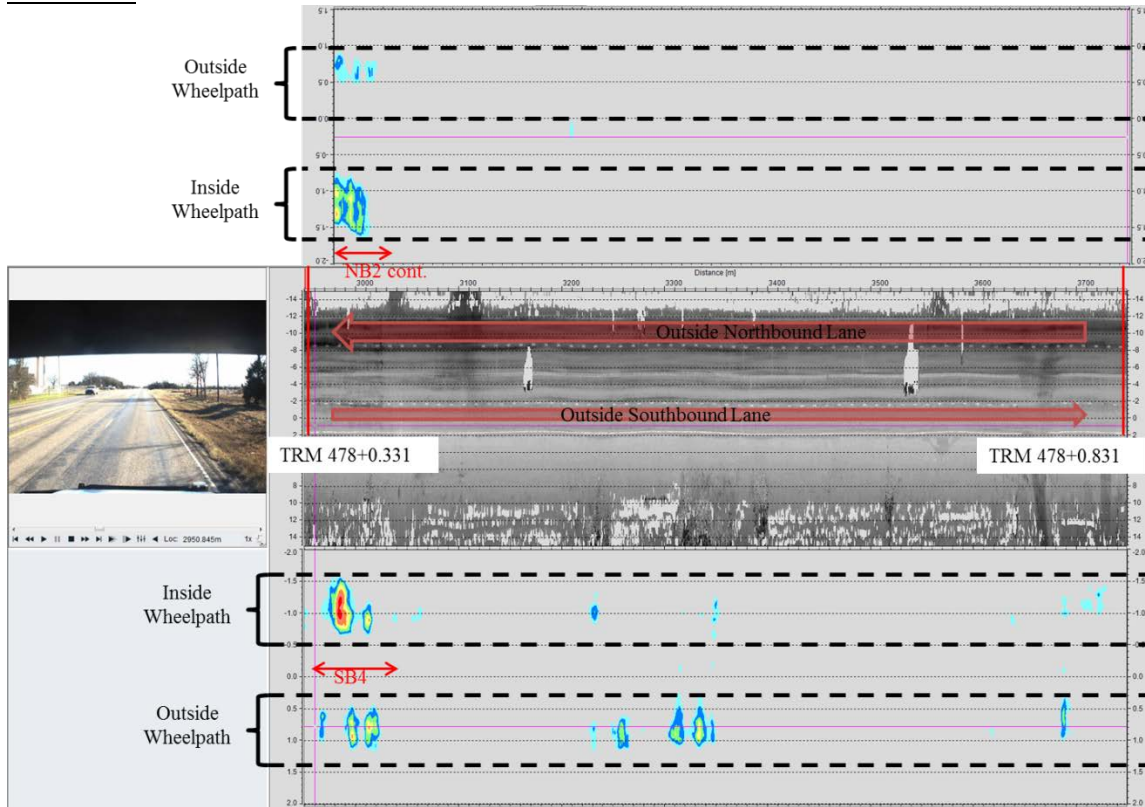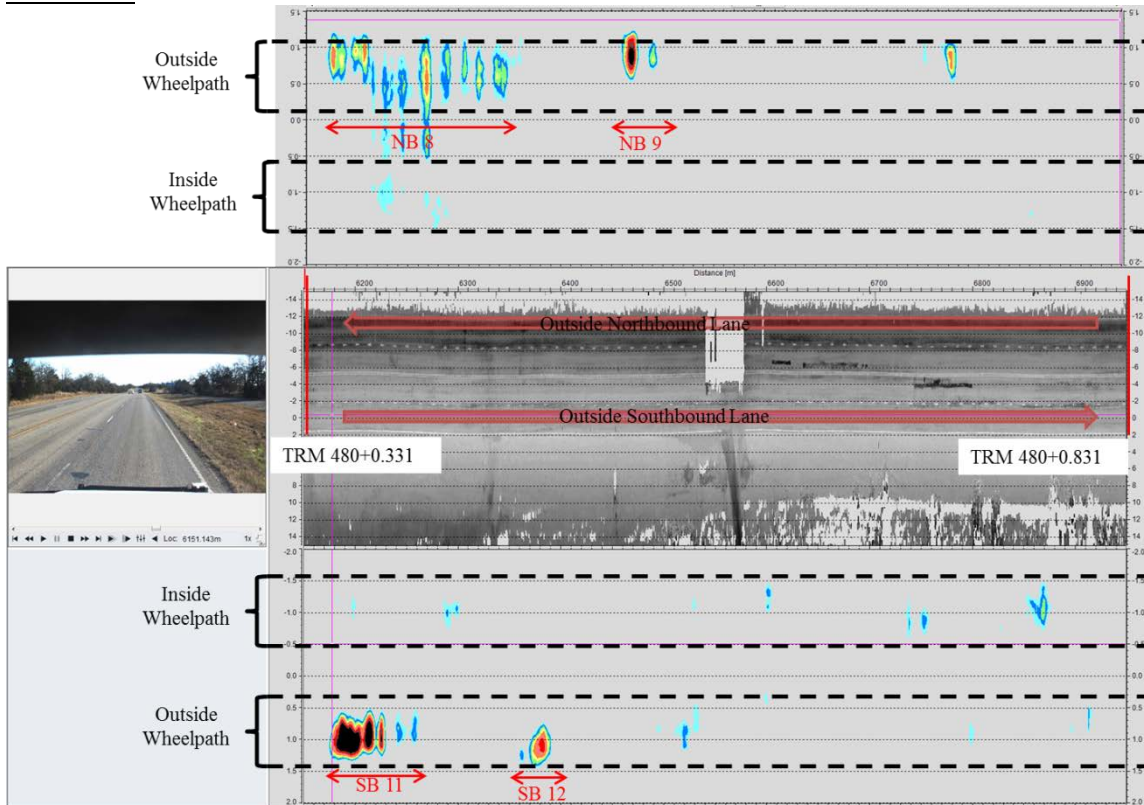

Section 3: *TRM 478+0.831 to 478+1.331*
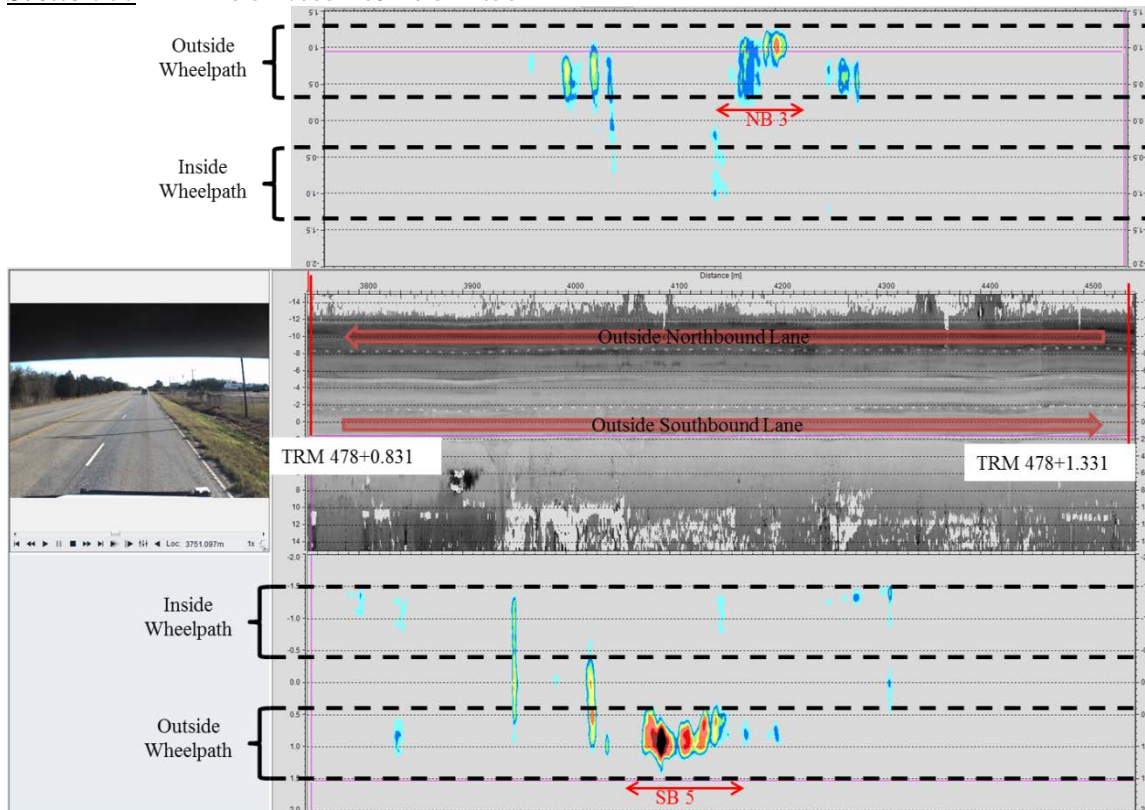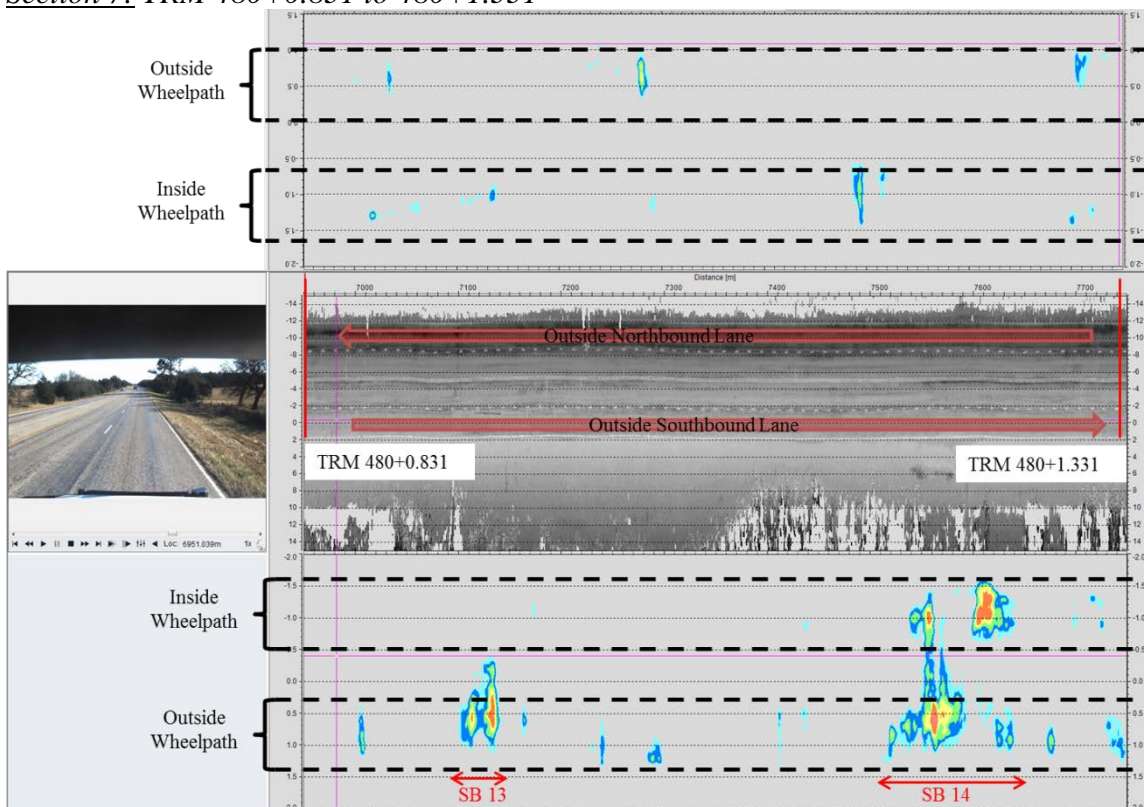
Section 4: TRM 478+1.331 to 478+1.831

201
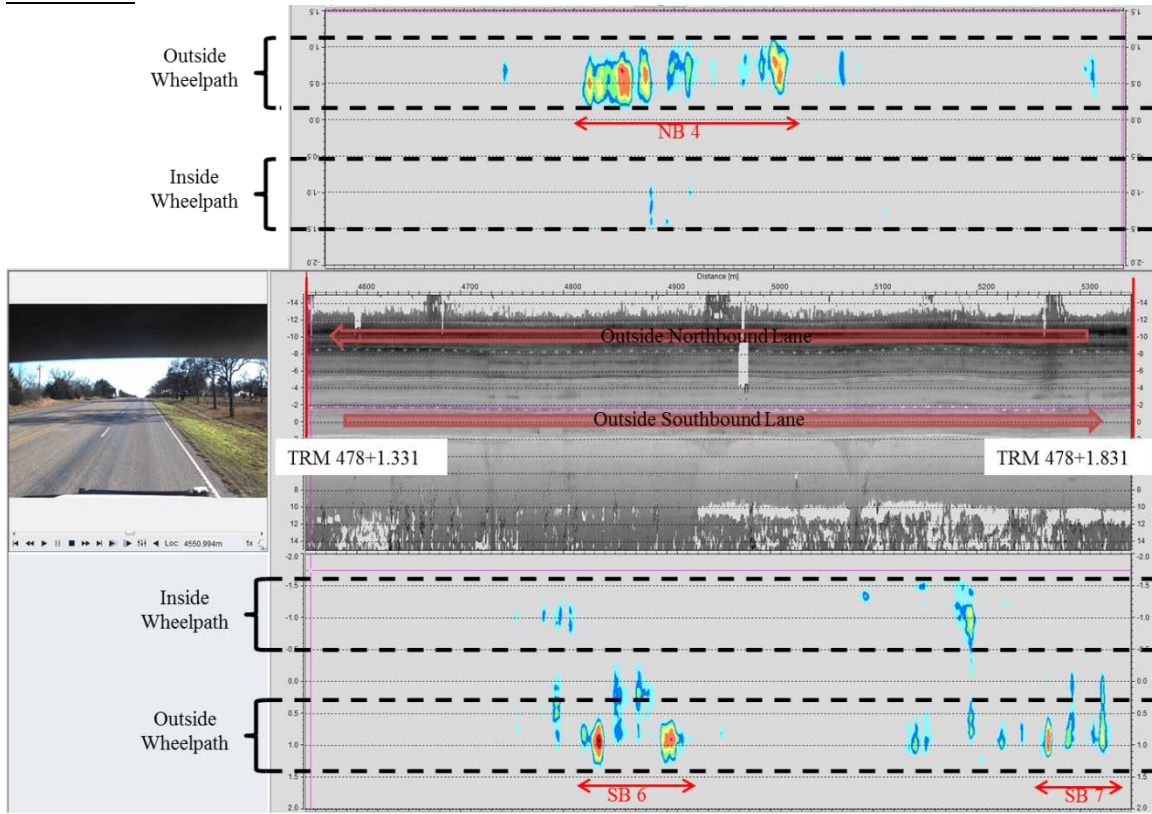
Section 5: TRM 478+1.831 to 480+0.331
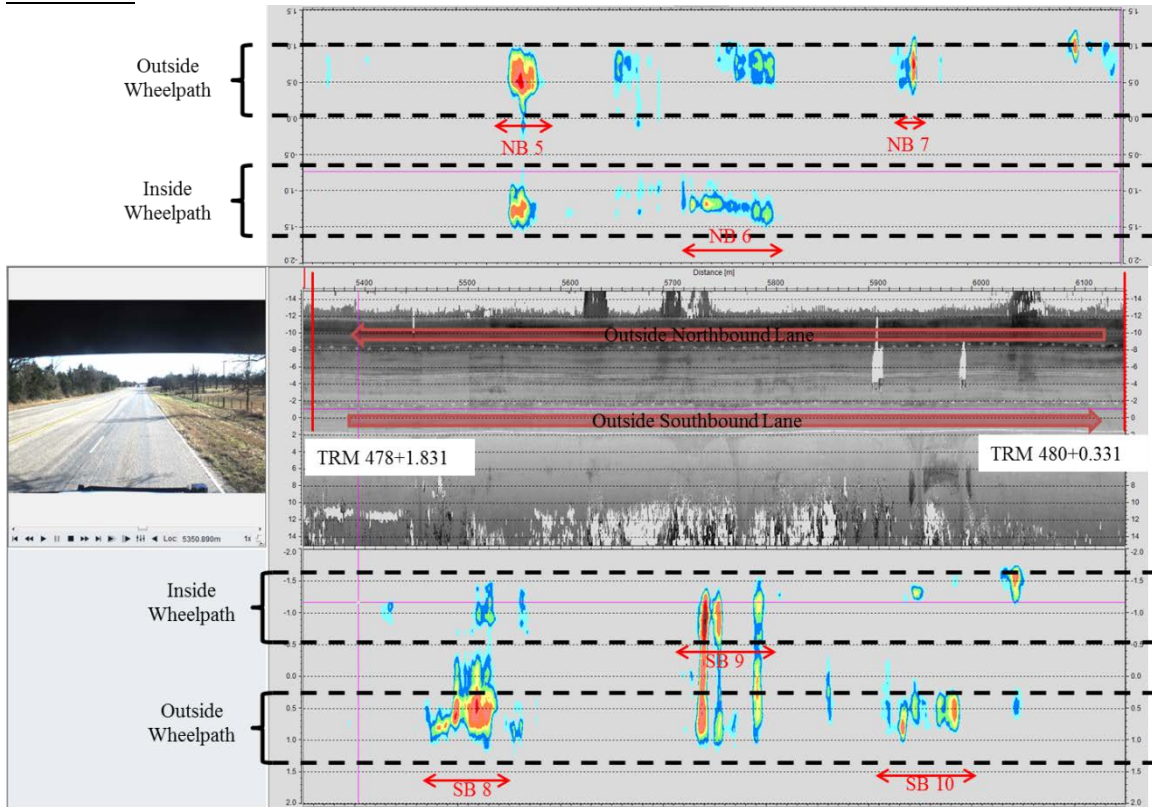
Section 6: TRM 480+0.331 to 480+0.831

Section 7: TRM 480+0.831 to 480+1.331

203

Section 8: TRM 480+1.331 to 480+1.831
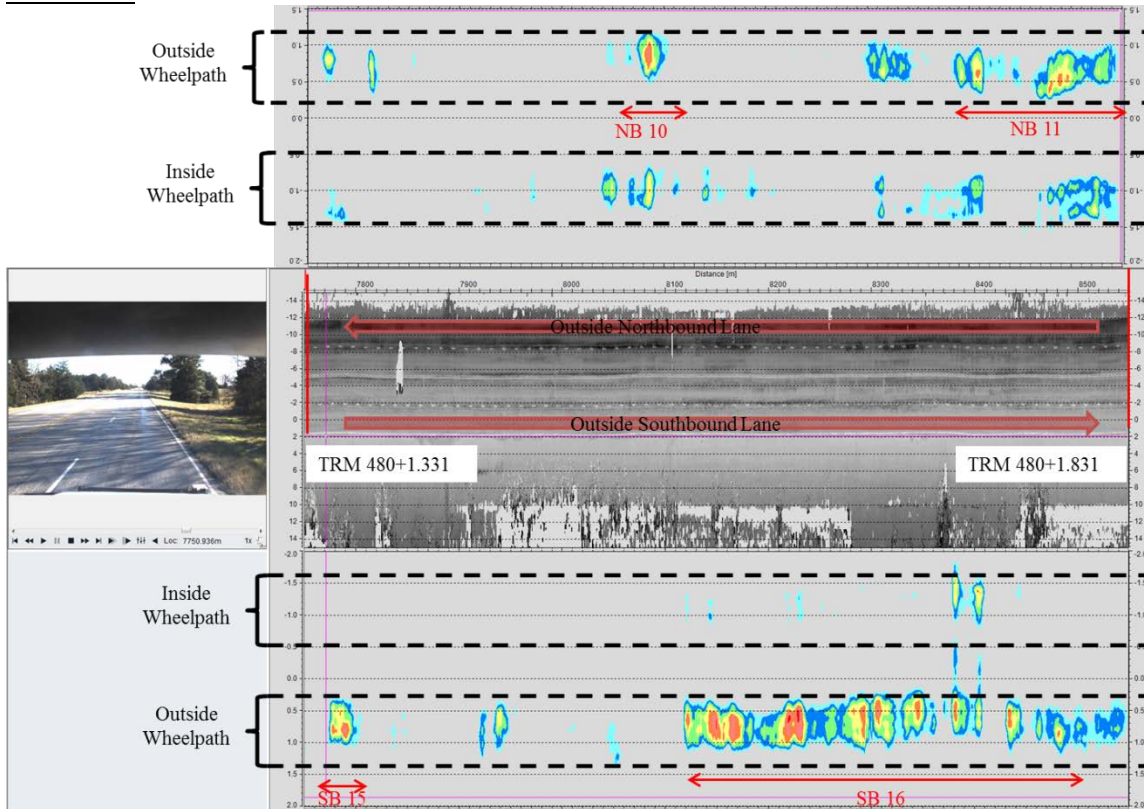
Section 9: TRM 480+1.831 to 482+0.331

204
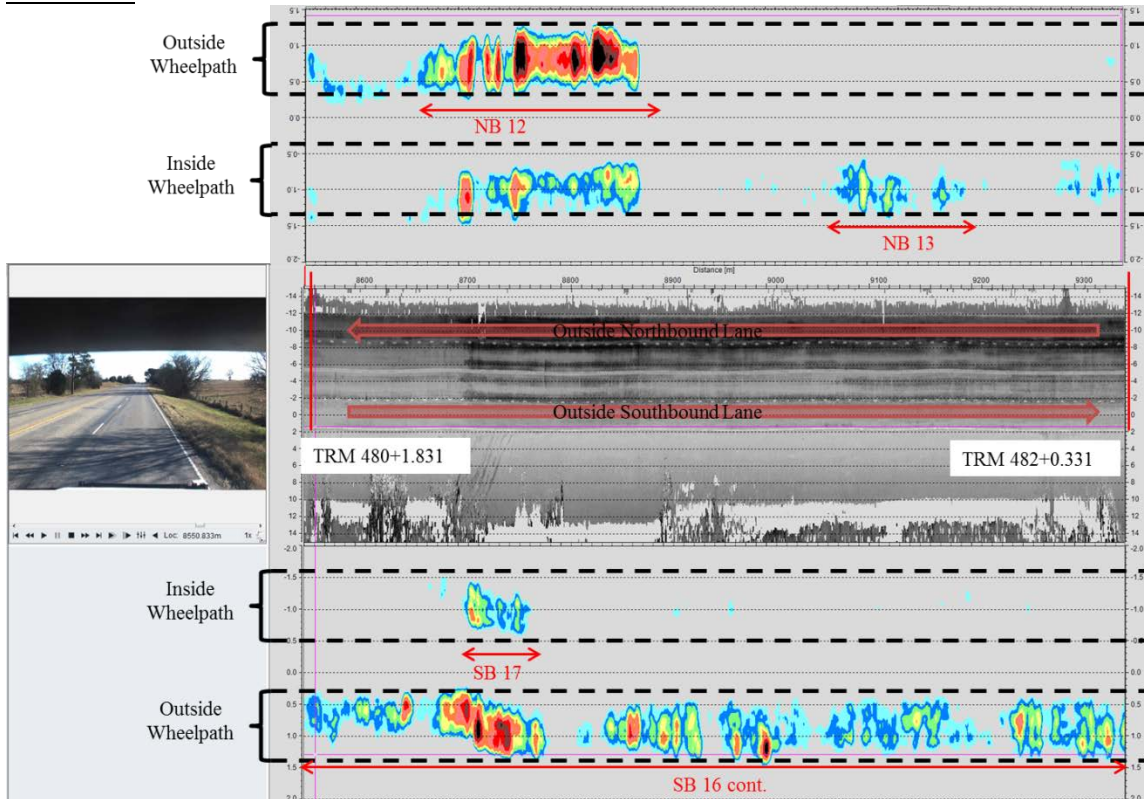
Section 10: TRM 482+0.331 to 482+0.831
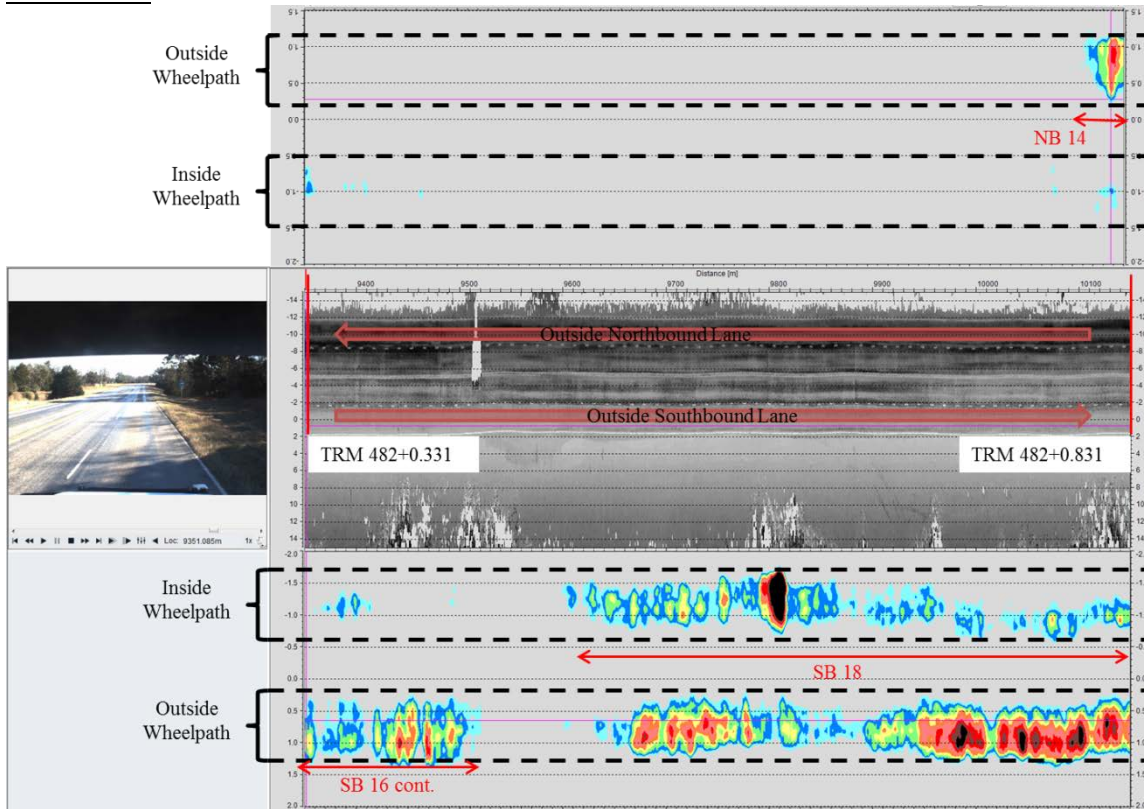
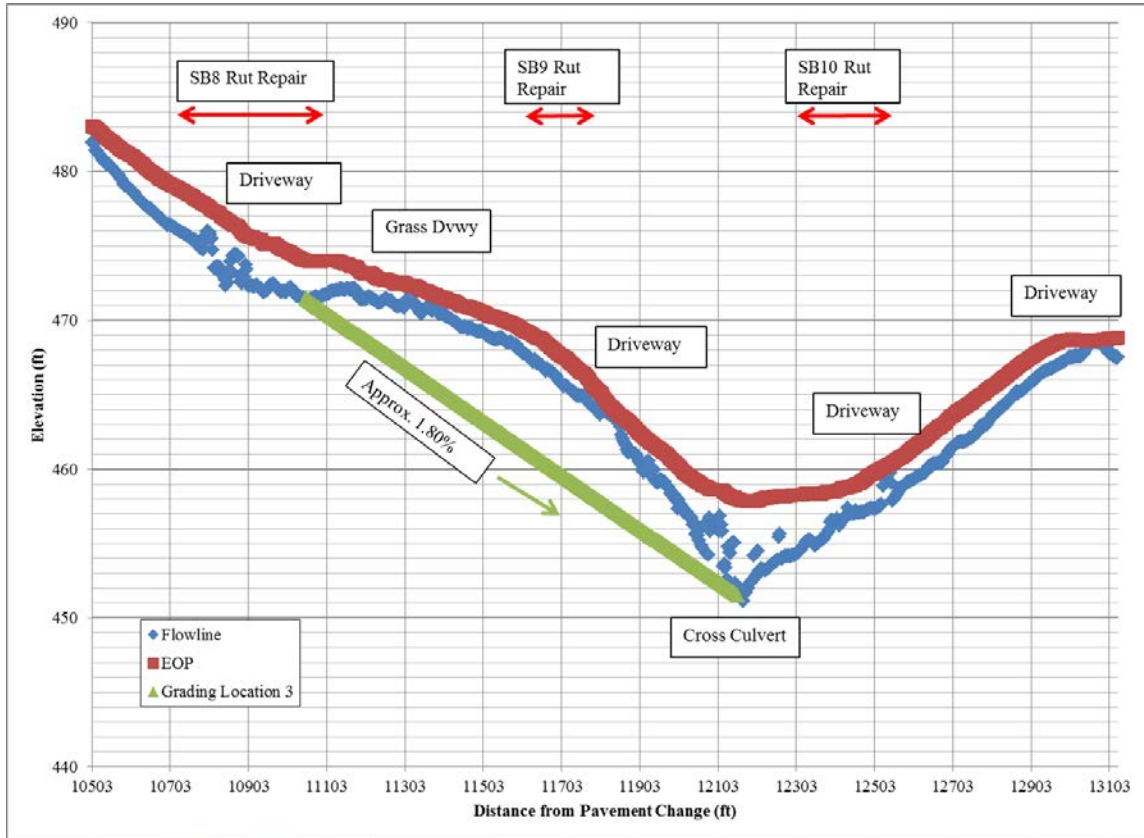## Section 11: TRM 482+0.331 to 482+0.831
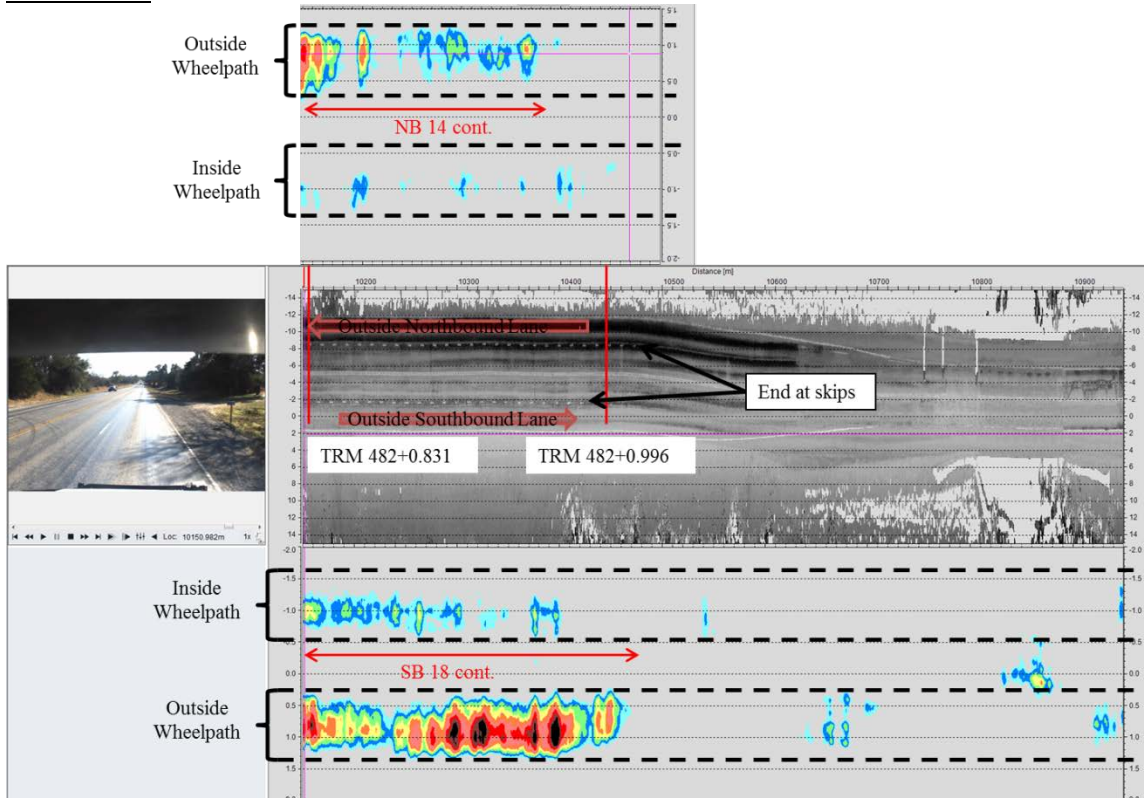
US 77—AUSTIN DISTRICT PROJECT LEVEL GRADING DETAILS

Southbound Section 2
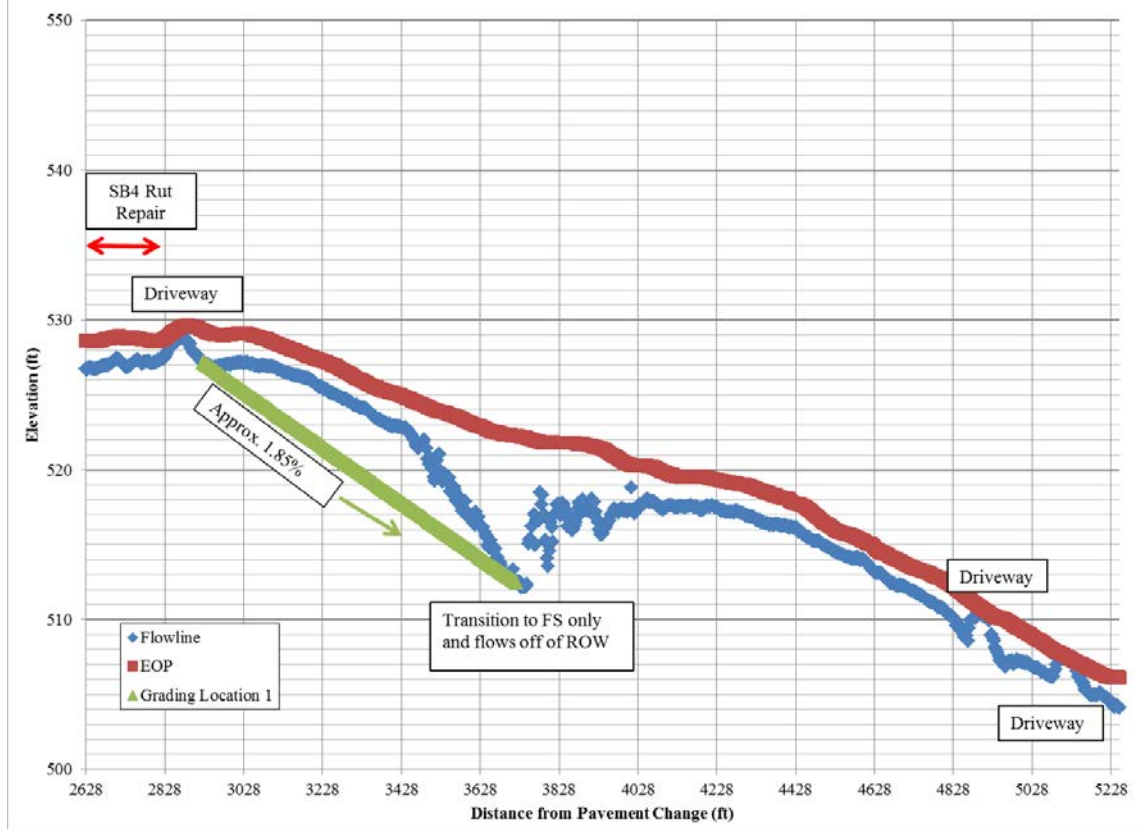
Southbound Section 3

Southbound Section 5